Science Research Council
RL-74-41
Rutherford Laboratory Report

THE WORK OF THE RUTHERFORD LABORATORY 1973

Wells KPL/Swindon Press, Swindon, Wilts.

THE WORK OF THE RUTHERFORD LABORATORY IN 1973

Edited by

J R Smith and F M Telling

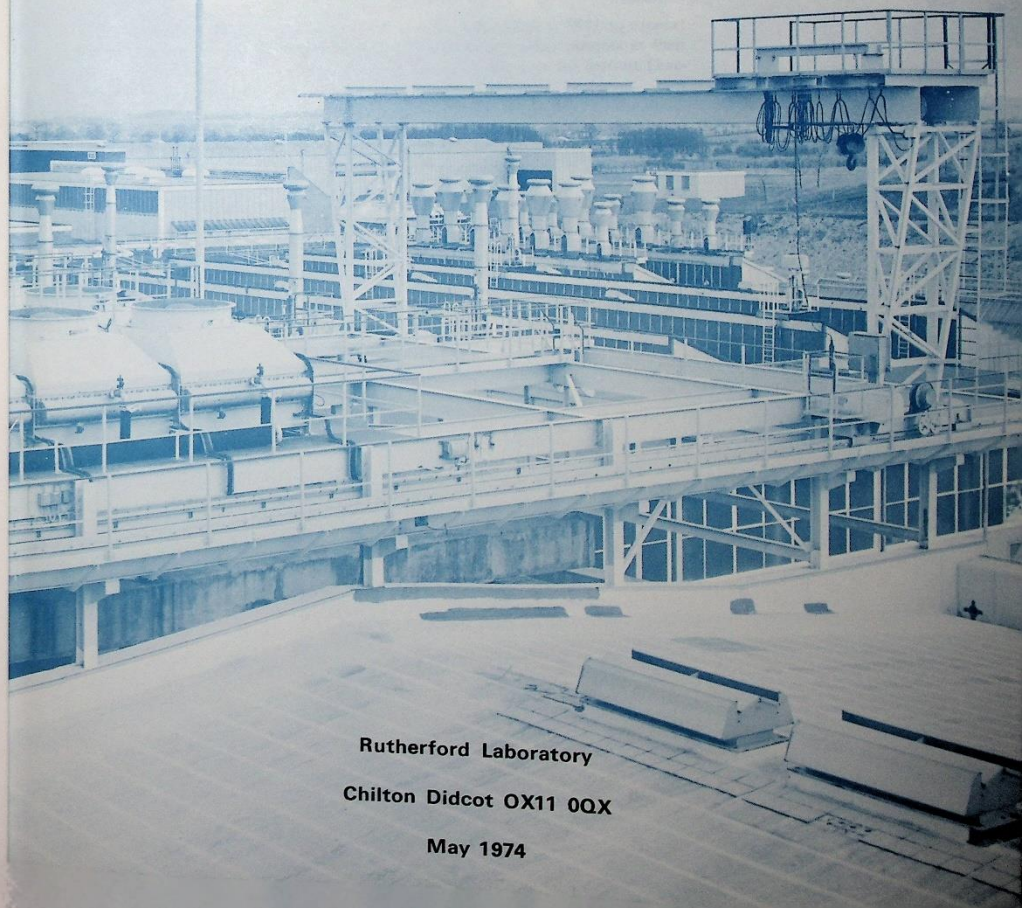

Rutherford Laboratory

Chilton Didcot OX11 0QX

May 1974

The Rutherford Laboratory was established in 1957 as the first Laboratory of the National Institute for Research in Nuclear Science to build and operate for the common use by university scientists, that equipment which was required for the conduct of research in the nuclear sciences and which by its scale or cost was beyond the resources normally available to individual universities. In 1965 the Laboratory became part of the Science Research Council retaining a similar principal role.

The experimental high energy physics research programme is based on the particle accelerator Nimrod, a 7 GeV proton synchrotron in the Rutherford Laboratory; the Laboratory also supports research carried out at international research centres, particularly at CERN in Geneva. Other fields of research at the Laboratory include theoretical physics, accelerator physics and branches of experimental physics which may have relevance to the long-term development of high energy physics.

A Neutron Beam Research Unit was established at the Laboratory in 1971 to support the community of scientists who use neutrons generated in nuclear reactors as their main research tool. The main European centre for this work is at the Institut Laue-Langevin in Grenoble.

The research and development programmes are supported by a computing system based on an IBM 370/195 computer which serves the requirements of the nuclear physicists and neutron beam users and also selected users in other fields.

There are 1160 staff employed by the Laboratory and 250 scientists in universities are associated with the nuclear physics programme. About 170 university scientists are involved in the SRC supported neutron beam research programme.

Contents

Laboratory Organisation (December 1973)

DIRECTOR: G. H. STAFFORD

HIGH ENERGY PHYSICS DIVISION
Experiments in particle physics and nuclear structure physics in collaboration with university groups; nuclear electronics.
DIVISION HEAD & DEPUTY DIRECTOR: G. MANNING
DEPUTY DIVISION HEAD: J. J. THRESHER

THEORY DIVISION
Studies in theoretical particle physics
DIVISION HEAD: R. J. N. PHILLIPS

NIMROD DIVISION
Operation and development of Nimrod (7 GeV proton synchrotron accelerator); accelerator design; experimental area management; development of beam line components and cryogenic targets; bubble chamber operations and development; radiation protection.
DIVISION HEAD: D. A. GRAY
DEPUTY DIVISION HEAD: G. N. VENN

NEUTRON BEAM RESEARCH UNIT
Support of research by universities using UK reactors and the reactor at the Institut Laue-Langevin, Grenoble; development of new instruments and techniques; study of new neutron sources; participation in experiments.
HEAD OF UNIT: L. C. W. HOBBIS

APPLIED PHYSICS DIVISION
Superconducting magnet studies; development of polarized targets; rapid cycling bubble chamber studies; superconducting power supplies and energy transfer.
DIVISION HEAD: D. B. THOMAS

COMPUTING & AUTOMATION DIVISION
Operation and development of the central computer (IBM 370/195) and satellite computer system; computer applications for bubble chamber and spark chamber film analysis.
DIVISION HEAD: W. WALKINSHAW

ENGINEERING DIVISION
Design and manufacture of equipment for nuclear and applied physics research; department of engineering science; mechanical, electrical and building services; chemical technology; safety services.
DIVISION HEAD & CHIEF ENGINEER: P. J. BOWLES
DEPUTY DIVISION HEAD: G.E. SIMMONDS

ADMINISTRATION DIVISION
Personnel, finance and accounts, general and scientific administration; library, photographic, stores, transport and security services.
DIVISION HEAD & LABORATORY SECRETARY: J. M. VALENTINE

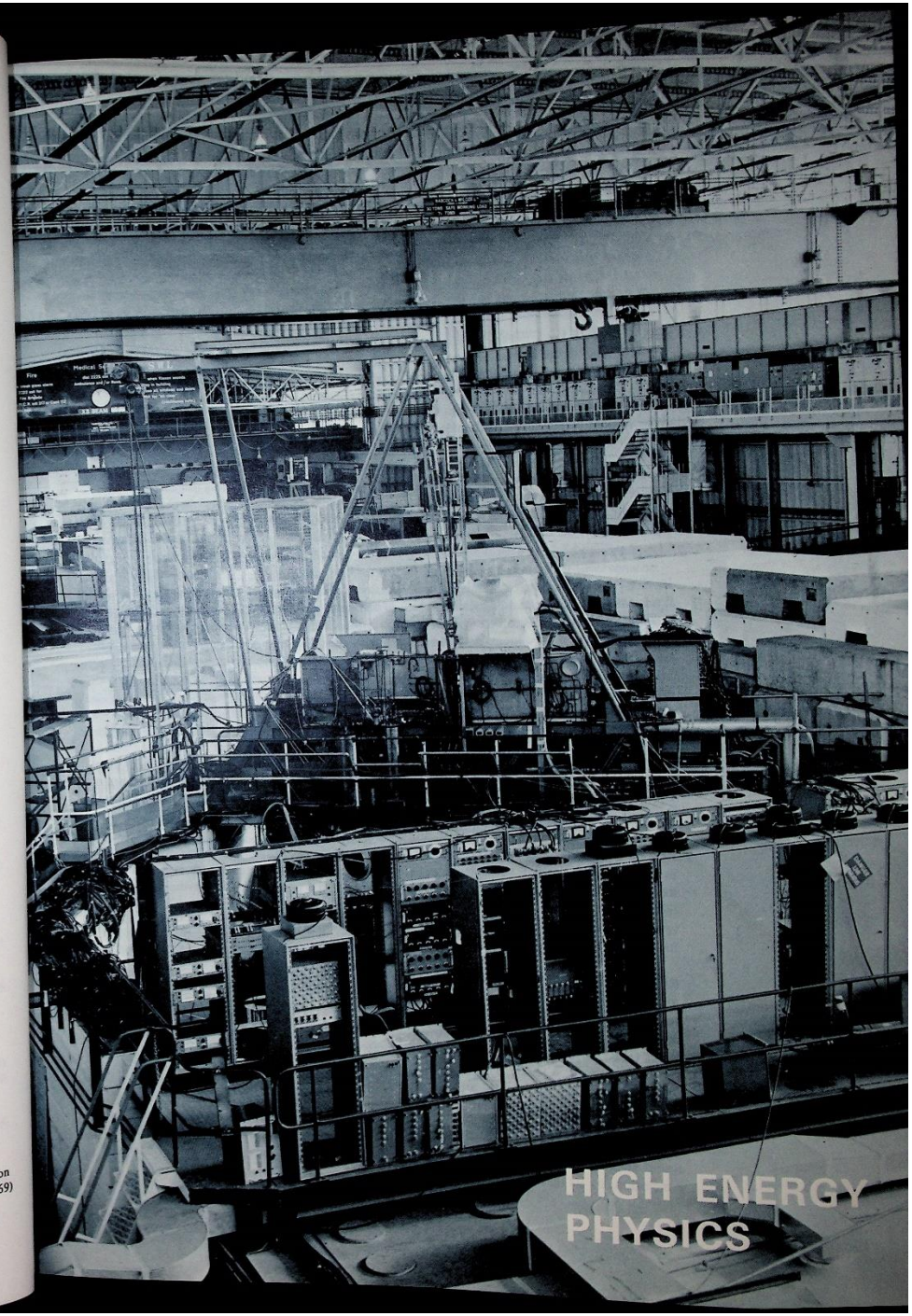

Experimental Hall 3 of the Proton Synchrotron complex at the Rutherford Laboratory (15269)

High Energy Physics

In the field of High Energy Physics much interest is currently being focussed on the possible substructure of the elementary particles e.g. the proton and neutron. By way of introduction to the reports on experiments in progress a review is given of the principles, ideas and experiments by which the substructure is being investigated and the relationship of the research programme at the Laboratory to this fundamental topic. Reference is made to the future development which could further these studies.

Hadrons resulting from the collisions of elementary particles at high energy are produced mainly with momenta closely parallel to the direction of motion of the incoming particles, However, a small fraction of events have particles emerging with large momenta and at large angles to the direction of the incident particles. Such events have large transverse momentum (p_T) and by Heisenberg's uncertainty principle, reflect the short distance behaviour of the interaction. "Large p_T" and "short distance" may be freely interchanged in what follows.

In the past three years it has become increasingly clear that these rare events are of crucial importance for understanding the structure of elementary particles. It is now believed that large transverse momentum scattering directly probes the fundamental constituents (called partons) of which hadrons may be made. This can be understood by analogy to nuclear or atomic scattering – for instance, by scattering electrons at small angles off a nucleus, one sees the nucleus as a whole; only by large angle (and so large transverse momentum) scattering can one investigate the constituent protons and neutrons in the nucleus. Similarly, large angle scattering off a proton probes the constituent partons within the proton. The parton picture abounds with paradoxes, the most obvious being: Why are the partons never seen in the final state of large p_T events? It is known that their properties should be quite different from ordinary hadrons – they must have point-like electromagnetic interactions (like a lepton) but probably have non-integral electric charge. Physicists are not discouraged by these paradoxes within the parton picture – they may indicate that the picture, like the Bohr atom (also paradoxical) is a step towards some completely new insight.

However, two things are certain. The first is that progress can only be made by detailed experimental investigation of these large p_T effects in lepton-lepton, lepton-hadron and hadron-hadron collisions. The second is that, whether or not the parton picture survives in anything like its present form the recent scattering experiments which give rise to the parton model have revealed effects unseen in other areas of particle physics, and that a rich new field of experimental and theoretical investigation has been opened up.

Recent studies at the Rutherford Laboratory have reflected this interest in large angle phenomena and the constituent structure of hadrons. Although Nimrod energies are not high enough to show these effects, the Laboratory is involved in several such experiments, either proposed or currently running on the CERN Proton Synchrotron (PS), on the CERN Intersecting Storage Rings (ISR), at the National Accelerator Laboratory (NAL), USA and at the CERN 400 GeV Proton Synchrotron (SPS). This year has also seen joint studies by physicists from British universities and from the Rutherford and Daresbury Laboratories of the feasibility and physics case for an e^+e^- and $e\pm p$ colliding beam complex, EPIC. This machine could carry further the investigation of short distance phenomena, thus probing the substructure of hadrons much more deeply than is possible with present machines. Several working groups, set up early in the year, have found that there is an extremely strong physics case for EPIC, and have reached encouraging conclusions on its feasibility.

Large angle scattering of high energy leptons on hadrons has played a seminal role in this new and rapidly developing field. This is because the interactions of the leptons (electrons, muons and neutrinos) are comparatively well understood, and are believed to be mediated by the weak and electromagnetic currents acting at a point. Thus the leptons act as carriers of currents which probe the substructure of hadrons.

Typical of these lepton-hadron scattering experiments is the Chicago-Harvard-Oxford large-angle muon-proton scattering experiment, supported by the Laboratory, which is currently running at NAL. (Experiment 20). This experiment is designed to investigate the hadronic final state produced in a muon-proton deep inelastic collision – or, in terms of the parton picture, to investigate the decay of the partons. This has been the subject of intense theoretical speculation over the past two years, but until now there have been practically no experimental data to confront the theoretical ideas.

Whereas in lepton-hadron collisions one uses a known probe (the weak or electromagnetic current) to investigate the unknown parton substructure of the hadrons, in a hadron-hadron scattering experiment one collides two unknowns with each other. The result of the collision depends on the interaction between the partons in the two colliding hadrons. Therefore hadron-hadron collisions can be used to investigate the interactions of the hadron constituents, in a way that lepton-hadron collisions cannot. The results of the British-Scandinavian collaboration (Experiment 17) on large transverse-momentum hadron production in pp collisions at the ISR, have contributed significantly to our experimental knowledge of these phenomena.

Meanwhile there has been continued activity in the study of two-body scattering processes at low and intermediate energies, a well-established area of Rutherford Laboratory involvement. All these experiments have a common aim – to accumulate enough data on a scattering process to enable the scattering amplitudes to be reconstructed without theoretical assumptions. In the past, the Laboratory has supplied a large fraction of the world's data in this area, and the many experiments proposed or currently under way ensure that this will remain so. Typical of the high quality experimental results for which the Laboratory has a responsibility are the differential cross-sections for $\bar{p}p$ processes produced by the Liverpool-QMC-Daresbury-Rutherford collaboration. The original aim of this experiment, and of the subsequent polarization measurements, was to investigate the formation of high mass bosons. This still holds good, but the results are also of great interest for parton models of large angle scattering.

Reconstruction of scattering amplitudes requires polarization data as well as cross-sections, so there has been continued emphasis on experiments with polarized targets. Work is progressing on an orientable polarized proton target which will allow important spin correlation measurements, greatly facilitating the extraction of scattering amplitudes. A design study has been completed on a polarized deuterated target which will allow measurements of scattering from polarized neutrons. This will be crucial to the understanding of the KN and $\bar{K}N$ systems.

In such small transverse momentum interactions, characterised by the formation of resonances and of peripheral peaks, hadrons appear as diffuse extended objects with a radius of the order of 1 Fermi (10^{-13}cm). The dynamics of these processes are extremely complicated, and it is known that they cannot be simply described by an elementary quantum field theory – any underlying substructure of hadrons is only hinted at indirectly by the symmetry laws. On the other hand, collisions at large transverse momentum show simple scaling laws, a behaviour which is not governed by any fixed unit of mass or distance. In this regime, the characteristic behaviour is pointlike, and the hadrons are described by field theories with fundamental pointlike constituents – apparently distinct from the complicated dynamics of small transverse momentum processes. Yet these two very different sorts of behaviour must be intimately related – not only because it is the same hadrons which are involved in the two cases, but also because we have direct evidence that the two regimes match up in a simple way through "duality". To reconcile and unify the spatially extended behaviour of hadrons at small transverse momenta, with the scaling pointlike behaviour at large transverse momenta, is one of the great challenges facing physicists today. The programme of research at the Rutherford Laboratory is exploring both these regimes.

Table 1

High Energy Physics : Electronic Counter Experiments

Experiments at Nimrod

Experiment Number	Proposal	Experiment Title	Groups
1	43, 83, 105 120	K^+, K^-, π^+, π^-, $-p$ elastic scattering differential cross-sections	University of Bristol University of Southampton Rutherford Laboratory
2	50, 99, 110 128	Studies of η, ω, X^0 and S* by missing mass technique	Imperial College, London University of Southampton
3	70, 76	Search for C-violation in η-decay	Westfield College, London Rutherford Laboratory
4	81, 101	Differential cross-sections for $\pi^-p \to \pi^0 n$, ηn	Rutherford Laboratory
5	87, 114	Differential cross-sections and polarization for $\pi^-p \to K^0\Lambda$	University of Cambridge Rutherford Laboratory
6	92	Study of neutral states in K^-p interactions	University of Oxford
7	126	Baryon and meson spectroscopy with a multiparticle spectrometer	Westfield College, London Rutherford Laboratory

Experiments at CERN Proton Synchrotron and Synchro-cyclotron

8	75	Differential cross-sections for $\bar{p}p \to \bar{p}p$, $\pi^+\pi^-$, K^+K^-	University of Liverpool Queen Mary College, London Daresbury Laboratory Rutherford Laboratory
9	103	Polarization in $\bar{p}p$ reactions	Queen Mary College, London Daresbury Laboratory Rutherford Laboratory
10	88	Studies of neutral bosons produced in π^-p reactions using the CERN Omega spectrometer	Univeristy of Birmingham Tel Aviv University Westfield College, London Rutherford Laboratory
11	93	Non-diffractive production of neutral K meson resonances	University of Rome Rutherford Laboratory
12	95	Coherent production of I=½ states on Helium	CERN University College, London University of Uppsala
13	100	Differential cross-sections and polarization in the reactions $\pi^+p \to K^+\Sigma^+$ $K^-p \to \pi^-\Sigma^+$	University of Birmingham University of Genova University of Stockholm CERN Rutherford Laboratory
14	107, 124	Spin rotation parameters in $\pi^-p \to K^0\Lambda$	Imperial College, London University of Southampton ETH – Zurich CEN, Saclay University of Helsinki

Experiment Number	Proposal	Experiment Title	Groups
15		Spin dependence of inclusive reactions (CERN PS and Nimrod)	CERN University of Paris-Sud University of Oxford
16	98	Measurement of the pion-nucleon scattering lengths (CERN SC)	Queen Mary College, London University of Birmingham University of Pisa University of Mainz Daresbury Laboratory

Experiments at CERN Intersecting Storage Rings and the National Accelerator Laboratory, USA

17	72	Search for quarks; Particle production at large transverse momentum Search for new particles by studying muon production (ISR)	University of Bristol University of Liverpool University College, London Rutherford Laboratory University of Bergen University of Lund University of Copenhagen University of Stockholm CERN
18	129	Study of high transverse momentum behaviour (ISR)	CERN University of Liverpool Daresbury Laboratory Rutherford Laboratory
19	131	Study of inclusive particle production of very low p_T and x = 0 (ISR)	CERN University College, London University of Bristol Massachusetts Inst. Tech. Niels Bohr Institute University of Stockholm
20	96	Muon-nucleon scattering (NAL)	University of Chicago Harvard University University of Illinois University of Oxford
21	118	Study of inclusive pp reactions from 30 to 400 GeV/c (NAL)	Rutgers University Imperial College, London
22	130	Study of large transverse momentum behaviour using a split field magnet (ISR)	University of Liverpool University of Paris-Sud Scandinavian Universities

EXPERIMENT 1

University of Bristol
University of Southampton
Rutherford Laboratory

K^+, π^+, π^-, K^-–p elastic scattering
Differential Cross-sections

(Proposals 43, 83, 105, 120)

K^+p scattering

The K^+p phase shift analysis of the Birmingham University-Rutherford Laboratory group (RL-73-071) shows first that particle exchange plays a dominant role for scattering in this channel and second that the particular exchange calculations of J W Alcock and W N Cottingham are in reasonably good agreement with experiment. Work is being done in Bristol to determine with small errors, the fundamental K meson coupling constants that appear in these calculations. The K^+p differential cross-sections in the incident momentum range 0.7 to 1.0 GeV/c measured at Rutherford Laboratory by the Bristol Group and described in previous Annual Reports have provided much of the data for these calculations.

π^+, π^-p scattering

During 1973 the momentum range over which differential cross-sections were measured for $\pi^\pm p$ elastic scattering was extended. Data-taking was completed and final analysis is now nearing completion. Details of the experiments and the experimental configuration have been described in previous Reports. Figures 1 and 2 show isometric plots of the differential cross-sections for $\pi^\pm p$ elastic scattering at a number of momenta in the range 0.04 - 2.20 GeV/c. Sufficient data has been collected to provide differential cross-sections continuously over this momentum range. The results will be used in new phase shift analyses being carried out both in Bristol and in the USA.

K^-p scattering

In contrast to the K^+p system, the K^-p system in the intermediate momentum range shows a large number of resonant states. To assist in the elucidation of these states, precision measurements of K^-p elastic differential cross-sections comparable to those already available in the pion-nucleon system are required. Construction and testing of a new beam line and apparatus to achieve this objective is now under way.

EXPERIMENT 2

Imperial College, London
University of Southampton

Study of the production of narrow width mesons in π^-p interactions

(Proposals 50, 99, 110, 128)

(ref. 26, 348, 403)

A series of experiments on the production of mesons in the reactions

$$\pi^- + p \rightarrow M^- + p$$
$$\rightarrow M^\circ + n$$

have now been completed though some have still to be fully analysed. All these experiments used the "missing mass" technique in which the mass of the recoiling meson system M was defined from the incident π and final nucleon momenta. The decay products of M were detected by an array of counters surrounding the hydrogen target, both gamma rays and charged particles being registered.

Figure 1 π^+p Differential cross-sections: Experiment 1 (15209)

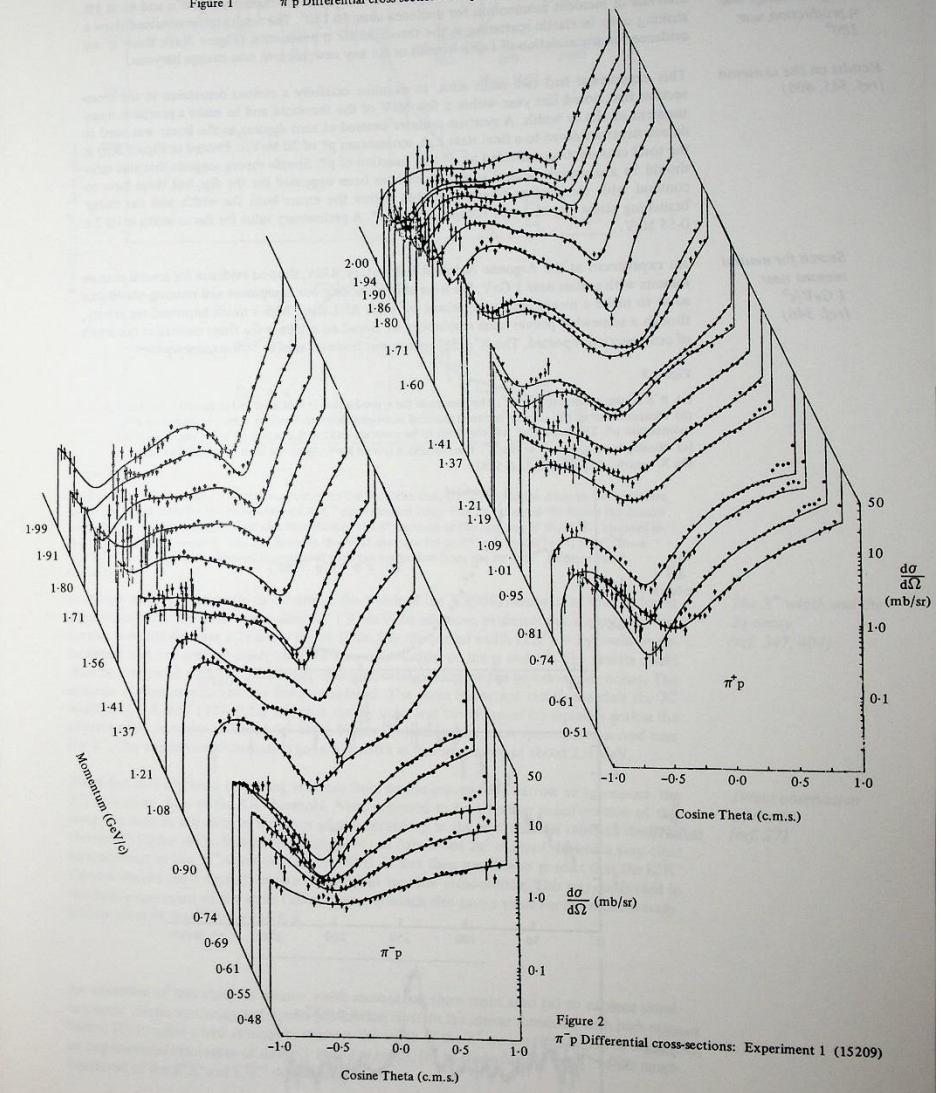

Figure 2
π^-p Differential cross-sections: Experiment 1 (15209)

Elastic scattering, charge exchange and η production near 180°

Data has been collected between 600 and 1000 MeV/c for the channels π^-p, π^0n and ηn at 1% intervals of incident momentum for nucleons close to 180°. The results so far obtained show a striking cusp in elastic scattering at the threshold for η production (Figure 3(a)); there is no evidence for any violation of I-spin bounds or for any new, narrow, non-strange baryons.

Results on the ω meson (ref. 345, 406)

This experiment had two main aims, to examine carefully a curious depression in the cross-section first noted last year within a few MeV of the threshold and to make a precision measurement of the ω width. A neutron counter centred at zero degrees to the beam was used to detect neutrons down to a final state c.m. momentum p* of 20 MeV/c. Plotted in Figure 3(b) is the total cross-section σ divided by p* as a function of p*. Simple theory suggests that this ratio should be a constant. Several explanations have been suggested for the dip, but these have to contend with the further observation that within the errors both the width and the decay branching ratios appear to be independent of p*. A preliminary value for the ω width is 10·2 ± 0·55 MeV.

Search for neutral mesons near 1 GeV/c² (ref. 346)

An experiment at the Argonne National Laboratory, USA, showed evidence for several narrow mesons with a mass near 1 GeV. We were able to modify our equipment and running conditions so as to make a meaningful comparison with the ANL data. With a much improved sensitivity, though a somewhat poorer mass resolution, we found no evidence for these mesons at the levels of cross-section reported. The X°(958) meson was however seen in both experiments.

Figure 3

(a) π^-p elastic scattering at 180°. The threshold for η production is indicated and coincides with the cusp.
(b) Measurement of the ω cross section (assumed isotropic) down to very low values of final state c.m. momentum p*. The ratio σ/p* was expected to be constant and the fall at low p* is not yet understood.
(c) Missing mass spectrum at the X°. The bin width is 0·49 MeV. An upper limit of 0·8 MeV is found for the X° width: Experiment 2. (15281)

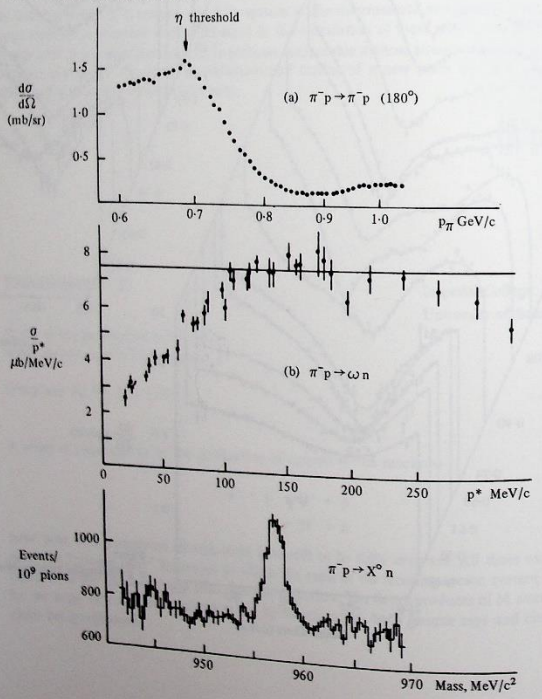

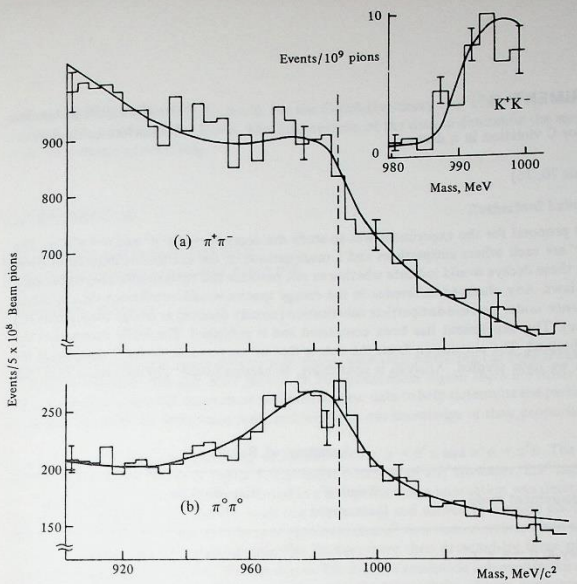

Figure 4

Evidence for the S* meson. The striking feature in the $\pi^+\pi^-$ channel, (a), is the sudden drop in the spectrum at the threshold mass for the production of K^+K^- pairs (dashed line). The $2\pi^0$ channel (b) shows the meson very clearly. The drop is explained as a distortion of the S* because of the opening of the K^+K^- channel to which it is strongly coupled. The full lines are the fit to the data for an S* pole at (987-i24) MeV. Inset: The K^+K^- mass spectrum observed is compared with the prediction from the ππ data: Experiment 2. (15282)

The X° width and the 2γ decay (ref. 347, 404)

A further attempt was made to determine the width of the X°(958) meson or at least to lower significantly our previous upper limit of 1.9 MeV. In addition, evidence was sought that the meson detected did have a 2γ decay mode. From this the partial width $\Gamma(X^\circ) \to 2\gamma$ could be determined and comparison made with the measured widths of the η and π^0. The results could then be compared with the predictions of singlet/octet mixing for the pseudo-scalar nonet. The analysis of this experiment has been completed. The most important results are that the X° width is < 0.8 MeV (95% C.L.) and that the 2γ mass and the X° mass are equal to within the experimental accuracy of about 0.5 MeV. Figure 3(c) shows the mass spectrum observed near the X°. The experimental resolution has a full width at half maximum of about 2.0 MeV.

Direct observation of the S (ref. 27)*

There has recently been increasing evidence from several groups for a narrow ππ resonance, the S*, at a mass close to the $K\bar{K}$ threshold. What appeared to be a further manifestation of this state was seen in our data in the form of a sudden drop in the $\pi^+\pi^-$ channel close to the K^+K^- threshold (Figure 4(a)). Subsequent analysis of our data in the $2\pi^0$ channel showed a very clear enhancement in the $2\pi^0$ spectrum (Figure 4(b)). It was then possible to predict that the K^+K^- channel should show a rapid rise to a defined, but very low cross-section. This was confirmed in the final experiment of the series (inset, Figure 4) which also gave a value for the relative coupling constant of the S* to ππ and $K\bar{K}$.

An extension of this study of narrow width mesons has three main aims (a) to explore simultaneously elastic scattering and meson production close to the meson threshold with high resolution, (b) to make a new attempt to measure the width of the X° meson (it is hoped to achieve an experimental resolution of under 1 MeV f.w.h.m.), (c) to study further the S* in the neighbourhood of the K^+K^- and $K^0\bar{K}^0$ thresholds.

EXPERIMENT 3

Westfield College, London
Rutherford Laboratory

Search for C violation in η decays

(Proposals 70, 76)

(ref. 202, 203, 407)

The first proposal for the experiment was to study the decays $\eta \to \pi^+\pi^-\pi^\circ$ and $\eta \to \pi^+\pi^-\gamma$. The π^+ and π^- are each others antiparticles and a measurement of the energy distributions of the π^+ and π^- in these decays would indicate whether or not particles and antiparticles obeyed the same physical laws. Any observed difference in the energy spectra would be evidence for a violation of invariance under particle-antiparticle substitution (usually denoted as charge conjugation (C) invariance). The experiment has been completed and is published. The Table summarises the results obtained. The conclusion from the data is that we see no evidence for C-violation in the η decays we have studied. Analysis is continuing, to extract further physics results from this data.

Summary of Results

Measurement made	Result if C conserved	Experimental Result	Comments
Asymmetry in $\eta \to \pi^+\pi^-\pi^\circ$	0	0.0028 ± 0.0026	Sensitive to C-violation due to I = 0 or 2 final state.
Asymmetry in $\eta \to \pi^+\pi^-\gamma$	0	0.012 ± 0.006	Sensitive to C-violation due to I = 0 final state.
Asymmetry vs $\lvert x \rvert$ in $\eta \to \pi^+\pi^-\pi^\circ$ Dalitz plot	Flat	Flat	Linear increase if C violated in I = 2 state.
Asymmetry vs y in $\eta \to \pi^+\pi^-\pi^\circ$ Dalitz plot	Flat	Flat	Linear increase if C violated in I = 2
Sextant asymmetry in $\eta \to \pi^+\pi^-\pi^\circ$ Dalitz plot	0	0.0021 ± 0.0025	Sensitive to C-violation due to I = 0
Quadrant asymmetry in $\eta \to \pi^+\pi^-\pi^\circ$ Dalitz plot	0	-0.0029 ± 0.0025	Sensitive to C-violation due to I = 2
Asymmetry vs $\lvert \cos\theta \rvert$ for $\eta \to \pi^+\pi^-\gamma$	Flat	Flat	Linear increase if C-violation due to I = 0 final state.
Asymmetry vs k for $\eta \to \pi^+\pi^-\gamma$	Flat	Flat	Increase if C-violation due to I = 0 final state.
d-wave amplitude in angular distribution for $\eta \to \pi^+\pi^-\gamma$	0	0.11 ± 0.11	Presence of d-wave would imply C-violation.

A further proposal was made to search for the C-violating decay $\eta \to \pi^\circ e^+e^-$. No convincing event for this decay has been found. The final analysis of the data to determine the sensitivity of the experiment is proceeding.

EXPERIMENT 4

Rutherford Laboratory

Differential Cross-sections in the Charge Exchange Reactions $\pi^-p \to \pi^\circ n$ and $\pi^-p \to \eta^\circ n$

(Proposals 81, 101)

The differential cross-section for pion-proton charge exchange scattering has been measured at 23 momenta between 600 and 3000 MeV/c. In this momentum region there are many known nucleon resonances, and the experiment will provide new data to help determine the partial wave amplitudes produced by these resonances, and so add to our knowledge of their properties.

Data has been recorded simultaneously on the reactions $\pi^-p \to \pi^\circ n$ and $\pi^-p \to \eta^\circ n$. The experimental arrangement is shown in Figure 5. The target consisted of a 2″ diameter, 2.5″ high cylinder of liquid oxygen. The neutron produced in a charge exchange interaction was detected in a large array of liquid scintillator cells, each one metre long, and viewed by a single photomultiplier. The γ rays resulting from the decay of the associated π° or η were converted into electron-positron showers by large sheets of lead. The showers were then detected by three planes of plastic scintillators placed behind the lead sheets. The angular resolution achieved in the neutron and γ-ray detectors was good enough to determine, unambiguously, charge exchange events from inelastic events by measuring the angles of the three final state products. Charged particle background is rejected by the use of plastic scintillation counters placed around the target and in front of each of the neutron and γ-ray detectors. Data taking was completed in February 1973.

Figure 5 Diagram of the apparatus for Experiment 4 with liquid hydrogen target installed. (13767)

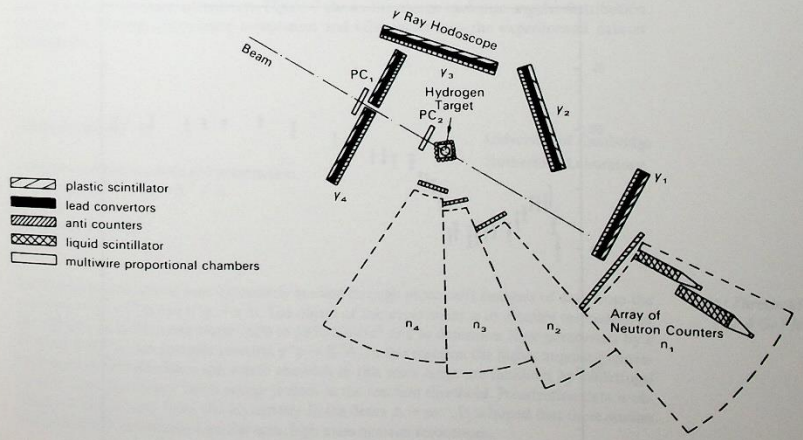

In order to evaluate the differential cross-sections from the experimental data it is necessary to know the detection efficiencies of the detectors.

The neutron counters were calibrated by three separate methods

(i) A low energy neutron beam, produced by the Harwell cyclotron, was used to investigate the efficiency of the neutron counters in the momentum range 200 to 450 MeV/c.

(ii) A neutron beam produced at Nimrod by the extracted proton beam, X3, was used to perform an np elastic scattering experiment (N4). The elastically scattered neutron was detected in the neutron counter arrays. The associated proton was detected in a sonic spark chamber spectrometer, which measured the angle and momentum of the proton. This enabled a prediction of the neutron angle and momentum to be made. By comparing the number of predicted neutrons with the number detected, the neutron counters could be calibrated between 1000 and 3000 MeV/c.

(iii) The πp charge exchange experiments were run at a few momenta below 1200 MeV/c in a mode where the trigger required only the detection of two γ-rays coming from the target; no neutron requirement was imposed. This enabled a prediction of the angle and momentum of the neutron to be made, assuming a charge exchange interaction had taken place. In this way the efficiency of the neutron counter arrays could be estimated between 200 and 1300 MeV/c.

It has thus been possible to calibrate the neutron counter arrays over a momentum range of 200-3000 MeV/c and to cross-check the normalisation by comparing the efficiencies obtained in the regions of overlap of the three methods. The slope of the efficiency curve as a function of momentum varies in the way expected from our knowledge of the processes involved in the production of knock-on charged and neutral particles by neutrons. The arrays have a minimum efficiency of 42% and a maximum efficiency of ~60% across the measured momentum region.

The γ-ray hodoscopes were calibrated using "tagged" photons of known energy. They were selected from the bremsstrahlung radiation produced in a thin radiator by electrons present in the π9 beam. The photon energy was obtained by measuring the electron momentum before and after the radiation. The hodoscope efficiency is determined by comparing the number of tagged photons with the number detected in the hodoscope. The measured efficiencies agree well with theoretical predictions.

Figure 6 Efficiency of neutron counter arrays: Experiment 4. (15411)

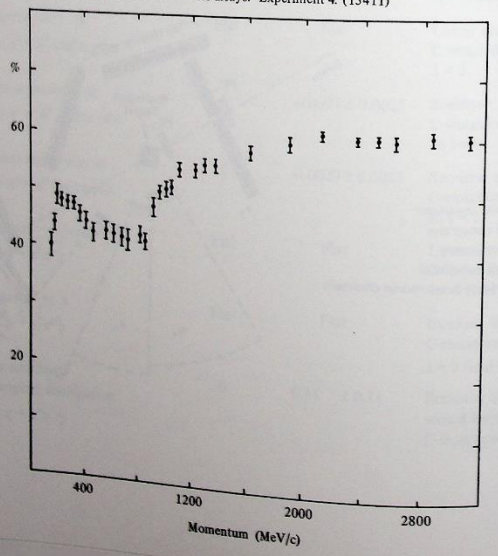

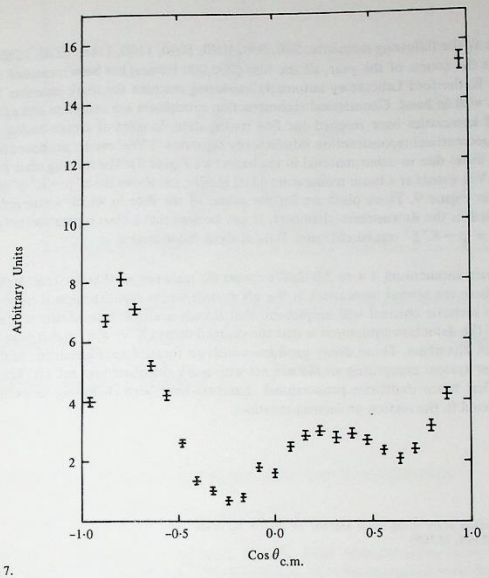

Figure 7.

Angular distribution for the reaction $\pi p \rightarrow \pi^{\circ} n$ at 1030 MeV/c. Errors are statistical only: Experiment 4. (15407)

The analysis of the various calibration data has been carried out in parallel with that of the charge exchange and η production data. Both are nearing completion.

Figure 6 shows the results of the efficiency measurements on the neutron counter arrays plotted as a function of neutron momentum. Figure 7 shows the charge exchange angular distribution obtained by folding approximate acceptances and efficiencies into the experimental data at 1030 MeV/c.

EXPERIMENT 5

University of Cambridge
Rutherford Laboratory

Differential Cross-sections and polarization
in the reaction $\pi^- + p \rightarrow K^{\circ} + \Lambda$

(Proposals 87, 114)

(a) Threshold to 1·4 GeV/c

Nucleon resonances have been extensively studied through phase shift analyses of data from the reactions $\pi^{\pm}p \rightarrow \pi^{\pm}p$ and $\pi^- p \rightarrow \pi^{\circ} n$. The object of this experiment is to identify resonances in the πN system in the mass range 1600 to 1850 MeV/c^2 and to determine their parameters by a detailed study of the inelastic reaction $\pi^- p \rightarrow K^{\circ}\Lambda$. In this reaction the higher angular momentum waves which dominate the elastic channels in this mass range are inhibited by centrifugal barriers since the chosen beam energy is close to the reaction threshold. Polarization data is obtained simultaneously from the asymmetry in the decay $\Lambda \rightarrow p\pi^-$. It is hoped that these studies will yield useful information on low spin, high mass nucleon resonances.

Data was taken at the following momenta: 940, 980, 1020, 1040, 1100, 1160, 1220, 1280 and 1340 MeV/c. In the course of the year, all the film (900,000 frames) has been measured using CYCLOPS, the Rutherford Laboratory automatic measuring machine for spark chamber film. Data analysis is well in hand. Geometrical reconstruction procedures are complete and pattern recognition and kinematics have reached the fine tuning state. In spite of a high background trigger rate the geometrical reconstruction satisfactorily separates '2 Vee' events produced in the hydrogen from those due to other material in the beam (see Figure 8). The missing mass to the K° vertex for 2 Vee events at a beam momentum 1160 MeV/c, i.e. above the $\pi^- p \to K^\circ\Sigma^\circ$ threshold, is shown in Figure 9. These plots are for the subset of the data in which 4 charged particles are detected in the downstream chambers. It can be seen that a clear separation between $\pi^- p \to K^\circ\Lambda$ and $\pi^- p \to K^\circ\Sigma^\circ$ can be obtained. Data analysis is continuing.

(b) 1·4 to 2·0 GeV/c

The range in beam momentum 1.4 to 2.0 GeV/c covers the mass region 1880 to 2160 MeV/c^2. In this region there are several resonances in the πN system whose identification is uncertain. The data in this inelastic channel will supplement that already available from elastic scattering. The principle of the detection equipment is that the charged decays $K^\circ \to \pi^+\pi^-$ and $\Lambda \to p\pi^-$ are observed in spark chambers. Those decay products which go forward are momentum analysed in a spectrometer system comprising an M5 magnet with spark chambers fore and aft. The properties of the first beam multiwire proportional chambers have been rigorously determined. Results are reported in the section on instrumentation.

Figure 8

Position of production point along beam axis for 2V events. Hydrogen flask is 6cm long (−6 to 0cm): Experiment 5. (15368, 15369)

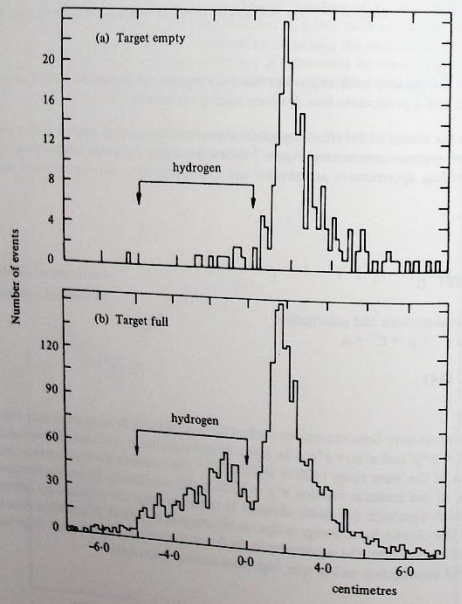

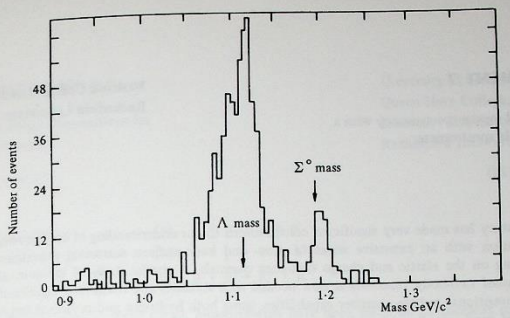

Figure 9

Missing mass to the K° for 2V events from hydrogen at p_π = 1·16 GeV/c: Experiment 5. (15360)

EXPERIMENT 6

University of Oxford

Neutral states from K^-p interactions

(Proposal 92)

(ref. 114, 334)

This experiment selected the following final states from K^-p interactions:

$$\pi^\circ\Lambda,\ \pi^\circ\Sigma^\circ,\ \eta\Lambda,\ \eta\Sigma^\circ,\ \pi^\circ\pi^\circ\Lambda$$

Our purpose is to find, by partial wave analysis, what resonant states decay into these final states, and with what amplitudes. The results may then be compared with the predictions of symmetry models based on quarks, such as that of Faiman and Plane. In the table we give the amplitudes deduced in our experiment, together with these authors' predictions, and we see good agreement in phase and in most cases also in amplitude.

Amplitudes for resonances decaying into the various final states

Channel	$\pi^\circ\Lambda$	$\pi^\circ\Sigma^\circ$	$\pi^\circ\Sigma^\circ$	$\eta\Lambda$	$\eta\Lambda$	$\pi^\circ\pi^\circ\Lambda$	$\pi^\circ\pi^\circ\Lambda$
Wave	D13	S01	D03	S01	D03	D03	S01
Resonant Mass	1660	1700	1670	1700	1670	1700	1670
Amplitude (expt.)	+0.10 ±0.02	−0.28 ±0.05	−0.20 ±0.03	+0.20 ±0.05	0.0 ±0.03	+0.16	+0.14
Amplitude (theory)	+0.18	−0.33	−0.32	+0.24	0	+0.14	±0.05

Further testing of the models requires extension to higher mass, in particular to cover the $\eta\Sigma^\circ$ threshold region and the F_{05} (1815) and D_{05} (1830) resonances in $\pi^\circ\Sigma^\circ$. We are analysing data up to 1180 MeV/c in K momentum, that is to 1880 MeV/c^2 in mass. This analysis uses a new principle, in which the only events inspected by scanners are those known to have a good 'V' fit in the magnetostrictive wire chamber data, found by automatic pattern recognition. We are at present evaluating the efficiency of this method to prove compatibility with data obtained by the pure optical method.

EXPERIMENT 7

Westfield College, London
Rutherford Laboratory

Baryon and meson spectroscopy with a multiparticle spectrometer

(Proposal 126)

The Laboratory has made very significant contributions to our understanding of baryon resonance formation with an extensive series of pion- and kaon-nucleon scattering experiments concentrating on the elastic and charge exchange channels. A similar study of inelastic, and especially quasi two-body reactions is now needed with statistics and resolution significantly beyond conventional bubble chamber capabilities, using both hydrogen and polarized targets. This type of work usually requires a large aperture spectrometer magnet: such magnets are being built or are running at Stanford Linear Accelerator Centre and Brookhaven National Laboratory in the USA and at CERN (the Omega spectrometer), usually at beam momenta higher than those accessible with Nimrod.

The Rutherford Multiparticle Spectrometer (RMS) Project will provide the Laboratory with such a spectrometer, to be operated as a facility with the improved Nimrod. Based on the 1·5 m Hydrogen Bubble Chamber magnet, suitably modified with new pole pieces and return yokes. the RMS will offer a useful volume of 2·7 m x 2·0 m x 1·24 m with a magnetic field of 1·0 to 1·2 tesla. Capacitative read-out spark chambers (with a total of some 65,000 wires with a 1 mm pitch) will be used, supplemented by proportional chambers in the beam and target region, where they can be used in the trigger. An atmospheric pressure Cerenkov counter will fill the 2 m x 1·24 m downstream aperture of the magnet, enabling pions and kaons above 2·8 GeV/c to be distinguished. Figure 10 shows the general layout.

Specific proposals for experiments are expected to be submitted in 1974. Some fields of study to which RMS could be expected to make substantial contributions include: (i) meson spectroscopy, for many predicted meson states are either missing or poorly established, (ii) the role of Regge cut contributions in scattering amplitudes, by providing data for model-independent amplitude analysis of quasi two-body differential cross-sections and polarizations, and (iii) baryon spectroscopy, via phase-shift analyses of differential cross-section and polarization data obtained from a study of multibody final states in the s-channel resonance formation domain ($s \leqslant 4$ GeV^2).

Both a 6 GeV/c unseparated pion beam and a 4 GeV/c separated beam are being considered for the first round of data taking.

Figure 10 The RMS magnet to be used in Experiment 7. (15366)

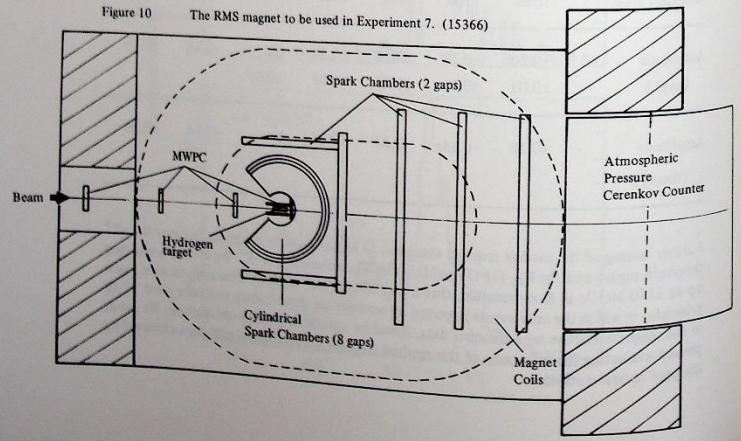

EXPERIMENT 8

University of Liverpool
Queen Mary College, London
Daresbury Laboratory
Rutherford Laboratory

Differential cross-sections for $\bar{p}p$ reactions.

(Proposal 75)

(ref. 158, 159, 331, 332, 339, 356, 387, 390, 414)

The processes:

(a) $\bar{p} + p \rightarrow \bar{p} + p$
(b) $\bar{p} + p \rightarrow \pi^- + \pi^+$
(c) $\bar{p} + p \rightarrow K^- + K^+$

have been studied in some detail. Measurements have been made at 21 incident antiproton momenta in the range 0·7 GeV/c to 2·4 GeV/c, with coverage of the full range of centre-of-mass scattering angles. At each momentum, typically 40,000 events were detected for process (a), 1,500 for process (b) and 400 for process (c).

Data taking ended in June 1972, and the extraction of differential cross-sections for all 3 reactions is now complete; the results for channels (b) and (c) have been published. Work is continuing on the physical interpretation of these results.

Figure 11 Angular distributions for $\bar{p}p$ elastic scattering at 1·85 GeV/c: Experiment 8). (15362)

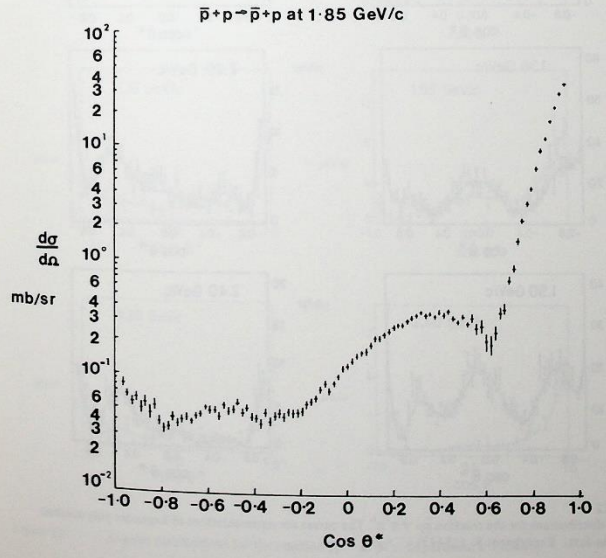

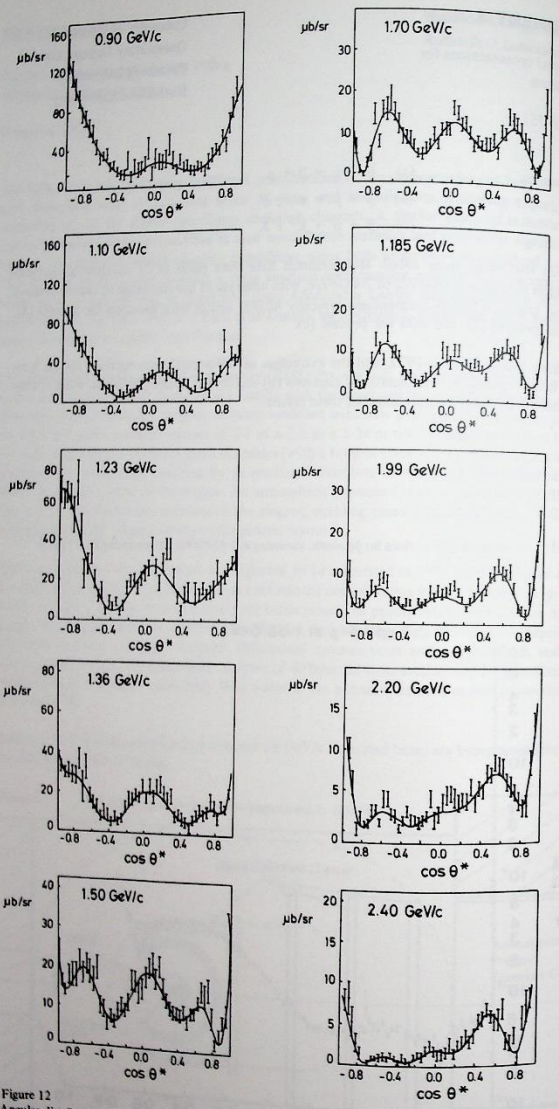

Figure 12
Angular distributions for the reaction $\bar{p}p \to \pi^- \pi^+$. The curves are representations of Legendre polynominal fits to the data: Experiment 8. (15443)

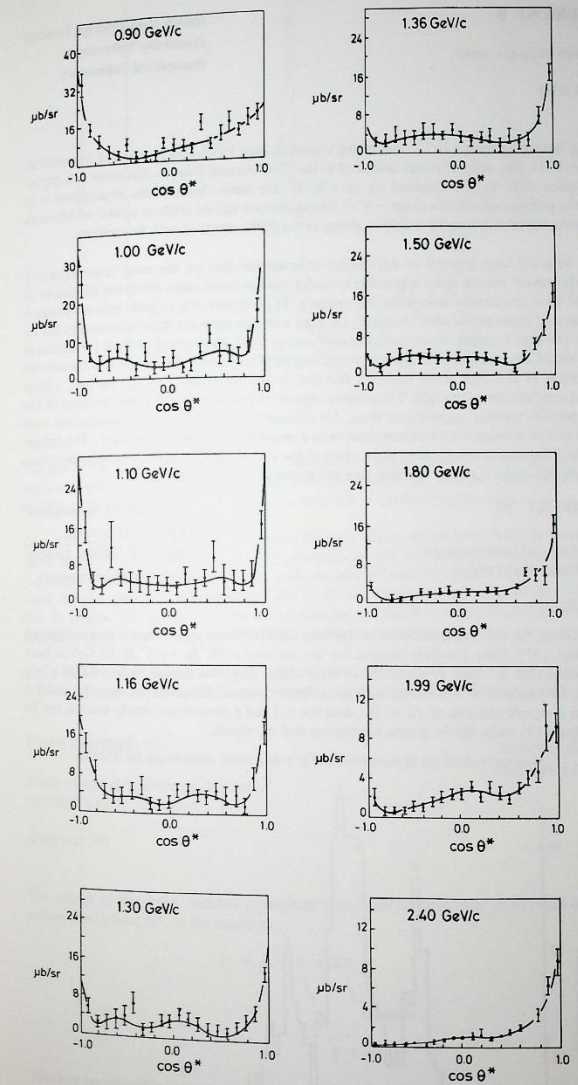

Figure 13 Angular distributions for the reaction $\bar{p}p \to K^- K^+$: Experiment 8 (15444)

EXPERIMENT 9

Queen Mary College, London
Daresbury Laboratory
Rutherford Laboratory

Polarization in $\bar{p}p$ reactions

(Proposal 103)

Following setting up during 1972, data taking started in May 1973, and is expected to continue until June 1974. The apparatus was described in the 1972 Annual Report. Although it is expected that some data will be obtained on $\bar{p}p \rightarrow K^-K^+$, the main object of the experiment is to measure the polarization effects in $\bar{p}p \rightarrow \pi^-\pi^+$. Measurements will be made at a total of 10 incident momenta between 1·0 and 2·2 GeV/c; giving about 5000 events at each momentum.

Together with the large amount of differential cross-section data on the same process (experiment 8) the results should make it possible to understand in much more detail the behaviour of the partial wave amplitudes describing the reaction. In particular, it is of great interest to know whether any of these amplitudes 'resonate', i.e. if an unstable resonant state is formed in the reaction. In the quark model, these states are expected to exist; observation of their formation in this way would be a further and important verification of the model. An alternative framework for discussion of the data arises from the fact that in the annihilation of the $\bar{p}p$ pair, a large amount of momentum is released. The reaction therefore has some of the characteristics of the high momentum transfer experiments done, for example, at the ISR. These experiments have suggested rather strongly that hadronic matter is composed of pointlike 'partons'. The behaviour of the differential cross-sections show some of the characteristics of such models; the polarization data will make it clearer whether they are useful in this energy region.

EXPERIMENT 10

University of Birmingham
Tel Aviv University
Westfield College, London
Rutherford Laboratory

A study of neutral bosons using a neutron time of flight trigger

(Proposal 88)

The data taking for this experiment which uses the CERN Omega spectrometer was completed in December 1973. Over 3 million triggers for the reaction $\pi^-(K^-)p \rightarrow nX^\circ$ at 12 GeV/c have been recorded (the K^- flux is about 1% of the π flux). The data contain over 50,000 $\pi^+\pi^-n$ events and even more $\pi^+\pi^-\pi^\circ n$ events with the effective mass of the pions between 0·8 and 2·2 GeV/c^2. In a sample analysis of 1% of the data the ρ, f and g mesons are clearly seen in the 2π system (Figure 14) while the 3π system contains ω and A_2 signals.

Figure 14 Mass spectrum of the 2π system in the $\pi^+\pi^-n$ final state: Experiment 10. (15359)

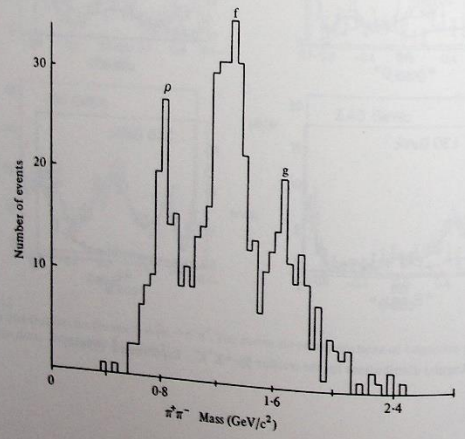

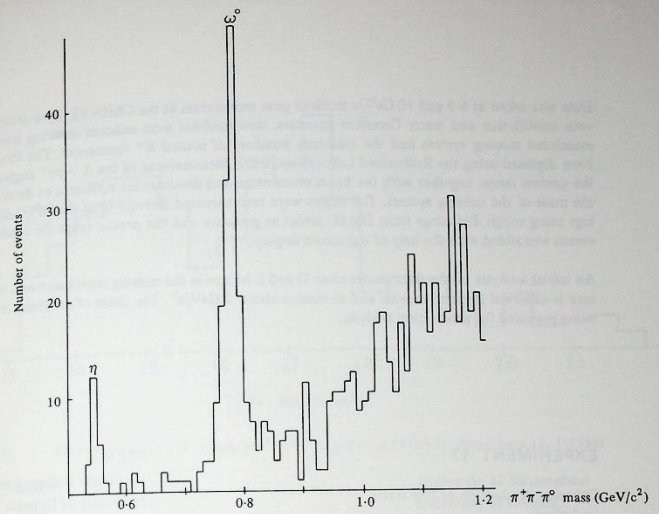

Figure 15 Mass spectrum of the 3π system in the $\pi^+\pi^-\pi^\circ n$ final state: Experiment 10. (15365)

The aim of the experiment is to look for evidence of new zero strangeness meson states by making a spin-parity analysis of the 2π and 3π events. Such states provide information about the validity of the quark model since they are composed of quark-antiquark pairs.

Over 10^5 4-pronged events are included in the data. These will be more difficult to analyse but there is every hope that useful physics information will be obtained from these events also. 2-pronged events will be analysed first with the aim of understanding the systematic biases for these simpler events. It should be possible to obtain complete decay angular distributions for the 2π events. The problems to be solved concern the pattern recognition efficiency and geometrical reconstruction and are common to all Omega experiments.

Some earlier test data, with 1 magnet coil only, have yielded a few hundred $\pi^-p \rightarrow \omega\, n$ events at 8 GeV/c (Figure 15). The differential cross-section for this reaction will be obtained.

EXPERIMENT 11

University of Rome
Rutherford Laboratory

Study of non-diffractive production of neutral K meson resonances

(Proposal 93)

The object of this spark chamber experiment is to study the peripheral production of neutral K meson resonances, K*, in the reaction

$$\pi^- + p \rightarrow \Lambda + K^* \quad (K^* \rightarrow \text{neutrals},\ \Lambda \rightarrow p + \pi^-)$$

There is considerable interest (and uncertainty) in the mass spectrum of resonances in the so-called Q region, 1200 to 1350 MeV/c^2, and the L region, 1600 to 1800 MeV/c^2. The experiment was designed to cover these mass regions with good resolution.

Data was taken at 6·5 and 10 GeV/c incident pion momentum at the CERN PS. By a system of veto scintillation and water Cerenkov counters, slow lambdas were selected ensuring that the associated missing system had the quantum numbers of neutral K* resonances. The film has been digitised using the Rutherford Laboratory HPD2. Measurement of the $\Lambda \rightarrow p\pi^-$ angles and the proton range, together with the beam momentum and direction are sufficient to determine the mass of the missing system. The angles were reconstructed directly from the HPD2 digitisings using rough digitisings from DMAC tables as guidance and the proton range for candidate events was added with the help of a graphics display.

An initial analysis of the data shows clear Q and L bumps in the missing mass spectrum. Structure is observed in these regions and at masses above 2 GeV/c^2. The chain of programs is now being prepared for production analysis.

EXPERIMENT 12

CERN
University College, London
University of Uppsala

Coherent production of I=½ states on helium.

(Proposal 95)

(ref. 372)

The object of this experiment, which is currently set up in a 19 GeV/c beam at the CERN PS, is to study the elastic and inelastic scattering of high energy protons on Helium nuclei. The principal inelastic channels of interest are:

$$p + {}^4He \rightarrow {}^4He\ (p\ \pi^+\pi^-)$$
$$\phantom{p + {}^4He \rightarrow} {}^4He\ (n\ \pi^+)$$
$$\phantom{p + {}^4He \rightarrow} {}^4He\ (p\ \pi^\circ)$$
$$\phantom{p + {}^4He \rightarrow} {}^4He\ (\Lambda\ K^+)$$
$$\phantom{p + {}^4He \rightarrow} \hookrightarrow p\ \pi^-$$

Measurements of the decay distributions of the short-lived I=½ states produced by diffraction dissociation of the incident proton will enable the spin and parity of such states to be investigated, free of possible I=3/2 contamination. The comparison of elastic and inelastic data is expected to provide information on the interaction of the produced states in nuclear matter.

The experiment was set up, inelastic trigger rates were established and a large quantity of elastic data was collected during a PS cycle in late April and early May. Preliminary results were presented to the Fifth International Conference on High Energy Physics and Nuclear Structure, Uppsala, Sweden, in June. Additional inelastic data were collected during a short PS cycle in October, and two further cycles, which will be sufficient to complete the data taking, have recently been allocated for 1974.

The most striking result of a recent analysis of a small sample of events of the type $p + {}^4He \rightarrow {}^4He\ (p\ \pi^+\pi^-)$ is the observation of resonance peaks, relatively free of background, at effective masses of 1·48 and 1·72 GeV/c in the $(p\ \pi^+\pi^-)$ system (Figure 16). Similar peaks have been observed in other reactions, for example, $p + p \rightarrow pp\ \pi^+\pi^-$ (G Kayes et al. Nucl. Phys. B5 (1968) 169 and S P Almeida et al. Phys. Rev. 174 (1968) 1638) and $p + C \rightarrow C\ p\ \pi^+\pi^-$ (J Rosen et al. Aix Conference 1973), but always in the presence of a large, non-resonant background. The smaller background observed in the current experiment provides one justification for the study of nucleon resonances by the coherent production technique and is expected to simplify the analysis of the decay distributions.

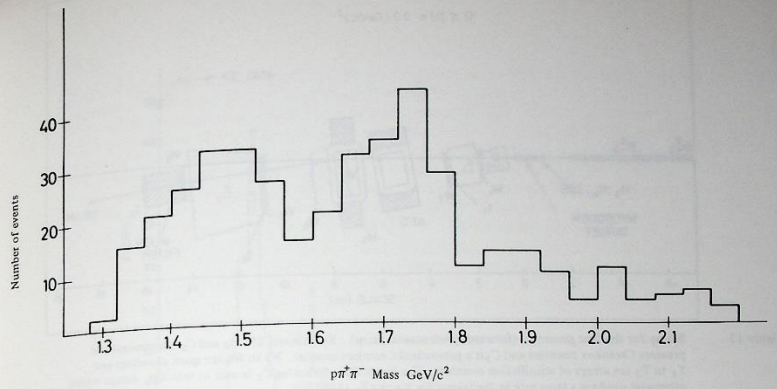

Figure 16 Effective mass of $p\ \pi^+\pi^-$ system in $p\ {}^4He \rightarrow {}^4He\ p\ \pi^+\pi^-$ at 19 GeV/c: Experiment 12. (15398)

EXPERIMENT 13

University of Birmingham
University of Genova
University of Stockholm
Rutherford Laboratory

Study of the reactions
$\pi^+p \rightarrow K^+\Sigma^+$ and $K^-p \rightarrow \pi^-\Sigma^+$

(Proposal 100)

Differential cross-sections and polarization for the two reactions $\pi^+p \rightarrow K^+\Sigma^+$ and $K^-p \rightarrow \pi^-\Sigma^+$, at the highest possible momentum (in practice 10 GeV/c) are being measured. Theoretically these reactions should be related in a simple way; in the most elementary model, the cross-sections should be equal. There is currently general confusion about the relative magnitudes of these cross-sections, with conflicting evidence from different experiments. For the first time this experiment measures both reactions with the same equipment, so an excellent comparison should be possible. A further aim of the experiment is to explore the hypercharge exchange cross-section to much wider angles than before. Such a measurement is of particular interest, in view of the possible dominance of parton interchange in the large angle region. So far the only exclusive channel studied to adequately wide angle is elastic scattering.

The experiment has had one period (3 weeks) of data taking at CERN, and in this time the small angle part of the running has been completed. The set-up is shown in Figure 17. In this geometry no attempt was made to detect the recoil Σ^+ or its decay products because their momentum is too low. Instead reliance was made on extremely efficient particle identification of the incident and outgoing mesons, and on a very accurate momentum measurement. The particle identification is achieved by the use of threshold Cerenkov counters, three in the incident beam, and another three (C_0, C_1 and C_2) in the forward spectrometer. Because it is always required for a meson to change its identity in the scattering process (from π to K or vice versa) and because of the small cross-section for such processes, there is a major problem in achieving adequate particle recognition. For example, below-threshold particles tend to be seen by production of δ electrons or by hadronic interactions in Cerenkov counters. By making these counters of the lowest possible mass, and by measuring the pulse heights of all signals and rejecting inadequate signals in the analysis, it is possible to keep the mis-identification problem to a low level. Finally, the spark chamber information can be used to eliminate hadronic interactions. For example, W6 is used mainly to eliminate interactions in C_2. Figure 18 shows a pulse height distribution in the pressurised Cerenkov counter C_1 where the pressure is set just below the K threshold, and the event trigger is set for the reaction $Kp \rightarrow \pi\Sigma$. The tail of small pulse height events is completely absent if one triggers on πp forward scattering, and so is due to the forward scattered kaons and (mainly) the beam kaons which pass through the counter. These background events are eliminated by a pulse height cut at the very beginning of the analysis.

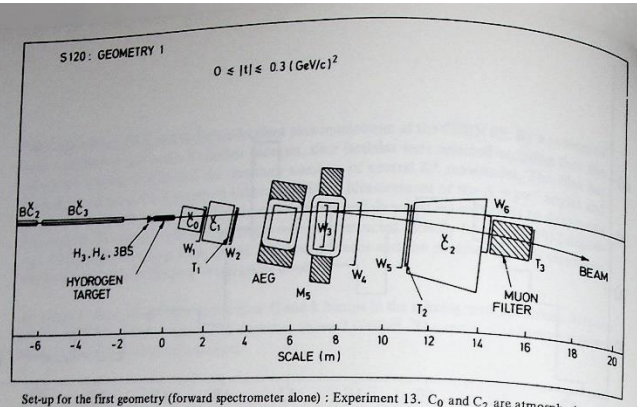

Figure 17 Set-up for the first geometry (forward spectrometer alone) : Experiment 13. C_0 and C_2 are atmospheric pressure Cerenkov counters and C_1 is a pressurised Cerenkov counter. W1 to W6 are spark chambers and T_1 to T_3 are arrays of scintillation counters. The muon filter following C_2 is used to veto $K\mu_2$ decays which otherwise produce a large rate in the trigger for $Kp \rightarrow \pi\Sigma$. (14972)

The forward spectrometer consists of two large aperture magnets (AEG from CERN and M5 from the Rutherford Laboratory) and a series of double gap spark chambers W1 to W6. These chambers are fitted with capacity readout which for the first time is being used on both low voltage and high voltage planes of the chambers. The choice of capacity readout is based on the very low spark energy needed for the readout (about one tenth of that needed with core readout or magnetostrictive readout). This enables extremely high multi-track efficiency to be achieved, since each spark barely loads the pulsing system. The spatial resolution on each plane is about 0.35mm, which will lead to a momentum resolution of 0.3% at 10 GeV/c. This is better than has ever before been achieved in studying these reactions. So far only a simple momentum fitting program, which does not use W3, has been used and already this has achieved 0.5% momentum resolution. Clean missing mass peaks are being seen corresponding to the Σ events with both incident π^+ and incident K^-, with very low background. Figure 19 shows a missing mass distribution for $\pi p \rightarrow K\Sigma$. The background due to the beam can be completely removed by an angular cut.

The data already obtained will allow the very interesting comparison of small angle cross-sections to be made. The next step will be to introduce a recoil detection system to observe the protons from Σ decay. This will enable further constraints to be placed on the wide angle events (where the cross-section is very low and the forward missing mass measurements alone would probably be inadequate). Furthermore, the $\Sigma^+ \rightarrow p\pi^\circ$ decay asymmetry will allow a measurement of the polarization in the reactions concerned. These measurements will be made during 1974.

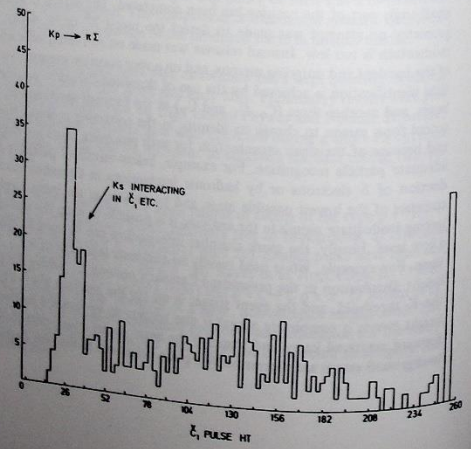

Figure 18
Pulse height distribution in C_1 for events from the trigger for $Kp \rightarrow \pi\Sigma$. The events in the low pulse region are mainly due to beam kaons which interact, decay, or produce δ rays in the gas of the Cerenkov counter: Experiment 13. (14971)

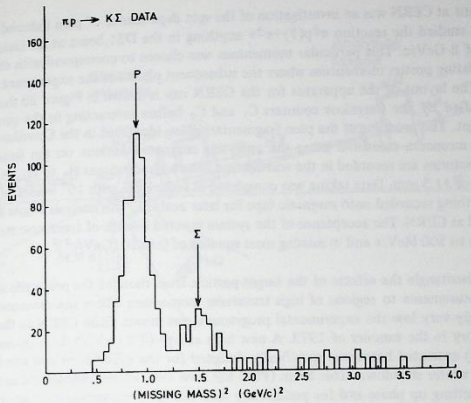

Figure 19

Preliminary missing mass distribution from an early data tape on the $\pi p \rightarrow K\Sigma$ trigger. Despite being essentially raw data analysed in a very simple way, there is a clear Σ peak with little background: Experiment 13 (14973).

EXPERIMENT 14

Imperial College, London
University of Southampton
ETH – Zurich
CEN – Saclay
University of Helsinki

Spin rotation parameters in
$\pi^- p \rightarrow K^\circ \Lambda$

(Proposals 107 and 124)

A group from Imperial College and Southampton is working at CERN in collaboration with the ETH–Zurich and Saclay. They have recently reported results on the differential cross-sections and polarizations in the charge exchange reactions $\bar{p} + p \rightarrow \bar{n} + n$ and $K^- + p \rightarrow K^\circ + n$; further results on the latter reaction and on $\pi^- p \rightarrow \Lambda K^\circ$ are now being analysed. They have reported on trials in the Omega magnet of a K^+ detector initially tested at Nimrod. The Imperial College and Southampton group is now collaborating with Zurich and Helsinki in the preparation of an experiment, to start in 1974, which will use a frozen spin polarized target for the measurement of the spin rotation parameters in $\pi^- p \rightarrow K^\circ \Lambda$. In this experiment optical spark chambers viewed by a lead oxide vidicon camera system will be used inside the CERN–ETH spectrometer magnet.

EXPERIMENT 15

CERN
University of Paris-Sud
University of Oxford

Spin dependence of inclusive reactions

(Proposal 112)

The spin dependence of hadron induced interactions is a sensitive probe of the interaction mechanism and may well reflect any substructure of the particles concerned. The investigations during 1973 have been particularly concerned with this substructure in that the reactions studied have been those in which fragmentation of the particles occurs and those in which the interaction occurs at a very small distance (large momentum transfer). The experiments have been carried out at both the CERN P S and the Rutherford Laboratory Nimrod accelerator.

The experiment at CERN was an investigation of the spin dependence of pion induced inclusive reactions and studied the reaction $\pi^{\pm}p(\uparrow)\rightarrow\pi^{\pm}+$ anything in the D31 beam at an incident pion momentum of 8 GeV/c. This particular momentum was chosen to correspond with that of the Nimrod circulating proton momentum where the subsequent phases of the experiment are being carried out. The layout of the apparatus for the CERN run is shown in Figure 20 the incident pion is identified by the Cerenkov counters C_1 and C_2 before interacting in the propanediol polarized target. The products of the pion fragmentation are identified in the Cerenkov counter C_3 and their momenta measured using the analysing magnet. Positions on the incident and scattered trajectories are recorded in the scintillation counter hodoscopes H_1 to H_3 with a spatial resolution of ±1.5 mm. Data taking was completed in June 1972 with 10^7 events of the type $\pi^{\pm}p\rightarrow\pi^{\pm}+$ anything recorded onto magnetic tape for later analysis. This analysis is now underway at Oxford and at CERN. The acceptance of the system covered a range of transverse momentum of 100 MeV/c to 500 MeV/c and in missing mass squared of 0 to 10 $(GeV/c^2)^2$.

In order to disentangle the effects of the target particle from those of the projectile and to extend the measurements to regions of high transverse momentum where the cross-sections are correspondingly very low the experimental programme was moved from CERN to the Rutherford Laboratory in the summer of 1973. A new high energy (7.9 GeV/c), high intensity (10^9 protons/pulse) extracted beam was specifically designed for the experiment and was built during the 1972 winter shutdown. This beam (P81) has now been commissioned and successfully used in the setting up phase and for preliminary data taking. The experimental layout of the experiment at the Rutherford Laboratory is shown in Figure 21. There are three major sections of the apparatus: (i) A forward arm with steering magnets M404 and M407 and an analysing magnet M402 to accept and measure the momentum of the fast forward particle from the inclusive reaction

$$p + p(\uparrow)\rightarrow\pi^{\pm} + \text{anything}$$
$$p + \text{anything}$$
$$K^{\pm} + \text{anything}$$

and the elastic reaction $p + p(\uparrow)\rightarrow p + p$. Positions along the particle trajectory are recorded in scintillation counter hodoscopes H_1 to H_6: (ii) A recoil arm with hodoscopes $H_7 H_8$ and H_9 which detects and records the spatial positions of the recoil proton in the elastic scattering region. (iii) A backward arm which detects and momentum analyses the fragmentation products of the polarized proton target. This arm uses multi-wire proportional chambers with a 1mm wire spacing to record position along the trajectory in order to obtain the required reconstruction accuracy.

Figure 20 Layout of Experiment 15 at CERN (D31 Beam line). (15357)

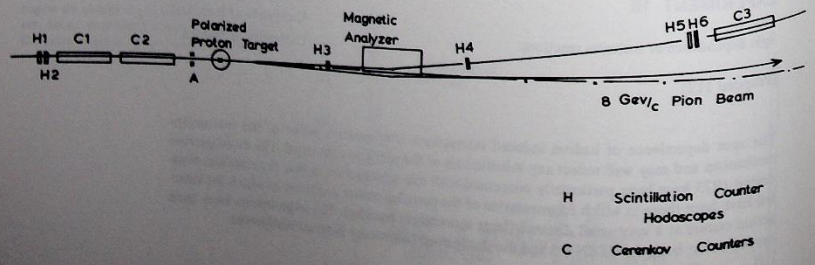

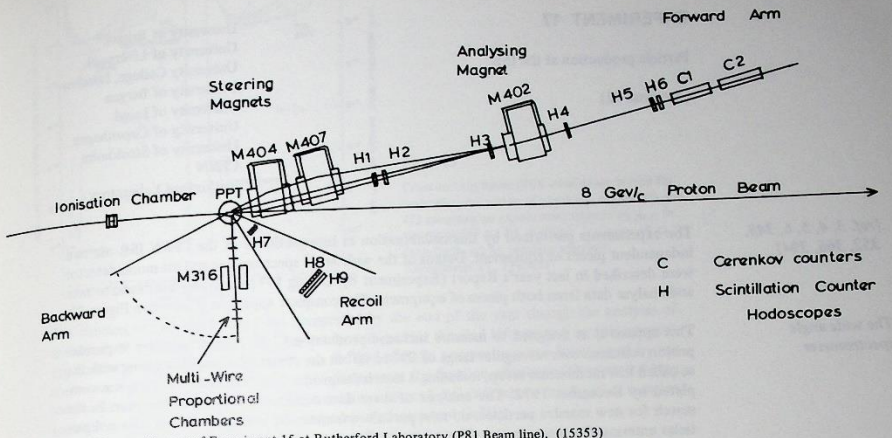

Figure 21 Layout of Experiment 15 at Rutherford Laboratory (P81 Beam line). (15353)

Sufficient data has already been taken in the elastic scattering phase to confirm, with better statistics, the trends shown in earlier CERN data out of a four momentum transfer (t) of 3.0 $(GeV/c)^2$. The full angular region extends to $|t| = 6.6$ $(GeV/c)^2$ and it is hoped to complete data taking in this new, unexplored region early in 1974.

EXPERIMENT 16

Queen Mary College, London
Daresbury Laboratory
University of Birmingham
University of Pisa
University of Mainz

The pion-nucleon scattering lengths

(Proposal 98)

The analysis of this experiment has been completed and a publication prepared. Details of the experiment have been given in previous Annual Reports. *(ref. 35)* The main result is:

$$a(\pi d) = -(0.049\ ^{+0.022}_{-0.016})\ m_{\pi}^{-1}$$

in satisfactory agreement with the theoretical prediction of $-0.043 \pm 0.005\ m_{\pi}^{-1}$. Despite the fact that the experimental errors are larger than those of the prediction, the result is a valuable systematic check on the many assumptions and extrapolations involved in the theory.

EXPERIMENT 17

Particle production at the ISR

(Proposal 72)

University of Bristol
University of Liverpool
University College, London
University of Bergen
University of Lund
University of Copenhagen
University of Stockholm
CERN
Rutherford Laboratory

(ref. 3, 4, 5, 6, 343, 352, 366, 394)

The experiments performed by this collaboration at Intersection 2 of the CERN ISR use two independent pieces of equipment. Details of the wide angle spectrometer and the muon detector were described in last year's Report (Experiment 8). During 1973 the group continued to take and analyse data from both pieces of equipment. The complete apparatus is shown in Figure 22.

The wide angle spectrometer

This apparatus is designed to measure inclusive production of all charged particles in proton-proton collisions over an angular range of 29° to 90° in the centre of mass. Data taking with the so-called low momentum setup, including a search for production of massive particles, was completed by December 1972. The analysis of these data continued throughout the year. In the search for new massive particles, no new particle was observed amongst 0.7×10^8 charged particles entering the spectrometer. The corresponding total cross-section limits for production of quarks of charge 2/3 e and 4/3 e compared to previous results are shown in Figure 23. A clear signal from production of antideuterons was seen in this experiment representing an increase of about 100 in the relative $\bar{d}$ to π^- ratio over the value found at lower energies at Serpukhov. The analysis of the low momentum pion data indicated that the invariant cross-section for fixed transverse momentum varied with rapidity over the central region, showing that theoretical predictions of a flat central plateau, are not yet at hand for the ISR-energies.

Throughout 1973 measurements were taken with the spectrometer in the high momentum mode. The data taken in this mode permit charged particle identification in the range of transverse momentum (p_T) from 1·5 GeV/c to 4·5 GeV/c. Results from this group and others at the ISR display a marked levelling off in the slope of the invariant production cross-section with increasing p_T. This 'excess' of high transverse momentum events fits in well with the parton model of the nucleon where point-like interactions of hadrons can occur.

Figure 22 Layout of Experiment 17 at CERN ISR (12614)

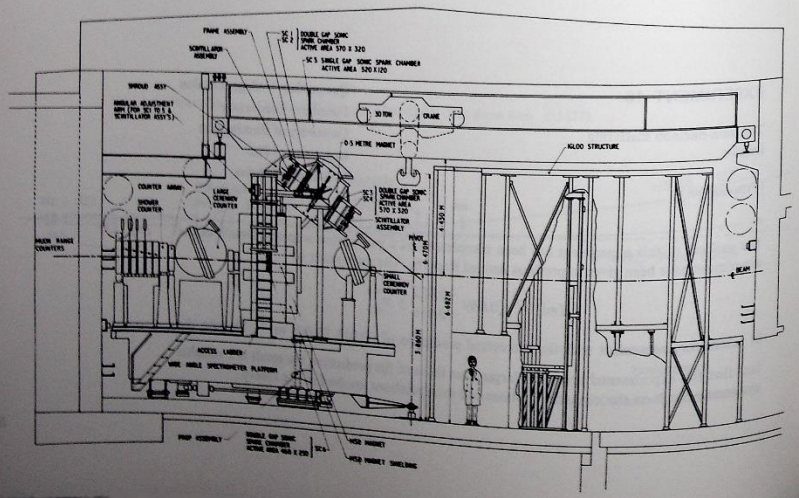

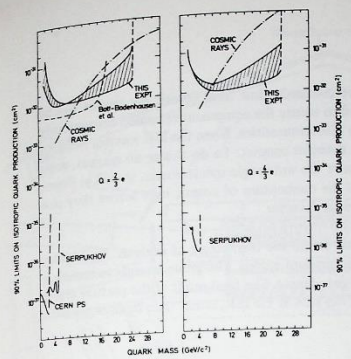

Figure 23

Cross-section limits (90% confidence levels) for isotropic production of quarks of charge 2/3 and 4/3 assuming an exponential slope in $p_{c.m.s.}$ in the range 1·2 to 2·1 $(GeV/c)^{-1}$ compared to their limits set by previous searches: Experiment 17. (15364)

The running of this experiment was completed by the end of the year though the analysis of the data will continue into 1974. The results will provide detailed information on this interesting class of events. Preliminary results on charged particle composition as a function of p_T are shown in Figure 24. The trend of a rapid decrease in the fraction of pions with interesting p_T seen in the low momentum data does not continue above 1.5 GeV/c where this fraction remains constant at approximately 65% of all charged particles up to 4 GeV/c.

Data were taken where the spectrometer was run in coincidence with the large solid angle magnetostrictive spark chambers of the muon detector. These data should provide information on correlation effects and associated multiplicities as a function of momentum.

The muon detector

This apparatus is used to study the momentum spectum of muons from the ISR for evidence of structure which would indicate the existence of new particles. If the weak interaction is not a 'point interaction', then a particle may exist whose function is to act as the 'messenger' between the interacting particles. Such a particle, being massive, can only be produced at high energy, and would decay into muons, having a characteristic high momentum. Other sources of muons at the ISR are the decays of mesons ($\pi^\pm$, $K^\pm$) and cosmic rays. A Monte Carlo simulation of the momentum spectra from meson decay, and the decay of a 20 GeV/c^2 Intermediate Boson (Drell-Yan Model) are shown in Figure 25. During 1973 the equipment was changed to reduce the number of triggers from meson decay as indicated in the Figure.

Figure 25 Monte-Carlo simulation of muon detector data: Experiment 17. (15354)

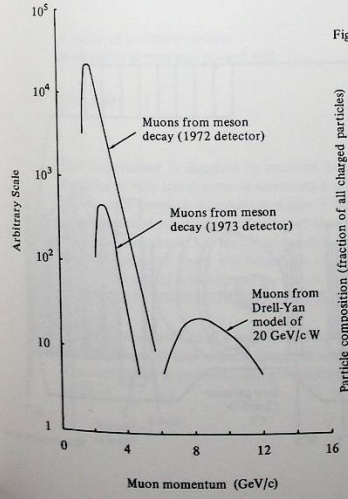

Figure 24 Particle composition as a function of transverse momentum p_T: Experiment 17. (15363)

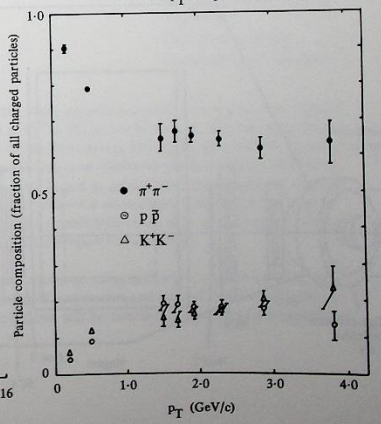

Preliminary analysis of the data indicates the contamination from cosmic ray muons will be negligible. However cosmic rays have been used to ensure the equipment remained continuously sensitive during periods of data taking at high ISR luminosities. When the ISR was not running, cosmic rays were used to calibrate the muon detector magnet. To do this an air magnet, sonic spark chamber spectrometer was mounted above the wide angle spectrometer, shown in Figure 22. This elevated spectrometer then measures the momentum of cosmic rays before they pass through the intersection region and into the muon detector.

To date 350,000 pictures have been taken, and are in the final stages of analysis. Preliminary data indicates the existence of very few high momentum muons. The group intends to complete this analysis before proposing an extension of data taking. The final result of the particle search will be limited by the integrated luminosity of the runs at the ISR, rather than by background.

EXPERIMENT 18

A study of high transverse momentum behaviour at the ISR

(Proposal 129)

CERN
University of Liverpool
Daresbury Laboratory
Rutherford Laboratory

This experiment is an extension of the investigation begun by the British-Scandinavian Group using the Wide Angle Spectrometer. (Experiment 17). In that experiment it was established that the single particle inclusive cross-section is not a simple exponential function of transverse momentum above 1 GeV/c. Several models have been advanced to explain this behaviour. The available experimental data is unable to provide sufficient information to distinguish between these models. Further, the general problem of high transverse momentum behaviour at the very high centre of mass energies available at the ISR is not well investigated nor understood, in particular for the heavier particles such as K^-, p.

This experiment will supplement the information so far obtained by investigating the multiplicity and rapidity distribution of secondaries associated with high transverse momentum events. The existing Wide Angle Spectrometer (with some small improvements) will be utilized to provide a high transverse momentum particle trigger. The spectrometer is shown in Figure 26. The

Figure 26 Plan view of apparatus on the wide angle spectrometer platform (side elevation shown in Figure 22): Experiment 18. (15358)

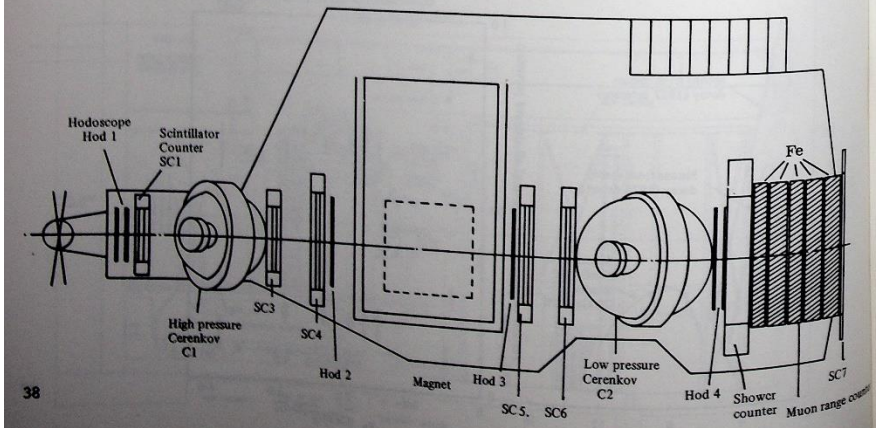

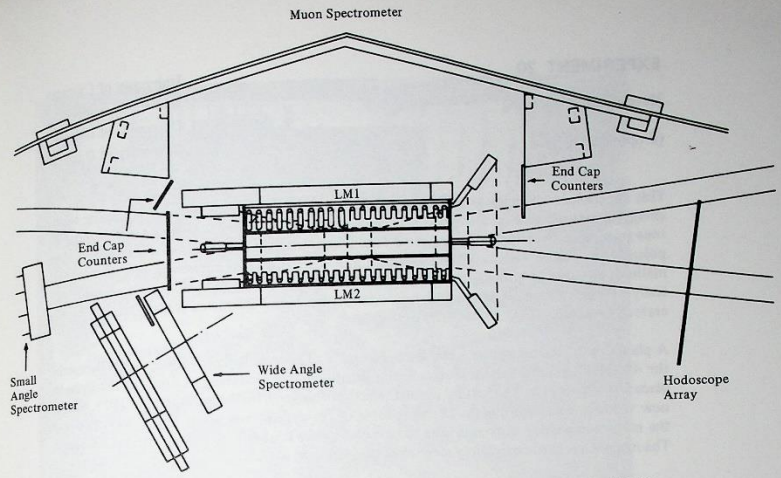

Figure 27 The charged particle detector to be used in Experiment 18. (15355)

associated charged particles will be detected by the apparatus shown in Figure 27. The principal detector is a barrel shaped assembly of scintillation counters surrounding the intersection region. The barrel is subdivided into longitudinal strips and lateral hoops to provide detailed information on the azimuthal and polar distribution of the secondaries. Large spark chambers on either side of the barrel detector will provide additional information on those secondaries roughly collinear with the high transverse momentum trigger. Scintillation counter hodoscopes covering the ends of the barrel complete the angular coverage giving an angular sensitivity of $\sim$ 99% of the total solid angle.

This apparatus is being prepared for installation during the winter shutdown of the ISR and should be ready to collect data at the start of the ISR programme in 1974.

EXPERIMENT 19

A study of inclusive particle production at very low p_T and x=0

(Proposal 131)

CERN
University College, London
University of Bristol
Massachusetts Institute of Technology
Niels Bohr Institute
University of Stockholm

This experiment is designed to measure the single particle inclusive cross-section for charged particles of very low transverse momentum at 90° in the centre of mass system. The experiment will be performed at intersection region 8 of the intersecting Storage Rings at CERN. Existing data on inclusive particle production at the ISR apply to transverse momenta above 150 MeV/c for pions, and above 300 MeV/c for protons. It is hoped to reduce these lower limits by a factor three in order to study the behaviour of the transverse momentum distributions as they approach the axis of symmetry at $p_T = 0$. A good normalisation of the data will be made, enabling predictions of violation of scaling in the pionization region to be checked.

The apparatus consists of a small magnetic spectrometer using multiwire proportional chambers. Particle identification is made from the results of momentum and time-of-flight measurements. The equipment is presently being constructed and will be installed in the ISR at the beginning of 1974.

EXPERIMENT 20

Muon-nucleon scattering

(Proposal 96)

University of Chicago
Harvard University
University of Illinois
University of Oxford

This experiment attempts to probe the internal structure of the nucleon by scattering high-energy muons off protons and neutrons. The electromagnetic interaction between charged leptons (muons or electrons) and nucleons is mediated by virtual photons whose mass, energy, and polarization can be varied. Because of this, muon-scattering from nucleons is one of the best methods available for probing the internal structure of the nucleon. A suitable high energy (typically 150 GeV) beam of muons with high intensity has been constructed at the National Accelerator Laboratory, USA.

A plan view of the apparatus is shown in Figure 28. The large spectrometer magnet (formerly the 450-MeV cyclotron at the Enrico Fermi Institute of the University of Chicago) has been in place for over a year. The setting up of the rest of the apparatus began in March 1973, and is now virtually complete. Figure 29 shows some of the apparatus in place. The hodoscopes and the magnet-measuring apparatus were constructed by the Rutherford Laboratory NPAG Group. The magnet has been completely mapped at two different currents.

Figure 28

Layout of muon scattering apparatus. The beam enters from the left: Experiment 20. (NAL photograph). (15356)

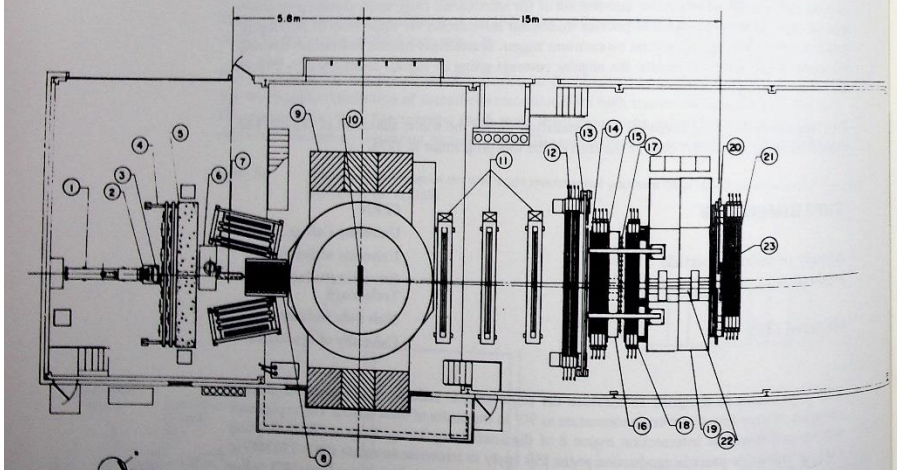

1 Cerenkov Counter
2 8" x 8" Proportional Chamber
3 Hodoscope
4 Halo Veto Counter
5 Backward Scattering Shield
6 Liquid H Target (1m Long)
7 Spark Chambers 8 Time of Flight System
8 8 - 1m x 1m Proportional Chambers
9 Cyclotron Magnet (4.3m dia. Poletip)
10 1m x 1m Proportional Chamber
11 3-2m x 4m Spark Chamber
4 Shift Readout Planes/Chamber
12 2m x 6m Spark Chambers (8 Mangnetostrictive Delay Readout Planes)
13 2m x 6m G Hodoscope
14 2m x 6m x 2" Steel Plate
15 2m x 4m Spark Chambers (8 Magnetostrictive Delay Line Readout Planes)
16 2m x 4m x 40.6 cm Pb Absorber
17 2m x 4m H Hodoscope
18 2m x 4m Spark Chambers (6 Magnetostrictive Delay Line Readout Planes)
19 Steel Hadron Shield
20 2m x 4m M Hodoscope
21 2m x 4m Spark Chambers (8 Magnetostrictive Delay Line Readout Planes)
22 Removable Shutters
23 N Hodoscope

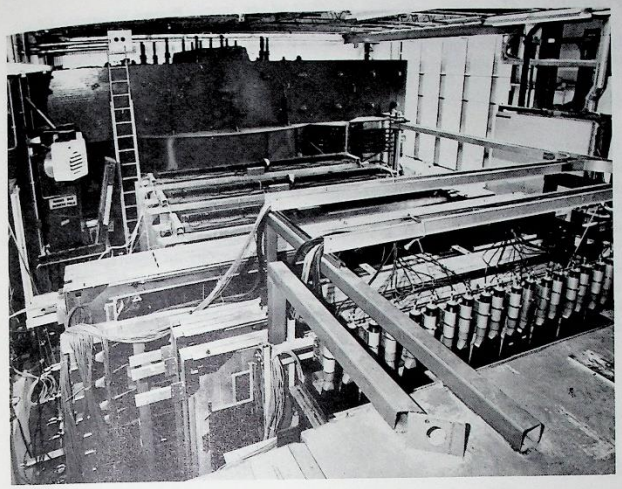

Figure 29

View upstream from the top of the steel hadron shield (see Figure 28): Experiment 20 (NAL photograph). (15361)

Some parasitic beam has been available for the experiment during the past few months. The first beam under realistic operating conditions was provided in October 1973. For that run a Be target was used as the liquid hydrogen/deuterium target was not yet operational. An on-line display of one of the events observed is shown in Figure 30. During 1974 a substantial amount of running with hydrogen and deuterium targets should take place, to yield information on the total photo-absorption cross sections, the structure functions in deep-inelastic scattering, and allow detailed studies of the hadrons produced to be made.

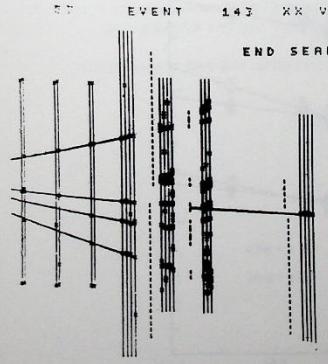

Figure 30

An event displayed in the downstream spark chambers (the ones labelled 11, 12, 15, 18 and 21 in Figure 28). The scattered muon is the particle passing through into the final spark chambers. Three charged hadrons and a photon shower are also visible: Experiment 20. (15370)

EXPERIMENT 21

Rutgers University, USA
Imperial College, London

Study of inclusive reactions pp → pX, nX between 30 GeV/c and 400 GeV/c

(Proposal 118)

The first and simplest inclusive reaction to be studied over the new energy range at the National Accelerator Laboratory was pp → pX. By pulsing an internal H_2 gas jet target at different instants during the acceleration ramp it was possible to measure the energy dependence of this reaction over the entire range of the new machine. The recoil proton was identified and its momentum measured by pulse height in a total absorption scintillation counter and by time of flight over 2m. Energy loss in intermediate counters provided additional constraints. The normalisation of the invariant cross-section was obtained by monitoring the rate of slow elastically scattered protons in small solid state detectors situated inside the main ring vacuum near 90° to the beam axis. The experiment was completed in May 1973 and the final results have been published (Figure 31).

Figure 31

Invariant cross-section $\frac{sd^2\sigma}{dtdM^2}$ for reaction pp → pX. s, t and M^2 are respectively, the squares of the center of mass energy, the four momentum transfer between the target and recoil protons and the missing mass. Data at fixed $x = 1\text{-}m^2/s$ and t are plotted against $s^{-1/2}$. The straight lines indicate the s dependence of the form $A + B/\sqrt{s}$ with B increasing with x: Experiment 31. (15367)

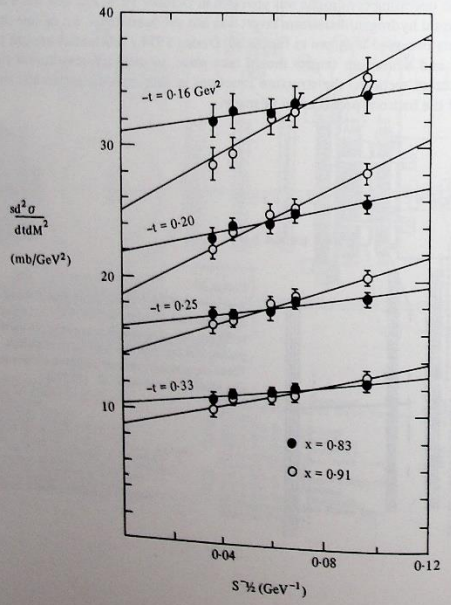

The second aim of the experiment was to study the inclusive reaction pp → nX for which the exchange of charge at the fragmentation vertex suppresses leading particle effects. High neutron backgrounds inside the main ring tunnel at NAL prevented direct measurements of this reaction. However, the same physical information can be obtained from a study of pn → pX for which a Deuterium gas jet target was used. Data on the two reactions, pp → pX and pd → pX, were collected under identical conditions and we are currently analysing these in order to extract the cross-section for pn → pX.

EXPERIMENT 22

University of Liverpool
Orsay
Scandinavian Universities

Study of large transverse momentum behaviour

(Proposal 130)

The experiment plans to study particle correlations associated with high transverse momenta events at the ISR using the split field magnet.

Recent data obtained at the ISR on single particle production at large angles have in particular drawn attention to the high p_T range. The explanation for the surprisingly large production in this region may be sought, according to the parton model, in the existence of point-like structures inside the hadrons, or it may possibly be accounted for by the same multiperipheral model which describes the production of low momenta particles. A choice between models requires studies of the correlations between particles when one, or several of them, is produced with high p_T.

A magnetic spectrometer, presently being designed, will be used to trigger the split field magnet detectors in order to select the very rare high p_T secondaries.

The collaboration hopes to start data taking early in 1975.

Bubble Chamber Experiments

Conventional bubble chamber experiments continue to be one of the main sources of information on the properties of the elementary particles and over the last year the Laboratory, working in collaboration with the universities and with other laboratories, has made a significant contribution to this effort. There has also been progress in the development and utilization of new techniques to overcome the two main limitations of conventional bubble chambers: neutral particle detection and limited statistics. The 1·5m bubble chamber at the Laboratory has further demonstrated the reliability of operations with a track sensitive target (TST). The usefulness of the TST is not in doubt and plans exist in other laboratories for the construction of targets based on the CERN-Rutherford Laboratory design. Work has also started at the Laboratory on the construction of a rapid cycling bubble chamber (or vertex detector).

Track Sensitive Target (ref. 45, 139, 173, 174, 175, 222, 323, 324, 375, 378, 380)

The TST considerably extends the domain of particle physics available for study. It consists of a perspex walled target filled with liquid hydrogen and situated inside the bubble chamber where it is surrounded by a neon-hydrogen mixture. Both regions are sensitive to charged tracks. Beam particles introduced into the target interact with free protons while their reaction products in general pass into the neon-hydrogen mixture, which is an efficient detector of γ-rays. Many particle reactions result in the production of several neutral particles (e.g. π°, η°, Σ°) and these particles commonly decay into γ-rays which remain undetected in a conventional chamber.

The 1·5m bubble chamber, with a TST installed, operated reliably throughout 1973 taking 1,100,000 pictures in a slow K^-beam (Experiment 34). TST's have now been constructed and are under test at the Argonne National Laboratory (ANL) and Brookhaven National Laboratory in the USA and are under consideration at CERN and at the National Accelerator Laboratory (NAL) in the USA. The processing of the data from the first two experiments in the TST (Experiments 30, 33) is well under way and is reported below. A programme for the geometrical reconstruction of tracks in the hybrid system has been developed. The Laboratory group has plans to collaborate in a further TST experiment, in the 12 foot chamber at ANL (Experiment 36). In order to exploit the technique fully, it remains to be shown that events can be measured on automatic systems so that measurement rate can match the data acquisition rate. First tests using the HPD at the Laboratory look promising.

Hybrid Systems (ref. 215, 342, 379)

In the future it seems likely that more and more bubble chamber experiments will make use of information from external electronic detectors, which will be used either to trigger the bubble chamber flash or to supplement its measurements. Such hybrid systems are being developed because the conventional hydrogen bubble chamber is non-selective so that in the study of rare interactions the data rate may be low. Current experiments are typically at the 20 events/μb level and all expansions have to be photographed irrespective of whether they contain an event of interest in a particular experiment. To solve this problem a small rapid cycling bubble chamber is being developed. At the proposed expansion rate of 60 hertz, experiments of up to 500 events/μb become possible and moreover, because of the thin walls and geometry of the chamber, selected reactions can be studied by controlling the photography from external detectors.

The rapid cycling chamber has several very attractive features as a detector for the local region around an interaction (the vertex region). The track efficiency is 100% in all directions and, because of the small bubble size and the fact that the chamber is both the target and the detector, the resolution near the vertex is excellent (approximately 1mm). This is particularly important for final states involving hyperon or K°_S production where decay lengths may be a few centimetres or less. The detection and measurement of spectator protons from deuterium also allows the study of interactions on quasi-free neutrons and the measurement of the range of short recoil protons in hydrogen allows the study of very low momentum transfer, $-t \simeq 0{\cdot}005$ $(GeV/c)^2$, processes. Because of the essential features of the design, secondaries can be extracted over a large solid angle and in addition to providing trigger information, measurements, particularly on momenta in the forward direction, can be augmented by external detectors i.e. spectrometer systems.

A group at the University of Oxford has been developing an external particle identifier which could be placed behind the large bubble chamber BEBC when it commences its operations at the CERN 400 GeV Synchrotron (SPS). This device, ISIS, will be used to measure the ionisation of energetic secondary tracks leaving BEBC, so enabling the particle masses to be determined. A model has been built and it was recently tested in a beam at the Rutherford Laboratory; it shows great promise.

High Statistics Experiments

For three experiments the year has been notable for the large amount of data which has been measured. All three were made in the 2m bubble chamber at CERN and each involves the Laboratory in a collaboration with other groups in the UK and in France. These experiments are: low energy K^-p interactions (Experiment 31) with over 800,000 pictures, a π^+d exposure at 4 GeV/c of 700,000 pictures (Experiment 23) and a 1,400,000 picture exposure to 14 GeV/c K^- interactions on protons (Experiment 32). A large amount of data from these and several other experiments are currently being analysed as a consequence of the powerful film analysis system which has been developed at the Laboratory over recent years. Although this system will continue to be improved, it seems probable that the next step forward in high statistics experiments will come from techniques such as the rapid cycling detector outlined above.

Special Beams

The Laboratory has been active in several experiments utilising rather unusual beams. Analysis is proceeding on an exposure at CERN (Experiment 29) which used a monochromatic K° beam. An extension of this experiment, with an improved beam, has been accepted.

There is a proposal from the University of Cambridge to carry out experiments in the 15 foot hydrogen bubble chamber at NAL (USA) with beams of high energy Σ^- hyperons and π^+, $K^\pm$ mesons. The experiments would use pulsed high-field dipole and quadrupole magnets constructed at the Rutherford Laboratory. The meson beams do not employ standard separation techniques but rely on reaction kinematics. The same group is currently analysing experiments in the CERN 2m chamber exposed to a high energy Λ beam (Experiment 26) and a medium energy neutron beam (Experiment 28).

Table 2 — High Energy Physics : Bubble Chamber Experiments

Experiment Number	Proposal Number	Beam and Chamber	Groups
23	36	π^+ ; 4 GeV/c ; CERN 2m (D_2)	University of Birmingham University of Durham Rutherford Laboratory
24	38	K^- ; 2·1 GeV/c ; RL, Heavy liq.	Free University of Brussels CERN Tufts University, USA University College, London Rutherford Laboratory
25	39, 86	π^+ ; 0·8 - 1·6 GeV/c ; RL 1·5m (H_2), Saclay 80 cm (H_2)	University of Cambridge Imperial College, London Westfield College, London
26	49, 82	Λ ; 0 - 2·33 GeV/c ; CERN 2m (H_2)	University of Cambridge
27	56	K^+ ; 2·3 GeV/c : RL 1·5m (D_2)	Imperial College, London Westfield College, London
28	85	n; 1·3·5 GeV/c ; CERN 2m (H_2)	University of Cambridge
29	89	K^0_L ; 0·4 - 0·8 GeV/c ; CERN 2m (H_2)	University of Bologna University of Edinburgh University of Glasgow University of Pisa Rutherford Laboratory
30	91	π^+ ; 4 GeV/c; RL/TST (H_2,Ne)	CERN Lawrence Berkeley Laboratory University of Turin Rutherford Laboratory
31	108	K^- ; 0·92 - 1·40 GeV/c ; CERN 2m (H_2)	Imperial College, London Rutherford Laboratory
32	109	K^- ; 14·3 GeV/c : CERN 2m (H_2)	Ecole Polytechnique, Paris CEN, Saclay Rutherford Laboratory
33	115	$\bar{p}$; 2 GeV/c . RL/TST (H_2,Ne)	Tata Institute, Bombay
34	117	K^- ; 0 - 0·58 GeV/c ; RL/TST (H_2,Ne)	University College, London Free University of Brussels University of Durham University of Birmingham
35	119	K^- ; 2·9 GeV/c ; RL/RCBC (H_2)	University of Oxford Rutherford Laboratory
36	121	π^+ ; 6 GeV/c ; ANL/TST (H_2,Ne)	Argonne National Laboratory, USA Rutherford Laboratory
37	134	π^- ; 22 GeV/c ; BEBC (H_2)	University of Oxford University of Pisa Rutherford Laboratory
Experiments proposed			
	122	Σ^-; 50, 100 GeV/c ; NAL 15ft (H_2)	University of Cambridge
	127	π^+,$K^\pm$; 50 -200 GeV/c ; NAL 15ft (H_2)	University of Cambridge
Letter of Intent to SPSC		K^- ; 45, 65 GeV/c ; BEBC (H_2)	University of Glasgow University of Oxford CEN, Saclay Rutherford Laboratory

EXPERIMENT 23

π^+d interactions at 4 GeV/c

(Proposal 36)

University of Birmingham
University of Durham
Rutherford Laboratory

(ref. 42, 395 349, 350, 351)

The study of boson resonance production, which is the main aim of this experiment, has commenced with an analysis of the reaction $\pi^+d \rightarrow pp\pi^+\pi^-$. More than 17,000 events have been obtained in this final state, and in the prism plot shown in Figure 32, strong bands corresponding to ρ° and f° production can be seen in the upper half of the plot. With such a large number of events available it has been possible to study in detail the production mechanism of these resonances, and also of their "daughter states" — resonances with lower spin, but the same mass as the parent states. This work has entailed developing new techniques for the analysis of the $\pi^+\pi^-$ spin density matrix.

In the lower half of Figure 32 can be seen another accumulation of events: these correspond to the relatively rare process whereby resonances such as ρ° and f° are produced by baryon exchange. These processes (together with the production of ω° in the backward direction) have been the subject of another study.

The f° meson has also been observed in different decay modes, $f^\circ \rightarrow 4\pi$ and $f^\circ \rightarrow K\bar{K}$, and new values for the branching ratios into these final states have been obtained.

An analysis of the reaction $\pi^+d \rightarrow pp\pi^+\pi^-\pi^\circ$ has started with a study of ω° production. Here again, the high statistics available have allowed a detailed study of the production mechanism.

The data reduction of the original 420,000 pictures taken in this experiment is now almost finished, and the first measurement of a further 315,000 pictures taken in December 1972 is also 80% complete.

Figure 32. Prism plot for the reaction $\pi^+n \rightarrow \pi^+\pi^-p$ at 4 GeV/c; ω is the Van Hove angle: Experiment 23 (14868)

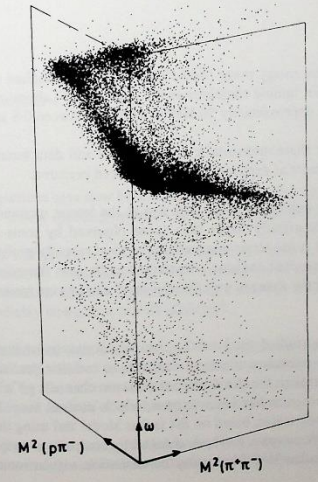

EXPERIMENT 24

K^- interactions in a heavy liquid bubble chamber

(Proposal 38)

Free University of Brussels
CERN
Tufts University, USA
University College, London
Rutherford Laboratory

(ref. 402) The experiment consists of a 640,000 picture exposure of the Rutherford Laboratory 1·4m heavy liquid bubble chamber to a 2·1 GeV/c K^- beam from Nimrod. The chamber was filled with a propane-freon mixture of radiation length 30cm.

Scanning of this film was originally completed in 1970 and enabled the properties of the Ξ hyperons to be studied. In addition about 350 events were recorded with a final state containing a K^+ or K° together with two Λ-hyperons. These events were attributed to the re-interaction of Ξ hyperons within the complex nucleus in which they had been produced. The invariant mass spectrum of the Λ pairs yielded an unexplained peak at 2367 ± 4 MeV/c^2, possibly the first example of a Λ-Λ resonance.

The film is now being re-scanned to find the remaining events which have two Λ's but without requiring that a K^+ or K° be recognised. This should yield a factor of 2-3 in statistics and clarify the nature of the peak. The rescan is nearing completion and the new analysis will be finished early in 1974. One of the advantages of the bubble chamber technique is that, since all events are recorded, a surprising result which was not foreseen at the time of the exposure can be investigated in this manner.

EXPERIMENT 25

π^+p interactions in the range 0·8 - 1·5 GeV/c

(Proposals 39, 86)

University of Cambridge
Imperial College, London
Westfield College, London

(ref. 368) The π^+p interaction in the energy range 1560-1930 MeV is being studied using film taken in the 80cm and 1·5m hydrogen bubble chambers at the Rutherford Laboratory. Data has been obtained at 14 momenta in approximately 50 MeV/c intervals between 0·8 and 1·5 GeV/c.

0·90, 0·95, 1·0, 1·05, 1·1, 1·2, 1·3, 1·4 GeV/c Processing of the film at these momenta is now complete and data summary tapes containing approximately 12,000 events at each momentum have been prepared.

In the elastic channel it was noted some time ago at the lowest momenta that our backward cross-sections were systematically lower than those observed by some counter groups. This effect persists, although it is not so pronounced, in the most recently analysed data at the higher momenta. An elastic phase shift analysis, constrained to lie near the solution of Ahmehed and Lovelace, has shown that the data are well fitted if small changes are made to these partial wave amplitudes.

In the energy range being studied the I = 3/2 s-channel resonances are highly inelastic so that a full understanding of the resonance structure demands an inelastic partial wave analysis. Such an analysis is being undertaken for the dominant inelastic channels $p\pi^+\pi^\circ$ and $n\pi^+\pi^+$. A maximum likelihood fitting program has been written, which uses all four independent variables which describe these 3-body states, based on the Isobar Model and using the formalism of Deler and Villadas. This complex program has been checked by comparison with an independent program again based on the Isobar Model but using the relativistic angular momentum formalism of Namyslowski, Razmi and Roberts as simplified by Capps, Maddin and Williams. Our analysis differs from those of Berkeley-SLAC and Saclay in that we fit both the $p\pi^+\pi^\circ$ and the $n\pi^+\pi^+$ channels. The analysis is energy independent and we are at present engaged in a comprehensive search for solutions from a large number of random starts at our lowest energy.

The question of the energy dependence and continuity of the solutions from this analysis is being tackled in two ways. A K-matrix fitting program is being written to fit the energy independent results using an energy dependent K-matrix formalism to incorporate the constraints of unitarity and the results of the, by now well established, elastic partial wave analysis. Secondly a simplified energy dependent PWA of the dominant $\Delta^{++}\pi^\circ$ final state is being undertaken. Only backward decaying Δ^{++} events are taken, eliminating the problems of overlapping Δ^+ and ρ^+ bands. Combined production and decay momenta of the Δ^{++} are fitted with simple background or Breit-Wigner parametrizations. The aim is to get an idea of what the gross features of the data indicate. The preliminary results appear to suggest the importance of the 0·8 and 0·85 GeV/c data which is not yet fully analysed, since there are at least two important I = 3/2 resonances in this region in the SD1 and DS3 waves.

At 1·4 and 1·5 GeV/c peripheral events in the single π production channels have been used to estimate the $\pi^+\pi^+$ and $\pi^+\pi^\circ$ scattering cross-sections by a Chew-Low extrapolation. From the $\pi^+\pi^+$ data values have been obtained for the I = 2 s- and d-wave phase shifts up to a centre-of-mass energy of 800 MeV.

0·80, 0·85, 1·15, 1·25, 1·45, 1·5 GeV/c All film has been measured and a quarter of the events have reached the data summary tapes. The remainder is being processed through the THRESH–GRIND–AUTOGRIND chain. Considerable difficulty has been experienced in determining optical constants for a large part of this film. The lowest two momenta will be particularly important for reasons outlined above and in addition because the Berkeley-SLAC collaboration does not have data in this region. They have found that the problems associated with the continuity of their solutions across this gap have increased the difficulties in determining the relative signs of resonant amplitudes. With data continuous throughout our energy range we hope to make unambiguous determinations of these signs which are of crucial importance for testing higher symmetry schemes such as l-broken SU(6)w, Melosh transformations and the Quark Model.

EXPERIMENT 26

Hyperon-Proton interactions

(Proposals 49, 82)

University of Cambridge

70% of the 290,000 pictures have now been scanned for Λ° decays, and the work of identifying the source of each Λ° is now speeding up with improved techniques, and more resources.

This association scan will produce about 20,000 $np \rightarrow \Lambda^\circ X$ events, up to 15,000 $np \rightarrow K^\circ X$ events, and several hundred identifiable $\Lambda p \rightarrow \Lambda X$ events, which should include all the visible elastic scatters. Measurement of some Λp elastic scatters at about 20 GeV/c, indicates that they may be identifiable reliably down to $-t \simeq 0{\cdot}01$ (GeV/c)^2.

In addition to the Λ-induced events and the $np \rightarrow \Lambda$-inclusive events data for several neutron-induced exclusive channels will be obtained at a level of about 25 events/μb. In order to obtain absolute cross-sections for the neutron-induced channels the neutron flux incident in the chamber is being obtained by an analysis of double np elastic scatters.

The channel $np \rightarrow pp\pi^-$ is also being studied and a preliminary report based on 2024 fitted events was submitted to the Aix-en-Provence Conference in September.

EXPERIMENT 27

Imperial College, London
Westfield College, London

K^+d interactions in the
2-3 GeV/c region

(Proposal 56)

(ref. 344) During 1973 about 150,000 events from this experiment have been measured on the Imperial College HPD. This almost completes measurements on the film which comes from an exposure of 750,000 pictures in the 1·5m bubble chamber at Nimrod. Some topics of interest have been pursued with a partial sample of data.

A preliminary partial wave analysis of $K^+\pi^-$ scattering has been completed. The channel $K^+n \to K^+\pi^-p$ has been shown to be dominated by π exchange at low values of the momentum transfer between the nucleons. It also has the advantage that t_{min} is lower than in π exchange reactions with a final state Δ. The procedure for extrapolation to the pion pole has been studied, and the partial wave results are almost independent of the remaining uncertainties in the extrapolation procedure.

The P½ wave is adequately parameterised at low masses by a Breit-Wigner K*(890) and the D½ wave also calls for a K*(1420). The S½ wave phase shifts are quite well determined at all masses, but the inherent phase ambiguities cannot yet exclude the possibility of some narrow structures.

Single and double pion production with a deuteron in the final state has also been studied. Single pion production is dominated by K^{*+}, which is adequately explained by ω° exchange. Double pion production is >75% $K^{*\circ}\pi^+d$ and can be fitted to a π-pomeron double Regge exchange mechanism, which explains most of the observed features (including a low mass $d\pi^+$ enhancement, in spite of the low beam momentum.

EXPERIMENT 28

University of Cambridge

Neutron-proton interactions
below 3·5 GeV/c

(Proposal 85)

The analysis of single and double pion production processes, arising from neutron-proton collisions below 3·5 GeV/c, is now complete. 54,000 three-prong events have been measured and reconstructed and of these 44,000 events have been assigned to the final states $pp\pi^-$, $pp\pi^-\pi^\circ$, $np\pi^+\pi^-$ and $d\pi^+\pi^-$.

Figure 33. Mass spectrum of the combination $(p_f\pi^-)$ in the reaction $np \to pp\pi^-$ (p_f is the forward scattered proton): Experiment 28 (15403)

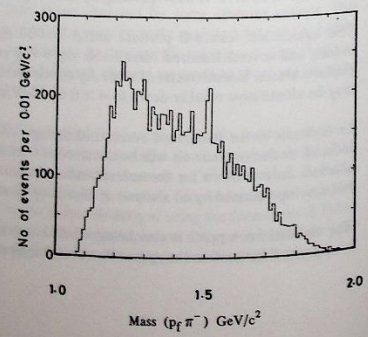

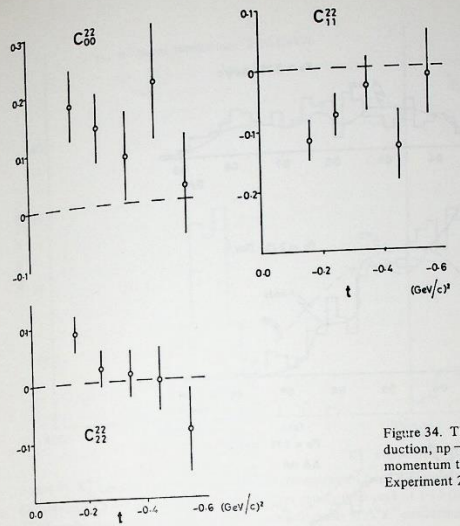

Figure 34. The correlation terms in double Δ production, $np \to \Delta^-\Delta^{++}$ plotted as a function of four momentum transfer squared (see below): Experiment 28 (15410)

The $pp\pi^-$ final state has been compared in detail with a modified one pion exchange model, which included the main interference term, and satisfactory agreement has been found. Unlike previous results at a similar beam momentum [1], the π^- centre of mass scattering angle shows a backward peak (corresponding to a π^- slow in the laboratory frame of reference), in good agreement with the model. No anomalous production of the N*(1470) is seen, though there is a narrow excess of events above the predictions of the model near an invariant mass of 1520 MeV at the neutron vertex (Figure 33). The production of N*'s, seen in the $pp\pi^-$ final state at masses of 1500 and 1700 MeV, is also seen, via the $N\pi\pi$ decay modes, in the $pp\pi^-\pi^\circ$ final state.

The use of the charge symmetry of the reaction $np \to np\pi^+\pi^-$ has demonstrated that a carefully prepared sample of 8,000 events in this channel is not significantly contaminated. The ratio of the numbers of events in the $pp\pi^-$ and $np\pi^+\pi^-$ final states, together with an estimate of the $pp\pi^-$ cross-section, obtained by interpolating in the cross-section data of other experiments, enable the $np \to np\pi^+\pi^-$ cross-section to be evaluated as 5·1 ± 0·2 mb at 3 GeV/c. The $np\pi^+\pi^-$ final state has been analysed as a sum of incoherently produced $\Delta(1236)$ resonances and the cross-section for the reaction $np \to \Delta^-\Delta^{++}$ (where the momentum transfer from the neutron to the Δ^- is small) is found to be 2·3 ± 0·4 mb. The reaction $np \to \Delta^{++}\Delta^-$ (which would require Q = 2 exchange) only contributes 1·3 ± 1·0% of the events in sharp contrast to the less sophisticated analysis at 3·7 GeV/c which indicates that approximately 1/3 of the $\Delta^{++}\Delta^-$ final state may be produced by Q = 2 exchange.

Statistical tensors for double-Δ production have been evaluated in the Jackson frame and show significant deviations from the predictions of a simple one pion exchange model; in particular the correlation terms:

$$C^{J_1\,J_2}_{M_1M_2} = T^{J_1\,J_2}_{M_1M_2} - T^{J_1}_{M_1}\,T^{J_2}_{M_2}$$

which are shown in Figure 34 as a function of t are non-zero and do not appear to tend to zero at t = 0 as would be required by the dominance of the pion pole. The absorption model of Svenson [2] predicts $C^{22}_{00} = 0{\cdot}05$ for all t, for the reaction $\bar{p}p \to \bar{\Delta}^{--}\Delta^{++}$ at 3·6 GeV/c and it would be expected that the absorption effects would be smaller in np interactions. The components of the statistical tensors have been fitted by the expressions given by Kotanski [3] derived from the Quark model [4]. The quality of the fits support the class A predictions but the class C predictions do not appear to hold in the Jackson frame.

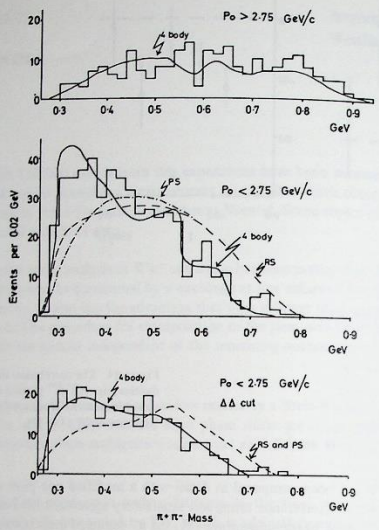

Figure 35. The $\pi^+\pi^-$ mass spectra in $np \rightarrow d\pi^+\pi^-$. The low mass enhancement known as the "ABC effect" is shown to be the result of deuteron formation: Experiment 28 (15404)

A low mass enhancement in the $\pi^+\pi^-$ mass distribution has been observed in the $d\pi^+\pi^-$ final state. This ABC effect [5] has been seen in several final states in which complex nuclei are formed from simpler constituents. A calculation of the neutron-proton interaction has been made and used to modify events in the $np\pi^+\pi^-$ channel to predict the $d\pi^+\pi^-$ distributions. This procedure successfully explains the ABC effect as a result of such deuteron formation. Figure 35 shows the $\pi^+\pi^-$ mass spectra compared with the predictions of the modified $np\pi^+\pi^-$ state ('4-body'), the model of Risser and Shuster [6] ('RS') and the phase space predictions ('PS').

REFERENCES

[1] G Alexander et al., Nucl. Phys. B52 (1973) 221.
[2] B E Y Svenson, Nuovo Cimento 29 (1965) 667.
[3] A Kotanski and K Zalewski, Nucl. Phys. B13 (1969) 119.
[4] A Bialas and K Zalewski, Nucl. Phys. B6 (1967) 465.
[5] A Abashian et al., Phys. Rev. 132 (1963) 2296, 2305, 2309, 2314.
[6] T Risser and M D Shuster, Phys. Letts. 43B (1973) 68.

EXPERIMENT 29

Parameters of the τ and semi-leptonic decays of K^0_L ; $K^0_L p$ interactions in the range 450-800 MeV/c

(Proposal 89)

University of Bologna
University of Edinburgh
University of Glasgow
University of Pisa
Rutherford Laboratory

An exposure of 520,000 pictures to a K^0_L beam in the 2m chamber at CERN was taken in October and November 1972. About 90% of the film has been scanned and measured. The Rutherford Laboratory, Bologna and Pisa groups have been using HPD machines successfully while Glasgow and Edinburgh have been using the Glasgow SMP and Polly systems.

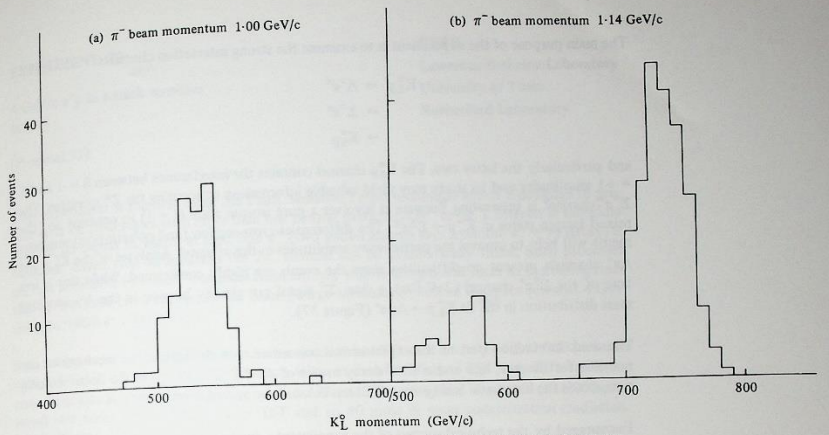

Figure 36. K^0_L beam momentum distributions reconstructed from measured events in the chamber fitting the hypotheses $K^0_L p \rightarrow K^0_S p$ and $K^0_L p \rightarrow \Lambda\pi^+$. The low momentum peak at 1·14 GeV/c corresponds to associated $\Sigma^\circ K^\circ$ production in the hydrogen target, the other peaks to $\Lambda^\circ K^\circ$ production: Experiment 29 (15408)

The K^0_L beam was formed by means of forward associated production ($\pi^- p \rightarrow K^\circ\Lambda^\circ, K^\circ\Sigma^\circ$) in a hydrogen target situated about 8m upstream from the chamber. Six discrete π^- momenta were taken covering the K^0_L momentum region 450-800 MeV/c, the lowest being in the monochromatic region below $K^\circ\Sigma^\circ$ threshold and the others in the dichromatic region. The success of the experiment depended critically on the K^0_L beam being truly monochromatic (or dichromatic). Figure 36 shows the measured K^0_L momentum distributions for π^- momenta of 1·00 and 1·14 GeV/c determined using the highly constrained events with no unseen neutral secondaries. The widths ($\Delta p/p \sim \pm 3\%$) are equal to the predicted values and no significant tails are seen.

Figure 37. Distribution of the $\Lambda\gamma$ invariant mass in events fitting the hypothesis $K^0_L p \rightarrow \Lambda\gamma\pi^+$. A clear Σ° signal is seen: Experiment 29 (15406)

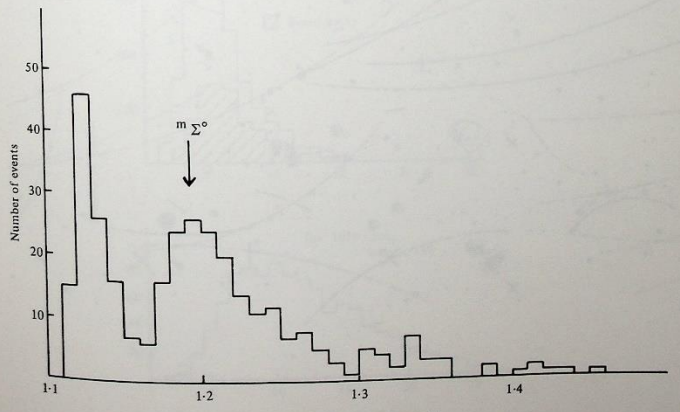

The main purpose of the experiment is to examine the strong interaction channels

$$K^0_L p \rightarrow \Lambda^0 \pi^+$$
$$\rightarrow \Sigma^0 \pi^+$$
$$\rightarrow K^0_S p$$

and particularly the latter two. The $K^0_S p$ channel contains the interference between S = -1 and S = +1 amplitudes and its study may yield valuable information concerning the Z* question. The $\Sigma^0\pi^+$ channel is interesting because it involves a pure isospin state (I = 1) in contrast to the mixed isospin states in $K^- p \rightarrow \Sigma^\pm \pi^\mp$. The differential cross-section (and polarization) measurements will help to unravel the partial wave amplitudes in this channel. Analyses of the $K^0_S p$ and $\Lambda\pi^+$ channels present no difficulties since the events are highly constrained. While this is less true of the $\Sigma^0\pi^+$ channel (2-C fits), a clear Σ^0 signal can already be seen in the $\Lambda\gamma$ invariant mass distribution in the fit $K^0_L p \rightarrow \Lambda\gamma\pi^+$ (Figure 37).

The weak interaction part of the experiment is concerned with elucidating the mechanisms responsible for the $\pi e\nu$, $\pi\mu\nu$ and $\pi^+\pi^-\pi^0$ decay modes of the K^0_L. Knowledge of the beam momentum avoids the kinematic ambiguity which has beset many previous investigations.

Encouraged by the technical success of the experiment a further 500,000 pictures have been requested. It is hoped to obtain them in summer 1974. A new beam is currently being designed which should yield significantly higher K^0_L fluxes.

Figure 38 shows a frame from this exposure showing a semi-leptonic K^0_L decay, a $K^0_S p$ event and a $\Sigma^0\pi^+$ event.

Figure 38. A frame from the K^0_L exposure showing a semi-leptonic K^0_L decay, a $K^0_L p \rightarrow K^0_S p$ event with backward K^0_S, and a $K^0_L p \rightarrow \Sigma^0\pi^+$ event with backward π^+ (and unseen γ). The other recoil protons in the frame are due mainly to the neutron background in the beam, and the Compton electrons are due to soft photons leaking through the lead filter: Experiment 29 (15397)

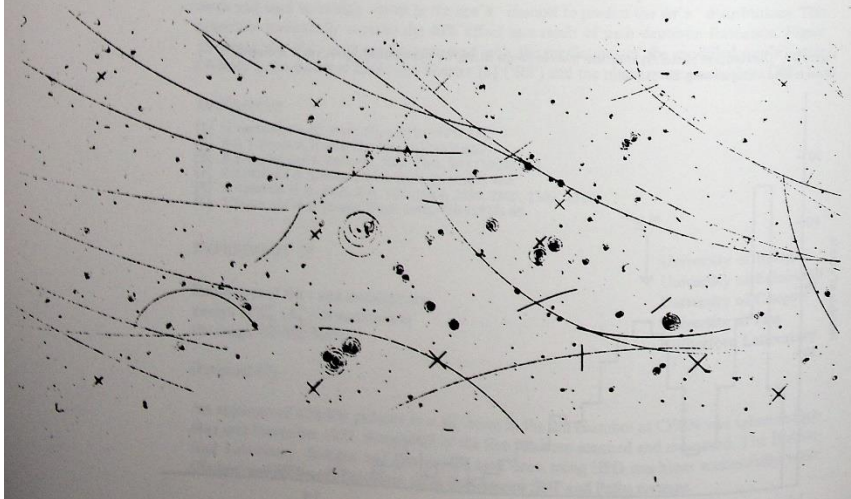

EXPERIMENT 30

4 GeV/c $\pi^+ p$ in a track sensitive target

(Proposal 91)

CERN
Lawrence Berkeley Laboratory
University of Turin
Rutherford Laboratory

This experiment is the first using the Track Sensitive Target technique which is designed to provide data on final states with more than one neutral particle ($\geqslant 2\pi^0$ or $n\pi^0$). Interest is therefore centred on events in which at least one π^0 (two paired gamma rays from the $\pi^0 \rightarrow \gamma\gamma$ decay) is detected. Given this information the $2\pi^0$ channel can be kinematically fitted. Such processes are not accessible to bubble chambers filled entirely with hydrogen and form an increasing fraction of the total cross section as the beam energy increases (~40% of σ_{Tot} for pions at 4 GeV rising to ~80% at 100 GeV/c).

Data taking in the 1·5 metre bubble chamber finished in 1972 with a total of 1,342,000 pictures with a 4 GeV/c π^+ beam. Two batches were taken in the metal framed TST with different neon concentrations in the neon-hydrogen mixture (73 and 77 mole %) and one batch (516,000 pictures) was taken with an all perspex TST and an 80 mole % neon concentration (radiation length 37 cm).

The past year has seen a large effort to develop the necessary techniques for the analysis of the TST pictures. Since the gamma conversion efficiency is greater we have concentrated on the film from the perspex TST. At the Rutherford Laboratory we have now measured more than 13,000 events each with more than two gammas converted using the Crystal measuring system. A similar number of events have been measured at Berkeley on "Cob-web". Because of the increased information content most of the events are complicated; they have two or more outgoing tracks and between two and five gamma rays. There are therefore considerably more tracks per event than in a simple experiment. The current output of the two Vanguard machines is in the region of 350 events per week (~2·8 events/hour/machine).

Figure 39. (a) The helix fit residuals from conventional measuring machines; tracks in hydrogen. (b) Helix fit residuals for tracks in neon/hydrogen mixture: Experiment 30 (15402)

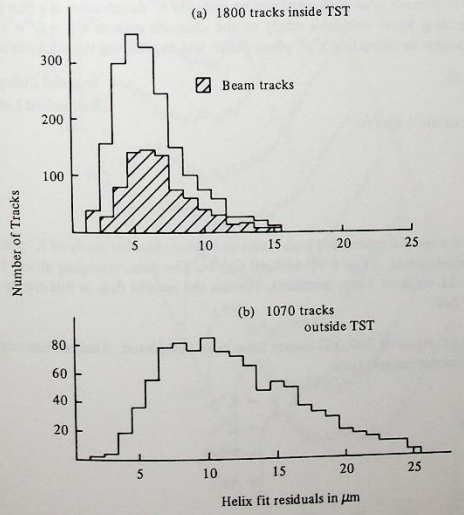

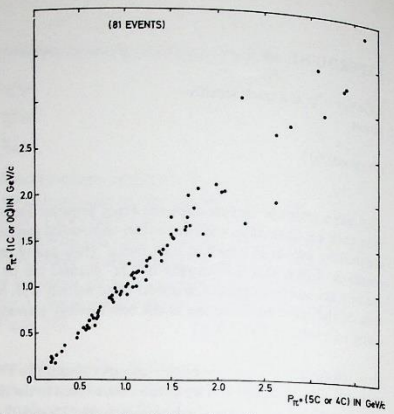

Figure 40. The π^0 momenta calculated from measurement of their decay γ-rays (0C or 1C fit) plotted against the same momenta after fitting both the production and the decay: Experiment 30 (15401)

A few rolls (some hundreds of events) have been measured with the automatic measuring machine (HPD). The HPD can detect and digitise tracks in both media in a very satisfactory way and after some minor program modifications it is now planned to go into production early next year.

The modified version of the geometry program is now essentially in its final form. Results were already presented at the 1973 Frascati Instrumentation Conference and show that track and vertex reconstruction in the hydrogen is as good as in the chamber with a pure hydrogen filling i.e. the presence of the TST and the neon-hydrogen mixture in no way limits the precision in hydrogen. Helix fit residuals on hadron tracks are histogrammed in Figure 39. The increase in the residuals in the neon-hydrogen mixture is as expected from the multiple Coulomb scattering. Hadron tracks in general are treated in two sections in the two media and a technique has been developed to combine information from both sections and to minimise the errors. A strong π^0 signal is seen in the distribution of the effective mass of gamma pairs and the determination of the π^0 momenta from the pairing of gammas can be checked from the production vertex fit in single π^0 channels. Such a check is shown in Figure 40.

The aim of the experiment now is to construct an inclusive π^0 distribution as a first physics result before proceeding to an exclusive study of the channels such as $\pi^+p \rightarrow \Delta^{++}\pi^0\pi^0$ and $\pi^+p \rightarrow \Delta^{++}\omega^0\pi^0$ with a view to extracting $\pi^0\pi^0$ phase shifts, and to studying the $\omega\pi$ system.

EXPERIMENT 31

Imperial College, London
Rutherford Laboratory

K^-p interactions in the 1 GeV/c region

(Proposal 108)

0·96-1·40 GeV/c

(ref. 333)

This experiment is a second generation high statistics bubble chamber study of K^-p interactions in the incident momentum range 0·96 to 1·40 GeV/c. The data, averaging about 1·4 events/μbarn at each of 11 incident beam momenta, increase the present data in this energy region by a factor of about two.

Final data summary tapes of 340,000 events have been completed. Analysis has concentrated on the two body formation reactions:

$$K^-p \rightarrow K^-p,$$
$$\rightarrow \bar{K}^0n,$$
$$\rightarrow \Sigma^{\pm}\pi^{\mp},$$
$$\rightarrow \Lambda\pi^0.$$

Angular distributions for the elastic channel, containing about 10,000 events at each energy, are shown in Figure 41. These numbers of events are comparable to statistics of counter experiments with the additional advantage from the bubble chamber technique of being bias free. This data should help to determine the weakly coupled Y* resonant structure, which is notably ambiguous in this energy region.

Energy dependent partial wave analyses are in progress and new analysis methods are being investigated.

In the three body channels 35,000 events of the highly constrained reaction $K^-p \rightarrow \Lambda\pi^+\pi^-(\pi^0)$ have been used to make a new measurement of the Λ lifetime: $(2{\cdot}61 \pm 0{\cdot}02) \times 10^{-10}$ s. Analysis of other final states is in progress.

The primary purpose of this exposure in the CERN 2m bubble chamber of four K^- momenta between 0·92 and 1·04 GeV/c is to provide a large increase in statistics, particularly at 0·96 GeV/c with about 4·5 events/μb, in order to reduce the number of ambiguous partial wave solutions. First measurements have been completed and work has started on the remeasures.

0·92-1·04 GeV/c

Figure 41. The differential cross section for elastic K^-p scattering as a function of the incident momentum from 0·96 to 1·36 GeV/c: Experiment 31 (14153)

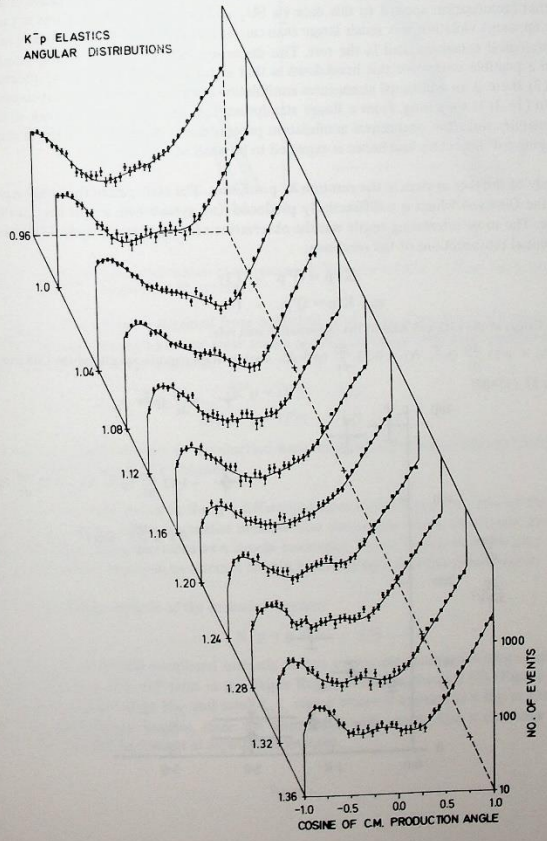

EXPERIMENT 32

Ecole Polytechnique, Paris
CEN, Saclay
Rutherford Laboratory

K^-p interactions at 14 GeV/c

(Proposal 109)

(ref. 19, 67, 72, 75, 257, 359, 360, 361, 362, 363, 364, 365, 367, 385, 386)

During 1973 additional data has been accumulated and at present the Data Summary Tapes contain about 290,000 events which is about 60% of the final number of expected events for the experiment.

The analysis of the data has proceeded both in the inclusive and exclusive reactions. The principal studies made are given below.

(i) A test of factorisation for the proton fragmentation processes in the inclusive reactions:

$$\pi^{\pm}p \to \Lambda + X \quad - \quad (1)$$
$$\text{and } K^-p \to \Lambda + X \quad - \quad (2)$$

The investigation was performed in collaboration with the Notre Dame (USA) group who supplied the data on reaction (1) at 18·5 GeV/c incident momentum. The result obtained (Figure 42) was that factorisation applied to this data via SU_3 and exchange degeneracy was not satisfied. The apparent violation was much larger than can be accounted for by uncertainties in the phenomenological constants used in the test. This discrepancy has created some theoretical interest and a possible source for this breakdown is that in the proton fragmentation process in reaction (2) there is an additional strangeness annihilation channel open which is not accessible in reaction (1). It is surprising, from a Regge standpoint, that the apparent violation is so large at these energies since the strangeness annihilation process can be represented by the exchange of a low lying ϕ-f' trajectory and hence is expected to be small at high energies.

(ii) A study of the $\bar{K}\pi\pi$ system in the reaction $K^-p \to \bar{K}N\pi\pi$. The main part of this study was devoted to the Q-meson which is a diffractively produced $\bar{K}\pi\pi$ system with a mass near its threshold value. The most interesting result was the observation of a cross-over (Figure 43) between the differential cross-sections of the reactions:

$$K^-p \to Q^-p \quad - \quad (3)$$
$$\text{and } K^+p \to Q^+p \quad - \quad (4)$$

Figure 42. Values of the LHS and RHS of the factorisation sum rule: $\frac{d\sigma}{dt}(p\overset{K^-}{\to}\Lambda) = 1{\cdot}13\,\frac{d\sigma}{dt}(p\overset{\pi^-}{\to}\Lambda) - 0{\cdot}33\,\frac{d\sigma}{dt}(p\overset{\pi^+}{\to}\Lambda)$. Factorisation requires equality of the LHS and RHS: Experiment 32 (15409)

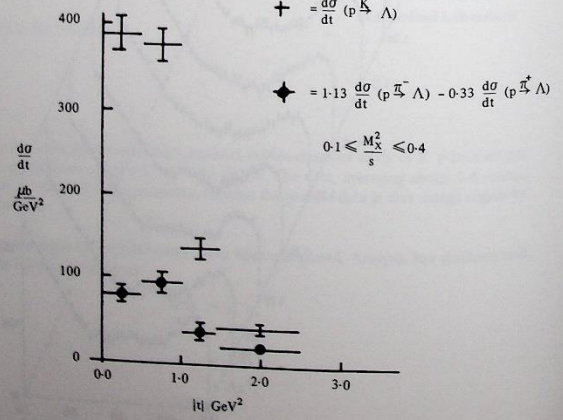

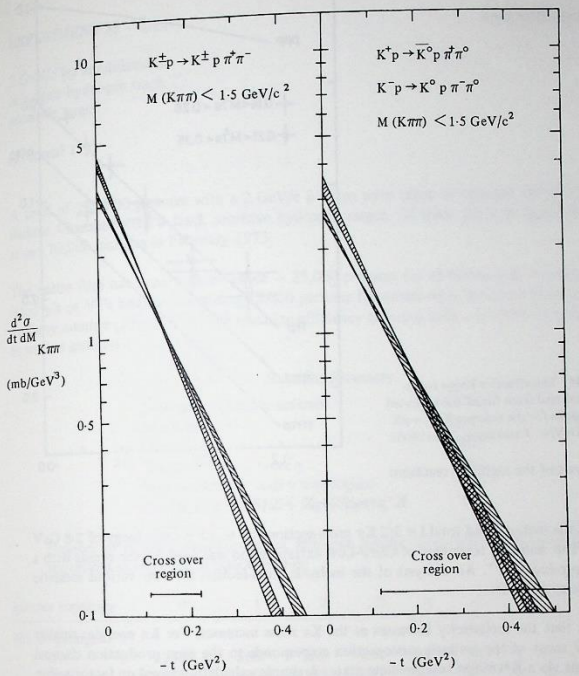

Figure 43. The differential cross sections of the reactions $K^-p \to Q^-p$ and $K^+p \to Q^+p$ for the decay modes $K^{\pm}\pi^+\pi^-$ and $\bar{K}^0\pi^{\pm}\pi^0$: Experiment 32 (15399)

Data on reaction (4) were obtained from published work. The direction of the cross-over obtained is incompatible with a simple Deck model and the cross-over observed between the differential cross-sections of the reactions:

$$\bar{K}^0p \to \bar{Q}^0p \quad - \quad (5)$$
$$\text{and } K^0p \to Q^0p \quad - \quad (6)$$

Also significant differences in Q^- production were observed according to whether the Q^- decayed into the $\bar{K}^0\pi^-\pi^0$ or $K^-\pi^+\pi^-$ channels.

The differences were found in the Q^- differential cross-sections and the ratio of the coupling constants $g_{K\rho}/g_{K^*\pi}$. These anomalies indicate that the system which constitutes the Q region is very far from being described as a simple resonance. In our future work we plan to partial wave analyse the Q region in an attempt to gain further insight into this phenomenon.

(iii) A triple Regge analysis of the inclusive reaction:

$$K^-p \to p + X \quad - \quad (7)$$

From a study of 56,000 peripheral inelastic proton events the most interesting result was the possible existence of a $\pi\pi\underline{P}$ term in the Triple Regge model for reaction (7) (Figure 44). This term is strong in the large M_X and small $t_{p,p}$ region where it appears as a dip in the effective trajectory. Its presence implies, since the term scales with energy, that π exchange processes with the proton will be present at asymptotic energies.

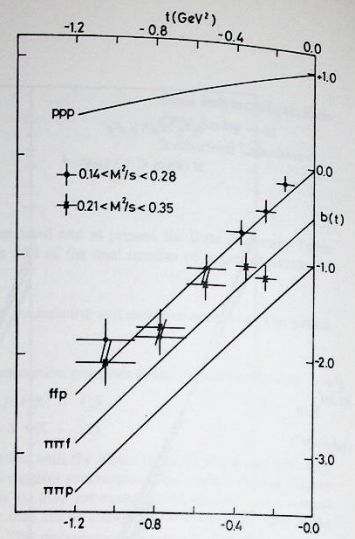

Figure 44. The effective Regge trajectories obtained from fits of the indicated M^2/s regions for the reaction $K^-p \to pX$ at 14·3 GeV/c: Experiment 32 (15405)

(iv) An analysis of the inclusive reaction:

$$K^-p \to \Delta^{++} + X \quad - \quad (8)$$

has extracted the inelastic and total I = 3/2 Kπ cross-sections up to a Kπ c.m. energy of 2·8 GeV (Figure 45). The standard technique of Chew-Low extrapolation was used for the events with a peripherally produced Δ^{++}. An analysis of the inelastic cross-section into the various inelastic channels was also possible.

It was found that the inelasticity increases as the Kπ mass increases. For Kπ energies smaller than 2·0 GeV most of the inelastic cross-section corresponds to the pion production channel which proceeds via a K*(890)π intermediate state. A simple calculation based on factorisation indicates that the total Kπ cross-section at 2·8 GeV is about 50% of its asymptotic value. The I = 3/2 Kπ s-channel quantum numbers are exotic and a comparison with other exotic reactions (e.g. K^+p, K^+n) would suggest that the total I = 3/2 Kπ cross-section should have reached its asymptotic value within the energy range we have studied. This slow rise of I = 3/2 $\sigma_{TOT}(K\pi)$ to its asymptotic value is somewhat surprising. A similar phenomenon is observed for the total I = 2 $\pi\pi$ cross-section. It may thus be a feature of meson meson scattering.

For the future it is hoped to analyse in detail the many exclusive channels, which with the accumulated statistics should reveal many interesting new results.

Figure 45. Values of the elastic, inelastic and total $K^-\pi^-$ cross sections: Experiment 32 (15400)

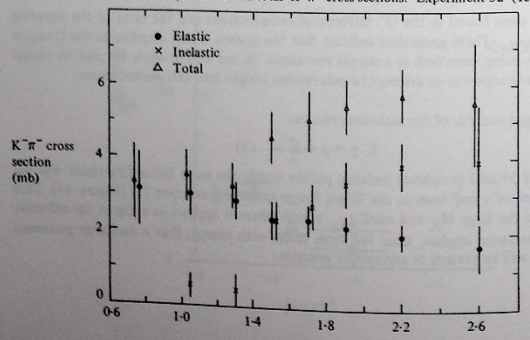

EXPERIMENT 33 **Tata Institute, Bombay**

2 GeV/c $\bar{p}p$ annihilations
in a neon-hydrogen track
sensitive target

(Proposal 115)

A total of 200,000 pictures with a 2 GeV/c $\bar{p}$ beam were taken in October 1972 in the 1·5 m Bubble Chamber with a track sensitive hydrogen target. Of these the Tata Institute received about 70,000 pictures in February 1973.

The entire film has been scanned twice – 25,000 pictures for all events with or without associated γ's or V°'s and the remaining 45,000 pictures for events with two or more associated γ's and any number ($\geq$0) of V°'s. The scanning efficiency is found to be over 95% for annihilations as well as gammas.

Scanning Summary

Number of pictures scanned	62748
Bad frames	2145
Good frames	60603
Events with 2 or more γ	7486
Events with 1 V° (all γ topologies)	855
Events with 2 V° (all γ topologies)	118

Number of events (annihilations) of different gamma topologies for different prong topologies as recorded in 60600 frames:

gamma topology	0	1	2	3	4	5	6	7	8	9
No. of prongs										
0	2740*	860*	283	134	61	18	11	0	1	0
2	7680*	4920*	2187	893	343	82	30	5	3	1
4	7800*	5020*	2168	701	176	34	9	1	1	0
6	1780*	757*	266	61	16	0	0	0	0	0
8	30*	8*	1	0	0	0	0	0	0	0
Totals	20030	11565	4905	1789	596	134	50	6	5	1

* These number are based on the scanning of a sub-sample of the film amounting to 23310 frames.

In order to reconstruct the events, we have modified the geometry program THRESH (which is being used in other experiments here) to accommodate the complications arising from the use of the TST and neon-hydrogen mixture. Measurements on events with two or more associated gammas will commence shortly.

Attempts are being made to deduce π° multiplicity distribution for each prong topology. Two approaches are being tried. In the first procedure, we use an average gamma conversion probability and assume that the gamma distribution for a given π° multiplicity is determined by a binomial distribution. The π° multiplicity distribution is then deduced by fitting the observed gamma distribution. In the second approach we use a Monte Carlo procedure assuming the π° momentum and angular distributions to be the same as those of $\pi^\pm$.

EXPERIMENT 34

University College, London
University of Birmingham
Free University of Brussels
University of Durham

Slow and stopped K^- interactions

(Proposals 84 and 117)

During 1973 a slow K^- beam was built in Hall 1, and 900,000 pictures were taken for this experiment. The quality of the beam was excellent, with well separated K^- over the whole range of momenta used, from 560 MeV/c to 680 MeV/c. The tracks entered a hydrogen filled track-sensitive target, surrounded by a neon-hydrogen mixture, in the 1·5m bubble chamber. Degraders of varying thickness were used to scan a range of K^- momenta in the hydrogen from rest up to 580 MeV/c.

The total exposure contains about 26 events per microbarn. In the $\Lambda\pi^\circ$ channel there are expected to be more than 750 events with one or more γ-rays detected in the neon-hydrogen mixture, for every 25 MeV/c bin between 100 MeV/c and 575 MeV/c. The $\Sigma^\circ\pi^\circ$ channel will have similar statistics. The stopping K^- part of the exposure (200,000 pictures – proposal 117) will have more than 20 times the statistics of the previous experiments on $K^-p \to \Lambda^\circ\pi^\circ$ and $\Sigma^\circ\pi^\circ$ below 250 MeV/c. The experiments have continuous data over a momentum range in which previous experiments have concentrated on narrow bands. No other experiment in this range has had γ-ray detection to help resolve the Λ°-Σ° ambiguity.

Differential and total cross-sections and polarizations will be measured for the $\Lambda^\circ\pi^\circ$ and $\Sigma^\circ\pi^\circ$ channels over the whole momentum range. The $\Sigma^-\pi^+$ and $\Sigma^+\pi^-$ channels will also be studied in some momentum regions. The general aim of the experiment is to improve the K-matrix fit to low-energy $\bar{K}N$ reactions. Particular topics of interest include:–

(a) The $\Lambda^\circ/\Sigma^\circ$ production ratio between 100 MeV/c and 200 MeV/c.

(b) Determination of S-wave effective ranges to aid calculations of the $\Lambda\bar{K}N$ coupling constant.

(c) The rate of increase of the P-waves over the 200 to 400 MeV/c range.

(d) The possible D_{13} $\Lambda\pi^\circ$ resonance at about 1485 MeV/c^2.

(e) The recently observed total cross-section peak at 550 MeV/c.

(f) Re-determination of the hyperon production ratios at rest.

Figure 46. A "$\Lambda + 2\gamma$" event in the 1·5 m bubble chamber with the track sensitive target. The fine tracks are in the hydrogen target, the heavier tracks are in the neon-hydrogen mixture. Two electron-positron pairs point back to the K^-p interaction point, with the V pattern of $\Lambda^\circ \to p\pi^-$ decay close by. The event is probably an example of the sequence $K^-p \to \Lambda^\circ\pi^\circ$, $\Lambda^\circ \to p\pi^-$ and $\pi^\circ \to \gamma\gamma$, where each γ + nucleus $\to e^+e^-$ + nucleus: Experiment 34 (15420)

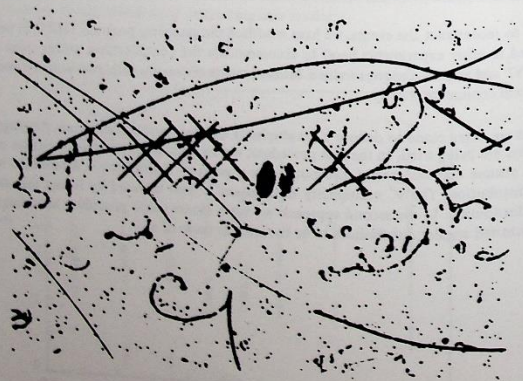

EXPERIMENT 35

University of Oxford
Rutherford Laboratory

The study of the S = –2 baryon resonance using the rapid cycling bubble chamber

(Proposal 119)

This experiment is designed to obtain a sample of ~ 20,000 events of the kind

$$K^-p \to \Xi^-K^\circ\pi^+(\pi^\circ) \quad - \quad (1)$$
$$\to \Xi^-K^+\pi^+\pi^-$$
$$\to \Xi^\circ K^\circ\pi^+\pi^-$$
$$\to \Lambda^\circ/\Sigma^\circ K^\circ\bar{K}^\circ$$

principally in channel (1), from K^- interactions at 2·8 GeV/c in the rapid cycling bubble chamber. The trigger for the photography will be provided by multiplicity $\geqslant 5$ in the particles leaving the chamber, detection being by multiwire proportional chambers surrounding the vacuum tank. Approximately 200,000 events are also expected in the channels $\Sigma/\Lambda\pi^+\pi^+\pi^-\pi^-(\pi^\circ)$, $K^\circ p\pi^+\pi^-\pi^-$ (π°) etc which should also provide interesting physics. A detailed Monte Carlo study of the experiment has been performed, however, data taking is not expected before 1975.

EXPERIMENT 36

Argonne National Laboratory
Rutherford Laboratory

6 GeV/c π^+p in a track sensitive target

(Proposal 121)

It has always been clear that the proper exploitation of the track sensitive target technique requires large chambers which allow highly efficient and unbiassed detection of neutrals. A preliminary proposal to study multineutral events in 6 GeV/c π^+p interactions using the ANL 12 ft bubble chamber has been approved for 100,000 pictures in the first instance. The physics interest is closely related to that of the current TST experiment in the 1·5m chamber (proposal 91). A prototype perspex target built by CERN and the Rutherford Laboratory in collaboration has been successfully tested in the chamber filled with hydrogen. It is hoped that the complete system will be ready for physics by the beginning of 1975.

EXPERIMENT 37

University of Oxford
University of Pisa
Rutherford Laboratory

π^-p interactions at 22 GeV/c

(Proposal 134)

It is proposed to make a small exposure of BEBC using a high energy beam from the CERN PS; 30,000 pictures with 22 GeV/c π^- have been requested. This is regarded mainly as an engineering run in view of the future exploitation of BEBC at the SPS. The RL–Saclay–Oxford–Glasgow collaboration is proposing to study high energy K^- interactions in BEBC at the SPS and this experiment should give valuable experience of the problems which may be encountered. However the experiment is not without physics interest and it is hoped to study inclusive γ-ray, Λ and K° production and inclusive channels such as $\pi^-p \to p + 3\pi$.

Nuclear Structure Experiments

The use of strongly interacting negatively charged particles such as K^-, Σ^-, $\bar{p}$ presents nuclear structure physics with an interesting and potentially extremely useful probe of the nuclear density distribution in complex nuclei. The formation of exotic atoms, where one of the atomic electrons is replaced by a negatively charged heavier particle, is followed by de-excitation of the atom accompanied by the emission of X-rays. Termination of the X-ray series by the nuclear absorption of the heavy particle, usually a meson, from a low lying Bohr orbit is now a well established process. This takes place via the short range strong interaction and it is the consequent localisation of the radial distance at which the absorption takes place outside the nuclear half density radius, which provides much of the interest in such studies. Conventional probes, using elastic scattering interactions, such as e^- and p are sensitive only to those parts of the nuclear density responsible for the gross properties like the surface thickness or r.m.s. radius.

Interest has been focused on pionic atoms for several years. With the increasing availability of K^- beams, attention is now being paid to the particular characteristics of kaonic atoms. These display an advantage over π^--atoms in that the nuclear absorption takes place primarily on single nucleons rather than on nucleon pairs because of the availability of several two-body $Y\pi$ channels (where Y is a Hyperon). For the same reason the absorption is stronger than in π^- atoms and as a consequence is both more localised and occurs at a larger radius – mainly in the 10-20% region of the density distribution. In principle therefore, kaonic atom studies may be a useful complement to elastic e^- and proton scattering, μ and π mesic X-ray measurements and the rather recent $\pi^\pm$ total cross-section measurements in investigating the elusive problem of relative neutron and proton distributions in medium and heavy nuclei. Before much progress can be made, however, a basic problem must be removed. The kaon-nucleus interaction, described using an optical potential, consists of folding the $\bar{K}$ N interaction into the nuclear density distribution. The free-space $\bar{K}$ N interaction is repulsive at threshold but attractive near a resonance of the $\bar{K}$ N system called the Y_0^* at -27 MeV. The extent to which this kinematic region is accessible to the $\bar{K}$ N system in the nucleus and what effect the Y_0^* resonance will have if it is, remain open questions.

A proper treatment of the way these free-space effects are modified in the nuclear environment to produce the effective $\bar{K}$ N interaction in a real nucleus is urgently required before much nuclear structure information can actually be extracted from experiments. Until then the flow of information is likely to be at least partly in the opposite direction. For example, the observation of nuclear de-excitation γ-rays following absorption of the kaon by the nucleus can be used to identify the residual nucleus from which the nature of the capture process can be inferred. A knowledge of the relative rates of capture on single neutrons and protons will help to show how the Y_0^* resonance affects the K^--nucleus system.

This observation of de-excitation gamma rays is also one of the fields where nuclear structure information may be extracted. About 20% of the K^- absorption processes in heavy nuclei take place on correlated nucleon parts ($K^- NN \rightarrow YN$), a figure which according to Wilkinson holds for absorption on ^{4}He also. This fact may be used to suggest the presence of alpha particles near the half density region of heavy nuclei. Some very tentative data gathered in the United States already indicates that one, two or even three clusters of four nucleons may actually be expelled from the nucleus when the K^- are absorbed. Although the evidence is so far very slight further corroborative observations of these processes would have far reaching implications for nuclear structure. In a rather similar way the intensities of gamma rays resulting from production of single hole nuclei can be used to give a direct indication of the relative populations of nuclear single particle states in a fairly specific region of the nuclear density. If this is afterwards augmented by similar studies using $\bar{p}$ and $\bar{\Sigma}$ particles each of which explores successively outer lying regions of the nucleus, the radial dependence of single particle occupation numbers can be investigated in a unique way.

To these ends in 1973 the activities of the Rutherford Laboratory Group in collaboration with Birmingham and Surrey Universities and the University of Williamsburg, Virginia, have largely centred on the design, construction and initial evaluation of a wide acceptance stopping K^- beam line. The first contribution below gives a summary of the status of the experiment at the present time.

The final analysis of the measurements of the total cross-sections for $\pi^\pm$ on light nuclei (Experiment 39) shows that the simple optical model of pion-nucleus interactions needs further refinement to include some second order effects. The differences in cross-sections between $\pi^\pm$ can be rather easily accounted for in a semi classical way.

Further optical model studies of helion and alpha scattering have been made by the Kings College Group in extending their energy range to 82·7 MeV on the Variable Energy Cyclotron at AERE, Harwell. The analysis at this higher energy for ^{3}He has removed the potential ambiguities found at lower energies and has revealed the interesting fact that this well defined real potential has a volume integral per particle pair which does not correspond to that obtained from the two nucleon force in contrast to the results at lower energies. Clearly the present trend in optical model analysis away from the purely phenomenological needs to continue particularly in the inclusion of exchange effects and the use of more refined effective interactions. Exchange effects have been included in the microscopic model of inelastic scattering from collective nuclei and an experimental program of α-scattering has begun to test this development.

Analysis of the program of work undertaken by a collaboration of AERE and several University groups on the AERE synchrocyclotron to study the few nucleon system is continuing. The work of n-p bremsstrahlung near 130 MeV is now completed and suggests that the off-energy-shell effects are not the only inclusion necessary to explain the cross-sections. Experiment 46 from this group involves a measurement of the n-p total cross-section around 100 MeV the results of which it is hoped may be explained by a constituent quark model of the hadrons. Experiment 47 is being set-up to measure the triple scattering parameters in n-p scattering between 250 and 500 MeV. The experiment will be performed at the new TRIUMF accelerator, in Canada.

In the final report on the search for superheavy elements in heavy metal targets irradiated with 24 GeV protons from the CERN PS (Experiment 48) it is concluded that the secondary reaction process seems unlikely to produce superheavy elements and the search for these must probably await the coming generation of heavy ion accelerators.

Table 3

Nuclear Structure Experiments

Experiment Number	Experiment ; Location	Groups
38	Experiments with stopping kaons; K17 beam Nimrod	University of Birmingham University of Surrey Rutherford Laboratory
39	Total cross-sections for pions on light nuclei; π10 beam Nimrod	University of Surrey University of Birmingham Rutherford Laboratory
40	$\pi^{\pm}$ – nucleus total cross-sections; CERN Synchro-cyclotron	University of Oxford CERN, Geneva University of Gothenborg SIN, Zurich University College, London
41	Scattering studies with helion and alpha beams; AERE variable energy cyclotron	King's College, London
42	Investigation of two step processes in nuclear reactions and of microscopic theories of inelastic scattering; AERE variable energy cyclotron, Oxford University Tandem	King's College, London Queen's University, Belfast
43	n-p bremsstrahlung near 130 MeV; AERE Synchro-cyclotron	Queen Mary College, London University of California King's College, London AERE, Harwell Rutherford Laboratory
44	n-d break-up between 50 and 150 MeV; AERE Synchrocyclotron	Queen Mary College, London Bedford College, London AERE, Harwell
45	Elastic scattering of polarized neutrons from deuterium; AERE Synchrocyclotron	Queen Mary College, London Bedford College, London AERE, Harwell
46	n-p total cross-sections between 90 and 155 MeV; AERE Synchrocyclotron	Queen Mary College, London Bedford College, London University of Surrey AERE, Harwell
47	Measurement of the triple scattering parameters of the free n-p system; TRIUMF H^- cyclotron, Vancouver	Bedford College, London AERE, Harwell University of Surrey Queen Mary College, London University of British Columbia, Canada
48	Search for superheavies; CERN Proton Synchrotron	University of Manchester University Research Reactor, Risley Rutherford Laboratory
49	Test for t-invariance in neutron beta decay; ILL High flux beam reactor, Grenoble	ISN, Grenoble ILL, Grenoble Yale University Rutherford Laboratory

EXPERIMENT 38

Experiments with stopping kaons

(Proposal 113)

University of Birmingham
University of Surrey
Rutherford Laboratory

The observation of nuclear γ-rays following the atomic cascade of a kaon and its capture by the nucleus should yield more information about the interaction mechanism of the capture process; in particular it should be possible to determine whether the existence of the Y_0^* (1405) causes a preferential absorption on protons. This data would also provide information about the existence of clusters of nucleons in the surface of the nucleus and should enable a more definitive interpretation of the kaonic X-ray width and shift data that are currently available.

Experimental apparatus, to perform measurements of γ-ray and X-ray spectra for a variety of nuclei, has been built. A diagram of the experimental arrangement is shown in Figure 47. The stopping kaon beam line is the sole user of a third target station of the X3 extracted proton beam from Nimrod. It is a single stage electrostatically separated beam with a transport momentum of 600 MeV/c. Solid state detectors are used to observe the spectra after the kaons have been slowed down in a degrader and stopped in the target to be studied. The kaons are identified using Cerenkov detectors and time of flight over a 4 metre flight path. Extensive studies of the beam line have been made and kaon yields and π/K ratios measured for a number of different production target lengths, cross-sections and materials. Kaon fluxes adequate for the above experiments are available. Some improvements such as the replacement of the first quadrupole by one with concrete insulation, necessary for long periods of high intensity running, will be made during the 1973-74 shutdown.

Whilst testing equipment for the stopping kaon experiment we have also investigated the 126 KeV γ-ray from the first excited state of ^{55}Mn. Godfrey and Weigand have reported that this state is strongly excited when kaons are brought to rest in a ^{55}Mn target. They discuss the possibility that this nuclear level is excited in a radiationless transition between the n = 9 and n = 6 levels of the kaonic atom. Our work has shown that the level is also strongly excited by pions and that the non linear variation of the γ-ray yield with target thickness suggests that the principal mechanism for the excitation is a two stage process of the type

$$\pi^- + {}^{55}\mathrm{Mn} \rightarrow \mathrm{X} + \mathrm{n}$$

$$\mathrm{n} + {}^{55}\mathrm{Mn} \rightarrow {}^{55}\mathrm{Mn}^* + \mathrm{n}$$

$$\hookrightarrow \gamma\ (126\ \mathrm{keV})$$

Ancillary experiments have confirmed that the state is strongly excited by neutrons. This work is being written up for publication.

Figure 47. K17 beam line and counter arrangement: Experiment 38 (15081)

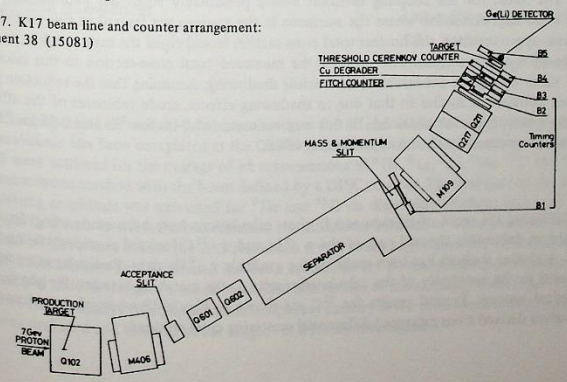

EXPERIMENT 39

Total cross-sections for pions on light nuclei

University of Surrey
University of Birmingham
Rutherford Laboratory

(ref. 44, 83, 95, 113, 369)

There has been a great deal of theoretical work on the scattering of π mesons by nuclei, particularly for energies in the region of the (3, 3) resonance for the pion-nucleon system. However the available experimental data has been rather limited, being confined to measurements of differential cross-sections at a few energies for Carbon and to total cross-sections for a few nuclei. There is a clear interest in extending these latter measurements to a wider range of energies and target nuclei.

In the present experiment measurements have been made of total cross-sections for π^+ and π^- mesons on ^{6}Li, ^{7}Li, ^{9}Be and ^{12}C at 14 different energies between 90 and 860 MeV and for Oxygen at 6 energies from 88 to 228 MeV. A preliminary analysis of the results for Carbon was presented in last year's Report. The results from the present work are in excellent agreement with those from other experiments. A comparison has been made for the T = O nuclei ^{6}Li, ^{12}C and ^{16}O between the measured cross-sections and the predictions of a number of simple optical models. It is generally found that, whilst these simple models give quantitative agreement with the results, there are a number of significant discrepancies. It seems that second-order corrections to the potentials must be considered if detailed qualitative agreement is to be obtained.

The measured cross-sections for positively and negatively charged pions on nuclei such as Carbon, which have zero isospin, can differ from each other and from the strong interaction cross-section due to the distortion of the incident pion wave-function by the Coulomb field of the nucleus. This distortion has the effect that the total cross-section for negatively charged particles is increased and for positive particles is decreased. The measured differences have been compared with the results of a semi-classical calculation and the predictions of optical model calculations using a variety of forms for the potential. Within the accuracy of the results the simple semi-classical calculation gives good agreement with the measured differences.

It has been shown by Ericson and Locher that the effective pion nucleus coupling strength can be obtained from pion scattering by nuclei with $T_z = \frac{1}{2}$ using dispersion relations. A similar analysis of the present results gives values of 0·058 ± ·008 for ^{7}Li and 0·051 ± ·007 for ^{9}Be. Ericson and Locher obtained the value 0·06 ± ·03 for ^{9}Be, whilst, using data from a Glauber model, Osland has recently obtained the value 0·042 ± ·008. Both these values are consistent with this work. The value for the coupling constant would presumably equal the pion-nucleon value (0·08) in an approximation where the nucleons in the nucleus are treated as free particles. In this same approximation the nuclear total cross-section would equal the mass number, A, times the free pion-nucleon value. The ratio of the measured total cross-section to this calculated "free" value then gives a measure of the nuclear shadowing. Assuming that the reduction in the coupling constant is similar to that due to shadowing effects, crude estimates of the effective coupling constant can be obtained. In this way estimates of 0·06 for ^{7}Li and 0·05 for ^{9}Be are obtained in agreement with the experimental values.

Also following the work of Ericson and Locher, calculations have been made using dispersion relations to determine the real part of the π^- ^{6}Li and π^- ^{12}C forward elastic scattering amplitudes. A similar analysis has been made of the available π^- ^{4}He data. Particular attention has been paid to the sensitivity of the calculated results to the matching between the physical and unphysical regions. Typical results for ^{12}C are shown in Figure 48 where they are compared with values derived from measured differential scattering cross-sections.

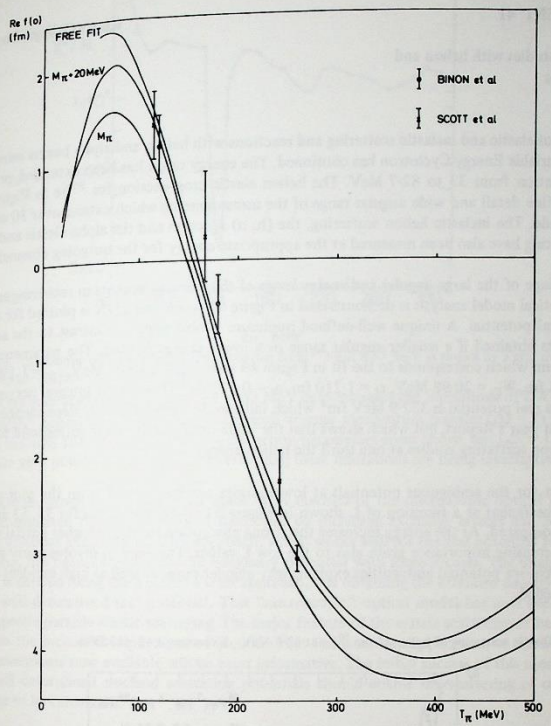

Figure 48. Values of the real forward scattering amplitude for carbon deduced using dispersion relations. Also shown are experimental values: Experiment 39 (13681)

EXPERIMENT 40

$\pi^\pm$- nuclear total cross-sections

University of Oxford
CERN, Geneva
University of Gothenborg
SIN, Zurich
University College, London

A precision comparison of nuclear total cross-sections for π^+ and π^- in the neighbourhood of the 3-3 resonance has been completed at the CERN synchrocyclotron. Statistical accuracies of about ½% were achieved for the average of $\pi\pm$ cross-sections of ^{4}He, ^{6}Li, ^{7}Li, ^{9}Be, ^{12}C and ^{32}S using a transmission method with the beam defined by a DISC counter. The real part of the forward scattering amplitude was extracted for ^{4}He and ^{12}C via dispersion relations and used to calculate the Coulomb interference correction to the difference between $\pi^\pm$ total cross-sections. The residual $\pi^\pm$ difference below the 3-3 resonance is very much larger than the statistical and systematic uncertainties. This difference has been accounted for by non-interference Coulomb corrections, but only in terms of a crude black disk description of the nucleus which is not very satisfactory. The possibility of an appreciable isospin asymmetry in the pion-nucleon interaction has not been excluded and this will be the subject of a future investigation. *(ref. 89)*

EXPERIMENT 41 — **King's College, London**

Scattering studies with helion and alpha beams

(ref. 88) The study of elastic and inelastic scattering and reactions with helion and alpha beams using the UKAEA Variable Energy Cyclotron has continued. The energy range has been extended, providing information from 33 to 82·7 MeV. The helion elastic cross-section for ^{56}Fe in Figure 49 shows the fine detail and wide angular range of the measurements which extend over 10 orders of magnitude. The inelastic helion scattering, the (h, α) reaction and the alpha elastic and inelastic scattering have also been measured at the appropriate energy for the outgoing channel.

The advantage of the large angular and energy range of these measurements in removing ambiguities in optical model analysis is demonstrated in Figure 50 where the χ^2/N is plotted for a grid over the real potential. A unique well-defined minimum is observed, in contrast to the ambiguous results obtained if a smaller angular range or a lower energy is used. The parameters for the minimum which corresponds to the fit in Figure 49 were V_R = 110·05 MeV, r_R = 1·195 fm, a_R = 0·765 fm, W_D = 20·98 MeV, r_I = 1·210 fm, a_I = 0·812 fm. The volume integral per particle pair for the real potential is 332·9 MeV fm^3 which falls on the smooth energy dependence plots given in last year's Report, but which shows that the value obtained does not correspond to that from nucleon scattering studies at one third the helion energy.

The reason for the ambiguous potentials at low energies can be inferred from the plot of absorption coefficient as a function of L shown in Figure 51 where the curves for 33, 53 and 83 MeV are compared. As the energy increases the strong absorption moves to higher partial waves with an increasing importance given also to the low L values. The need to involve many partial waves to remove potential ambiguities explains why angular range as well as high incident energies are needed.

Figure 49. Elastic scattering of helions from ^{56}Fe at 82·7 MeV: Experiment 41 (13536)

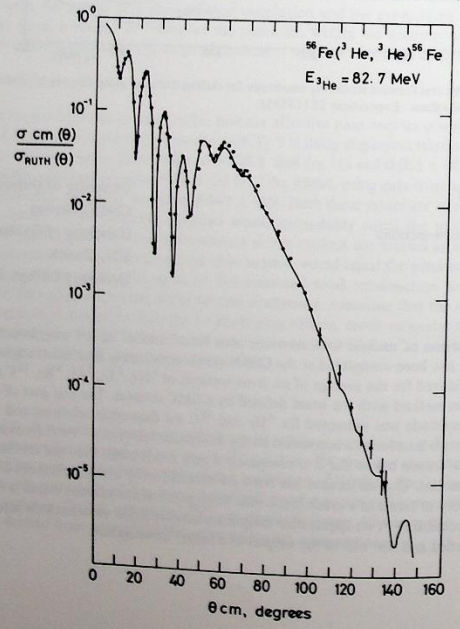

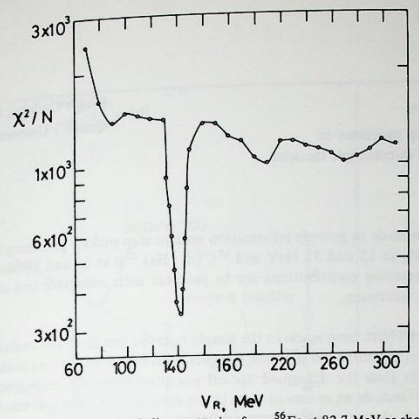

Figure 50. The unique minimum for helion scattering from ^{56}Fe at 82·7 MeV as shown by a grid over the real potential: Experiment 41 (13535)

The (h, α) data also obtained on ^{56}Fe at 83 MeV demonstrates the limitations of DWBA under "mismatch" conditions. The predominant high angular momentum transfer ($\Delta\ell = 3$) states observed, are well fitted using the unique distortion parameters given above, but ($\Delta\ell = 1$) transfer states are very poorly fitted. Ways of overcoming these limitations are being investigated.

Considerable progress has also been made with theories of the microscopic optical potential. The reformulated optical model was developed by including exchange effects and comparing various effective interactions. This approach, which works well for the real potential for proton scattering, has been extended to the imaginary potential with some success. The imaginary potential is derived using the Thomas-Fermi approach, but obtaining the effective density in terms of the well determined real potential. This "microscopic" optical model has now been applied to composite particle elastic scattering. The major feature of the elastic scattering of helions and alphas is the increased importance of second order terms so that application to the wide range of measurements now available will be most informative. The initial success of this model shows that well determined nucleon scattering potentials should enable the scattering of composite particles to be calculated.

In collaboration with Oak Ridge National Laboratory our measurements on the even isotopes of samarium have been extended and a program to study target spin and spin orbit effects in helion scattering has been initiated.

Figure 51. Absorption coefficient as a function of partial wave number for 33, 53 and 83 MeV helions on ^{56}Fe: Experiment 41 (13537)

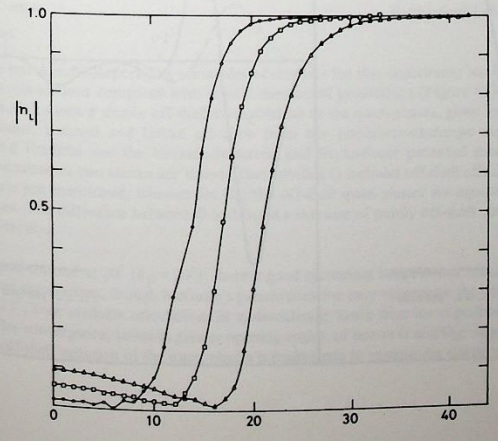

EXPERIMENT 42

King's College, London
Queen's University, Belfast

Investigation of two step processes to
nuclear reactions and of microscopic theories
in inelastic scattering

Measurements have been made to provide information on two step pickup processes in the reactions ^{26}Mg (^{3}He, α) ^{25}Mg at 15 and 33 MeV and ^{12}C (d, ^{3}He) ^{11}B at 28 and 50 MeV. Calculations of the two step reaction contributions are in progress with collective and microscopic models for the inelastic scattering.

Two further developments have been made to the simple microscopic model of inelastic scattering from collective nuclei mentioned in previous Reports. This model used as its basis a deformed nuclear density rather than the deformed optical potential normally employed. The first development has been to include an exchange term in the calculation of the real scattering form factor. Secondly we have almost completed a study of the anisotropic momentum spectra in deformed nuclei (see Figure 52) which is required to extend this model to the imaginary form factor. A series of forward angle inelastic cross-section and gamma correlation measurements has been commenced with 18 MeV α particles to test the above model in the Nuclear-Coulomb interference region where the DWBA predictions are very sensitive to the scattering form factor.

Figure 52. Anisotropic momentum spectra for neutrons and protons in ^{238}U. The probability of finding a nucleon with momentum between $\underline{k}$ and $\underline{k} + \underline{dk}$ is $\left[\sum_{\lambda} A_{\lambda}(k) \sum_{\mu} \alpha_{\lambda\mu} Y_{\lambda\mu}(\hat{\underline{k}})\right] \underline{dk}$ where $\alpha_{\lambda\mu}$ are the nuclear deformation constants and $\hat{\underline{k}}$ is the angle between $\underline{k}$ and the nuclear symmetry axis: Experiment 42 (15425)

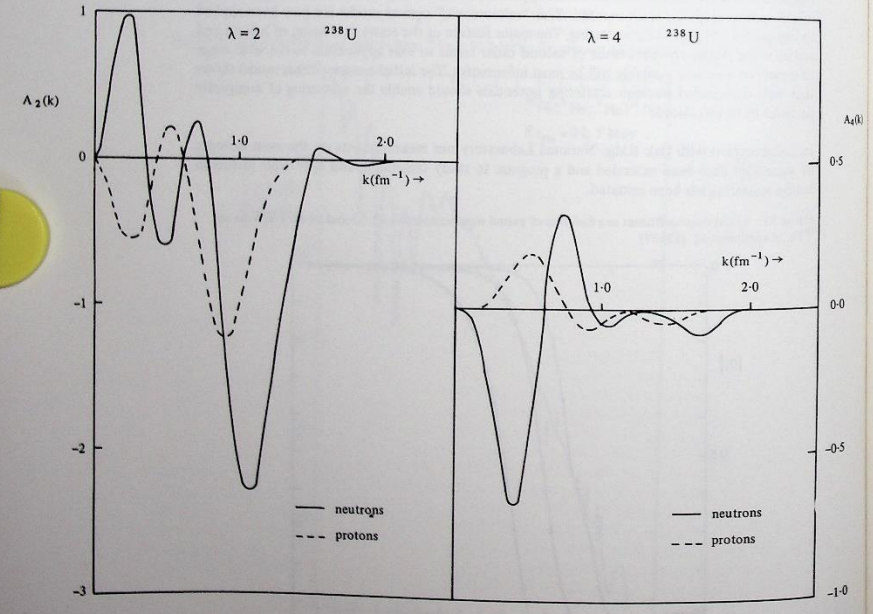

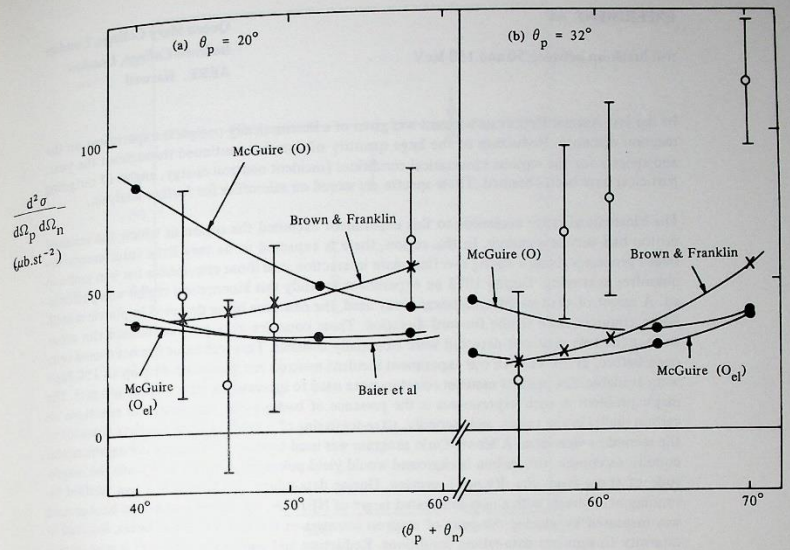

Figure 53. np bremsstrahlung cross-sections at 131 MeV. Open circles are the results of this measurement. The other symbols (connected merely to guide the eye) denote various theoretical calculations: Experiment 43 (15422)

EXPERIMENT 43

Queen Mary College, London
University of California
King's College, London
AERE, Harwell
Rutherford Laboratory

n–p bremsstrahlung near 130 MeV

Since the last Annual Report, the remainder of the data for this experiment has been analysed, and the cross-sections compared with several theoretical predictions (Figure 53). The calculation of McGuire uses a simple off-shell extrapolation of the quasi-phases, given by one-pion exchange. Baier, Kühnelt and Urban calculate from the one-boson-exchange model, whereas Brown and Franklin use the Hamada-Johnston and Bryan-Scott potential models. For McGuire's calculations two curves are shown; that labelled O includes off-shell effects in the parametrization just mentioned, whereas for O_{el} the off-shell quasi-phases are equated to their on-shell values. The difference between O and O_{el} is a measure of purely off-shell contributions to the cross-section. *(ref. 157)*

For protons emitted at 20° ($\theta_p = 20°$), there is good agreement between our measurements and the various calculations, though McGuire's parametrization may exaggerate the off-shell effects. At $\theta_p = 32°$, both available calculations lie systematically lower than the experimental measurements. The convergence, towards greater opening angles, of curves O and O_{el} suggests that even extreme off-shell variation of the quasi-phases is inadequate to explain the discrepancy.

EXPERIMENT 44

n–d break-up between 50 and 150 MeV

Queen Mary College, London
Bedford College, London
AERE, Harwell

In the last Annual Report an account was given of a kinematically complete experiment on the reaction d(n,np)n. Reduction of the large quantity of data has continued throughout the year, and spectra for the various kinematical conditions (incident neutron energy, angles of outgoing particles) have been obtained. These spectra are stored on microfilm for further analysis.

The kinematical range accessible to this experiment excluded the region in which the residual proton had very low energy. In this region, there is expected to be very little interference between processes giving a strong n–n final state interaction, and those responsible for n–n and n–p quasi-free scattering. During 1973 an experiment to study this kinematical region was performed. A target of deuterated cyclohexane was used, the neutrons being detected in plastic scintillation counters close to the forward direction. These counters were set, one behind the other, so that the two neutrons detected were essentially colinear. This technique has been used only once before, at 14 MeV. In our experiment incident neutron energies extending up to 150 MeV were available. Six pairs of neutron counters were used to increase the data acquisition rate. The major problem in such experiments is the presence of background, due firstly to reactions on carbon nuclei in the target, and secondly, to re-scattering of a neutron from the first detector to the second or vice-versa. A Monte-Carlo program was used to show that, under the experimental conditions chosen, the carbon background would yield pulses of (at most) one-tenth the magnitude of those from the d(n,nnp) reaction. During data-taking this conclusion was verified by running at intervals with a non-deuterated target of NE102A. The second source of background was measured by placing the pairs of neutron counters in the direct neutron beam, lowered in intensity to simulate data-taking conditions. Reduction and analysis of the data is now in progress.

EXPERIMENT 45

Elastic scattering of polarized neutrons from deuterium

Queen Mary College, London
Bedford College, London
AERE, Harwell

(ref. 200)

At energies of 50 MeV and below, the nd and pd systems seem to show systematic differences in differential cross-section, especially close to the deep minimum near 90°cm. Evidence is accumulating, first, that these differences remain pronounced at higher energies; and second, that differences occur also in the polarization parameter. An earlier experiment to measure the differential cross-section in nd elastic scattering near 130 MeV also showed differences between the pd and the nd systems.

The analysis of an experiment, to measure the asymmetry on scattering a beam of polarized neutrons from liquid deuterium, has now been completed. The beam polarization was determined by Schwinger scattering from a uranium target. This gave a measurement of the polarization parameter, P, in nd scattering. By replacing the deuterium with hydrogen, P for np scattering was also determined. This was found to agree well with previous determinations, giving confidence in our method of data-reduction. Our data has been divided into six energy intervals from 60 MeV to 110 MeV; at each energy we measured P at 5 or 6 angles. An example of the results is shown in Figure 54, this is an energy at which no pd polarization data are available. When these results are compared with existing pd data, no great discrepancy near the polarization maximum at θcm $\sim 100°$ is found, but it does seem that the nd measurements have a smaller (positive) maximum near θcm $\sim 155°$, than the pd.

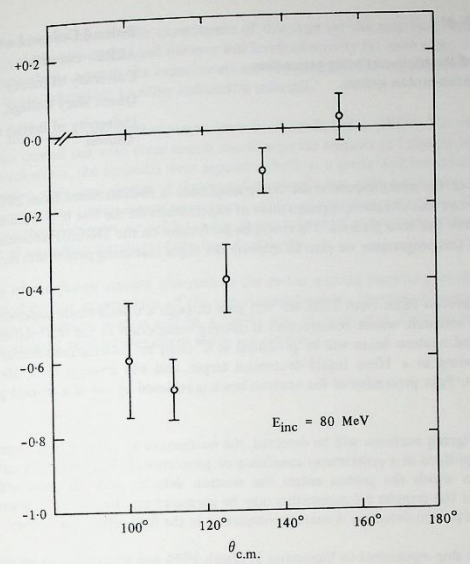

Figure 54. The polarization P (θ) in nd elastic scattering at an incident neutron energy of 80 MeV: Experiment 45 (15423)

EXPERIMENT 46

np total cross-section between 90 and 155 MeV

Queen Mary College, London
Bedford College, London
University of Surrey
AERE, Harwell

In an unpublished preprint (RPP/H103) Astbury drew attention to correlations between the structure seen in various hadron-nucleon total cross-sections. It was noted that "bumps" appear whenever the c.m. momentum reaches a value at which, in the πN system, production of nucleon isobars can occur in the s-channel. This peculiarity could have a simple explanation, on the basis of a naive constituent quark model of the hadrons.

A significant test of the universality of these correlations is afforded by the np system, in which the c.m. momentum, corresponding to Δ (1236) production in the πN system, is reached at 112 MeV. Present total cross-section measurements do not exclude the presence of a bump near this energy. A re-measurement of this quantity has been made, using the slow-spill neutron beam of the Harwell synchrocyclotron. Attenuation measurements were made in targets of graphite, and of paraffin wax of approximate composition $(CH_2)_n$. Both materials contained less than 5 ppm of impurity. The objective was to perform a highly precise measurement of the relative n–p total cross-section, as a function of energy. Because of Fermi motion within the nucleus, any narrow structure should be smeared in the n–C total cross-section. The data are now being reduced; we hope to have measurements in 15-20 energy bins, with relative errors of between ½% and 1%.

EXPERIMENT 47

Measurement of the triple-scattering parameters of the free neutron-proton system.

Bedford College, London
AERE, Harwell
University of Surrey
Queen Mary College, London
University of British Columbia, Canada

The I = 0 part of the neutron-proton scattering amplitude is ill-determined from 200 MeV upwards. To improve this situation, a programme of experiments on the free n–p system between 250 and 500 MeV has been planned. These will be performed on the TRIUMF accelerator, Canada. As part of this programme we plan to measure the triple scattering parameters R, A, D, R_t, A_t, D_t.

The polarized proton beam from TRIUMF will pass through a 6 tesla-metre super-conducting spin precession solenoid, whose construction is nearing completion in the Rutherford Laboratory. A polarized neutron beam will be produced at 8° (lab) by polarization transfer in quasi-free p–n scattering in a 10cm liquid deuterium target, and will impinge on a 30cm liquid hydrogen target. Spin precession of the neutron beam is achieved by use of a crossed pair of dipole magnets.

Both of the outgoing nucleons will be detected, the neutrons in an array of large plastic scintillators and the protons in a polarimeter consisting of proportional chambers and a carbon scatterer. Events in which the proton enters the neutron detector and vice versa will also be recorded so that the transfer ($_t$) parameters may be measured simultaneously. Construction of the neutron and proton detectors is nearing completion in the Rutherford Laboratory.

It is intended to ship equipment to Vancouver in March 1974, and to start the experiment when TRIUMF commences operation later in the year.

EXPERIMENT 48

Search for superheavy elements

University of Manchester
University Research Reactor, Risley
Rutherford Laboratory

(ref. 20, 21, 236)

In two previous Annual Reports experiments were described in which attempts were made to produce superheavy elements by secondary reactions in targets irradiated by high energy protons. It was suggested that energetic heavy recoils from proton-nucleus interactions might interact with other target nuclei to produce superheavy elements. These elements have been predicted to exist in the region of the possible closed shell of protons at around Z = 114.

In the early experiments spontaneous fission activity was observed in a mercury source separated from a Tungsten target which had been irradiated with 24 GeV protons from the CERN PS. It was suggested that the observed activity could be due to element 112 which would be the chemical homologue of mercury. Such an identification could be in error due to contamination of the source and this point was considered in some detail. Subsequent work in which some physical properties of the fission activity were measured did indicate that some of the activity at that later time could have been due to contamination by ^{252}Cf. However it did not seem that either all the activity then observed could be explained in that way, or that the activity observed in the early stages of the experiment was due to Californium contamination.

Two of the main problems with experiments of this type are the very long target irradiations required (typically 6 months) and the very low levels of activity (at most a few counts per day) to be measured. As a result the experiments are very time consuming, difficult to repeat and also open to contamination by other radioactive material.

Since the initial work two further targets have been irradiated at CERN. The chief aim of the experiments carried out with these targets was to separate element 112 and, in order to test the reaction mechanism, the actinides were separated both as a group and individually. The chemical techniques were very similar to those used previously but with some improvements. However no spontaneous fission events were seen in either the mercury or actinide fractions. These experiments therefore gave no evidence for the existence of superheavy elements or for the occurence of secondary reactions of the type postulated.

The origin of the fission activity observed in the earlier sources remains unexplained despite a very detailed further examination of the experimental results. However it seems unlikely that the secondary reaction process will be a useful way of producing superheavy elements and future experiments must rely on direct heavy ion reactions.

EXPERIMENT 49

Test of T-invariance in neutron beta decay

ISN, Grenoble
ILL, Grenoble
Yale University
Rutherford Laboratory

An experimental test of time-reversal invariance in the beta decay of the neutron is now in progress in collaboration with the Institut des Sciences Nucléaires (ISN), Grenoble, and Yale University. The test consists of a search for a term in the neutron decay rate proportional to $\vec{p} \cdot (\vec{p}_e \times \vec{p}_p)$ where $\vec{p}$ is the neutron polarization and $\vec{p}_e$ and $\vec{p}_p$ are the momenta of the decay electron and proton respectively.

Previous experiments testing time-reversal invariance in neutron beta decay have reached a precision of only about 1%, where the limiting factor has invariably been the extremely low coincidence counting rate, of the order of one per minute. This experiment is being performed at the ILL, Grenoble, where the use of a polarizing cold neutron guide tube yields a large increase in beam intensity over previous experiments. Further improvement is achieved with more efficient detection geometry. The overall count rate for 8 detector pairs is therefore about 100 per minute. By the end of 1973, 1·5 million events had been observed which, when analyzed, will permit a limit of 0·3% for time-reversal violation in neutron beta decay.

Radiological Experiments

π^- mesons are potentially superior to γ and X rays for radiotherapy. The basic properties which are important in this application are (i) the well defined range, for mesons of a definite momentum, with most of the energy being given up at the end of the range and (ii) the nuclear absorption process of stopped mesons; the resulting heavily ionizing products can cause local damage even in oxygen starved cancerous tissue.

During the year the programme of evaluating these predictions using a number of different cell systems has been continued. The results of further π^- irradiations of cultured cancer cells (HeLa type), mice haemopoietic colony forming units and broad beans are contained in the following reports. In addition two new systems have been introduced: aberrations in the chromosomes of human lymphocytes and the formation of cataracts in mice. Results are also reported for these experiments.

In support of the radiobiological experiments the parallel programme of physics measurements using specially designed instruments has been continued. A detailed design study for a new π^- beam, suitable for a clinical trial, has been carried out. Using the predicted intensity for Nimrod with the new injector a π^- irradiation dose rate of $\sim$ 10 rads min^{-1} over a volume $\sim$ 10 x 10 x 10 cm^3 looks feasible. Details of this work are given below.

Experiments with frozen cancer cell cultures (HeLa)

Glasgow Institute of Radiotherapeutics
Rutherford Laboratory

The group from the Glasgow Institute of Radiotherapeutics have continued their collaboration using frozen HeLa cells which enable the physical effects of various pion doses to be monitored at the Laboratory with subsequent assay of the biological response in Glasgow. The main reason for using frozen cells is that there is negligible dose rate effect. A much smaller sized polypropylene ampoule has been designed to enable cell samples to be irradiated at better defined positions along the depth dose profile on the beam axis and on either side.

Previous studies had established the Relative Biological Efficiency (RBE) for pions at the peak to be 1·86 ± ·15 (and 3·73 ± ·3 for 14 MeV neutrons) compared with 300 kV X-rays, using this frozen HeLa cell system assayed for survival of colony forming ability. Further studies in 1973 have now shown that the dose response curve with cells irradiated at the pion plateau region is not significantly different from that obtained using 300 kV X-rays, i.e. the RBE is unity. Intermediate values are observed just in front of the peak and in the tail behind. The data are being analysed.

Haemopoietic colony forming unit (CFU-S) survival

Medical College of St. Bartholomew's Hospital, London

Following the results from 1972, a further CFU-S experiment irradiated bone marrow cells for one exposure for 4·5 h, in three positions – the peak, plateau and behind the peak. Figure 55 shows the three π^- meson survival points in relation to a dotted reference curve for CFU-S irradiated with 14 MeV electrons at a dose rate of 400 rad s^{-1}. There is no significant difference in effectiveness between peak and plateau π^- mesons. This finding confirms our 1972 results, and is in line with much current data for RBE values for CFU-S irradiated with fast neutrons and X-rays.

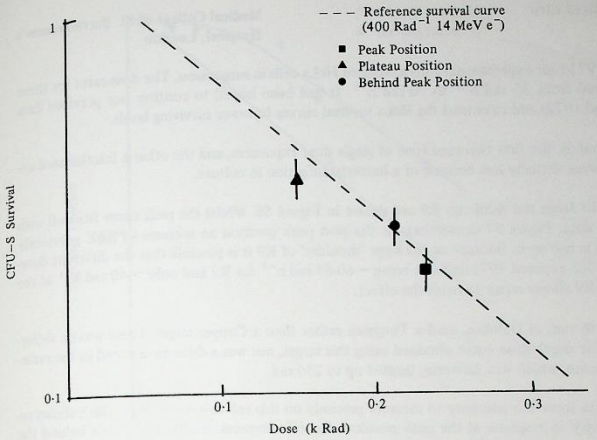

Figure 55. Haemopoietic colony forming unit survival when irradiated by π^- mesons (15426)

Lens Opacities

Medical College of St. Bartholomew's Hospital, London

About 450 1-day old mice were irradiated in three out of four runs in 1973. Eight mice were irradiated per exposure – 4 in the plateau and 4 in the peak. The irradiations were to the head only since the 2 cm^2 80% isodose field was too small for whole body radiation. For comparison purposes a group of mice were given 200 rad ^{60}Co γ-rays at 1·5 rad min^{-1} – a dose rate strictly comparable with that of the π^- mesons. (Subsequent scoring of the lens opacities was with the naked eye).

The results to date are encouraging, and more opacities are expected with time. The preliminary data by December, from SAS/4 mice irradiated in June and August are given in the Table below, with results from the ^{60}Co irradiation. At present no RBE values can be obtained from these early results but they do provide ample evidence of the need for further data at both lower and higher π^- meson doses, as well as the relatively high 'sham' incidence over 25%, compared with control mice with 15-18%.

Incidence of Lens Opacities in Irradiated Mice

Group I; 6 months after irradiation π^- mesons 1-2 rad. min^{-1}		Group II; 4 months after irradiation π^- mesons 1-2 rad. min^{-1}		Group III; 5 months after irradiation ^{60}Co γ 1·5 rad. min^{-1}	
Dose (rad)	% incidence of lens opacities	Dose (rad)	% incidence of lens opacities	Dose (rad)	% incidence of lens opacities
O-sham	15 (2 out of 13)	O-sham	28 (31 out of 109)	O-sham	19 (5 out of 27)
40-plateau	14 (1 out of 7)	O-(control*)	18 (12 out of 66)	200	68 (42 out of 62)
60-peak	58 (7 out of 12)	136-plateau	57 (30 out of 53)		
120-plateau	65 (11 out of 17)	200-peak	71 (34 out of 48)		
180-peak	53 (8 out of 15)				

(* mice taken to Rutherford, but not 'sham' irradiated in block house)

A further group, C3H neonates irradiated in January 1973, have not been possible to score for lens opacities.

HeLa cells in vitro

Medical College of St. Bartholomew's Hospital, London

During 1973 four experimental runs irradiated HeLa cells in suspension. The dose-rates for these runs varied from 35 rad h^{-1} to 70 rad h^{-1}. It had been hoped to confirm our previous data (1971 and 1972) and to extend the HeLa survival curves to lower surviving levels.

Unfortunately the first two runs (one of single dose exposures, and the other a fractionated exposure) were virtually lost because of a bacterial infection in culture.

The results from the third run R9 are shown in Figure 56. Whilst the peak curve fits well with previous data, Figure 57 shows that for the post peak position an increase in RBE previously observed is not seen. Because of the large 'shoulder' of R9 it is possible that the different dose-rates for R2 exposed 1972 and R9; being ~ 60-65 rad h^{-1} for R2 and only ~ 40 rad h^{-1} at the peak for R9 allows repair to mask the effect.

The fourth run, in October, used a Tungsten rather than a Copper target. There was no difference in the depth-dose curve obtained using this target, nor was a difference noted in the radiation response, which was, however, limited up to 250 rad.

These data show the necessity to measure precisely on this cell culture system, which shows reproductivity in response at the peak position, the effectiveness at different points behind the peak. The problems of dose-rate effects must also be clarified, as to whether they are due to low LET contamination components only or would be expected in a clean π^- meson beam also.

Figure 56. HeLa survival in peak positions. Position C straddles the peak of the ionization curve which is similar to that of Figure 59. Position B is 1·4 g/cm^2 before this, and the post peak position (as for data on Figure 57) is a similar depth beyond the peak (15427)

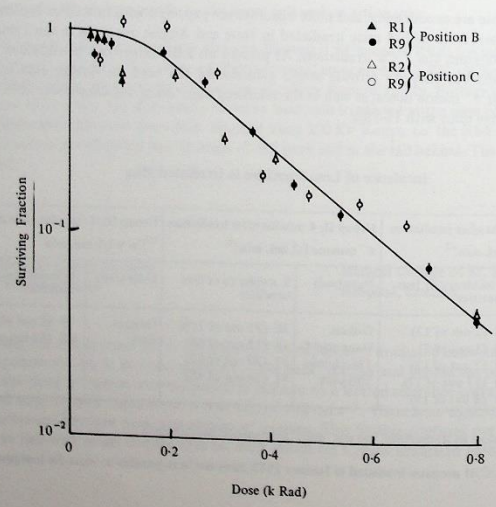

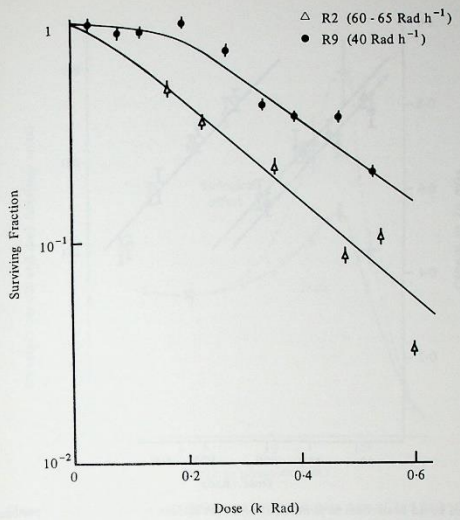

Figure 57. HeLa survival in the post peak position (15421)

Effects of the radiation at the entrance point of a negative pi-meson beam on broad bean roots

Churchill Hospital, Oxford
Rutherford Laboratory

During 1970-72, a group from the Research Institute of the Churchill Hospital, Oxford used the broad bean root to investigate the biological effect of the radiation in the peak and plateau region of the π^- beam.

Because of the unexpectedly high effectiveness of the plateau region which was found in these studies, an additional experiment was performed during 1973 to investigate the effects of the radiation at the entrance point of the beam from air into the water phantom.

The perspex water tank phantom used in the original experiments was modified to facilitate irradiations as close to the surface as possible. The point at which the beam entered the water was closed with a sheet of Melinex of thickness 0·05 mm. A new irradiation rig was constructed, which enabled irradiations to be performed simultaneously at the surface position and, for comparison, at the original plateau position 1. The front face of the root compartment was also constructed from 0·05 mm Melinex sheet so that the average distance of the bean roots from the air was half the thickness of the root compartment, or 3·4 mm.

Eighteen groups of twelve beans each were used in the experiment, giving four dose points under each set of conditions (aerobic or hypoxic, plateau or surface position), together with two control groups. The results with standard errors are shown in Figure 58.

The Oxygen Enhancement Ratio (OER) was 2·08 in the plateau region with 95% confidence limits of 1·83 - 2·32 (cf. 2·04 with confidence limits of 1·89 - 2·19 in the original series). In the surface position, the value was 2·33 (limits 2·07 - 2·60). The RBE of the surface position relative to the plateau was 1·14 (limits 1·01 - 1·27). The results show an apparent inconsistency in that both the OER and the RBE increase from the plateau to the surface.

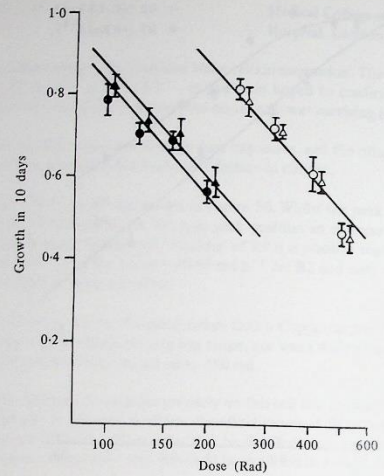

Figure 58. Response of broad bean roots to pion radiation at the surface (circles) and at the plateau (triangles) of the depth dose profile in a water phantom. The open symbols refer to data taken under hypoxic conditions. (14916)

Experiments with human lymphocytes

National Radiological Protection Board
Rutherford Laboratory

Human blood samples were placed at various positions in a plastic phantom, exposed in the π 11 beam, and analysed for damage to lymphocyte chromosomes. The purpose of the work is to provide initial biological information as a function of depth in the phantom. The data on aberration yield will be useful in extending the basis on which the human lymphocyte is used as a dosemeter for people exposed to radiation. Three experiments have been performed and the microscope analysis of the aberrations is almost complete.

Study of the chromosome damage along the depth/dose profile

1 ml blood samples were exposed in the plateau and at four positions about the peak for doses of 70, 130, 210, and 360 rads at the peak position. This provided a profile of biological damage for comparison with the ionization depth profile, and showed that, for example, at the 360 peak rads case the biological effect peak to plateau ratio was 2·6 ± 0·4, an enhancement over the dose ratio of 1·6 ± 0·3. At a distance of 2 cm behind the peak the damage had declined to below plateau values, and we did not observe the further enhancement expected at the rear edge of the dose peak. Figure 59 shows the profile obtained for the 5 positions for a peak dose of 360 rads.

Study of dose rate dependence

Experiments using ^{60}Co and 250 kV X-rays reveal a dose rate effect on the production of chromosome aberrations. Exchange aberrations such as dicentrics normally require damage to two adjacent chromosomes (two hits) and for low LET radiation these are each produced by separate ionising tracks. Thus when the dose is spread out in time the chance of two damaged chromosomes recombining to form a dicentric is reduced. As the LET is raised a greater proportion of the two hits are produced by a single ionising track thus removing the dose rate effect. In the first exposure the doses were delivered at 25 rad/hr as measured in the peak position. Further exposures were carried out at 18 and 70 rad/hr and all the peak points have been plotted in Figure 60. There is no detectable dose rate effect and this is in accord with the high LET events occurring in the peak position. The plateau data have yet to be analysed.

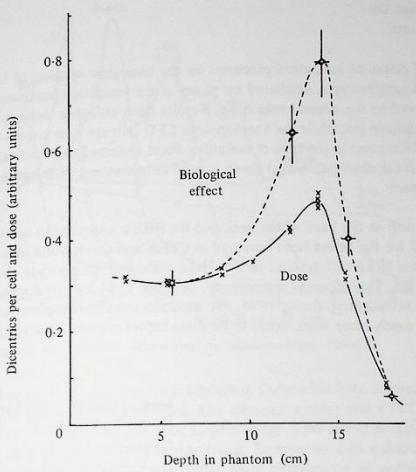

Figure 59. Chromosome aberrations in lymphocytes for a peak pion dose of 360 Rad. (15424)

Study of the fractionation effect

Fractionation is an alternative method of spreading a dose out in time. With low LET radiation, as in the pion plateau, it reduces the dicentric yield, but this effect was xpected to be less marked in the high LET peak. To investigate this effect on the peak to plateau ratio, tubes of blood were exposed so that those in the peak received 200 rads. The dose was delivered in two equal fractions separated by 0, 0·5, 4·2, 6·3 and 24 hours. With a 24 hour interval, such as is commonly used in radiotherapy, the dicentric yield was found to be 26% lower in the peak and 41% lower in the plateau than when the dose was not split. Should this indication of an improved peak to plateau ratio (by 1·25 ± 0·4) be confirmed it will make the π^- beam even more attractive for radiotherapy.

Figure 60. Chromosome aberration in lymphocytes for various doses and dose rates at the peak (15428)

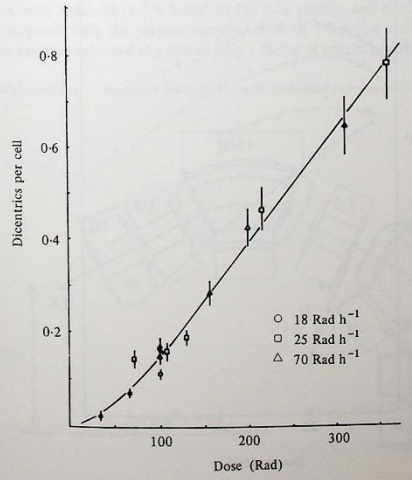

Summary of results from the
radiobiology experiments

There is an enhanced effect of ionization processes on the biological systems of broad beans, frozen HeLa cells and lymphocytes, irradiated by pions, at the ionization peak near the end of the pion range compared to the normal behaviour. Results from unfrozen HeLa cells and mice cataracts are too preliminary yet, while the haemopoietic CFU cells are now known to be particularly insensitive to differences in the type of radiation. Plant systems like broad beans are very sensitive, so the additional observation that there is little enhancement at the surface is of obvious practical importance.

Pions predominantly stop at the back of the peak and the RBE is expected to be highest there. This was seen in 1972 for the broad bean here and at CERN and also for unfrozen HeLa cells. But this year this same HeLa cell system, frozen HeLa cells, and lymphocyte aberrations all failed to show the effect. This apparent discrepancy, be it due to biology or dosimetry, will be subject to a thorough investigation during 1974. The situation remains that pions are promising for radiotherapy, but much more work needs to be done before anyone can attempt to treat a patient.

Physics experiments

Medical College of St. Bartholomew's Hospital, London
University of Leeds
Rutherford Laboratory

Small volume, parallel plate, tissue equivalent proportional counters, after the design of Rossi, are being developed. Spectra of ionizing events at various positions in the pion beam have been obtained, but suffer from instability problems. Work continues to make these tools reliable, and to simulate different types of tissue.

Figure 61. Particles leaving carbon surface at 90° within the pion peak region (15013)

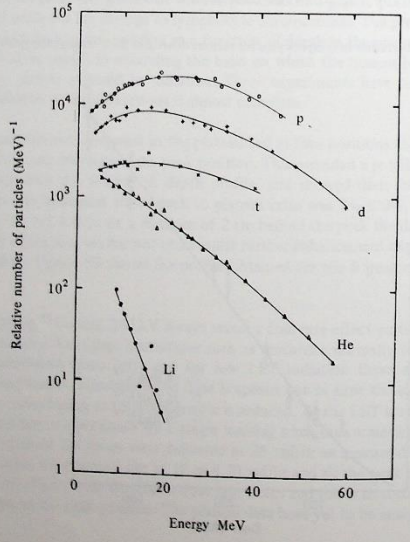

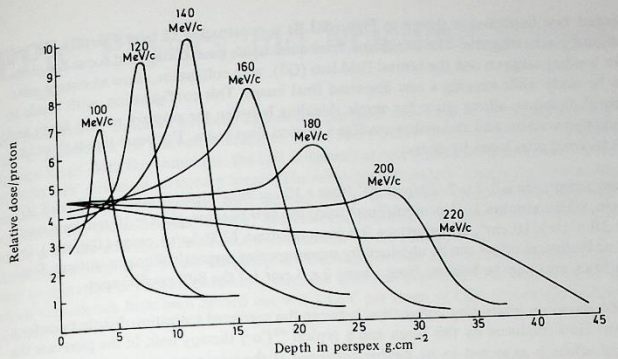

Figure 62. Depth-dose profiles for various beam momentum settings (14681)

The charged particle spectra from pion capture in Carbon has been studied. Protons, deuterons, tritons, He and Li nuclei were identified. The detector system was a Si/CeI vacuum telescope, measuring rate of energy loss and total kinetic energy. Two sets of detectors of different thicknesses were used to cover a wide energy range. To improve data collection rates a very thick target was used, particle production spectra being obtained by an unfolding technique. However, the unmodified thick target spectra are also relevant to radiobiological studies, as they represent a good approximation to the particle fluxes crossing a small volume element in a solid absorber. Some results are shown in Figure 61. A further study underway is to observe changes of the flux of secondaries at a bone soft tissue interface using thin emulsions.

New modes of operating the meson beam have been explored. It has been discovered that use of a Tungsten target yields 40% more pions than a Copper target, with no obvious increase in electron contamination as indicated by the similarity of the depth dose profile and the biological effect on HeLa cells. Further the second harmonic RF cavity in Nimrod is expected to add 50% to the flux. A series of depth dose profiles for different beam momentum settings are shown in Figure 62. By using suitable settings sequentially it will be possible to study the biological response to a flat peak of any reasonable thickness. Further by using new focussing conditions a larger spot has been obtained (3·5 x 5 cm^2 at the 80% profile, and 6 x 7·5 cm^2 full width at half height compared with the present standard spot of 1·9 x 2·4 cm^2 with 3·4 x 4·4 cm^2 f.w.h.h.). This has been achieved at a loss of only a factor of two in peak intensity.

Figure 63. A high intensity π^- beam line designed for radio-biological experiments (14693)

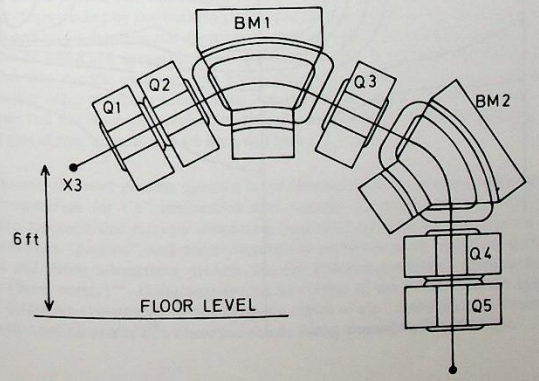

A high intensity π^- beam for radiobiological experiments (ref: 125, 126)

A proposed new beam line is shown in Figure 63. It is constructed of large aperture (40 cm) conventional electromagnets. The initial and final quadrupole pairs collect and focus the pions. The two bending magnets and the central field lens (Q3), with collimator, allow an energy selection to be made while keeping a non dispersed final image. This configuration, with bends in the vertical direction, allows space for ample shielding between the primary proton beam and the irradiation volume, and also makes possible a vertical final beam. The beam line is short (8·1 meters) to avoid pion losses by decay.

The basic acceptance is 1·2 sr % $\Delta p/p$ at 90° from a 10 cm long target. A predicted flux of 10^{10} pions/min, which assumes 10^{13} protons/burst using the new injector, gives ~ 10 rads/min over a volume 10 x 10 x 10 cm^3. Distributions flat in momentum (20%$\Delta p/p$), range (10g/cm^2), ionization or biological effect can be obtained by superimposing magnet/collimator settings. Similarly the beam area may be built up from a basic 2 x 5 cm^2 (at the 80% profile) spot.

Figure 64 shows an interesting comparison between the predicted ionization distributions for a three port field produced by this beam and a typical ^{60}Co γ therapy unit. In the pion case the biological effect is expected to be further enhanced at the treatment region where the pions stop.

Figure 64. Triple field isodose contours for π^- and γ (15112)

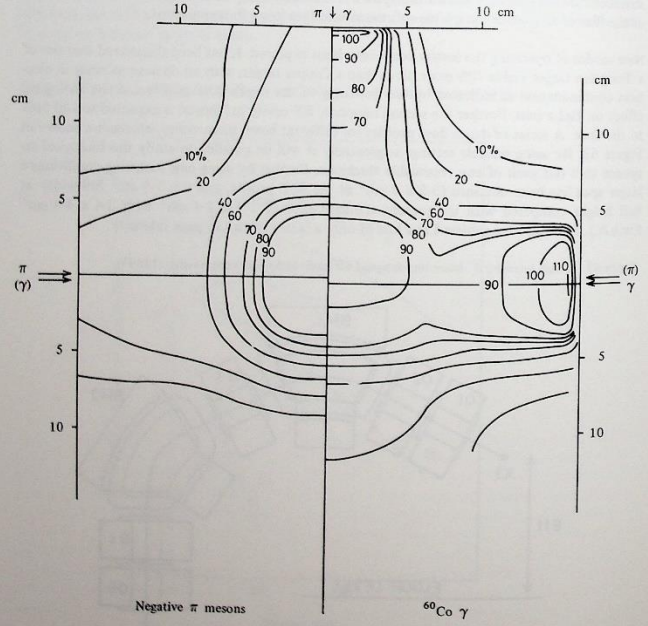

EPIC Physics and Machine Studies

The most violent collisions between elementary particles which can be produced in the laboratory at present are the head-on interactions in the two 30 GeV beams at the CERN Intersecting Storage Rings. With this technique, the ISR is equivalent to a conventional beam with an energy of 1900 GeV striking a stationary target. The reliability of modern storage ring technology has stimulated interest in exploiting their unique ability to outstrip conventional accelerators in equivalent (or center-of-mass) energy, despite their limitation to collisions between particles which are stable and can be stored for several hours. At the present time, in addition to the proton-proton storage rings of the ISR, there are electron-positron and electron-electron rings in or near to operation in France, Germany, Italy, the USA and the USSR. The maximum energy at which experiments have been carried out is 2·5 GeV per beam at CEA (Harvard), in electron-positron collisions.

Electron-proton intersecting storage rings with a center-of-mass energy in the ISR range were first suggested in 1971 by a SLAC-LBL group. Before the end of that year, accelerator physicists from the Rutherford and Daresbury Laboratories came to the conclusion that it might be possible to build an Electron Proton Intersecting Complex on the Rutherford Laboratory site. Design work in 1972 had such promising results that it was decided to invite the high energy physics community in the universities to join with the staff of the laboratories in a detailed assessment of the physics interest and feasibility of a complex at which one could study the collisions of 14 GeV electrons with 14 GeV positrons and up to 200 GeV protons and deuterons. With a luminosity of about 0·4 x 10^{32} cm^{-2} sec^{-1} reasonable event rates (event rate = luminosity x cross-section) can be achieved.

More than 78 people, the majority from the universities, met in 8 working groups throughout the summer of 1973, and came together at the Rutherford Laboratory in October for a full week to assess progress. The very exciting programme of fundamental physics which emerged from this work is described below. A much smaller group is now preparing a summary of the case for building EPIC, to be submitted to the SRC in 1974. The present idea is to begin with 14 GeV e^- on 14 GeV e^+ in a single ring, to which a proton ring could later be added. International collaboration would be welcomed at any stage, and would be necessary to go beyond the initial e^+e^- stage, which could be built by the UK alone. The physics programme covers many important areas inaccessible to the CERN programme and would be comparable in size with the present research programme on our national machines.

The Physics Case (ref. 101, 108, 116, 118-123, 138, 141, 145, 153, 176, 211, 212, 235, 249, 253, 254, 256, 260, 269, 274, 282-284, 292, 293, 309, 328)

The breadth of the physics case can be seen from the Table, which is an attempt to summarise the many reactions studied by the working groups and discussed in some 95 reports. In the case of both e^+e^- and ep(D), fundamental questions relating to weak, electromagnetic and strong interactions can be asked and answered. These questions will still be relevant when EPIC is built. They are also very specific questions. We know about them now and can only suppose that EPIC will be like other machines which broke new ground in the past, where the most significant questions had not been conceived at the time it was proposed to build the machine. A few of the highlights of this minimal case are discussed below.

In e^+e^- collisions, the most pressing question is the ultimate form of the energy dependence of the total cross-section for e^+e^- annihilation into strongly interacting particles. The parton model, which supposed that strongly interacting (hadronic) particles are made up out of elementary, point-like "partons", and which successfully correlates many results in electromagnetic, weak and strong interactions, predicts that this hadronic annihilation cross-section will decrease as (beam energy)$^{-2}$. Unfortunately, the translation of the model from the space-like domain of scattering experiments to the time-like region of e^+e^- annihilation is theoretically difficult so that one cannot be sure where this simple energy dependence should begin.

Reaction	Experiments, Significance
$e^+e^- \rightarrow e^+e^-$	Tests of QED.
$\gamma\gamma$	Absolute luminosity monitors.
$\rightarrow \mu^+\mu^-$	Test of QED. Photon-neutral current interference.
→ new particles	Heavy leptons, bosons etc., $M \leqslant 14$ GeV, if they exist.
→ e^+e^- + leptons e^+e^- + photons	Direct study of higher order QED processes.
→ hadrons	Asymptotic behaviour of total cross-section. "Measure" parton charges or observe breakdown of old theories or new interactions.
	Final state hadron distributions, multiplicities and types for energy → matter in $J^{PC} = 1^{--}$ state.
→ e^+e^- + hadrons → $e^+e^-\rho^\circ\rho^\circ$	Total cross-section, particle distributions, specific final states. Are these "photon-photon" collisions like hadron-hadron collisions?
ep → e hadrons	Small q^2 limit ≡ photoproduction beyond energy range reached by ISR for pp. Does σ_{TOT} rise? Production of high mass diffractive states? Final state particle distributions. Individual channels.
	Finite q^2, large ν gives measure of structure functions at large ω. Is scaling still observed? Are there thresholds for new quantum numbers, such as Charm?
	Deep inelastic tests scaling to limit. Interference with weak neutral current?
	Studies of final state hadrons vital to models. Can be said "measure" parton quantum numbers.
ep → ν hadrons	Is P-violating weak interaction stronger than EM? What is mass of intermediate boson?
eD → e hadrons	Complementary questions to ep case.
→ ν hadrons	Target viewed as D (coherent diffractive) or n.

Recent experimental results from CEA at Harvard and SPEAR at Stanford show an unexpectedly large and apparently constant cross-section at beam energies between 1·5 and 2·5 GeV. The energy of 14 GeV per beam proposed for EPIC is sufficiently high that a serious re-examination of the significance of the model would be necessary, if the $(\text{energy})^{-2}$ behaviour were not by then established. If the predictions of the parton model were fulfilled at EPIC, then the sum of the squares of the charges of the partons could be deduced from a knowledge of the absolute value of the cross-section, and it would be possible to decide which (if any) of the quark models is correct, though the significance of such a measurement goes far beyond any model. In a sense, one would be counting the total number x (charge)^2 of all independently existing fundamental sub-units of matter. A study of the detailed distributions of the final state hadrons would then give important information about the interaction which turns the unobserved partons into the particles we know.

Independently of any model, an indefinite continuation of the present behaviour would lead to serious trouble with quantum electrodynamics (QED) and with unitarity. Since QED is the only theory we have which is capable of apparently unlimited precision in both low and high energy phenomena, it is of the utmost importance to make sure that the cross-section for $e^+e^- \rightarrow$ hadrons has an acceptable high energy behaviour and also to check QED directly in the EPIC kinematic range. Several e^+e^- reactions permit tests of complementary aspects of QED at EPIC.

The very specific predictions of QED for certain reactions provide sensitive tests for new phenomena. For example, a weak neutral current of the type suggested by the results of recent neutrino experiments at CERN would behave like a heavy photon and would be expected to interfere with the ordinary photon of QED. One of the most popular models for this new current predicts easily measured effects of the order of 14% in the angular distribution of the muons in the reaction $e^+e^- \rightarrow \mu^+\mu^-$, at EPIC energies. The effect is proportional to the square of the beam energy and cannot easily be studied at lower energy machines. The transverse polarization expected in the EPIC e^+e^- beams is important for this experiment.

Reference could also be made to searches for new pair-produced particles, about photon-photon collisions and about each of the many reactions which can be studied in the ep or eD case. We will just comment on one more.

In ep collisions at EPIC energies, the weak interaction process ep → ν + anything will have a larger cross-section than the electromagnetic ep → e + anything in a substantial fraction of the kinematic region, if the scaling behaviour observed at SLAC, CERN and NAL in electromagnetic and weak interactions persists. Detailed studies show that event rates for the weak process would be between 10 and 50 per day in that case. They also show that the momentum and energy transfers, q^2 and ν can be measured with an accuracy of a few percent even in the weak processes where there is no observable final state lepton. The event rates quoted are comparable with those in previous neutrino experiments. The physics interest is to see whether the parity violating weak interaction does approach and exceed the electromagnetic in strength or if it is suppressed by some mechanism, such as the intermediate boson. At the very least, such an experiment would measure the mass of the boson.

Technical aspects of experiments (ref. 106, 154, 155, 166, 171, 177, 201, 205, 206, 270, 305-308, 314, 321)

The technical aspects of experiments with EPIC were studied in detail. These included estimates of electromagnetic backgrounds, studies of desirability of bunched beams, the amount of energy variation required, the provision of test beams, the possibility of rotating the natural transverse polarization of the electron beam into the longitudinal direction, and many other topics.

The design of apparatus was carefully examined. A most encouraging result is that all of the experiments proposed could be carried out with apparatus of the type currently in use at many laboratories, using known technology. The apparatus is not very different in size from several at present in use. The most versatile and the largest of the devices proposed during the study is shown in Figure 65. This large solenoid and its associated detectors would be expected to be continuously in use for both e^+e^- physics and for ep physics throughout the life of EPIC, and to be used by several different groups of physicists.

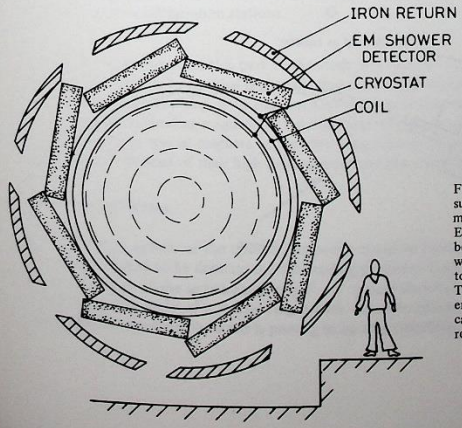

Figure 65. Schematic diagram of superconducting solenoid spectrometer 3 m diameter, 6 m long, for EPIC. The magnetic field would be 1·0 tesla. Wire spark chambers with a total of 10^5 wires are used to measure particle trajectories. The walls of the solenoid are thin enough to permit particle identification outside the magnetic field region.

Machine Studies (ref. 149, 150, 192, 193, 195, 216-220, 223, 224, 226-234, 261, 271-273)

A complex consisting of two storage rings has been designed in collaboration with Daresbury Laboratory and the Physics Working Parties. The rings, of average radius 349 metres, occupy the same tunnel, and four collinear interaction regions are provided by means of vertical bending magnets. The system could be built in two stages: the first ring would be used to study electron-positron collisions at centre of mass energies up to 28 GeV. The second ring for protons would comprise either conventional or superconducting magnets, allowing momenta of 80 or 200 GeV/c respectively. The essential parameters of the e^+e^-, e^-–p options (other options are theoretically possible) are shown in the Table below:

Beam Momenta (GeV/c)			Centre of Mass Energy (GeV)	Luminosity/Interaction Region (cm^{-2} sec^{-1})
Electrons	Positrons	Protons		
14	14		28	$0{\cdot}4 \times 10^{32}$
14		80	67	$0{\cdot}25 \times 10^{32}$
14		200	106	$> 0{\cdot}25 \times 10^{32}$

Electron-Positron Ring

The 5 GeV electron synchrotron, NINA, will be modified for use as the booster-injector for EPIC. Inserted into its lattice will be 20 quadrupoles (for changing the Q-values) and 10 damping triplets, which will serve to reduce the beam size in NINA. The repetition rate will be reduced to 4Hz and an additional 10MHz RF system installed. Alternate pulses of electrons and positrons will be accelerated to 5 GeV/c and injected into EPIC at a rate of approximately 10^9 particles per pulse.

The filling time is expected to be about 15 mins when operation is to be at the maximum energy.

After acceleration to the required energy the beams are brought into collision and remain so until the event rate is no longer satisfactory. This "luminosity" lifetime is expected to be greater than 2 hours. The beams are then separated, decelerated back to 5 GeV/c, and topped up with the booster. The macroscopic duty cycle should therefore be about 90%.

Figure 66. A possible site layout for EPIC, showing the approximate dispositions of the linac injectors, the booster and the main ring (15466)

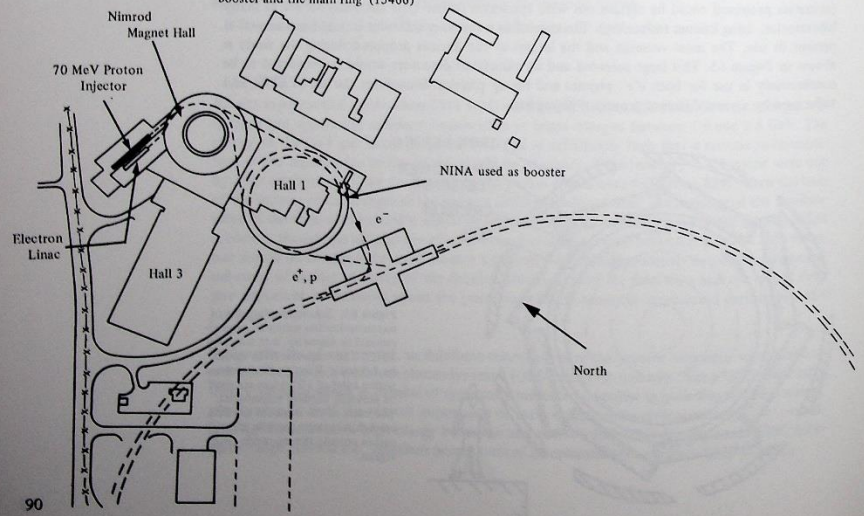

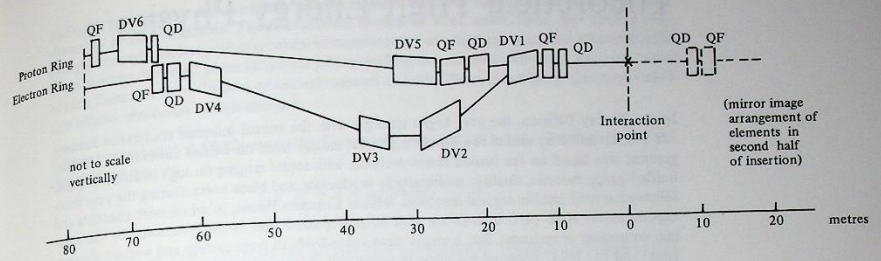

Figure 67. Vertical arrangement of lattice elements in a half e–p insertion (15465)

Electron-Proton System

The proton ring normal cells will lie 0·86m above the electron ring. Extra path length has to be provided for the electrons in order to maintain synchronism between them and the slower protons; this is introduced in the insertions by means of vertical bending magnets, which also serve to bring the beams together in the plane of collision.

The fact that there is negligible radiative damping of the proton betatron oscillations has many consequences, some of which are: (i) each of the four bunches in the proton ring must be filled from just one booster pulse, (ii) the proton RF accelerating system must have an extremely low noise content, (iii) the proton transition energy must be crossed with very little increase in longitudinal emittance, (iv) machine induced resonances must be minimised. The present indications are that these difficulties can be solved, but much further effort remains to be expended on them.

Superconducting Aspects

Superconducting magnets have two possible roles in EPIC: in the main ring to maximise the proton energy, and in the insertions to maximise luminosity. To assess at what stage the use of this technology would be technically and economically appropriate, a feasibility study has been made on the production of suitable magnets, assuming only slight improvements on existing technology.

It was necessary to assume special quadrupoles (using reverse shielding windings to cancel the fringe field) for the insertions, but very simple coil designs were chosen for the main ring, with the magnetic field restricted to 4·5 tesla at 4·2 K. Future experience may in fact allow higher magnetic fields (and correspondingly higher particle energies) particularly if a technology based on the superconductor Nb_3Sn (rather than NbTi) can be used. The refrigeration system would not require any great extrapolation of existing technology; about 10-15 kW at 3·6 K would be supplied from four refrigeration stations.

The overall conclusion from this part of the study was that the superconducting system would be technically feasible. In practice this means that the particle energy could be a factor of about 3 higher for a given size ring, with the cost/GeV no greater than that of conventional magnets. The use of superconducting magnets for the insertions may prove necessary to obtain acceptable luminosities. These special magnets will involve a significant amount of new development and prototype work because of their high field gradient and low fringe field specification.

Conclusions and Status

An e-p colliding system of the quoted luminosity could be built, although it is apparent that much work remains to be done on the outstanding problems. Current effort is being concentrated on the design of the initial single ring e^+ - e^- system for which a strong physics case exists. In this continuing study of a storage ring system, the close collaboration between theorists, experimenters and machine physicists is proving to be very stimulating.

Theoretical High Energy Physics

In the Theory Division, the year began strongly with the annual informal conference January 3rd-5th, attended by about two hundred people, mainly from the British universities. The programme was based on ten invited review lectures, with topics ranging through neutrino physics, unified gauge theories, duality, multiparticle production and black holes. During the year there followed several smaller topical meetings, held at Coseners House, in which both theorists and experimenters took part. Interaction with other physicists was further promoted by the summer consultant programme, that brought ideas and individuals from eastern and western Europe, Israel and the USA. Some of the areas in which our theorists have been active during the year are outlined in the paragraphs below.

Unified gauge theories (ref. 11, 54, 55, 68, 69, 70, 281, 304)

Among the most interesting and important developments in particle physics are unified gauge theories of the weak, electromagnetic and strong interactions. The coupling constant characterising the strength of the weak interactions is of order 10^{-6}, compared to values of order 10^{-2} and 10 for the electromagnetic and strong interactions, respectively. Despite their huge dissimilarities in coupling strengths, it has long been hoped to unify all these interactions in a single complete theory. In fact in other respects the weak and electromagnetic interactions are strikingly similar. The electromagnetic current couples to electric charge and all charges are found to be multiples of the charge on an electron; similarly all weak charges seem to be simply expressible in terms of one fundamental charge. Also both the electromagnetic and weak interactions appear to be vector in nature.

Models that unify the weak and electromagnetic interactions were originally proposed by Salam and by Weinberg in 1967. They suggested that the fundamental interaction may be mediated by vector bosons, associated with a gauge invariance of the second kind. This would explain naturally both the vector nature of the interaction and the universal charge associated with it. The difference in interaction strengths is explained if the bosons mediating the weak interactions (the $W^{\pm}$) have very large masses – more than 37 GeV/c^2. The square of this mass appears in the denominator of the lowest-order weak amplitude (see Figure (a)):

$$T(ab \to cd) = \frac{g^2}{q^2 - M_W^2}$$

where $g^2 (g^2 \geqslant e^2)$ is a universal coupling and q^2 is the square of 4-momentum carried by the W-boson. For small q^2 the large W mass will clearly make the effective strength of the interaction very weak compared to the corresponding electromagnetic process, mediated by the massless photon.

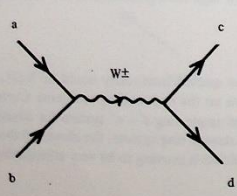

Figure (a)

Although such models are extremely elegant, interest was not fully aroused until they were shown to be renormalizable. The conventional models of weak interactions, that involve only charged currents, violate unitarity when extrapolated to very high energies. The renormalizable gauge theories, however, preserve unitarity by cancelling the conventional terms with new terms coming from new heavy leptons or neutral currents or both. Thus unified gauge theories predict new effects, observable at high energies.

A recent experiment at CERN, using the Gargamelle heavy liquid bubble chamber. looked for events of the type

$$\nu + N \to \nu + \text{anything}$$
$$\nu_\mu + e \to \nu_\mu + e$$

with neutrinos of 2-10 GeV. Since the photon does not couple to neutrinos, any such events can only be mediated (to lowest order) by a new neutral current. The exciting result is that such events were found, and at the level predicted by the Salam Weinberg model. Further experiments to check neutral currents are being run or planned, at several laboratories. Beside the neutrino scattering process above, it is also interesting to examine the reactions

$$e^+ + e^- \to \mu^+ + \mu^-$$
$$\mu + p \to \mu + \text{anything}$$

where the neutral current effects appear first as an interference with the electromagnetic term. In the former reaction, the purely electromagnetic term is precisely calculable. Other ways to isolate the new neutral current term are to exploit its parity-violating properties (using polarization) or to look for the effects of the associated neutral W-boson's mass.

There are difficulties in extending these models to include hadrons, because of $\Delta S = 1$ strangeness-changing terms. The conventional Cabibbo approach constructs the weak charged current using the combination $(n\cos\theta + \lambda\sin\theta)$ of n-quark and λ-quark operators. Thus the strangeness-changing and non-changing hadronic currents have comparable strength, and the same will be true of neutral currents constructed in this way. However, experimental evidence from $K_L \to \mu^+\mu^-$ and the K_1-K_2 mass difference shows that $\Delta S = 1$ semileptonic and $\Delta S = 2$ nonleptonic neutral currents are much smaller than the strangeness non-changing currents. Some reformulation is clearly required, at the very least.

It has been found possible to avoid direct strangeness-changing neutral currents for example by redefining the Cabibbo rotation. Alternatively, some models have been suggested which have no direct neutral weak currents. However the difficulty reappears in higher-order calculations, since strangeness-changing neutral currents can also be generated, from charged currents alone, via higher-order graphs (see Figure (b)). The contributions of these processes to the $K_L \to \mu^+\mu^-$ rate and to the K_1 - K_2 mass difference are enhanced, relative to second-order weak interactions, by a factor proportional to the W-boson mass – and exceed the experimental limits. Three ways to overcome this difficulty have been suggested.

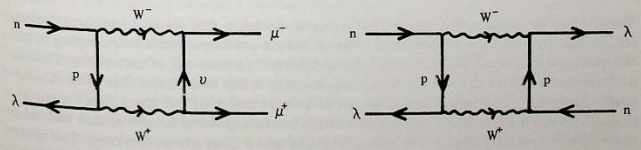

Figure (b)

Perhaps the most elegant solution is to introduce new "charmed" hadronic states. In the simplest example, one adds a new charmed p-quark p′ to the conventional triplet p, n, λ. If the observed low-mass hadronic states do not contain p′, there will be no new effects at low energy. However, the loop integrals implied in the second-order processes of Figure (b) will bring in high-mass charmed states: the graphs must be calculated with p′ as well as with p, and their contributions may be made to cancel. The direct neutral current is also cancelled. The degree of cancellation depends on the mass of charmed states, and can only be made consistent with experiment if charmed hadrons exist with masses of a few GeV – a prediction that should be testable. One difficulty with the simple charmed model above is that its basic hadronic symmetry is SU(4) rather than the observed SU(3). A solution is to have three quark triplets, which can naturally be classified in the leptonic symmetry while still generating SU(3) symmetry for low-mass hadronic states. Once again, new hadronic charmed states are predicted and should be observable.

An alternative way to suppress induced strangeness-changing neutral currents is to modify the scaling properties of the $\Delta S = 1$ current. This may happen through the appearance of anomalous dimensions (due to the strong interactions) or through the introduction of light vector bosons. The W bosons mix with these new bosons; it is the smallness of the mixing angle, rather than the boson mass effect, that makes weak interactions weak compared to electromagnetic, in this case. As a result, the second order effects are not enhanced. In either case, the non-scaling of the $\Delta S = 1$ charged semileptonic current provides a clear test of this idea.

Finally, one can arrange to suppress second-order effects without charmed hadrons or light vector bosons, by modifying the parity structure of the hadronic current from the conventional V-A form. Again this has consequences that should be accessible to experiment.

It is clear that any theory that incorporates hadrons is likely to predict new effects at presently available energies. Since purely hadronic weak interactions involve the product of two hadronic currents, they may display effects of the charmed current at energies below the charmed hadron threshold. Neutral weak currents give parity violating effects that can be looked for in nuclear transitions. The calculation of other higher-order effects is very interesting, in a renormalizable theory. For example, in the proton-neutron mass difference calculation, there is hope that the divergence coming from the electromagnetic contribution may be cancelled by the weak contribution, yielding a calculable result. In this and other ways, an immediate outcome of the unified theories has been to stimulate a re-examination of weak interaction effects.

The models discussed above have only dealt with the electromagnetic and weak interactions. Due to the strength of the strong interactions a perturbation series in the strong coupling constant does not converge and at the moment it is impossible to compute the physical effects of a field theory for the strong interactions. However, we do know that strong interactions must be included in a way that does not violate the gauge invariance corresponding to the weak and electromagnetic interactions. If this were not the case the renormalizability of these models would be spoilt and most of their attractive features lost.

Moreover in one region, the deep inelastic region, we know that strong interactions "switch off" in the sense that the experimental observations are consistent with a bare coupling of the electromagnetic or weak currents with fermion "parton" constituents of the nucleon. There is no form factor due to the strong-interactions. Recently it has been shown that a non-Abelian gauge theory for the strong interactions would indeed "switch off" in the scaling region. Although this result applies only to massless strongly interacting vector bosons, models with massive vector bosons may display this scaling behaviour over a finite momentum range. This raises again the exciting prospect of a unified field theory of the strong, weak and electromagnetic interactions.

Tests of the quark parton model in lepton scattering (ref. 107)

The scaling phenomenon in deep inelastic electron scattering has suggested that the proton contains pointlike constituents ("partons"). Further specific details, and preliminary results from inelastic neutrino scattering, are consistent with the exciting notion that these partons are in fact the quarks suggested long ago by Zweig and Gell-Mann as the basic building blocks for hadrons. More exacting tests of this idea can be made when better neutrino data become available. Since these tests are usually formulated for separated structure functions, requiring high quality data beyond the present or immediate future possibilities, it is important to see what can be done with low-quality data. It has been shown that significant predictions can be made for raw cross sections, for unnormalized event rates $N^{-1}\ dN/dx$ etc., and for distributions where the incident neutrino spectrum is not determined.

Proton-proton scattering (Ref. 17, 18)

Proton-proton scattering has particular interest in that it allows measurements both at the highest energies and also at the largest momentum transfers, thanks to the CERN intersecting storage rings and the high intensity of primary proton beams.

The high energy cross-section $d\sigma/dt$ gives a clear picture of pure diffraction scattering, that is also described as Pomeron exchange. Interesting structure is seen in the t-dependence, including a dip that develops near $t = -1{\cdot}4$ at ISR energies, suggesting that several interfering amplitudes are present with different phases and energy-dependences. An empirical analysis of this dip phenomenon has shown that it may be explained by three simple components: a Pomeron Regge pole, a constant background and a falling background contributing $d\sigma/dt \sim s^{-2}$, all with phases defined by their s-dependence and even $s \leftrightarrow u$ crossing. A resulting prediction is that the dip is most pronounced near 200 GeV/c where future NAL experiments are planned.

At large momentum transfers, any point-like "parton" constituents within the proton are expected to give characteristic effects. It can be argued that the dependence on transverse momentum p_T should be through a scale-independent formula, and indeed the formula $d\sigma/dt = a\ s^{-10}\ (p_T/\sqrt{s})^{-14}$ is known to describe pre-ISR pp data quite well for $p_T > 1{\cdot}5$ and $s > 15$. On the other hand, the new ISR data (extending to $p_T = 2{\cdot}5$) lie far above this formula and suggest that a limiting distribution $d\sigma/dt = f(p_T)$ is being approached instead. A resolution of this difficulty is to note that a two-term scaling formula can both reproduce the lower-energy fit to data and also reduce to a limiting distribution asymptotically. It is tempting to go further, and identify these two terms with the two background terms appearing above in the explanation of the dip, but a fully satisfactory form has not yet been constructed.

Extrapolating the πN amplitude to the $\pi\pi$ cut (ref. 133)

In the theory of nucleon-nucleon forces, the two-pion-exchange cut plays an important role. Since strong interactions are involved, there is no way to calculate this cut directly, but it can be determined from πN scattering amplitudes if the latter can be extrapolated from the physical ($t \leqslant 0$) to an unphysical ($t > 0$) region. One possible scheme is to take the first few terms in the partial wave series, eliminate $\cos\theta$ in favour of t, and extrapolate in t. This is unreliable, since the partial wave series itself diverges at the Lehmann ellipse; also there is no way to estimate the uncertainty in extrapolating. A new scheme has been devised, using the reproducing kernel of Hilbert spaces. Within this scheme, it is meaningful to speak of the error of the extrapolation – the norm of the difference between a function and its approximate. It has been proved that, requiring the approximate to have certain values at certain points in the physical region, there exists a unique set of basis functions for constructing the approximate. The criterion used is that the upper bound for the error is at its minimum. Furthermore, this procedure is independent of the original function, save that it must belong to the Hilbert space. Therefore, by constructing a Hilbert space that takes into account all our theoretical knowledge of the amplitude, we have an extrapolation procedure that is optimal and that also provides a measure of the uncertainties involved. As an example, the basis functions and the error functional have been constructed for πN scattering amplitudes. The final application to NN scattering is rather complicated and has not yet been completed.

Two-body amplitude analyses (ref. 52, 53, 58, 93, 136, 267, 312, 358)

There has been continued progress in the study of Regge exchanges in two-body processes at intermediate energies, mainly using the tool of amplitude analysis. The first amplitude analyses (see the 1971 Annual Report) concentrated on the momentum-transfer dependence at fixed, isolated energies; they showed the inadequacy of all existing Regge models and gave rise to several new models. Recent work has concentrated more upon the energy-dependence of amplitudes; it has again upset theoretical prejudices and has given valuable clues about a new, more realistic picture of Regge exchanges.

High energy amplitudes contain Regge pole contributions (which are fairly well understood) and absorptive cut corrections (which are not). In most models, these two components have different energy dependences, so the energy dependence of their sum is rather complicated. However, recent analyses of data have shown a simple energy-dependence, contradicting the models. In the πN system, amplitudes at relatively low energies show typical high-energy features and, taken together with high energy amplitudes, show that absorptive corrections have unexpectedly the same shrinkage as Regge poles. A study of the energy-dependence of the crossover effect gives the same conclusion, and K^0_S regeneration phases show that absorptive corrections have a Regge-pole-like phase. Furthermore, an FESR analysis of $\pi^- p \to \pi^0 n$ shows that amplitudes do not have the complicated energy dependence predicted by conventional absorption models. A consistent picture of the phase and energy dependence of absorptive corrections is beginning to emerge.

An amplitude analysis of the isoscalar exchange nonflip amplitude in $\pi N \to \pi N$ has given valuable information about the real parts of Pomeron and f^0 exchange amplitudes, over a range of intermediate energies and momentum transfers. Further evidence about duality and energy-dependence comes from an FESR study of the reactions $\pi N \to K\Sigma$ and $\pi N \to K\Lambda$. The results confirm that duality is alive and well in these reactions, but that the folklore that there are no cuts in spinflip amplitudes cannot be true for K*(890) and K*(1400) exchanges.

Amplitude analysis needs a concentration of different kinds of data (cross-sections and polarization parameters) for a given reaction. It therefore requires a co-ordinated experimental program, with collaboration between theorists and experimenters to establish which polarization measurements offer the best value for money. These questions were extensively discussed at a weekend meeting at the Coseners House in April.

Spin relations for pure natural or unnatural parity exchanges (ref. 147)

For elastic scattering, time-reversal invariance gives well-known relations between spin effects, such as the equality of recoil polarization from an unpolarized target and the asymmetry of scattering from a polarized target. Strikingly similar spin relations have been derived also for inelastic reactions, when the amplitudes are restricted in a particular way corresponding asymptotically to having purely natural or purely unnatural parity exchanges (called M-purity). Data indicate that high-energy vector meson photoproduction proceeds by purely natural parity exchange, so this case has been considered in some detail and compared with the analogous elastic case of Compton scattering, to bring out the similarities and differences between M-purity and T-invariance relations. The former relations can in general apply to much wider classes of situation than the latter.

Magnetic moment of Δ^{++} (ref. 132)

A recent attempt to measure the magnetic moment of Δ^{++} by $\pi^+ p \to \gamma\pi^+ p$ radiative scattering seemed to indicate a serious discrepancy between experiment and the magnetic moment $\mu = 5{\cdot}6$ given by the quark model. Since there were no alternative theoretical predictions for comparison, a new calculation has been performed within the bootstrap model of Δ. The resulting magnetic moment ($\mu = -2{\cdot}3$) is surprisingly different from the quark model values. Since there are still some unresolved questions in the experiment itself, there is no way yet to distinguish between these two models.

Multiparticle production, a probe for the Pomeron (ref. 38, 39, 56, 57, 62, 63, 64, 77, 78, 79, 130, 131, 210, 221, 259, 276, 353, 382, 383, 384)

The nature of the Pomeranchuk singularity, describing high energy elastic scattering and total cross sections, is a long standing mystery. It seems to have nothing to do with the t-channel particle spectrum, unlike ordinary Reggeons, and differs from the latter in other ways too. Nevertheless, a simple phenomenological description of multiparticle production has been possible, using two components: a non-diffractive part corresponding to multiperipheral production via Reggeon (R) exchange, and a diffractive part corresponding to Pomeron (P) exchange. The former part gives most of the total cross-section, and is regarded as generating a Pomeron pole in the elastic t-channel; the latter part generates a P–P cut correction: see Figure (c). However, this picture has lacked a precise dynamical description; many important details about cluster formation and decay were unknown, and also there was little knowledge of the overall diffractive component.

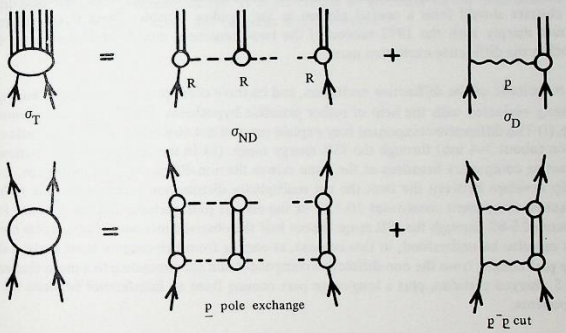

Figure (c) The two component picture

The last year has seen substantial progress, in which Rutherford theorists have played an active role. Firstly a dynamical model has been constructed for elastic scattering as a shadow of cluster production by Reggeon exchange. It uses semilocal duality in Reggeon-particle scattering, previously abstracted from the analyses of inclusive data (see 1972 Annual Report). Hence the cluster formation in Reggeon-particle (and Reggeon-Reggeon) channels may be expressed in terms of a few triple-Reggeon couplings, which are partly known from inclusive reactions: Figure (d). This approach can roughly reproduce the slopes, energy-dependences and shrinkage of elastic and charge-exchange scattering. There has also been an investigation of pp elastic scattering, using experimental non-diffractive and diffractive production as input; the observed break in the slope of $d\sigma/dt$ near $t = -0{\cdot}1$ is attributed to an interplay between the two components.

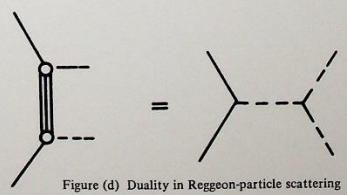

Figure (d) Duality in Reggeon-particle scattering

Progress in understanding the diffractive component was made possible by the ISR and NAL measurements of the inclusive reaction $pp \to pX$. Although the diffractive component is a small part of the complete cross-section, it is expected to peak in a specific kinematic region near $x = 1$, where $1 - x = M^2/s$ in terms of missing mass M and total c.m. energy squared s. The proton spectra from NAL and ISR clearly exhibit this peak, and show that the diffractive component dominates in this region. They provide a direct measure of the diffractive excitation, or in other words the Pomeron-proton cross-section (see Figure (c)). A significant feature is that the observed peak in $d\sigma/dx$ seems to scale (become independent of s) in the NAL–ISR range. In the Regge language this means that Pomeron-proton scattering is dominated by Pomeron exchange. This scaling of the leading proton peak had in fact been predicted from an analysis of Pomeron-particle scattering, based on 6–40 GeV data for $\pi p \to pX$ (see 1972 Annual Report).

The scaling of diffractive excitation implies that the excitation mass M has no cut-off. Instead the range of M^2 grows linearly with s: as energy increases, heavier clusters are excited. This has three important implications: the diffractive cross-section σ_D should increase with s; the diffractive multiplicity distribution should get broader with increasing energy, since heavier clusters are expected to decay into more numerous secondaries; the pions from high-mass diffractive clusters should form a central plateau in the rapidity variable. These three features all contrast sharply with the 1972 version of the two-component model, which assumed a fixed cut-off in the diffractive excitation mass.

The magnitude of the diffractive excitation, and its three consequences above, have been quantitatively evaluated with the help of rather plausible hypotheses. The tentative conclusions are these. (i) The diffractive component may explain most of the observed rise in the inelastic cross-section (about 3–4 mb) through the ISR energy range. (ii) In the multiplicity distribution, the diffractive component broadens at the same rate as the non-diffractive peak moves out, so that no dip develops between the two; the net multiplicity distribution broadens like ln s. (iii) The diffractive component constitutes 10-15% of the central pion plateau, and can account for an increase of 5-8% through the ISR range (about half the observed increase). Two-particle correlations can also be understood, in this context, as coming from two roughly equal parts: a short-range part coming from the non-diffractive component and corresponding to a mean cluster size of 2·5 charged particles, plus a long-range part coming from an interference between the two components.

The conclusions above have in fact been reached independently by several groups. In this connection, a weekend meeting at Coseners House on the subject of the Pomeron was very useful in bringing together an international cross-section of workers in the field. The Pomeron still has its mysteries, but a promising start toward solving them has been made.

Finally, some work has been done on the use of coherent states in multiparticle theory. Most models for hadronic scattering do not incorporate crossing symmetry. It has been shown, however, that if the connected T-operator is constructed as an outer product of coherent states, the corresponding amplitude is automatically crossing-symmetric. This idea has been applied in an attempt to relate dual resonance models to field theories. As might be expected, the field theory corresponding to the Veneziano model with unit intercept turns out to be highly non-linear.

Strong electro-magnetic potentials

A subject of possible relevance both to weak interactions and to experiments in heavy ion collisions, is the study of bound and continuum solutions of the Dirac equation for electrons or muons in critical electromagnetic potentials. These are potentials sufficiently strong to transfer levels from the upper to lower continuum or vice versa, and solutions for the Coulomb case have generated considerable interest in recent years because of the prediction that, for example, in high energy uranium-uranium nucleus collisions, or in high-Z superheavy nuclei, the critical potential will be exceeded and spontaneous delayed emission of positrons should be observed. There is, however, some uncertainty regarding the possible effects of vacuum polarization, and the present work has concentrated on analytical and computer studies of the distortion of the continuum levels by strong potentials. The initial results have already suggested several unexpected new physical effects, in particular that a transient short-range critical potential could induce a permanent shift in the entire set of continuum levels, renormalizing the vacuum state by one unit of charge, and reducing an electron (or muon) at rest to a state of zero observable charge and energy; alternatively a charged lepton could be produced, accompanied by a new vacuum state of zero observable charge. It is interesting to speculate on the resemblance between this effect and the leptonic and hadronic weak currents.

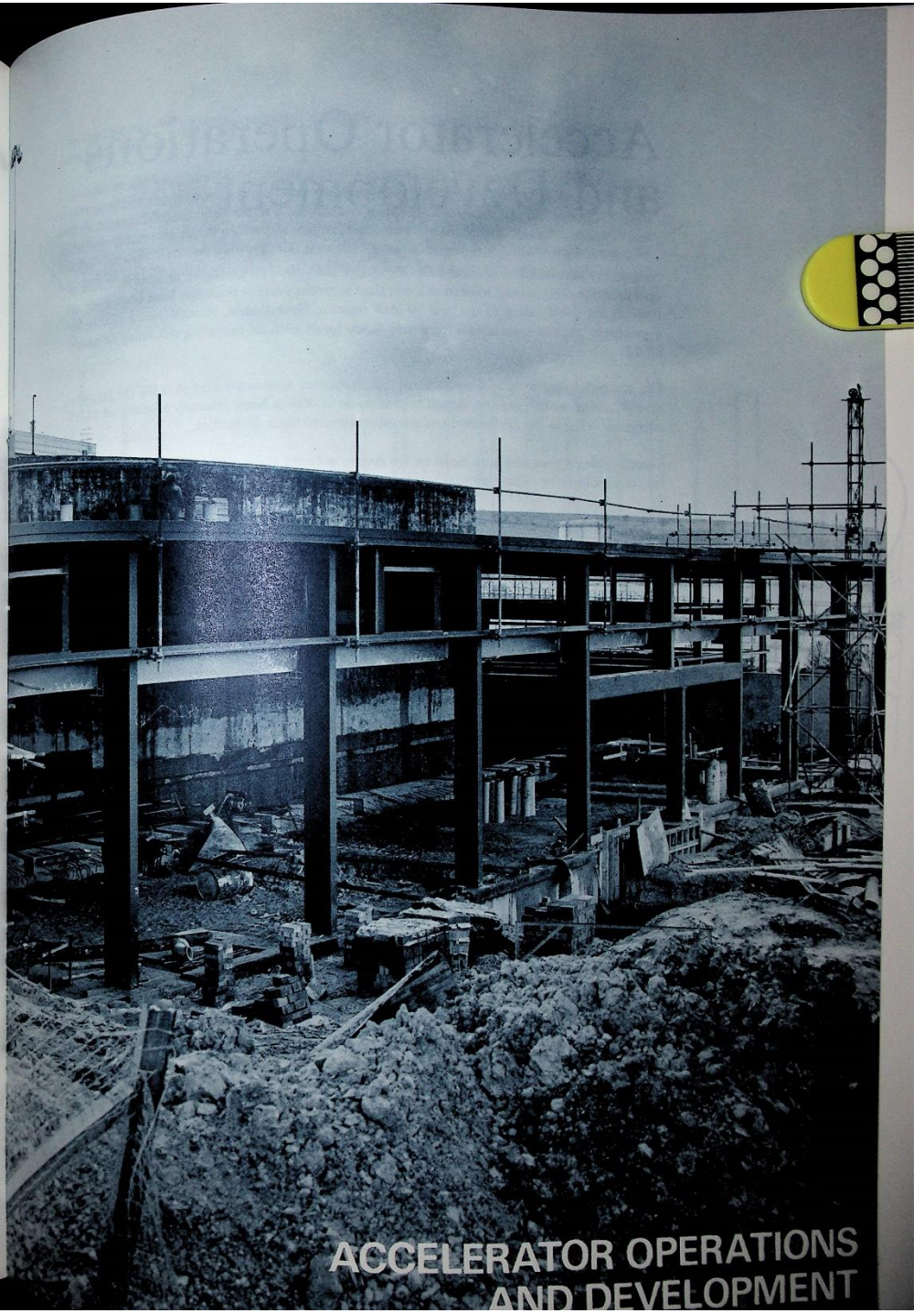

Construction of the building for the 70 MeV injector for Nimrod (15763)

ACCELERATOR OPERATIONS AND DEVELOPMENT

Accelerator Operations and Development

Nimrod has continued to operate well throughout the year. The scheduled number of hours of operation for the year was somewhat lower than in recent years as resources have been diverted towards the provisioning of the new 70 MeV injector. Nevertheless, Nimrod was available for high energy physics experiments for nearly 4,300 hours with an operating efficiency of nearly 87·6%.

The successful operation of the additional radiofrequency system working at twice the frequency of the basic system gave the design improvement of 40% in beam intensity accelerated to full energy. This led to the achievement of record accelerated beam intensities.

Considerable progress has been made on the design, ordering and construction of the equipment for the new injector. The building is under construction.

Four new secondary beam lines have been installed during the year; two have already been used for experimental data taking and the other two have been commissioned successfully.

The initial design work has been carried out on the new beam system for Experimental Hall 1 in 1975.

OPERATION OF NIMROD (Ref. 184, 185, 186)

The pattern of operation of Nimrod, the 7 GeV proton synchrotron accelerator, continued as previously, in 3-week cycles. The major portion of each cycle, usually about 17 days, being devoted to high energy physics research, with the remainder accounted for by accelerator development, maintenance and start-up time.

The accelerator was run from January to mid-February and then again from mid-April until end-November. The shutdown periods, mid-February to mid-April, and the whole of December were for major modifications and maintenance work.

The operations record is summarised as follows:–

High Energy Physics Research	Hours
Scheduled time	4878·6
Good beam time	4199·6
Available beam time	4271·7

ie beam on for 86·1% of scheduled physics research time. (Beam available for 87·6% of scheduled time).

The remainder of the year is accounted for as follows:–

	Hours
Machine physics and start up	1336·1
Routine maintenance and minor modifications at 3-weekly intervals	255·4
Shutdown periods for major modifications and maintenance, including Christmas holiday	2289·9

The total number of protons accelerated during the year was about $15{\cdot}5 \times 10^{18}$. Machine pulses with beam totalled $6{\cdot}26 \times 10^{6}$.

Throughout the year, the pattern of operation was such that, in principle, all installed experiments could be supplied with beam every machine pulse. During the first two cycles, in January and February, Nimrod operated at a momentum of 6·9 GeV/c with a flat-top of 500 ms, and a pulse repetition rate of 28 pulses per minute. Following the shutdown operation continued at 7·9 GeV/c with flat-tops between 300 ms and 900 ms in length and pulse repetition rates of between 15 and 27 pulses per minute, according to experimental teams' requirements.

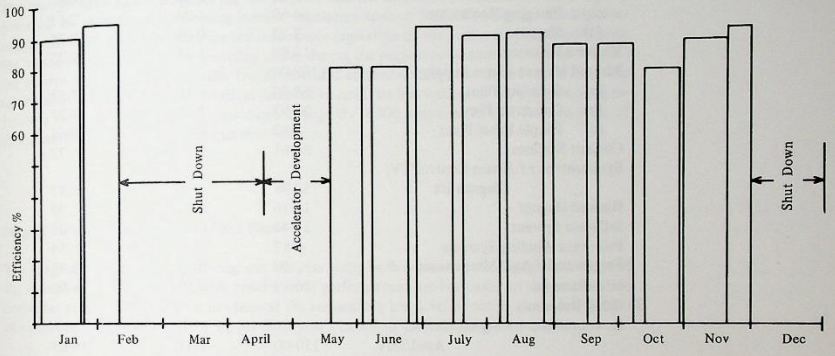

Figure 68. Nimrod operation record for high energy physics during 1973 (15548)

Nimrod Operations 1973

Date: From	To	Hours: Clock	Shut-down	Maint	HEP Research: Sched	Beam On	Exp Off	Nimrod Off	Nimrod Avail	Machine Physics and Development: Sched	Beam On	Exp Off	Nimrod Off	Nimrod Avail
Jan 1	Mar 31	2159·00	1155·32	23·75	930·85	854·35	0·53	75·97	854·88	49·08	31·09	4·05	13·94	35·14
Apr 1	June 30	2184·00	384·00	74·92	872·55	699·12	8·08	165·35	707·20	852·53	270·86	395·24	186·43	666·10
Jul 1	Sep 30	2208.00		108·96	1833·63	1590·03	62·79	180·81	1652·82	265·41	172·81	33·58	59·02	206·39
Oct 1	Dec 31	2209·00	750·57	47·84	1241·54	1056·07	0·77	184·70	1056·84	169·05	109·98	23·22	35·85	133·20
Totals		8760·00	2289·89	255·47	4878·57	4199·57	72·17	606·83	4271·74	1336·07	584·74	456·09	295·24	1040·83
Percent Clock Time		100·00	26·14	2·92	55·69					15·25				
Percent HEP Scheduled Time					100·00	86·08	1·48	12·44	87·56					
Percent MP Scheduled Time										100·00				77·90

Analysis of Nimrod Off Time during Scheduled Operating Time in 1973

Scheduled Operating Time 6214·64 hours
Off Time 902·07 hours

	Beam Time Lost Hours	% of Scheduled Op Time	% of Nimrod Off Time
1. Fault and Routine Inspections			
Injector	153·93	2·48	17·06
Extraction Systems	(144·97)		
(a) Power Supplies	78·05	1·25	8·65
(b) Plunging Mechanisms	64·69	1·04	7·17
(c) Magnets	2·23	0·04	0·25
Vacuum Systems	114·82	1·85	12·73
Nimrod Magnet Power Supply	(103·09)		
(a) Rotating Plant	68·30	1·10	7·57
(b) Converter Plant	28·97	0·47	3·21
(c) Ripple Filter Plant	5·82	0·09	0·65
Coolant Systems	60·61	0·98	6·72
Synchrotron r.f./Beam Control/TV/ Diagnostics	52·98	0·85	5·87
Nimrod Magnet	16·16	0·26	1·79
Inflector System	11·44	0·18	1·27
Pole Face Winding Systems	4·87	0·08	0·54
Targets and Target Mechanisms	2·94	0·05	0·33
Miscellaneous	36·12	0·58	4·00
2. Other Reasons			
Re-commissionioning of Nimrod, April/May	150·00	2·41	16·63
Start-Up	39·20	0·63	4·35
Public Electricity Supply	10·94	0·18	1·21
	902·07	14·52	100·00

Figures for Vacuum and Extraction Systems include routine inspection time.

External Beams : Operations Summary

Hall 1 X1/K19, the fast spill extracted proton beam for the 1·5 metre cryogenic bubble chamber, was supplied with a portion of the Nimrod circulating beam on current rise, generally at 7·6 GeV/c. P81, a low emittance, full energy beam, peels off some of the X3 protons before they are finally extracted from the machine.
P.71. This is a scattered out beam, parasitic on the internal machine X3 target, and mainly used for apparatus test.

Hall 2 π7, a scattered out beam from a machine internal target, completed data taking in the early part of the year, and has been dismantled.

Hall 3 X3, an extracted proton beam, services all experiments installed in this Hall. There are three target stations, known as X3, X3X and X3Y. Secondary beams off these stations are:

X3 – π8, π11 and K15
X3X – π9 and π12
X3Y – K17

Installation commenced during the Spring shut-down of two new beams π12 and K17. The other beams in Hall 3 have continued unchanged since 1972.

Plunging Mechanisms

The plunging mechanism in straight section 2, which is associated with the X1 and P81 extracted proton beams, was fitted, during the Spring shut-down, with a digital position control system similar to that developed for the X3 beam extraction system. The essential difference between that system and the X1/P81 system is the provision of a second "step" reference facility, whose output is used to control the position of the kicker magnet for the subsidiary, P81, extracted proton beam. This permits the plunged kicker magnet to be positioned accurately in radius, at two successive positions, one for X1 and the other for P81, every machine pulse. The two references are triggered independently. The time taken for the magnet to move the distance of about 6 cm from the greater radius to the lesser radius, ie X1 to P81, is about 100 milliseconds. Positional re-setting accuracy of the positions is better than $\pm$ 0·5 mm pulse to pulse.

The two plunged kicker magnets for the X1/P81 and X3 extracted proton beams are primarily powered via separate programming current regulators from a 900 kW, 12-phase static power supply. In order to compensate for the inadequate regulation of the power supply coupled with the voltage-drop on the interconnecting cables during the current programme, a voltage regulating system was designed and built. Installation and commissioning was carried out during the Spring shut-down. The system which is designed to hold the bus voltage of the programming regulators to 40 Volts $\pm$ 1 Volt in the current range 0 - 16000 Amperes permits the operation of all extracted beams during every machine burst.

Magnet Power Supplies and Ancillary Plant

The magnet has been pulsed throughout the year using both motor-alternator-flywheel sets and the complete converter plant with good overall performance. Arc-back rate on the mercury-arc converter plant during the year has been at the remarkably low level of one in about 1300 hours of operation – even better than the previous year's excellent performance.

Operational statistics are as follows:-

Machine running time	5,742 hrs
Machine pulsing time	5,521 hrs
Total pulses	7,048,620

No. 1 Alternator

This was dismantled during the planned synchrotron shut-down in February 1973 for replacement of the Vee coil support bolts on the rotor as they had been subjected to 26 x 10^6 pulses. The balance of 4 x 10^6 pulses required to reach their service life of 30 x 10^6 was insufficient for a further year of operation.

During this period a routine check on the field windings revealed a shorted turn on pole 5. Following removal of the pole caps, repairs were carried out on site by the manufacturer. The mating surfaces of the pole caps and the pole body were found to be in excellent condition. The pole cap retaining bolts on the poles were checked for elongation. Bolt elongation (and therefore pre-stress levels) were found to be unchanged. The stator of No. 1 alternator has been subjected to specialised testing to ascertain the condition of the insulation of the windings. The tests comprised polarization index, loss angle/applied volts and dielectric loss analysis checks and the insulation was found to be in excellent condition. All machine stators on the magnet power supply rotating plant have now been checked in this manner as well as the rotor of No. 1 motor.

All Vee coil support bolts removed from No. 1 solid pole rotor and which had been subjected to 26 x 10^6 pulses, were subjected to a thorough visual examination. Six bolts were further subjected to magnetic particle crack detection, three before and three after removal of the glass fibre insulation and adiprene coating. No trace of any cracking was found. In addition, Lloyds Register of Shipping carried out an independent visual examination of the remaining bolts.

Bolts which showed certain markings in the thread region or slight corrosion on the shank region, were selected for test by Lloyds Register. These tests comprised magnetic particle crack detection, visual examination, and microscopical examination of sections of thread root and head fillet radius. All bolts were pronounced to be free from any cracks and fit for further service. In view of this, it has been agreed with Lloyds Register of Shipping that the working life of bolts in the future will be increased by 15% from 30 x 10^6 pulses to 34·5 x 10^6.

Flywheels

Each of the two flywheels now in service has one half-shaft integrally forged with the disc. This half-shaft is coupled to the alternator, thus the limitations of the original bolted and keyed construction in this location are avoided. The half-shaft on the other side of the disc is, however, of bolted and keyed construction and two bolts were removed from this assembly on each flywheel for inspection. Visual examination and magnetic particle crack detection showed them to be in excellent condition and they were replaced.

Excitation Rectifiers

The excitation equipment for each alternator contains two steel-tank mercury-arc rectifiers. The manufacturers have advised us that manufacture of such units has ceased and that the reconditioning service for existing units is to be discontinued. A number of reconditioned spares is held but tests are to be carried out in the 1973/74 shut-down with thyristor equipment with a view to eventual replacement of the mercury-arc units.

New Master Timer

The timer has been in continuous service throughout the year and has been virtually trouble-free in operation. A few minor changes have been made as a result of experience gained during the commissioning and operating periods but the basic design has proved to be very sound.

Inter-phase Reactor Examination

No. 1 300/600 Hz unit has been inspected during the shut-down (the previous examination was five years ago). In addition to electrical tests all windings were checked for shrinkage and the only adjustment found necessary was to one winding retaining spring on the 600 Hz reactor assembly. The condition otherwise was virtually the same as when it was returned to service after the 1967 inspection.

ACCELERATOR DEVELOPMENT

Shut-down 1973-74

The 1973-74 shut-down which started on 1 December and will last until April has been extended beyond the normal length to allow the diversion of resources to the new injector project. It has been timed to take place when electricity is most expensive and to dovetail with the programme for the new injector building.

In addition to the maintenance required a large programme of work is planned.

The beam access tunnel between the 70 MeV injector building and the synchrotron hall will be built, mechanical services will be installed in the tunnel and the earth shielding back-filled over the tunnel. Holes for the proton beam and an access door have already been made.

It is intended to install the electrostatic inflector associated with the new injector at the end of 1974. It will be located in straight section 2, and in order to allow access some equipment needs to be relocated. In particular, the inflector 200 kV EHT set is being re-sited in one of the chambers underneath the main synchrotron hall, and the power supplies for the 15 MeV transfer line magnets are being moved to the 15 MeV injector hall.

Before embarking on the new injector project careful consideration had been given to the likely effects of the increased intensity of the circulating proton beam. It was concluded that all major components would still have an acceptable life.

The low density polythene closure plates for the Nimrod vacuum vessel, fitted as a temporary measure when Nimrod was built, had already suffered some damage due to post irradiation oxidation. A review of materials suitable, both mechanically and for radiation integrity, led to the choice of low density polythene loaded with carbon black. This material should be chemically more stable thus reducing damage due to oxidation. Replacement of the existing closure plates will be possible with no modification to other parts of the machine. The closure plate on octant 1 is being replaced by the new type in this shut-down period.

The r.f. accelerating cavity in straight section 8 is to be removed from the Nimrod ring in order to permit a detailed examination and refurbishment to be carried out where necessary. The opportunity will be taken to replace the pole face winding nylon cooling pipes in straight section 8 by a system of nylon-coated copper pipes as part of the programme of replacing the nylon pipes which are susceptible to radiation damage.

Second Harmonic r.f. System (ref. 393)

At the beginning of 1973 the second harmonic r.f. system had been completely assembled for pre-installation tests and high power r.f. tests had started. These were completed satisfactorily with atmospheric pressure in the straight box, but multipactoring (a form of r.f. discharge) occurred when tests were started with a vacuum in the straight box. Multipactoring depends on the operating frequency, the configuration and surface condition of the electrodes and the state of the vacuum. Modifications gave partial improvements: it was, however, completely suppressed by a d.c. electric bias field provided by two large flat electrodes installed on either side of the drift tube with a potential of 12 kV applied to them.

Before installation of the system into Nimrod the insulation of the bias turn conductors was improved and further modifications were made to the r.f. monitoring probes.

Installation and Commissioning

Installation in straight section 6 was completed by the end of the 1973 annual shut-down (see Figure 69) and operation with Nimrod began as soon as an accelerated beam was established. Initial tests confirmed there was no serious interaction between the drift tube or the ferrite bias field and the normal Nimrod beam, and no r.f. discharge when operated under normal conditions. The temperature control of the ferrite and r.f. valve remained good. In the experiments that followed, effort was concentrated on maintaining synchronisation of the normal (fundamental) and 2nd r.f. accelerating fields to produce and sustain an accelerated beam of increased intensity. Soon a considerable increase (about 40%) in the beam accelerated to 22 MeV was obtained, however this was somewhat inconclusive as at this time Nimrod was not operating at full intensity. Acceleration of the increased beam to higher energies was prevented by severe distortion of the beam bunches and oscillations in their phase. At this stage a number of variants in beam control were tried; the best results were obtained with a system with enhanced phase loop bandwidth. The increased beam was maintained up to 100 MeV with intensities of 4·7 x 10^{12} compared with 3·3 x 10^{12} for the normal (fundamental only) field. Further experiments brought the increase up to 260 MeV. Here, severe bunch instabilities became apparent over the period where steering in Nimrod is normally very critical and the beam is held near the inside wall of the vacuum vessel. It was shown that considerable oscillations in bunch width occurred during this period. A mean bunch length detector was used to demonstrate the existence of bunch length oscillations at twice the phase oscillation frequency. By damping these oscillations full energy beams of 4·2 x 10^{12} protons/pulse were obtained which also remained stable throughout flat top – see Figure 70.

This successful test took place a few hours before the start of the 73-74 annual shut-down and during the test an attempt was made to extract a beam down the X3 external proton beam line. With partial operation of the second harmonic r.f. system it was shown that the extraction efficiency was normal, but a fault on the extraction magnet power supply precluded further tests.

The present status of the system is that the second harmonic cavity and all its associated equipment (r.f. drive chain, bias supply and beam control electronics) operates satisfactorily for the acceleration of protons and gives a 40% increase in beam intensity. Further tests are needed to demonstrate that the intensity of external beams will be similarly increased and to measure the quality (r.f. structure and effective spill time, etc.) of the external beam.

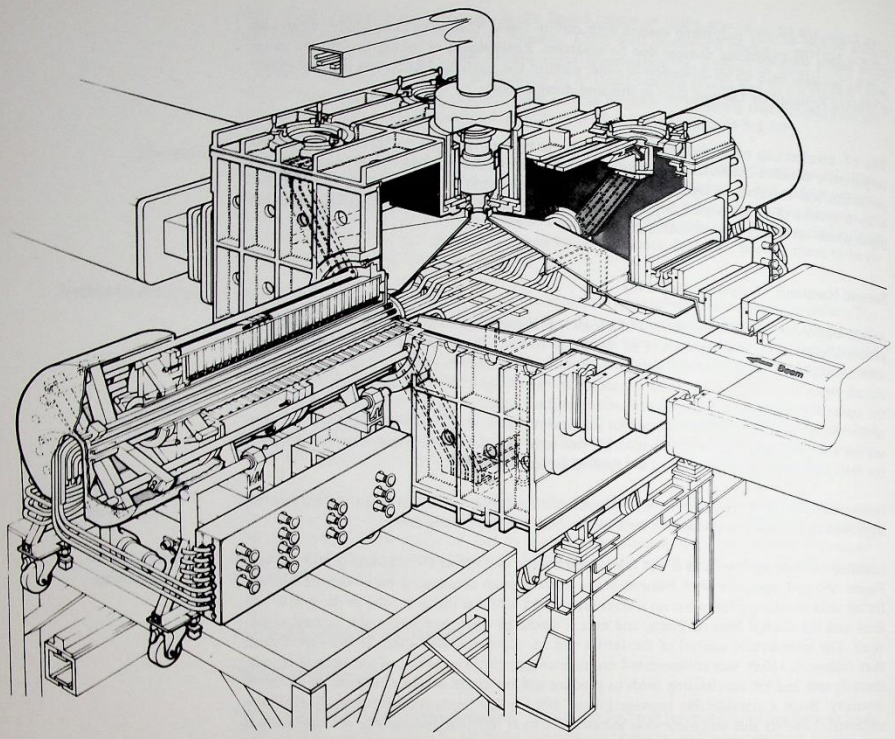

Figure 69. The second harmonic r.f. system in straight section 6 of Nimrod (15212)

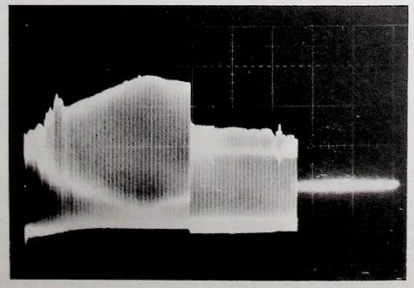

Figure 70. Beam pulse envelope from 15 MeV to 7 GeV showing stable bunches accelerated with the combined fields. The uneven form of the envelope is due to slow changes in bunch shape as the energy is increased. At 7 GeV flat top begins, the bunches immediately become longer and more symmetrical with a corresponding reduction in amplitude of the beam pulse signal, time base 0·2 sec/cm. (15572)

70 MeV Injector for Nimrod (ref. 161-163, 241-246, 248, 288, 320)

A description of the main parameters and requirements for a new injector for Nimrod was given in the 1972 Annual Report. Financial approval for this development was received at the end of December 1972.

During 1973 considerable progress has been made on the design and ordering of the necessary equipment. The building to house the new injector for Nimrod is now under construction. It is situated alongside the existing 15 MeV injector hall and has three floor levels. These are : (i) the equipment area, (ii) a large trench along the length of the building with its floor approximately 3m below the level of the equipment area floor. Radio frequency equipment and vacuum equipment will be housed in this trench. (iii) the EHT area; the whole of this floor will be covered by aluminium plates each one connected to the next and secured to the floor to provide electrical continuity. The walls of the EHT area will be lined internally with galvanised steel wall cladding electrically bonded to the floor to form a conductor box.

The injector building is linked to the synchrotron hall by a reinforced concrete tunnel 3m square and 15m long with a doorway into the synchrotron hall, for services and access, and the 300 mm hole through which the injected proton beam will pass. Some of the earth mounding which was removed to enable the tunnel to be constructed will be restored for radiation shielding purposes.

Components for the pre-injector are being assembled in a test area for operational trials. The high voltage equipment platform and the accelerating column support structure have both been re-built from former Proton-Linac (PLA) equipment. A new accelerating column is being assembled. A duoplasmatron ion source, together with all its power supplies and services, is ready for installation on the column and has delivered a proton beam of the required 200mA pulsed current on test. Components for the Cockcroft-Walton set have been delivered and both the reservoir capacitor and potential divider have been ordered.

The linac tanks (r.f. cavities), which will be located above the trench, are enclosed by concrete blocks to reduce radiation in the adjacent equipment area to an acceptable level. The first and fourth tanks are being manufactured from copper-clad steel plate and are due for delivery early in 1974, when the drift-tubes are also due. The other two linac tanks (second and third) which are ex-PLA equipment required only minor modifications and re-furbishing. Suitable 12 inch and 20 inch diffusion pumps for the evacuation of all 4 tanks are also available from the old PLA. Alignment of the tanks when being installed in their final positions will be done using existing optical equipment.

The manufacture of the main components of the r.f. system is well advanced and design is proceeding on a 200 kW fast ferrite phase shifter for the debuncher-ramper cavity.

All d.c. stabilised power supplies have been ordered and design of the pulsed power supplies for the drift tube quadrupoles in Tank 1 is now finalised. The requirement of producing pulses of 300A stable to $\pm 0{\cdot}2\%$ over 500 μs has been met by the use of capacitive storage and thyristor controlled resonant discharge.

The 7 quadrupole triplets used for beam matching and momentum recombination in the beam transfer and achromatic inflector system will be composite units, each consisting of two ex-PLA quadrupoles acting as end-elements and a water cooled quadrupole of somewhat similar geometry as a centre-element. The conventional sector magnet for the first deflection towards Nimrod in the inflector system and the septum magnet and electrostatic element which together give the second (opposite) deflection are all currently in manufacture. The septum magnet has 8 water-cooled turns in a stack, and a nominal pulsed current of 7000A. The electrostatic inflector operating voltage is approximately 140 kV, and the high voltage electrode is being manufactured from a plate of 5% magnesium-aluminium alloy. The earthed electrode will either consist of a thin sheet of the same alloy or a grid of 0·125mm dia molybenum wires. Preliminary experimental grids have been made, and voltage-testing of both solid plate and grid electrodes will commence early in 1974 so that a final choice can be made based on the results obtained in the tests.

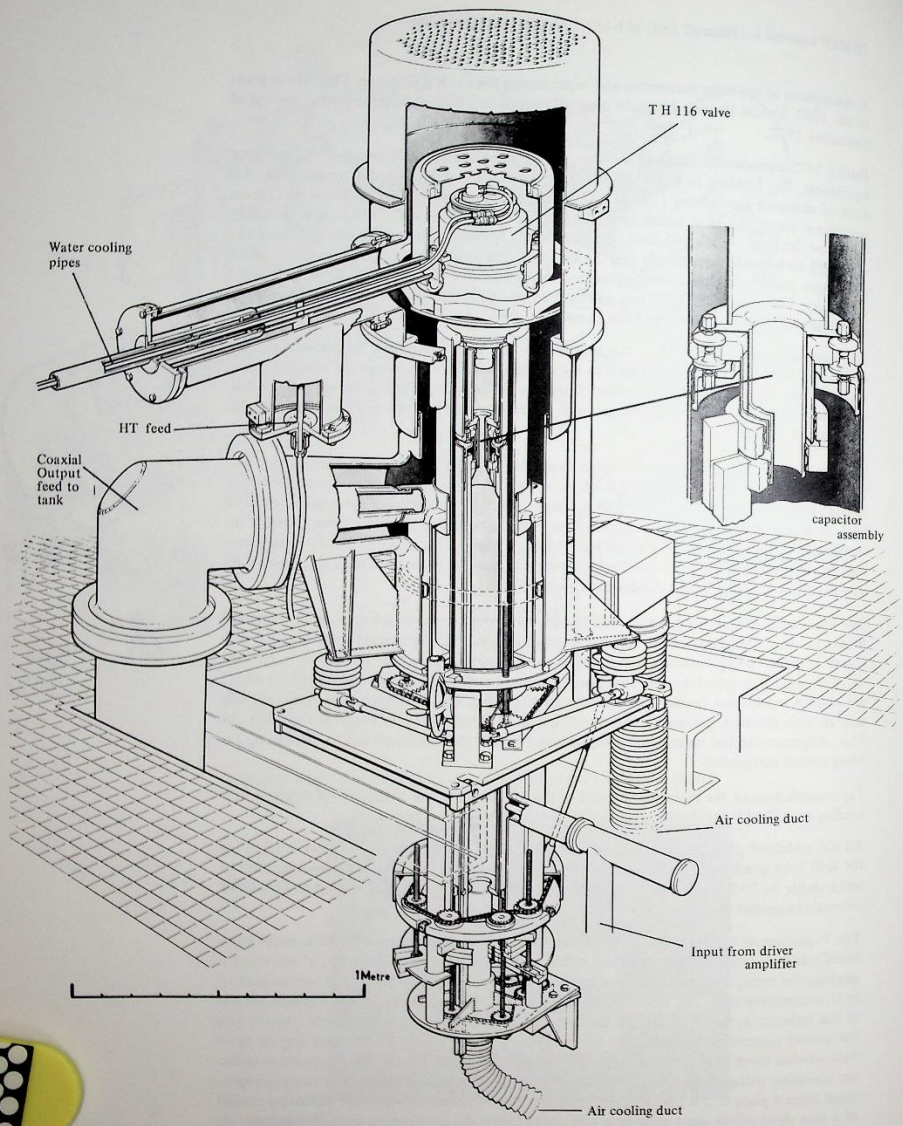

Figure 71. An r.f. power amplifier for the 70 MeV injector: each tank will have its own amplifier (15211)

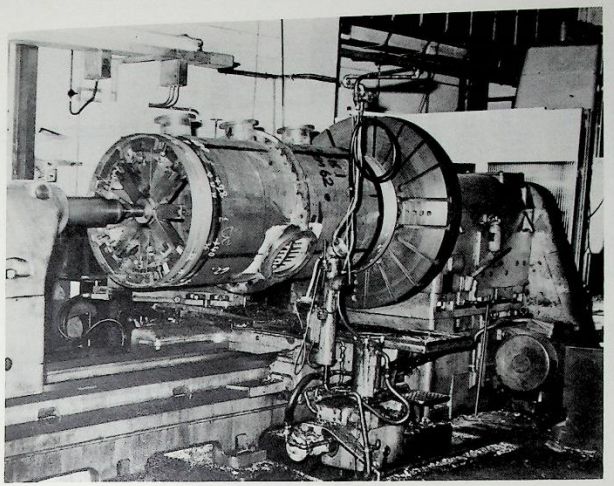

Figure 72. 70 MeV injector; tank 1, one quarter section under construction
(Photo by courtesy of Morfax Ltd.)

Protons from the injector will enter the synchrotron at the 2nd straight section. An available vacuum box has been modified to accept the electrostatic inflector, the septum magnet, and the existing kicker magnet associated with beam extraction.

The problems associated with running Nimrod alternatively with the 15 MeV Linac or with the 70 MeV Linac has led to a design of manually operated equipment that allows rapid and precise location of equipment within the 2nd straight section with operation sufficiently remote to reduce to acceptable levels the radiation dose absorbed by the operators.

Transmission of data and control signals from the 70 MeV Injector will be largely based on the use of a CAMAC system, which will have the potential for interfacing to a computer. Initially a continuously cycling data-transfer programme, held in a programmable read-only memory will be used. This programme will provide the acquisition and control functions basically necessary to operate the machine. There will be 3 CAMAC sites, one in the equipment area near tank 4, one in the injector control centre (I.C.C.), and one in the main control room. An infra-red light-link using 4 channels will provide control and acquisition at the EHT platform, in the form which is compatible with the CAMAC system operating mode. Prototype equipment for the control system is nearly complete and preliminary tests have been started.

BEAM LINES AND ASSOCIATED EQUIPMENT

During the year, four new secondary beam lines were installed and commissioned. Modifications were made to a fifth beam. A major reorganisation of beam lines in Hall 1 was undertaken.

Hall 1; K19 Beam

K19, a low momentum K meson beam to service the 1·5m bubble chamber replaced the K9 beam, which had been in use for five years. K19 is a two-stage electrostatically separated beam of high acceptance designed to provide negative kaons in the momentum range 600 to 800 MeV/c. It was designed to have a very high purity; in particular the muon background has to be very low so that degrader techniques can be used to take bubble chamber photographs of kaons from 700 MeV/c right down to stopping. The necessary proximity of the target to the chamber required careful arrangement of shielding to minimise the low energy background to the chamber.

SETTING	SEC	TIKH	CR7	CR8	CR9	CR10	RATIO	PULSES
210.13	295	4	0.00	166.00	16.60	10.40	0.0563	25
215.02	338	5	0.00	352.80	39.30	33.55	0.1162	31
219.98	367	5	0.00	515.05	64.20	56.75	0.1853	45
225.93	345	5	0.00	721.55	137.10	128.70	0.3979	25
230.10	327	5	0.00	860.20	328.85	320.65	1.0055	45
235.12	344	5	0.00	944.90	622.50	613.40	1.8106	43
240.13	352	4	0.00	862.85	711.60	705.95	2.0239	54
245.07	348	5	0.00	776.70	668.90	661.40	1.9221	39
250.15	338	5	0.00	676.15	506.15	497.35	1.4973	32
255.13	296	4	0.00	519.65	282.00	274.40	0.9517	31
260.17	341	5	0.00	456.65	165.70	158.70	0.4859	26
265.12	293	4	0.00	297.20	86.80	80.40	0.2967	21
270.18	308	4	0.00	191.35	47.10	41.90	0.1528	24
274.92	337	5	0.00	104.65	22.15	16.05	0.0658	24
279.91	275	4	0.00	51.50	8.45	3.80	0.0308	28

CENTROID OF PEAK AT 242.3 BACKGROUND 2%

AT 50% LEVEL; LHS 230.2, RHS 254.4, MID-POINT 242.3, FULL-WIDTH 24.2
AT 25% LEVEL; LHS 226.1, RHS 259.7, MID-POINT 242.9, FULL-WIDTH 33.6

S101 PROVISIONALLY SET TO 242.0

S101 0 1 2 3 4 5 6 7 8 9 10 CR9 /SEC (ARB.SCALE)

MAX RATIO OF CR9 /SEC COUNTS 2.024 DATA TABLE NO. 38

Figure 73. Output from the automatic scanning program, K19 computer

FAST SHUTTER MAGNET E.H.T. = 7.500
SLOW SHUTTER MAGNET E.H.T. = 1.500
FAST SHUTTER MAGNET CLAMP DELAY = 2.00
SLOW SHUTTER MAGNET TRIGGER DELAY = 0.50
SLOW SHUTTER MAGNET CLAMP DELAY = 9.50
UNSHUTTERED CR10 COUNT ABOUT = 7000
SHUTTERING AT CR10 = 6300
ONLY POINTS WITH SEC BETWEEN 10 AND 30 WERE INCLUDED.

NUMBER OF PULSES IN EACH BIN (ONE + EQUALS ONE PULSE)

CR10 COUNTS

0 TO 199
200 TO 399
400 TO 599
600 TO 799
800 TO 999
1000 TO 1199
1200 TO 1399
1400 TO 1599
1600 TO 1799
1800 TO 1999
2000 TO 2199
2200 TO 2399
2400 TO 2599
2600 TO 2799
2800 TO 2999
3000 TO 3199
3200 TO 3399
3400 TO 3599
3600 TO 3799
3800 TO 3999
4000 TO 4199
4200 TO 4399
4400 TO 4599
4600 TO 4799
4800 TO 4999
5000 TO 5199
5200 TO 5399
5400 TO 5599
5600 TO 5799
5800 TO 5999
6000 TO 6199
6200 TO 6399
6400 TO 6599
6600 TO 6799
6800 TO 6999
7000 TO 7199
7200 TO 7399
7400 TO 7599
7600 TO 7799
7800 TO 7999
8000 TO 8199
8200 TO 8399
8400 TO 8599
8600 TO 8799
8800 TO 8999
9000 TO 9199
9200 TO 9399
9400 TO 9599
9600 TO 9799
9800 TO 9999
0.1000E+05 AND MORE

Figure 74. Performance of the random shutter magnet K19 beam (14689)

A total of 1399 tons of steel and 1662 tons of concrete was used as shielding in the construction. The beam was commissioned successfully and was used to take over 900,000 pictures in the bubble chamber. It was computer controlled very effectively right from the start. Figure 73 shows typical output produced by the automatic scanning programme. A tandem shutter magnet, using the principle of moving the external proton beam off the external target, gave much cleaner shuttering than the previous method of moving the secondary beam into a beam stop. Figure 74 shows the quality of the results achieved. After the bubble chamber experiments were completed in November the beam was used to make some yield measurements of kaons and anti-protons at two different momenta of incident protons.

Hall 1; P81 Beam (ref. 160)

The P81 beamline (Experiment 15) was installed during the early part of 1973 and subsequently commissioned to allow experimental data taking. It utilized 1200 tons of cast iron and 1000 tons of concrete shielding. The beam requirements dictated that six of the collimators were fitted with heavy metal faced jaws. (Heavy metal is an alloy of tungsten, copper and nickel, with a specific gravity of 17·5).

A special secondary emission chamber was incorporated in this beamline. The main features of this chamber are its compact design, its ability to be mounted directly into a 34 cm gap in the beamline and its easy removal without disturbance to adjacent components. The major problem with this beam was the provision of a well defined proton spot at the polarized target.

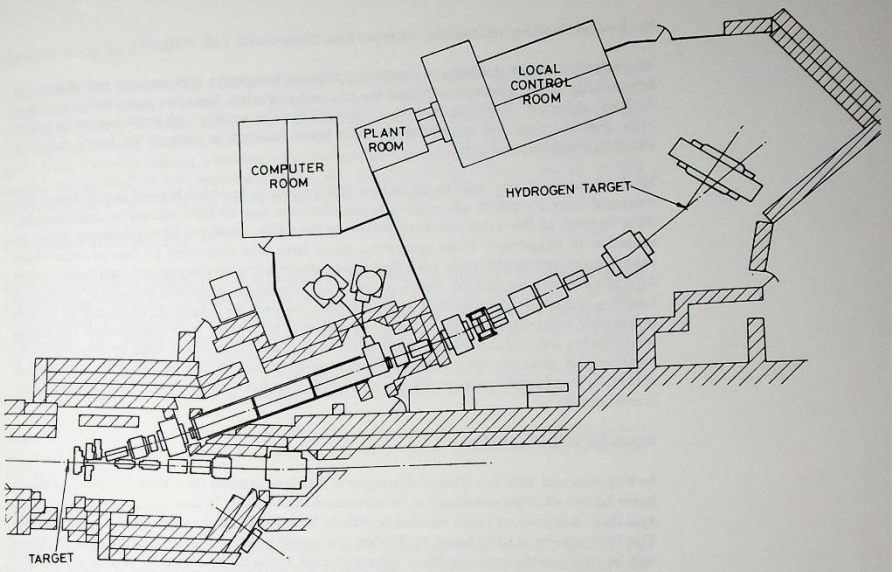

Figure 75. K15 beamline (15547)

Hall 3; π8, K15 and π11 beams

Minor modifications were carried out to the π8 beamline to make it suitable for use by a new user group. π8 shares the first target station, X3, in Hall 3 with the K15 and π11 beams. The K15 beamline has been re-designed to take a three tank separator to enable it to reach higher energies. This installation work will be done in the 1973-74 shut-down.

Hall 3; π12, π9 beams

From the second target station, X3X, in Hall 3, a second beam, π12, a 1 to 5 GeV/c pion beam, has been set up. This new beam is very similar in design to the existing π9, the other beam sharing the same target station.

Hall 3; K17 beam

The external proton beam which feeds the two target stations X3 and X3X was extended to provide a third-stage target station called X3Y. Any one of six targets can be selected manually at this station, which is located inside a quadrupole, to provide the source for K17 (Experiment 38). This kaon beam of nominal momentum 0·6 GeV/c is designed to provide K^- at rest. The beamline incorporates a single grid electrostatic separator. To minimise background radiation for the K17 experiment, a cast iron beam dump weighing 16 tons has been developed which can be lowered into the path of the external proton beam. The device provides an experimental facility for beam attenuation studies by the Radiation Protection Group. The blockhouse extension incorporates 2733 tons of cast iron together with 1121 tons of concrete shielding.

Mechanical Handling and Stability of Beam Line Components (ref. 300)

The effective use of the Nimrod accelerator requires progressive improvement and changes to beams both with regard to layout and the physical properties. Beamline equipment is necessarily large and heavy, involving magnets of up to 50 tons in weight. Such items have to be accurately positioned to the requirements of the beam structure in spite of the heavy radiation shielding placed around them.

Much of this work can only be carried out during periods in which Nimrod is shut down. The increased intensity which will come into use when the new 70 MeV injector is commissioned, adds impetus to the requirement for improving the safety, speed and labour demands during installation of equipment. These operations unavoidably arise from time to time in areas which cannot be served by the main travelling cranes. Major beamline components have been studied carefully to establish stability limits to guide the installation teams and designer in developing handling techniques. An improved design has been prepared for a turntable which will be used in positioning components of up to 9 tons in weight in areas away from main cranes. The design incorporates low friction bearing pads between the upper and lower table to ensure smooth rotation and minimise the rotational force needed. To ensure ease of operation and smooth action, hydraulic jacks will provide the rotational effort between the tables. Development work is continuing.

Beams for Hall 1 in 1975

In Experimental Hall 1, a phased development has been studied for a proton and a secondary beam layout allowing construction to commence in the 1974/75 shutdown. The scheme envisages three independent target stations capable of being illuminated with protons simultaneously. The final scheme is to be based on 'Peeling' the proton beam with a thin septum magnet. There will be two conventional secondary beams; one for kaons in the region 0·7-1·4 GeV/c and the other for pions at momenta up to 6 GeV/c. The third beam, for the rapid cycling vertex detector, requires special consideration. The device requires about 50 fast spills during the period of one flat top spill. To obtain compatibility with the counter beam spill, a kicker magnet will be synchronised with a fast spill on top of the counter spill, to divert this short burst of enhanced intensity spill to the RCVD-beam target. The 'holes' in the spill to the counter beams will lead to a 5 to 10% reduction in effective spill time.

Figure 76. Beam lines planned for Hall 1 in 1975 (15210)

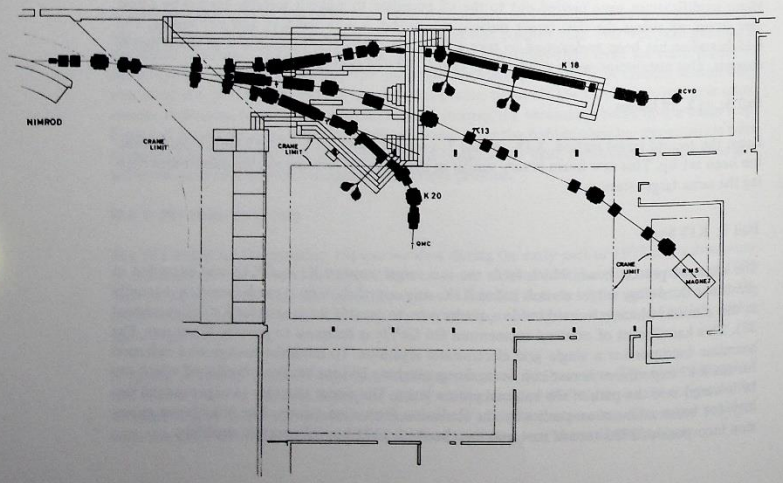

Hyperon Beam for CERN

Design work has continued on a charged hyperon beam for use at the SPS (SPSC / P 73-2). The design aim is to achieve hyperon identification up to 150 GeV/c. The beamline has to be as short as possible to minimise decay losses yet allow adequate mass resolution and muon shielding. Superconducting beamline elements are used to produce a channel of overall length 12m and a DISC Cerenkov counter is included as an integral part. Estimated fluxes within a total (including background) of 10^6 particles/machine pulse are; 7 x 10^4 Σ^-, 100 Ξ^-, 0·6 Ω^- at 150 GeV/c and 150 Σ^+ at 100 GeV/c, from a 200 GeV/c proton beam.

Electrostatic Separators (ref. 330)

Four separators have been in operation in three beam lines during 1973. These have comprised a double tank unit in K15, a single tank unit in K17 and two single tank units in K19. All these separators are of the flattened tube electrode construction and their performance has been most satisfactory. The electric field strength in gaps of these separators has ranged from 7·5 kV/mm for an 80 mm gap on K19 through 6·0 kV/mm for a 100 mm gap on K15 to 5·83 kV/mm for a 120 mm gap on K17. Work is now going ahead to construct a new 3 tank separator for K15 and several more multitank separators are proposed for new beam lines in 1974 and 1975.

Alumina insulators are currently on order and these will eventually replace the existing porcelain type which have shown an inherent weakness probably due to difficulty of quality control during manufacture.

Inorganic Insulation (ref. 247)

The increasing levels of radiation around Nimrod and in experimental area blockhouses has led to an investigation into the use of inorganic insulations such as oxides. An urgent need exists to improve the insulation of certain beamline magnets. Tests have been conducted on copper conductors sprayed with a range of metallic oxides. Simple coils are being wound to test further this insulation, and also to exploit further cement and concrete as insulation with asbestos tape as a binder.

Inorganic Insulation Quadrupole

A concrete filled encapsulated quadrupole magnet has been constructed for eventual installation to the high radiation environment of the X3Y-K17 target. The quadrupole is designed to have a comparable size and performance to the standard Rutherford type 1 quadrupole. The aperture is 8 inches with a gradient of 1172 gauss/cm and a length of 30 inches.

The conductors are pre-wrapped in asbestos tape which is soaked in a cement slurry. Individual coil pancakes are formed and mounted on the quadrupole yokes to form complete clamped coils. The whole magnet is then encased and a suitable concrete filling pumped into the casing.

This will be the third and largest working magnet using concrete insulation, but the first magnet employing this constructional technique.

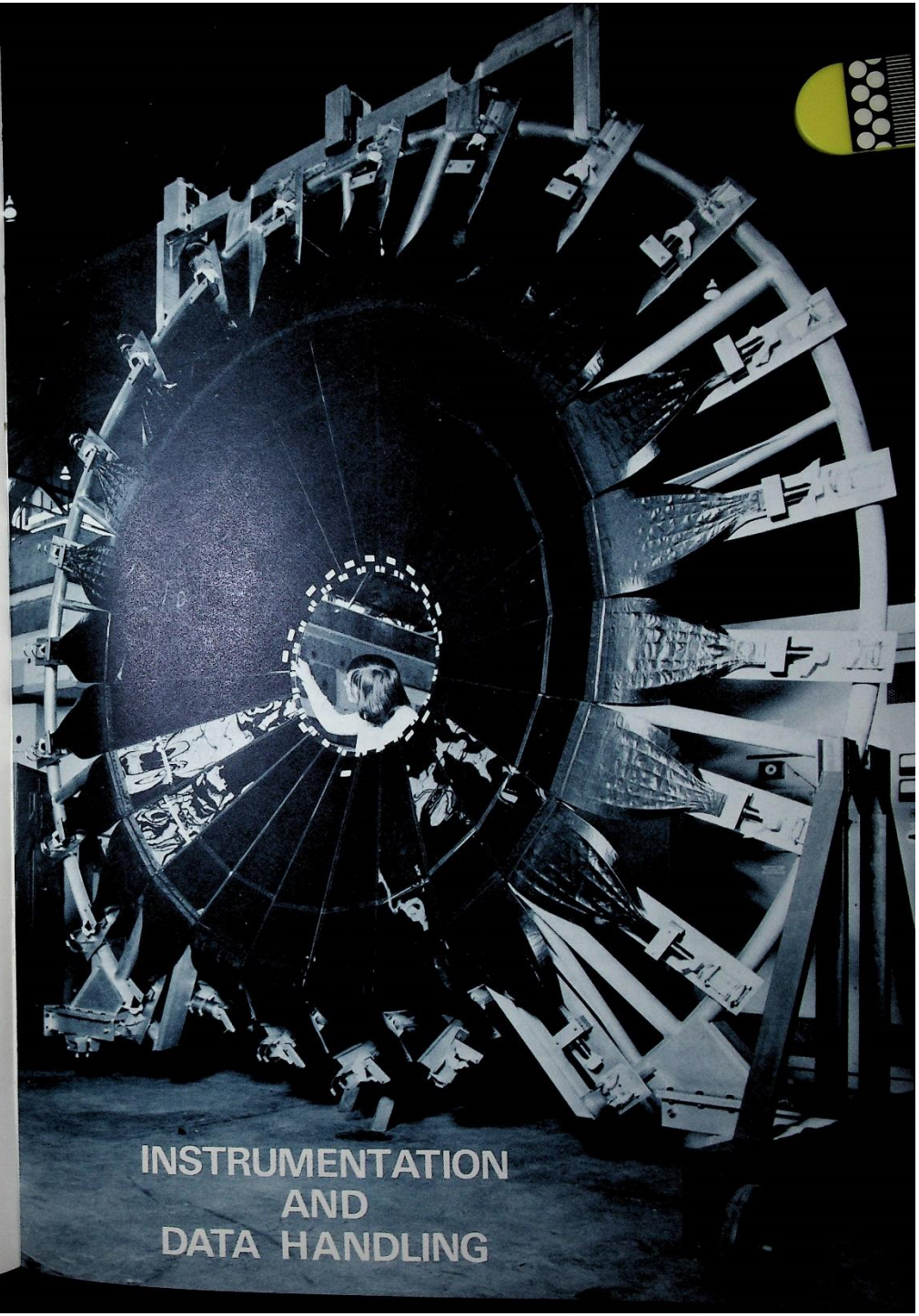

INSTRUMENTATION AND DATA HANDLING

A scintillation counter hodoscope for Experiment 5 during construction (see page 123) (14949)

Instrumentation and Data Handling

Bubble Chamber Operations

1·5m Bubble Chamber (ref. 10, 45, 139, 178, 375, 380)

In November 1973 the bubble chamber successfully completed its scheduled physics programme and has now been closed down. During the year two experiments requiring track sensitive targets (TST) were carried out and nearly a million data photographs taken.

For Experiment 34 a large stainless steel framed TST was installed. An aluminium block was fitted inside the metal frame of the TST to degrade the beam to its correct energy after it had passed through the chamber magnets. To assist in the beam tuning, an extra scintillation counter was located inside the main chamber vacuum tank.

Proposal 84 required some modification to the chamber complex. An all perspex TST manufactured by CERN was installed in the chamber. This was unique in shape, being designed to follow the beam contour; it was inclined at an angle of 128 milli-radians to the horizontal plane of the chamber and diverged in section from the beam entry along the beam path. A degrader system was installed inside the chamber vacuum tank, designed so that its total thickness could be altered by a pulley and lever system from outside.

For much of the running time Nimrod was operated at a pulse rate of 27 per minute, and picture-taking rates of 30,000 per day were typical. During the exposure using the perspex TST the chamber performed 830,000 expansions without maintenance to its mechanical, electrical or optical systems.

A brief history of the 1·5m bubble chamber

In May 1957 a meeting of physicists from several institutions was convened in London by Professor C C Butler to consider the desirability of constructing a large hydrogen/deuterium bubble chamber for use at CERN with the 25 GeV proton synchrotron and at the Rutherford Laboratory with Nimrod. As a result a working party consisting of members of the physics departments at Birmingham University, Imperial College, Liverpool University and Oxford University together with staff from the Rutherford Laboratory, was formed to prepare basic designs. The main parameters were fixed by the Summer of 1958 and approval for the project was granted in the Autumn of 1958. Design work proceeded in the separate institutes and in 1961 a construction team was assembled at the Rutherford Laboratory under the direction of Dr W H Evans.

The first successful operation of the chamber occurred at the Rutherford Laboratory in January 1963 when cosmic rays and electron tracks from $Co^{60}\gamma$ conversions were seen in liquid hydrogen. The chamber was dismantled and moved to CERN where, after re-assembly, the experimental programme commenced in June 1964. Operation of the chamber finished at CERN in July 1965 after 1,500,000 physics pictures had been obtained.

Once more the chamber was dismantled and shipped back to the Rutherford Laboratory where during 1966/67 it was re-installed and improved. Operation of the chamber for physics data-taking commenced in January 1968; running with hydrogen and deuterium fillings took place for 2½ years during which time $2{\cdot}5 \times 10^6$ pictures were obtained. In 1971 technical running took place to develop the use of track sensitive hydrogen targets operating in neon/hydrogen mixtures and in the Autumn of that year the chamber became the first in the world to successfully carry out a physics programme using this new technique. Up to the time of its closure the chamber remained unique in having a track sensitive target operating capability, and in the last two years of operation $2{\cdot}7 \times 10^6$ pictures were taken in the TST – Ne/H_2 system.

A TST in the NAL Bubble Chamber (ref. 100, 174, 175, 323, 324)

The unique experience obtained by the Laboratory in the use of track sensitive targets is being used in collaboration with CERN and the Argonne National Laboratory (ANL) to provide a track sensitive target in the 12ft bubble chamber at ANL. The target was constructed of Plexiglas by the CERN target group who have been collaborating in the development of the technique in the Rutherford Laboratory's 1·5m chamber.

The target was installed at ANL in October 1973 and successfully completed the first engineering trials by the end of the month. For these tests both the chamber and the target were filled with hydrogen, but it is expected that in 1974 the complete physics system will be operated. Then, the chamber will be filled with neon/hydrogen mixture and the target with hydrogen.

Rutherford Laboratory staff are involved in many technical aspects of this programme, the commissioning and operation of the system, and will be part of the first team to use the system for physics data taking.

Design for a Multiparticle Spectrometer (Experiment 7)

A design is being prepared converting the 1·5m hydrogen bubble chamber magnet into a multiparticle spectrometer magnet. This involves turning the magnet on its side, removing some coils and re-building with new poles and modified yoke. The field will be 12 kG and the magnet will be powered by an existing 1·2 MW power supply.

The counter system consists of a configuration of ten cylindrical shaped capacitive read-out spark chambers, cylindrical proportional chambers up to 1 m diameter and height, and circular flat chambers concentrated around a hydrogen or polarized target. In addition a number of large flat plane capacitive read-out chambers are to be installed between the poles of the bubble chamber magnet. Circuits have been designed to investigate the problems which have been found to occur in capacitor read-out systems. Other items to be provided for this facility will include Cerenkov counters, disc counters, numerous beam proportional counters, and gas systems.

Construction of this spark chamber facility using present techniques would require approximately 320,000 soldered joints. To overcome this a film/wire system is being developed. It basically consists of strands of wire adhered on to a 0·001 inch thick melinex backing at 1mm pitch, which in a continuous form will be used for both the active area of chambers and connectors to their respective read-out boards thus avoiding all the usual intermediate soldered connections. A small flat prototype chamber using this principle has been built and successfully tested.

Figure 77. Schematic of the proposed Rutherford Multiparticle Spectrometer system (15182)

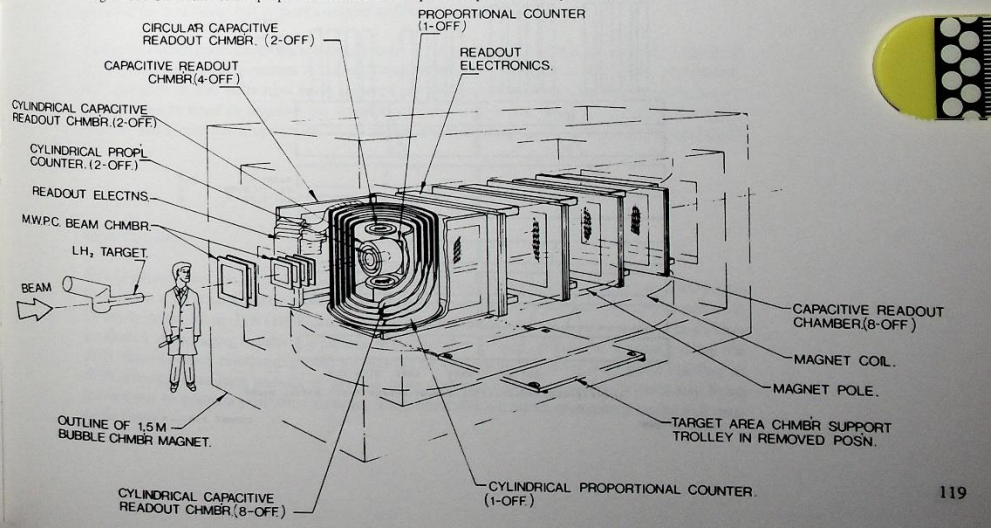

Television Cameras for Spark Chamber Read-out (Ref.377)

A proposal, by the Birmingham, Westfield College, Rutherford Laboratory collaboration, to record the spark chamber information from the Omega Spectrometer at CERN using a set of television cameras was approved in 1972. The cameras were designed and built by the Rutherford Laboratory and installed on the magnet in June 1972. No great problems were encountered in bringing the system into operation and data were quickly available for evaluation of the performance of spark chambers, cameras and analysis programs. Some parameters describing the specification and performance of the camera system are given below.

Number of cameras	8
Maximum rate capability	16 ms. per event
Maximum number of particle tracks in an event	10
Spatial measuring accuracy	$< 0{\cdot}5$ mm.
Spatial two spark resolution	~ 1 cm.
Spatial stability of system	~ 1 mm. per day
Life expectancy of camera tubes	> 2000 hours

By the end of 1973 six separate experiments had used the Omega facility, four having taken data for subsequent physics analysis, and two having tested the feasibility of their proposed triggers. Approximately ten million events have been written on magnetic tape.

The limited experience with the system has suggested a number of possible improvements and additions. Originally only the spatial position of each spark was measured but since March 1973 signal processing circuits have been introduced to give information on spark intensity. This is needed to correct a small intensity dependent spatial distortion which exists in television cameras. In the near future it is hoped to stabilise the camera sensitivity which at present depends slightly on the event rate. Also it may be possible to increase the event rate capability, possibly to one event every ten milliseconds. This is being investigated. Two other camera systems have been constructed, one of seven cameras for Experiment 14 and one of four cameras for Experiment 5.

Figure 78. A computer reconstructed event from an Omega experiment (Experiment 10). The spark-chambers are viewed by television cameras (15646)

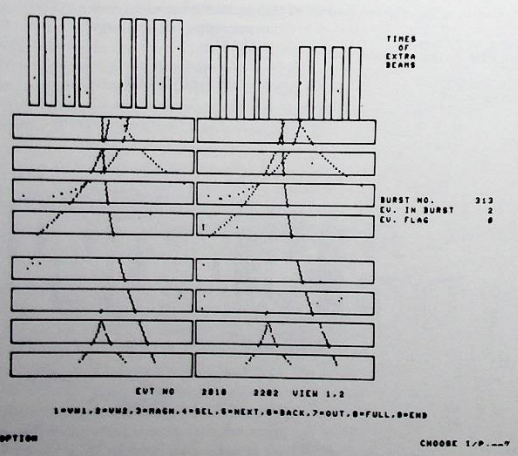

Multiwire Proportional Chambers (MWPC) (ref. 110, 112)

The operating properties and conditions of MWPC are being studied in detail. Results are based mainly on 20cm x 20cm x 2mm pitch chambers, using a beta source, however, chambers of 1mm pitch have been constructed and are in use in Experiment 5. Results from the beam-line tests agree well with those obtained with the beta source. The main results can be summarised as follows: (i) Chambers show a plateau of the order of 900 volts with detection efficiency greater than 99·5% using 'magic gas'; the efficiency remains undamaged (within a few tenths of a percent) for beam rates increasing from 5×10^4 to $1{\cdot}4 \times 10^6$ per second. (ii) Time resolution is limited only by the electron drift time i.e. 10ns for the 1mm spaced chambers. (iii) 'Magic gas' (with Methylal) suppresses breakdown and leakage current particularly in large chambers which inevitably contain some residual dust. (iv) At beam rates of the order of 10^6 per second, multiple activation of wires occurs on about 10% of the triggers.

Construction of MWPC requires considerable care and precision, particularly in the spacing and tensioning of the wires in the sense plane. The wires are typically made of gold-plated tungsten wire of 20μm dia, with a minimum tension of 45 grams per wire. The sense plane is located between planes of aluminium foil with a gap of 6·35mm. Ease of manufacture, within the close tolerances required to achieve reliable operation, is an important aspect of the design. Forty seven chambers of size 20cm x 20cm x 2mm pitch have been produced for use at the Rutherford Laboratory and CERN.

For the large scale use of multiwire proportional counter systems an economic stabilised EHT power supply unit has been developed. Operating from mains supply, it will provide a voltage range of 0 to 10 kV; overall stability of output is better than 1 part in 10^3

The gas handling rigs for these chambers have been further developed. The aim here is to control flow and mixture of gases within fine limits to maintain the properties of the chambers as constant as possible. A mixture of 56% Argon, 40% Isobutane, 4% Methylal and 0·4% Freon is passed continuously through a chamber.

Two types of electronic equipment have been developed for signal amplification and read-out for multiwire proportional chambers. One of them has the signal storage circuits and read-out bus incorporated into the electronics mounted on the chamber so that only wire addresses need be transmitted from the chambers. The other uses pre-amplifiers mounted on the chambers and the outputs, one for each wire, are transmitted to remote storage and read-out circuits. This gives higher sensitivity but is more complex and expensive than the former.

The lower sensitivity electronics is being used for a system of 12 chambers having a total of 2,250 wires used in Experiment 47. The commissioning of the equipment is nearly completed, H T plateaus of 400 volts have been achieved with high uniformity across the chamber. Developments are in hand to improve the sensitivity of this equipment. The higher sensitivity equipment is being used for a system of 16 chambers incorporating 3,200 wires used in Experiment 5.

Drift Chambers

Development work on drift chambers has been continued throughout the past year. Two prototype units with graded potential wire cathode planes of the type proposed by G Charpak et al (Nucl. Instrum. Meth. 108 (1973) 413) have been constructed. Initial tests with these units have produced encouraging results confirming the possibility of high positional accuracy using the drift time/distance relationship over a range up to 40 mm and showing very good stability in drift velocity over long periods of time. A more ambitious test programme is currently being carried out to evaluate positional accuracy limitations and the effect of inclined tracks and magnetic fields.

Low impedance amplifiers have been developed which will enable two-dimensional information to be obtained from one chamber. One dimension being obtained from drift-time measurement the other from current division ratio measurements. These circuits have not yet been used on chambers but bench measurements indicate that the required performance will be achieved.

X-ray Transition Radiation (XTR) (ref. 109, 111)

Measurements have been made on the π–8 beam line of the flux of XTR obtainable from various radiators, to assess the potential of the XTR phenomenon as an electron identification technique at energies above 5 GeV when simple Cerenkov counters become ineffective.

Measurements of the XTR flux from 1·5 GeV/c electrons, using a NaI (T1) detector agree well with theory. (The electrons were deflected to miss the detector). The detection efficiency of nearly 60% at 1·5 GeV/c implies that efficiencies of about 95% are obtainable above 5 GeV/c with stacks consisting of about 500 polythene foils.

In most applications, magnetic separation of the electron from its XTR X-ray is impossible and so experiments were carried out to assess the ability of a Xenon MWPC to resolve the X-rays from the particles. The best results obtained for electron/pion discrimination at 1·5 GeV/c were a pion suppression ratio of 5 with respect to electrons, with an electron efficiency of about 20%. Extrapolation of these results to 10 GeV/c electrons shows that suppression ratios of 20:1 can be obtained but the absolute electron detection efficiency remains disappointingly low at around 30%. Thus, while the technique has been shown to work, considerable improvement is necessary for general application in high energy physics.

Figure 79. Observed pulse height distribution in a NaI (T1) detector from XTR X-rays from 1·5 GeV/c electrons traversing a stack of polythene foils (15647)

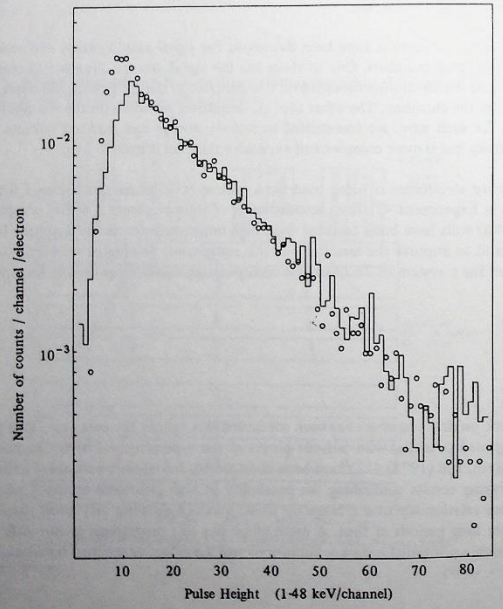

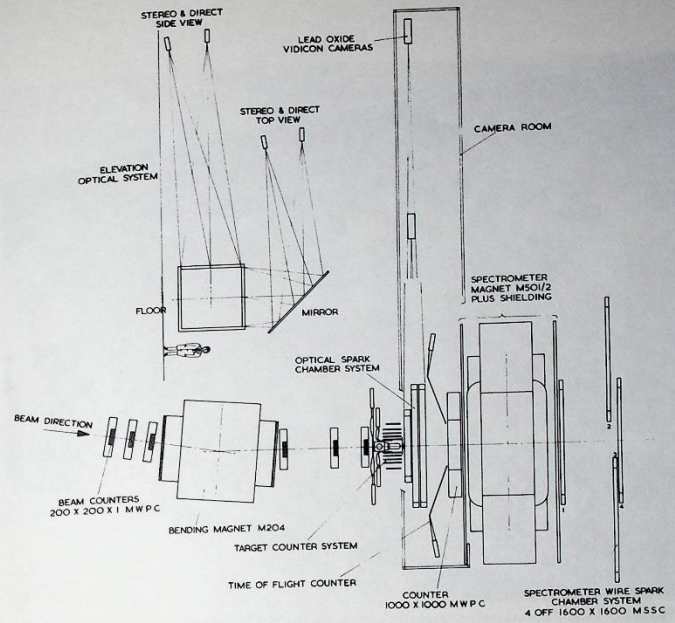

Figure 80. Arrangement of the apparatus for studying associated production (Experiment 5) (15185)

Apparatus for Individual Experiments

Apparatus for Experiment 5

Construction of the apparatus for this experiment, to study the reaction $\pi^- p \rightarrow K^\circ \Lambda$ was completed during the year. A lay-out of the apparatus is shown in Figure 80. The incoming pion beam is monitored by twelve 20cm x 20cm proportional chambers with 1mm pitch sense wires. The hydrogen target is completely surrounded by beam and veto scintillation counters, small hodoscopes, and, normal to the beam direction, sixteen low mass magnetostrictive spark chambers. The chambers are each 50cm x 30cm in area.

The downstream detectors consist of large optical spark chambers, viewed by vidicon cameras, followed by a time-of-flight hodoscope (shown during construction in Figure on Page 117) consisting of twenty four trapezium shaped scintillators with associated light guides and photomultipliers. The detection system is completed by a magnet spectrometer with a four-plane multiwire proportional chamber of 1m square active area, and four magnetostrictive spark chambers each of 1·6m square.

Apparatus for Experiment 13

A system of twenty large wire spark chambers with capacitative read-out, for this experiment at CERN, have been produced. Most of the chambers are of the order of 2m x 1m active area and the system involves about 90,000 wires. Tests were carried out to check the efficiency and overall performance of each chamber before shipment to CERN.

The atmospheric pressure Cerenkov counter for Experiment 13 has been commissioned. Figure 81 shows the fourteen concave mirrors, covering an area of 4·2m^2, each viewed by a photomultiplier and light collecting cone. The mirrors are required to have low mass while retaining their surface shape; the surface consists of aluminised melinex, coated with magnesium oxide.

To monitor the refractive index of the gas in the atmospheric Cerenkov counter and a pressurised Cerenkov counter used in this experiment, a Jamin refractometer has been built. This uses a low power HeNe laser as light source; the interference fringes are counted electronically.

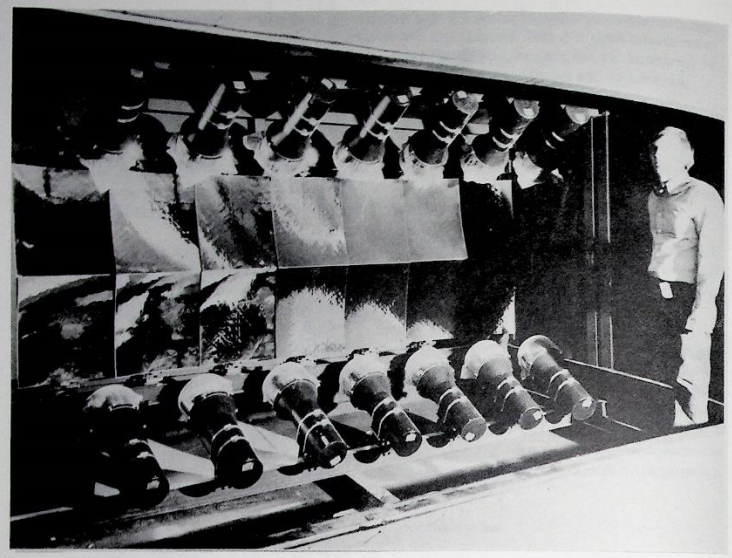

Figure 81. View of the atmospheric pressure Cerenkov counter used in Experiment 13, showing the mirrors and Winston cones (courtesy CERN 119-4-73)

Apparatus for Experiment 14

For the detection system of this experiment to be mounted at CERN, six optical spark chambers, each with dimensions of approximately 82cm square and fourteen gaps of 10mm, together with associated electronic units, stereo viewing systems and veto counters, have been supplied. The sides through which the chambers are viewed by plumbicon cameras are constructed as hollow box sections from 3mm thick perspex to reduce the refractive distortion effect. Ten multiwire proportional counters complete with gas systems have also been provided.

Apparatus for Experiment 17

An additional spectrometer system was installed for this experiment at CERN ISR, in January 1973. Sonic spark chambers are attached to either side of a magnet to form an integrated assembly; this is mounted 3·5m above the main spectrometer platform at intersection region 2.

Apparatus for Experiment 38

In this experiment gamma rays resulting from the reactions of stopped kaons with nuclei are to be studied. The main component of the detection system is the gamma ray detector, which is attached to a universal mounting enabling it to be positioned anywhere around the target. Scintillation counters and a Cerenkov counter define the arrival and stopping of a kaon in the target, after it has been slowed down by an energy degrader. Multiwire proportional counters are installed to study the characteristics of the slow kaon beam.

Apparatus for Experiment 47

The neutron proton scattering amplitude between 200 and 500 MeV will be studied in an experiment which will be staged at the TRIUMF accelerator in Vancouver. The experimental hardware has been designed and built at the Rutherford Laboratory: this consists of two large detector systems, one for protons and one for neutrons. The component parts consisting of scintillation counters, proportional counters, carbon scatterer, electronic controls and gas systems are mounted on two base frames. Thus the detectors can be shipped in assembled form and easily positioned about a hydrogen target in the arrangement for the experiment.

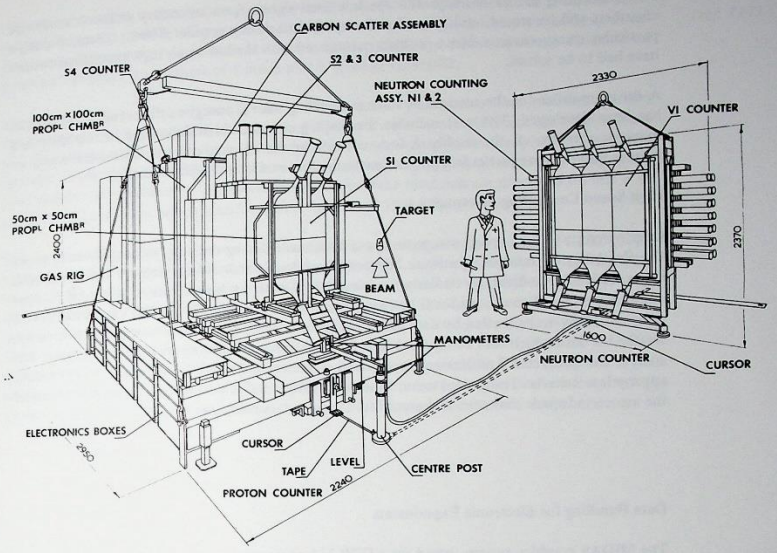

Figure 82. Arrangement of the proton and neutron detector systems for Experiment 47 (15648)

Spectrometer Arm for Beam-line P81

A spectrometer arm carrying a bending magnet and spark chamber array has been produced. The complete arm weighs about two tons and is designed to be rotatable about a polarized target, with a positional repeatability of 0·1mm at a radius of 4m from the target. It can be rotated about the target with very little effort using air bearing pads, the apex of the arm being mounted on a spherical bearing.

Electronics Development for the Nimrod 70 MeV Injector

Various aspects of the electronics development for the new injector have been undertaken. These have now passed the development phase and are being prepared for manufacture.

An expandable CAMAC system for monitoring and remote control purposes has been designed. Particular emphasis has been placed on data integrity and noise immunity. The system is based on an autonomous processor using the recently developed non-volative, re-programmable, read-only memories to provide the control program.

Development work on a beam current monitor has now reached an advanced stage with design of the toroid current transformer completed. Details of the processing electronics are at present being finalised prior to commencing the production of the main system which will have sixteen beam current monitor stations. A prototype system comprising toroid current transformer with vacuum enclosure, head amplifier, line receiver and calibration electronics has been produced for use in the pre-injector test programme. Test results obtained from this prototype confirm that the system will be suitable for monitoring current pulses with pulse durations of from 1 μs to 500 μs. The range of current pulse amplitude over which the prototype has been tested is from 200 mA down to 50 μA. The lower limit is a function of the signal to noise ratio which can be tolerated and this level may have to be raised when the system is used in the more noisy environment conditions encountered on an accelerator. It is planned to complete the design and development programme by March 1974 and to have the complete system available for installation on the injector by September 1974.

For monitoring of the beam profile the low level signals from secondary emission multiwire chambers will be stored, multiplexed and amplified to show a profile of beam intensity along a particular transverse axis. Many problems associated with the low level, high impedance circuits have had to be solved.

A drive amplifier for the modulator valve controlling the r.f. energy in the accelerating cavities has been developed. The unit includes the shaping circuits which determine the stability and dynamic response of the feed-back loop controlling the r.f. energy level. This work was a reminder that in some particular applications transistors cannot yet replace valves.

High Speed Computing Electronics

Developments in high speed computing have been made during the year, principally to improve the flexibility of control. Hardware additions have been made which improve the speed with some classes of problem, particularly those associated with track recognition. A special purpose computer directed to this end will be incorporated in Experiment 19. In this experiment event rates are likely to be limited by data recording speeds. It is important that recording time is not wasted on data which will be rejected later in the off-line computing chain. The computer will analyse the data from 5 multiwire proportional chambers and reject events which do not satisfy appropriate criteria. The computation time of 1 millisecond is well within the recovery time of the associated spark chambers and much less than the data recording time.

Data Handling for Electronic Experiments

The MIDAS graphics system, based on a DDP 516 computer, is now fully operational and provides event displays and interaction facilities as an aid to the analysis of spark chamber experiments. Both the ISR Muon Spectrometer team and the CERN Omega Spectrometer team are making extensive use of the system to rescue events which have not successfully passed through the analysis programs on the IBM 370/195. A batch of events is edited at a graphics terminal and later submitted to the IBM 370 for recomputation. Full on-line interaction with a 370 analysis program is also possible and has been used by the ISR team to tune program constants and to assess the effects on event analysis of deleting or adding sparks to tracks.

Alphanumeric display units interfaced to the MIDAS DDP 516 computer via CAMAC are used to record scanning information for film from the ISR Muon Spectrometer and from the Cambridge-Rutherford Laboratory associated production experiment (Experiment 5) with on-line checking of the typed information.

Attempts are being made to introduce standardisation of software and to create a repertoire of general techniques both for the small computers used in data acquisition and for the data analysis programs on the IBM 370. SPINE, a modular operating system for the DDP 516 computer, has been written for data acquisition on the charge-exchange experiment (Experiment 4) and handles data rates in excess of 300 events per Nimrod burst. Its structure allows simple modification for other experiments. Work is in progress on a data acquisition system for the new GEC 4080 computer to be used in the nuclear structure experiments with stopping K mesons (Experiment 38).

Data Handling for Bubble Chamber Experiments

Computer Programming (ref. 190)

There has been a continuing development of the data analysis computer program chain. The geometry reconstruction program has been extended to handle the problems of the track sensitive target and an improved convergence method has been added to the kinematics hypothesis fitting program. The CERN HYDRA system has been implemented on the 370/195 computer and is being used as a basis for a new large scale data summary and decision making program. A large program for the partial wave analysis of systems of three pseudo-scalar mesons has been implemented and is currently being used by several users at the Laboratory and from the Universities. Several programs using graphics display have been introduced to aid the analysis of experiments. These programs include histogram, scatter plot, Van Hove and three dimensional prism plot displays; an example of a prism plot is given in Figure 32.

Film Analysis (ref. 117)

The bubble chamber film analysis system at the Laboratory consists of two sections; one is a number of measuring machines used to rough-digitise events for the HPD and the other utilises two film plane measuring machines which handle the more complex events. In 1973 two machines able to take film from BEBC have been added to the rough-digitisation system, bringing the total number of machines to 14. Measurements from these machines are processed on-line with an IBM 1130 computer which interfaces with the central IBM 370/195 computer.

The system of two film plane measuring machines is now connected on-line to a PDP8E (12K) computer with extended arithmetic unit, and a high speed, high capacity disk. These improvements to the computer hardware have enabled the software to be expanded and the checks on the measurement process extended and refined. A real-time clock has been added to monitor operator measuring rates and Visual Display Units are in use for computer-operator communications. During the year the system has been used to measure 16,000 events from the 4 GeV/c π^+p experiment using the TST (Experiment 30). A single view circle fit check is applied to the tracks. For tracks which pass from the hydrogen into the neon-hydrogen medium the check is applied separately to the two segments, using separate tolerances for the two media.

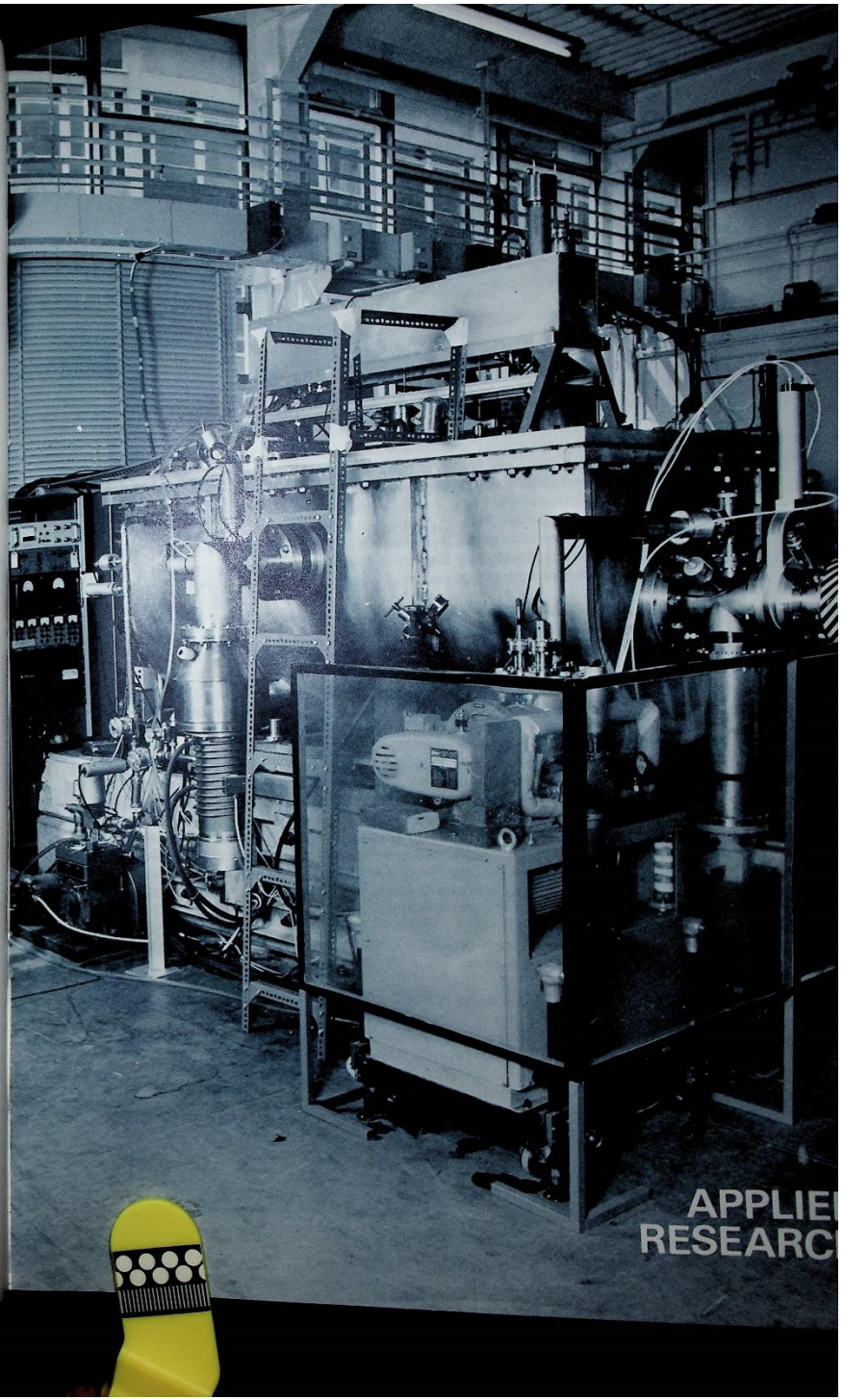

The superconducting r.f. charged particle separator which completed test operation in 1973 (13330)

Applied Research

STUDIES IN APPLIED SUPERCONDUCTIVITY

Magnet Studies

Pulsed Dipole Magnet AC5 (ref. 146)

Following the encouraging performance of the magnet AC4 in 1972, work has concentrated on improvements to the design before starting the construction of AC5. The main aims are improved field homogeneity by better symmetry in the geometry of the windings as manufactured and a reduced "training" effect, i.e. an increase in the lowest quench current (the current at which the conductor becomes non-superconducting), so that it is then not significantly lower than the full short sample current of the conductor having regard to the operating conditions.

There are indications that "training" may be due to imperfections in the coil structure which allow small, even microscopic, movements to occur with magnet excitation (c.f. the creaking of conventional coils), and the attendant heat release is sufficient to drive the local superconductor normal as the enthalpies are so low. It is therefore desirable to make the thermal contraction of the different component parts of the coil construction as nearly equal as possible to avoid local stresses and imperfections when cold. Development work to this end has been in progress for the whole year. A further development is to sleeve the winding with stainless steel rings so that it will be tightly contained at room temperature and remain so at liquid helium temperature.

Terylene braid, though strong and excellent as a conductor insulation, is anomalously bad thermally with a volumetric contraction $\Delta V/V \sim 33 \times 10^{-3}$ from room temperature to operating temperature and must be replaced. Glass fibre and cotton are good thermally but poor in resistance to abrasion from winding. If adopted, they will require that the part helical ends of AC4 be replaced by more natural curves. The problem is still amenable to design for a good field integral in the case of an iron yoke with a circular bore, which is now possible as the coil to iron gap has been increased to accommodate the stainless steel bands. The high density flat strip cable, reported last year, also indicates a need for an easy shape to wind in the ends.

A limited discussion of this sort illustrates how the design of a high field superconducting magnet involves many new inter-related and often conflicting factors.

On the question of improving the winding geometry, recent trials with double layers showed that better symmetry can be achieved by 'potting' as complete circular units with no division on the equator. Although it makes the provision of cooling channels more difficult, it is hoped to extend this so that four layers, e.g. for AC5, can be impregnated as a single unit so avoiding internal surfaces, possible sources of frictional heating.

The basic research and development for AC5 is almost complete and detail design has started. The aim is to produce a dipole magnetic field of 6 tesla.

"Training" Research

"Training" as discussed above in connection with magnet AC5 is an effect shown by all large superconducting magnets working at high current density. The magnet is seen to quench (become non-superconducting) at currents and fields considerably below the short sample critical currents. Repeated quenching usually produces some improvement, hence the name "training", but the full critical current is rarely attained. The hypothesis that this effect is caused by small movements occurring within the magnet winding, releasing heat, has now been confirmed by a series of training experiments on small 'race-track' shaped coils. It has been found that test coils will always "train" if their electro-magnetic forces are not adequately supported and also that this "training" can be completely removed by applying the correct force support. The implications for magnet design are obvious but are difficult to achieve, particularly in transverse field magnets such as dipoles and quadrupoles.

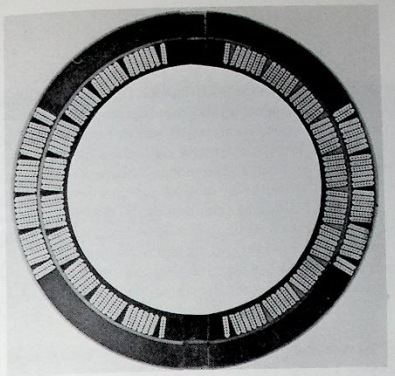

Figure 83. Section through a superconducting pulsed dipole magnet. Note the grouped winding of conductors, with wedges placed between groups to form the circular geometry (15018)

Potting Materials Research

The enhanced mechanical integrity of superconducting magnet assemblies, potted with epoxy resins formulated for resistance to thermal shock and large temperature gradients, has still not resulted in the elimination of "training". Studies, however, on curing and cooling stresses have indicated that curing resins under high pressure could serve to further control dimension changes during cooldown and also improve the mechanical integrity of the composite structure.

Measurements have been made on strain rate effects in superconducting materials with particular emphasis on serrated yield phenomena as another contribution toward an understanding of the "training" phenomenon.

D.C. Dipole Magnet

Work has started on the construction of a large d.c. dipole magnet as a further "training" experiment. It is designed to produce a transverse field of 5T in a 1·1 m long 130 mm diameter bore. The coils will be impregnated with epoxy resin using a new high pressure technique in which the resin is pumped into the magnet and cured at a pressure of about 300 atmospheres. It is hoped that most of this precompression will be retained throughout the life of the magnet. The magnetic forces should thus be very effectively supported and training effects should be reduced.

Superconducting Composites

The collaboration between the Laboratory and Imperial Metal Industries Limited has produced several new superconducting composites during the year. Figure 84 shows a large composite containing 177241 niobium titanium filaments of 5μ diameter in a matrix of copper. The composite is intended for pulsed use (approx. 2 sec rise time) and resistive barriers of cupro-nickel alloy are interspersed throughout the matrix to reduce eddy current effects. For a field of 5 tesla the composite should carry a current of more than 4000A and may thus be used to replace the multistrand cables which have so far been used in the construction of pulsed magnets. Its performance is currently being evaluated in a series of short sample tests.

Figure 84. Micrographs of a superconducting cable composite of niobium titanium filaments in a matrix of copper

(a) magnification X 20 (15701)

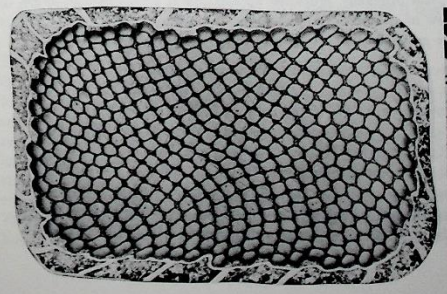

(b) magnification X 400 (15702)

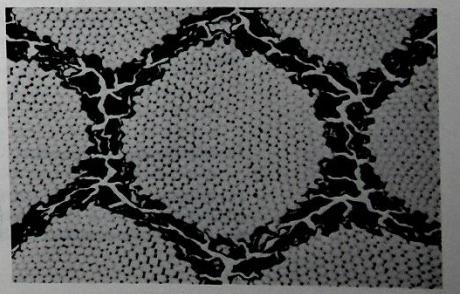

A new collaboration has been established with Process Technology Division, AERE Harwell, with the object of exploiting the filamentary niobium-tin composites developed at AERE. The superconducting properties of niobium tin are vastly superior to those of niobium titanium but its brittle mechanical properties make it extremely difficult to produce or handle. The Harwell process is based on the idea of processing pure niobium filaments in a tin-copper bronze alloy and then reacting the finished composite to produce niobium tin. Rutherford personnel have participated fully in the improvement and extension of the AERE process to produce composites suitable for large magnets and also for pulsed use. Techniques developed at the Laboratory should allow large magnets to be wound from an unreacted composite which is then finally reacted, thus eliminating all possibility of damage to the brittle niobium tin filaments during winding. Two small solenoids have been made so far and many tens of short samples have been tested.

Flux Pump

A small flux pump or superconducting current supply has just been brought into operation. It supplies a current of 1000 A at 20 mV, ie. 20 W of power from a unit about the size of a teacup. The supply works on the transformer rectifier principle. An alternating current of ±7 A at 30 Hz is fed from room temperature to a superconducting primary where it induces heavy currents to flow in a secondary winding. The secondary current is rectified by thermally activated cryotrons, or superconducting switches, and supplied to the magnet. If supplies of this type can be made sufficiently reliable for the routine operation of superconducting magnets, they should effect considerable economies by removing the heat leak caused by heavy current leads and also eliminating the need for large conventional power supplies.

Superconducting Solenoid Magnet

A solenoid magnet being constructed for use in Experiment 47 at the TRIUMF accelerator is now nearing completion. It will produce a field of 6T in a 1 m long 100 mm diameter room temperature bore and will be a fully operational unit, able to function for many weeks at a time without the need for operator access or maintenance. Each of the five magnet sections has been tested and reached full short sample performance with no training. The cryostat (supplied by Oxford Instruments Limited) has been tested and found to have a heat leak of less than 1 watt, a very satisfactory result.

Design Studies on Superconducting Magnets

Design studies have been made on a large number of superconducting magnets, including solenoids 4 m diameter x 6 m long providing magnetic fields of 1 to 2 tesla, dipoles with bending powers of 6 Tm, quadrupoles and sextupoles for possible use in particle physics. Most of these magnets have been investigated within the GESSS collaboration (the Group for European Superconducting System Studies which includes Saclay, Karlsruhe and Rutherford Laboratories).

Superconducting Energy Transfer System

Engineering design calculations on the 1 m diameter model have confirmed that the concentric spherical coil system can be constructed to maintain the required tolerances during operation. Trial coil sections were wound from multistrand superconducting tape, and low temperature tests on the bearings required for rotation of the inner coil showed that friction losses would be acceptably small. This work has confirmed the general feasibility of low loss inductive energy transfer systems, and their large scale use has been proposed, for example, in possible future pulsed fusion reactors. However, the originally proposed application as a synchrotron power supply now seems unlikely, in view of the trend towards slower cycle times or d.c. storage ring systems, and for this reason it is probable that no further work will be carried out on this scheme.

Superconducting r.f. Separators

The building and successful test running of the first superconducting r.f. separator has been achieved during 1973. The complete separator was in fact assembled and tested 3 times during the year, with the modifications from the first two runs leading to successful operation in the third.

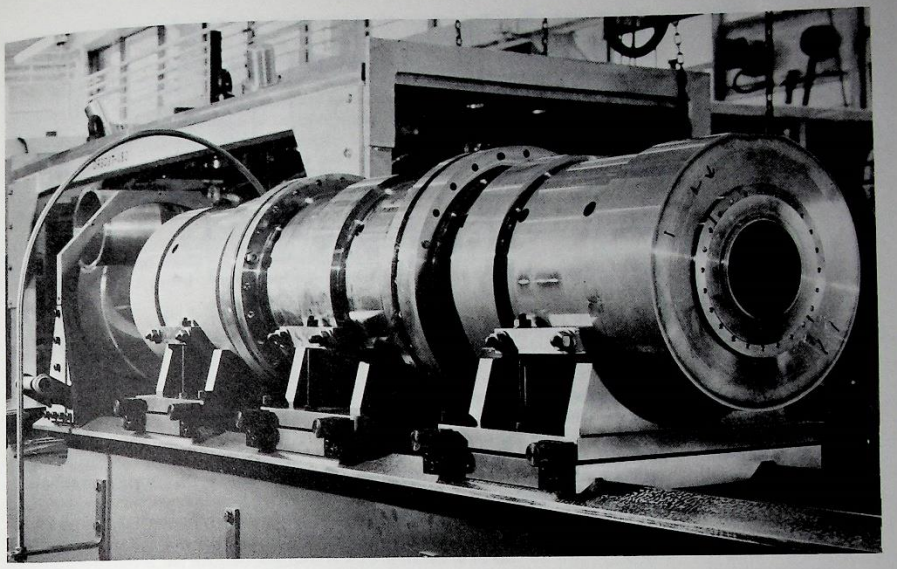

Figure 85. Pre-plated cavity sections of the superconducting r.f. separator undergoing alignment checks (12270)

Plating System

The r.f. cavity consists of three sections each of which is separately lead plated, using an enclosed plating system. A rough vacuum is used to remove totally any gas bubbles during critical stages in the cleaning and plating processes, and high purity acetone is used in the final water removal and drying stages, with the final vacuum drying being done through liquid nitrogen traps to ensure minimal contamination of the lead surfaces. To retain the good quality of the lead surfaces, all inspection and assembly processes are done in a pure nitrogen atmosphere (oxygen content less than 0·1%), requiring an elaborate system of glove boxes.

r.f. System and Components

The frequency stabilised source and main amplitude control have been further developed. The frequency stabiliser now operates over the range 1·3 GHz ± 7 MHz, with a stability of 2 parts in 10^{10}. The automatic level control provides an r.f. amplitude stability ($\alpha A/A$) less than 0·6%, well within the required tolerance. The automatic fine (varactor) tuning control has been shown to give up to 20 Hz tuning (depending on coupling) when it comes within the sensitivity of the mechanical tuners.

The main r.f. feed, mechanical tuners, r.f. tuners and samplers now generally operate satisfactorily. The first cryogenic test showed that the coupling factors of the main r.f. feed were too small; this has been corrected by reducing the wall thickness of the cavity coupling aperture and by changing the simple probe to a loop coupler. Coupling factors of up to 100 are now available, with an overall r.f. feed loss of 17 mW per watt. Small modifications to the mechanical tuners and r.f. samplers have also been made. Some difficulty has been experienced in obtaining coaxial ceramic windows reliable at extreme cryogenic temperatures. This has been overcome by selecting and vacuum testing the windows as individual items and in sub-assemblies at 77 K. Components tested in this manner have been leak tight even at temperatures below the helium λ-point.

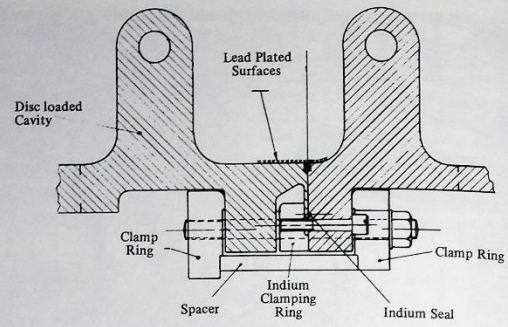

Figure 86. The cantilever joint between the cavities of the superconducting r.f. separator (14866)

r.f. Cavity

As stated above, the r.f. cavity is built in 3 sections, one of four, and two of three cells. The cantilever joint between the sections was intended to provide simultaneously a good r.f. contact and a vacuum seal for super-fluid helium. However, in the first two cryogenic tests, the mode dependence of the cavity Q-value indicated that though the vacuum seal was good, the contact for superconducting r.f. currents was poor. Later examination showed that the joints had become distorted. The joints were re-machined and are now as shown in Figure 86, where it can be seen that though the vacuum seal is still made by the cantilever, the clamping force is taken wholly by the r.f. joint itself. This joint now performs satisfactorily.

High Field Tests

After completion of the component modifications, the separator was assembled for the third series of tests. The complete separator is shown on Page 129. Prior to cooldown the cavity vacuum was $1{\cdot}5 \times 10^{-7}$ torr (from which pressure less than one monolayer of gas condenses on the lead surface); no vacuum problems were encountered on cooldown to 1·85 K. During cooldown the temperature differences across the cavity, at the critical temperature of lead, was 0·16 K for the first test, and 0·04 for the second. The cavity was warmed to 77 K between tests, as would occur in normal operation. The low power limiting Q_L-values were:– at 4·2 K, $1{\cdot}31 \times 10^8$, which is 75% of theoretical Q_O; at 1·85 K, $2{\cdot}1 \times 10^8$. No significant difference in Q-value was seen on varying the cavity mode, indicating satisfactory operation of the joints. On the application of even a few tens of mW of r.f. power the unloaded Q-value degraded to $8{\cdot}1 \times 10^7$, but remained constant thereafter, up to the highest power levels. During the second test, the Q_O-value retained the degraded figure up to the highest field levels, during runs of several hours. The cavity was easily run up to the equivalent deflecting field E_O = 2·18 MV/m, and with little conditioning run for a few hours at E_O = 2·23 MV/m. Beyond this level, more careful conditioning was required, due to the onset of E-field emission. However the highest field obtained was E_O = 2·6 MV/m (preliminary figure), with corresponding peak surface fields H_p = 377 Gauss, E_p = 9·96 MV/m. At this level X-radiation along the axis of the separator was 60-70 mR/hr, with occasional bursts of 300 mR/hr with voltage breakdown.

The experience obtained during the tests indicates reliable operation is obtainable in the range E_O = 2·25 to 2·50 MV/m.

RAPID CYCLING BUBBLE CHAMBER DEVELOPMENT

Rapid Cycling Vertex Detector

During the year, the development phase of the Rapid Cycling Vertex Detector programme has continued. Significant progress in many areas has been achieved and detailed designs for the construction of the detector are in course of preparation. The development programme has concentrated on the areas where this device departs from established bubble chamber design. These are: the expansion piston/optics cartridge, the illumination system, the expansion system actuator and the high speed camera.

Optics

In order to minimise wall interaction background in the external particle detectors, the base and walls of the chamber must be as thin as possible. This aim is achieved by forming the concave mirror used in the bright field retrodirective illumination system by deposition directly on to the body of the chamber. The first stage is to turn a spherical surface on the chamber by a copying process. This surface is then smoothed by normal polishing techniques to remove turning marks and to correct any minor geometrical errors. A thin layer of nickel (about 0·03 mm thick) is then deposited chemically and the surface is finally polished to high optical quality. Small sample mirrors have been made to the required standard and a full size mirror has also been produced which has only one small defect. Cryogenic tests on the small mirrors have been successfully carried out in the Bubble Chamber Test Rig.

A complete optics-expansion system cartridge has been tested at 50 Hz at room temperature in a vibration test rig. Nearly 4·5 million cycles have been completed at strokes of up to 4 mm. It is expected that a stroke of not more than 3 mm will be required in normal operation of the chamber.

Expansion System

The electromagnetic vibrator which will drive the expansion cartridge has been tested at 50 Hz. The linearity and force characteristics have been measured and experience in operating this piece of equipment has been acquired. Tests show that operation of the chamber at 60 Hz is within the capability of the vibrator. Further tests using a high power amplifier to power the vibrator will follow in 1974.

Cameras

Development work on the rapid cycling camera has progressed throughout the year using a bread-board model. The film transport mechanism is now capable of taking 5 pictures per Nimrod flat top at a rate of 10 pictures per second. The fastest wind-on sequence achieved is 26 ms resulting in a total camera dead time of 70 ms. A detailed study of the film motion made using a high speed cine film indicated that disturbances caused by a shock wave travelling back down the film when transfer was complete may limit reliable operation to 10 Hz.

Final design and construction is now in hand and it is expected that the first operation of the completed chamber will occur in late 1975.

Fast Cycling Bubble Chamber Test Rig

The test rig has been fully commissioned with liquid hydrogen. Four experimental runs were carried out with successive modifications between runs to optimise the system. After initial problems the chamber produced good tracks of a Cobalt 60 pulsed gamma source and also of cosmic rays. Experiments were carried out to determine the bubble growth and decay characteristics as a function of overpressure and operating frequency. Double-pulsed operation determined the over-pressure required to recondense bubbles when operating at a fast repetition rate and some tests were also done on multiple pulsing to obtain data for the design of the new Vertex Detector.

Over 1 million expansions were carried out at liquid hydrogen temperatures using the glass reinforced plastic (GRP) piston/bellows assembly at strokes of up to 5 mm. The material suffered no ill effects and has been shown to be completely suitable for applications in bubble chamber expansion systems at liquid hydrogen temperatures.

The Linde cycle hydrogen refrigerator which was designed and built at the Laboratory performed very reliably. Performance tests showed that its capacity was 230 W at 25 K with a liquefaction capability of 9·6 litres/hour of liquid hydrogen.

Expansion System

Electronic modifications to the resonant expansion system permitted reliable operation with liquid hydrogen. The mass carrier was lightened for the final experiment to give as rapid an expansion pulse as possible and this gave an expansion pulse width of 21 ms. The chamber was run in short bursts continuously at this basic frequency without re-applying the brakes between successive expansions. Multiple bursts were executed re-applying the brakes to hold the chamber in the compressed state between pulses with a basic pulse separation of 54 ms. Up to 9 expansions per burst at a repetition frequency of 1 burst every 2 s were performed very reliably. No difficulties were experienced in running the chamber continuously at 4 Hz.

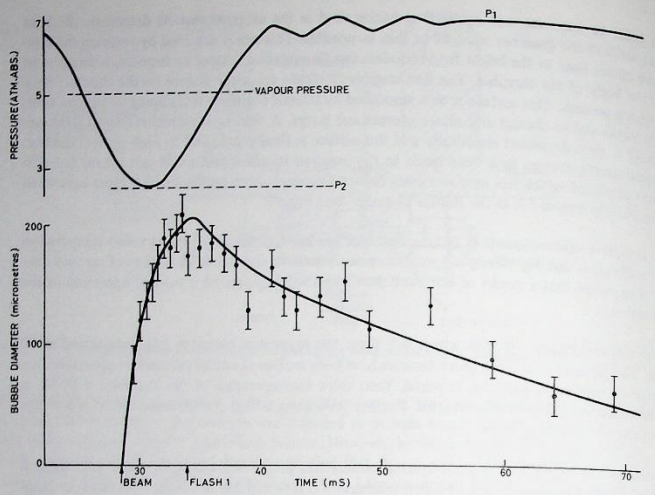

Figure 87. Bubble size as a function of time measured as part of the development programme of the rapid cycling bubble chamber (15704)

The Experimental Programme

The Fast Cycling Rig was used to carry out two series of experiments. Observations were made to determine rates of bubble growth as a function of operating parameters and a study of the effects governing the re-nucleation of track bubbles was undertaken.

It was found that for very low over-pressures bubbles re-nucleated readily giving rise to larger bubbles on the second expansion than on the first. As the over-pressure was increased a condition was reached in which the bubbles formed reappeared on the second expansion but with greatly reduced optical contrast. This was due to the presence of warmer liquid around the regions of recompressed bubbles giving a sufficiently high refractive index mismatch to give images in bright field. A further increase of pressure led to complete extinction of bubbles on the second expansion.

When measuring bubble growth rates the chamber was run continuously at 1 Hz and the two light sources were timed to flash on the same expansion pulse. One light source was set to take a picture at a fixed point during the expansion corresponding to maximum bubble size, ie. a growth time of about 4 ms. The other flash was scanned over the entire expansion cycle time to record the bubble size as a function of time. The results are shown in Figure 87.

POLARIZED TARGET DEVELOPMENT

PT55

This horizontally polarized proton target is required for Experiment 5 to study the reaction:

$$\pi^- + p \rightarrow \Lambda^\circ + K^\circ$$

For secondary particle detection a large exit cone of half angle 60° has been specified from a target volume 5 cm long and 3 cm diameter. Figure 88 shows how these requirements have been achieved in the design by the use of a superconducting magnet. The angled design of the target cryostat allows upstream counters defining the incident particle direction to be placed close to the target volume.

The target material will be propanediol prepared with Cr V complexes and at the design temperature of 0·5 K a proton polarization close to 80% is expected. The optimisation of the coils, for the superconducting magnet, to produce the required 2·5 tesla central magnetic field to an accuracy of 2 parts in 10^4 has been completed. Techniques for manufacturing the superconducting wire to tight tolerances on diameter and parallelism, and methods of winding the required coil shapes have been developed. Full scale dummy coils have been manufactured using copper wire and a cross-section of one of the large coils is shown in Figure 89. The detail design for the magnet cryostat and other support equipment has been completed and orders for manufacture placed with industry.

Design of the target cryostat and helium$_3$ refrigerator has been completed and most of the pump and vacuum systems have been ordered. The helium$_4$ refrigerator/liquefier has been delivered and installed in building R25 and prior to operating in a closed cycle mode for target work it has been systematically used to produce liquid helium for site requirements. Initial installation of structural items has proceeded in building R25 where the complete target system will be installed and commissioned before installation in the Hall 3 beam line.

Development has been carried out on a mechanism for traversing the target horizontally within the cryostat in order to remove the target assembly for loading in situ. This has involved investigation into microwave losses at the break in the copper wave guide and the system has been checked out at liquid nitrogen temperature. Methods of loading and unloading the target material have also been carried out at liquid nitrogen temperature. The majority of the micro-wave and NMR components have been ordered and initial assembly work has commenced.

Figure 88. Design of PT55, the horizontally polarized target (15703)

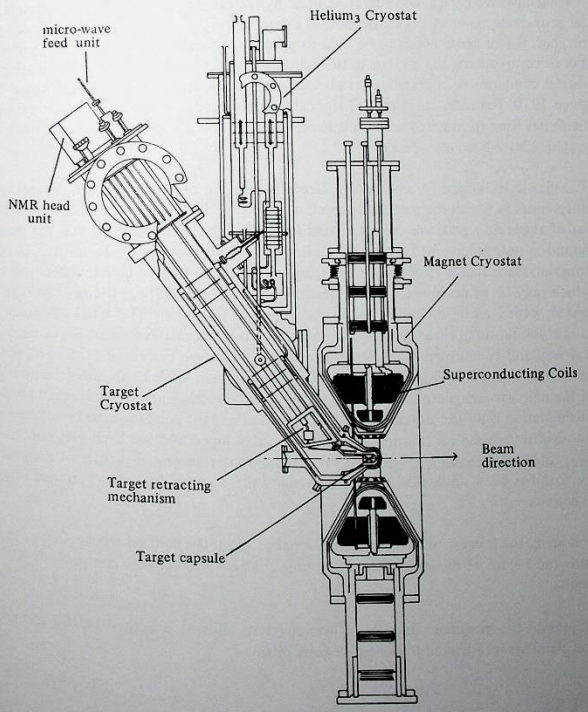

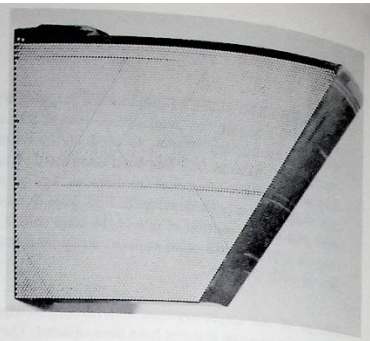

Figure 89. Section through a proto-type superconducting magnet coil for PT55 (14169)

The Frozen Spin Polarized Target

Polarization was achieved early in the year but faults in the superconducting magnet system prevented any further progress.

The magnet system has been repaired and rebuilt with an additional booster coil incorporated. This coil will raise the field between the polarizing and holding magnets hence reducing the polarization loss during the movement between these magnets.

A new material, 1,2-propanediol doped with Cr.V complexes, has been prepared for use in the target.

COMPUTER AIDED DESIGN OF MAGNETS (ref. 381)

Electromagnets are an essential part of apparatus used in HEP experiments. The design of a magnet involves careful consideration of many factors, such as geometric constraints and material properties, to meet a specification at a reasonable cost. In carrying out a design study for a magnet, the designer needs to be able to predict the field shape, the electromagnetic forces between components, the stresses in the materials used in construction and many other factors. A digital computer with graphics peripherals has been in use for magnet design at the Laboratory since 1970. Recently an improved algorithm based on a new method for computing magnetic fields has been formulated and implemented and improved ergonomic features, using interactive graphics, have been introduced.

New Method of Calculating the Field

The classic technique for computing magnetic fields in two dimensions is the method of finite differences in which the partial differential operation, describing the field, is approximated by a set of algebraic equations. An important limitation of this approach is that the magnetic field boundary values have to be prescribed. In practice this requires the boundaries to be located a considerable distance from the magnet, and requires the field to be calculated over this region, which may be of no interest to the designer. Another difficulty is the need to span the whole system with a mesh, including conductor, iron and free space. This latter difficulty becomes a crucial limitation in three dimensions. An alternative approach is to treat the problem in a physical way and to consider the magnet as a system of known current and unknown induced magnetisation sources. This way of formulating the problem leads to an integral equation in terms of the unknown magnetisation (dipole strength and direction per unit volume). In order to solve this equation only the iron needs to be discretised and the need for false boundaries is avoided. An algorithm based on this approach has been developed and has been very successful in two dimensions; for example, Figure 90 shows a computer generated picture of a dipole in which the iron has been subdivided into elements and the 'arrows' show the computed magnetisation directions.

Following the success of the two-dimensional program the method was applied to three dimensions and Figure 91 shows results for a bubble chamber magnet with comparisons with measurements.

At present the maximum number of iron elements allowed is limited to 100 and the shape of iron elements is restricted to right triangular prisms.

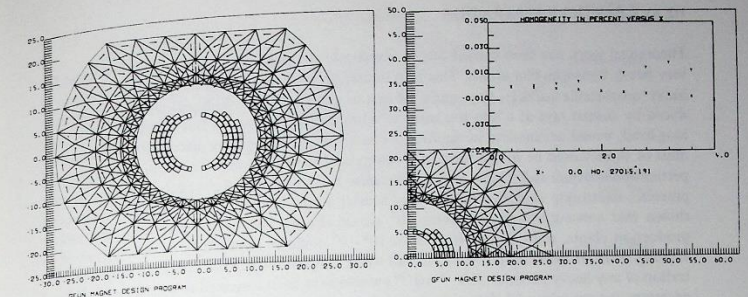

Figure 90. A computer generated design for a dipole magnet showing the field pattern in the iron yoke (15706, 15708)

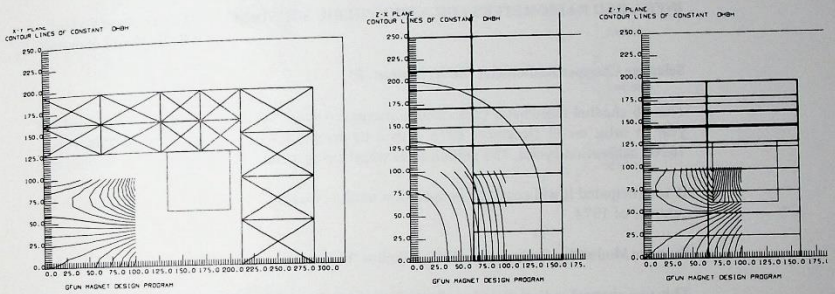

Figure 91. Results from a three-dimensional magnet design program (15705, 15710, 15707)

Interactive Graphics as an Aid to Design

The introduction of graphics hardware and communications software into the Laboratory's computing resources enabled a fresh approach to be considered in organising the structure and operation of computer programs used in design problems. Accordingly the new field computing algorithms were incorporated, into an interactive graphics program for magnet design. With this program it is now possible for a designer to create and modify data defining a magnet by typing simple commands at a graphics terminal which is on-line to the Laboratory's central computer. At any stage the geometry of the magnet can be displayed, enabling errors to be detected and design concepts checked. On completing the data-definition stage, the designer can request the program to calculate the magnetic field and display graphs of the magnetic field along selected lines or contour maps over selected regions. On the basis of these results, the designer can change the geometry of magnet in an attempt to find a better design. Automatic optimisation, in which selected parameters are varied in a continuous manner in order to achieve a desired field shape, can be used. For some three dimensional geometries stereo pairs are generated which can be examined with a stereo viewer.

The remote graphics terminals are used as an aid to general engineering design from various fields of work such as structural analysis, heat transfer and fluid flow. Investigations are being made also in the field of computer aided detail drawing and a system developed by PERA is being evaluated for the type of work at Rutherford Laboratory.

HEAVY PARTICLE SEPARATION

Theoretical work has been carried out to investigate the possibility of enrichment of water for very heavy hydrogen-like atoms. This is of interest in connection with the possible existence of heavy quasi-stable particles (e.g. quark or parton constituents of hadrons) which may be produced by cosmic rays at a rate too small to allow direct observation but which, if sufficiently long-lived, would accumulate in significant concentration in ordinary matter. If singly charged, most of these would be in the form of a heavy isotope of hydrogen, and from the known properties of deuterium and tritium, calculations have been made of the physical properties (vapour pressure, electrolyte evolution rate) of any heavier atoms of this type. From these it has been shown that concentration by a factor 10^5 would already have been achieved in heavy water production plants, and that a further factor 10^5-10^7 could be achieved by the electrolysis of an existing stock of heavy water, giving a final water sample in which the predicted initial concentration of any heavy particles, (10^{-26}-10^{-20}) would have been increased to the 10^{-8}-10^{-14} level necessary for experimental detection. It has also been established that such processing could be carried out using equipment already operational in the UKAEA.

INFRA-RED RADIOMETERS FOR ATMOSPHERIC SOUNDING

University of Oxford
Rutherford Laboratory

Selective Chopper Radiometer (SCR) Nimbus 'E'

This 16 channel radiometer (described in previous Annual Reports) successfully completed one year in orbit on 11 December 1973. This is its design lifetime and it now totals 5500 orbits, 16500 calibration cycles, 136 million filter wheel changes and 680 million chopper revolutions.

It is anticipated it will continue in operation until its successor on Nimbus 'F' is launched in the summer of 1974.

Pressure Modulated Radiometer (PMR) Nimbus 'F'

This two channel radiometer (described in last year's Annual Report) is nearing completion with the two flight modulators now being filled and sealed off in the Laboratory. After installation, final testing and calibration it will be shipped to NASA (USA). All the test gear, test targets and calibration targets have been completed by the Laboratory during this year and the engineering model of this radiometer has been integrated with the spacecraft using this test gear. The radiometers were manufactured by Marconi.

Figure 92 (a). Location of the Chopped Pressure Modulated Radiometer as it will be mounted on Nimbus 'G', showing the scanning modes (15709)

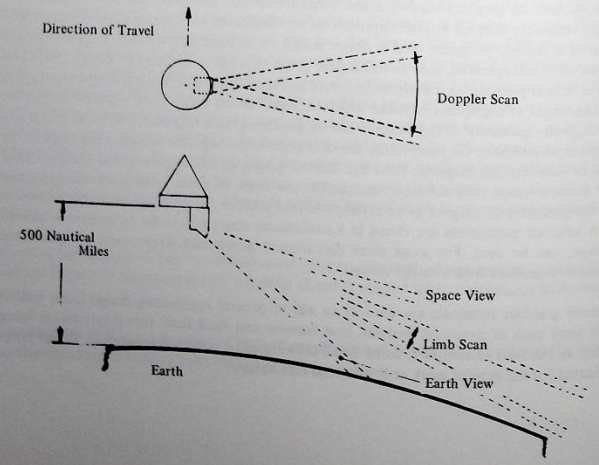

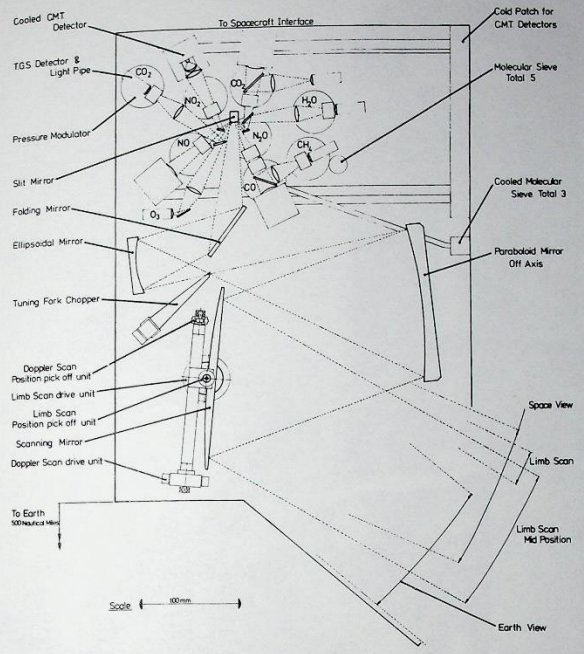

Figure 92 (b). Arrangement of components in the Chopped Pressure Modulated Radiometer (15022)

Chopped Pressure Modulated Radiometer (SAMS) Nimbus 'G'

This Stratospheric and Mesospheric Sounder is a 10 channel radiometer for temperature and composition remote sounding. It has been accepted by NASA for inclusion on Nimbus 'G' to be launched in 1978 and the proposal is now awaiting DES authorisation.

The general arrangement of the radiometer is shown in Figure 92 with a cluster of 8 pressure modulators filled with various gases (CO, CO_2, CH_4, NO, NO_2, N_2O and water vapour) and by selective absorption the concentration of these minor constituents of the atmosphere can be monitored on a global basis. Two CO_2 cells are included: one provides the temperature data and the other a height reference. Preliminary experiments have been made on pressure control techniques for the gases mentioned. These experiments suggest that all the gases except NO_2 could be amenable to control using the molecular sieve technique.

The scanning mirror looks at the limb of the atmosphere (i.e. tangential to the earth's surface) so that only the atmosphere is viewed, unlike the method of vertical scanning where signals from the earth's surface confuse the measurements. The mirror scans forward and backwards along the track on the limb to provide a doppler scan. This scan will allow wind measurements to be deduced. The scan on the limb is from the satellite at a height of 900 km and the height resolution of the atmosphere is required to be within 100m thus requiring the positional accuracy of the mirror to be known to within 2 arc seconds for each signal integration period (up to 4 seconds). The radiometer also includes a 150 Hz resonant chopper and this, being about 4 times the PMR frequency, allows the separation of wide band information from the PMR information. A firm design has been produced with accurate cost estimates for this very complex unit.

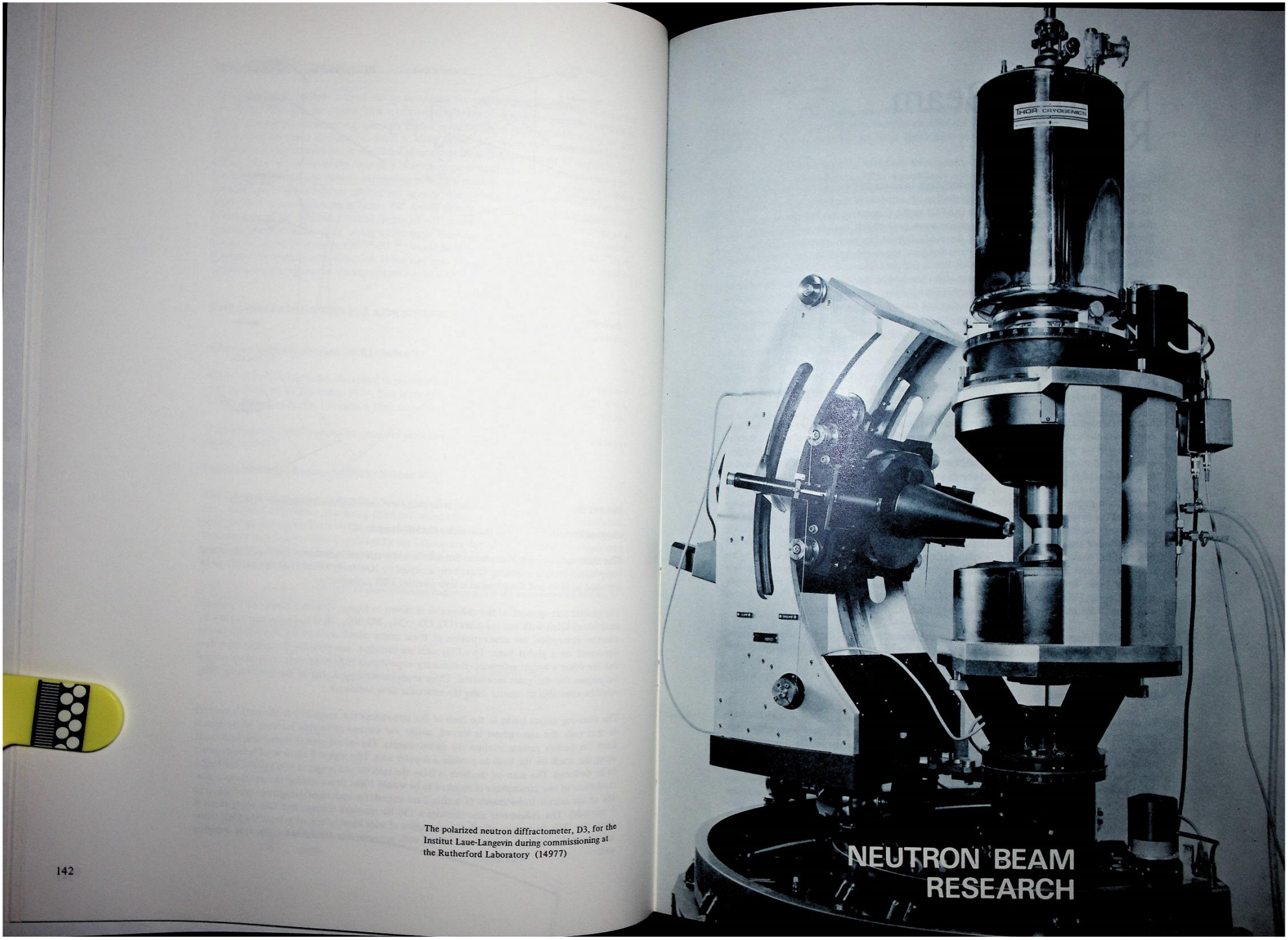

The polarized neutron diffractometer, D3, for the Institut Laue-Langevin during commissioning at the Rutherford Laboratory (14977)

NEUTRON BEAM RESEARCH

Neutron Beam Research

The SRC became a full partner in the Institut Laue-Langevin (ILL) with effect from 1 January 1973 and UK scientists are now closely involved in the activities of the Institut. The responsibility of the Neutron Beam Research Unit (NBRU) at the Laboratory has broadened to include the provision of support for approved neutron beam experiments both in the UK and abroad. During the year activities have included the production of two new instruments for the ILL, development work on new neutron beam techniques, secretariat work for the Neutron Beam Research Committee (NBRC) of the Science Board, and participation by NBRU staff in neutron beam research programmes. The total direct effort involved in the above work was 20 man years and by the end of the year the direct strength of the Unit was 24. 80% of this effort was divided roughly equally between development studies and current programme support, the remaining 20% being absorbed in participation in neutron beam science, general management, secretariat duties and ILL instrument construction.

DEVELOPMENT OF NEUTRON BEAM TECHNIQUES

Polarization Analysis (ref. 325)

In a polarization analysis experiment a monochromatic polarized neutron beam is scattered by a sample and the scattered neutrons are analysed in momentum, spin, and also sometimes in energy. The spin (or polarization) analysis allows neutron spin-flip and non-spin flip scattering processes to be distinguished and provides additional information about the nature of the scattering to that obtainable by momentum and energy analysis alone. Up to now polarization analysis of thermal neutron scattering has only been carried out on triple axis diffractometers at high-flux reactors and magnetised Cobalt (92) : Iron (8) single crystals were used on the first (polarizing) and third (analysing) axes. A considerable advance in the instrumentation required for such experiments is possible if a polarizing filter is used as the spin analyser and from earlier studies it was concluded that a material containing polarized ^{149}Sm nuclei, which operates by selective spin capture, would be the most efficient polarizing filter for thermal neutrons. A CSMN polarizing filter is now being constructed, and it is later planned to use it as the spin analyser in a polarized beam diffractometer. (The term CSMN refers to a cerous magnesium nitrate single crystal, $Ce_2Mg_3(NO_3)_{12}24D_2O$, in which $\sim 8\%$ of the Ce^{3+} ions are replaced by $^{149}Sm^{3+}$ ions in which the ^{149}Sm nuclei can be highly polarized by the 'Rose Gorter' method.

A theoretical treatment of the separation of the spin-dependent partial double differential cross-sections by polarization analysis has been carried out, and a method suggested to allow for multiple scattering effects.

Diffractometer Control

To obtain experience required for application to instrument control a test bed system has been set up to allow the testing and assessment of shaft-positioning and ancillary units which conform to the CAMAC standard. This standard has been adopted for the interface equipment in use at the ILL and for the control of the new diffractometers at AERE. The control systems for simple diffractometers may not justify the use of a digital computer. However, it is still desirable to allow for a degree of flexibility in their automatic sequencing. Experiments have been carried out using a Programmed Dataway Controller, coupled with a 256 word random access store, to control a single CAMAC crate. Such an arrangement allows the programme which specifies the diffractometer operation to be changed within minutes. Experience with the system has been gained by writing a suite of programs suitable for the control of and data acquisition by a two-circle polarized beam diffractometer.

Position Sensitive Detectors

Work on the application of channel electron multipliers to neutron detection has continued throughout the year. Light from a neutron scintillator is coupled to a photocathode-channel plate-electron collector assembly, the latter operating in vacuum.

Two methods of optical coupling have been investigated. In the first, suitable for a two dimensional position sensitive detector (PSD), a scintillator screen, which could be as large as $1m^2$, is coupled by a lens to the channel plate electron multiplier. Light from a neutron capture event is focussed onto the photocathode, the photo-electrons produced being multiplied in the channel plate by a factor of 10^5 to 10^6. The resulting electron avalanche is collected by an array of crossed wires. When simultaneous signals are observed on two wires, the positions of those wires are related to the x-y co-ordinates of the original event. The electron detection part of this proposed device has been satisfactorily demonstrated.

In the latter part of the year, priority was given to the second method of optical coupling which is suitable for a one dimensional PSD with high spatial resolution. This is considered to be the form of detector likely to find an immediate application (for example in a Marx spectrometer). The scintillator consists of a stack of thin strips, each one optically isolated from its neighbour, for example by aluminising the surface. The scintillator stack is in vacuum and the photocathode is deposited directly on the ends of the strips. Thus each strip forms its own light guide and a scintillation anywhere along a strip produces copious photoelectrons which are amplified by a channel plate and detected by a simple array of metal collector strips. The width of these collector strips is the same as the width of the scintillator strips.

Figure 93. Schematic diagram showing the components of an experimental linear position sensitive detector under development at the Laboratory (15072)

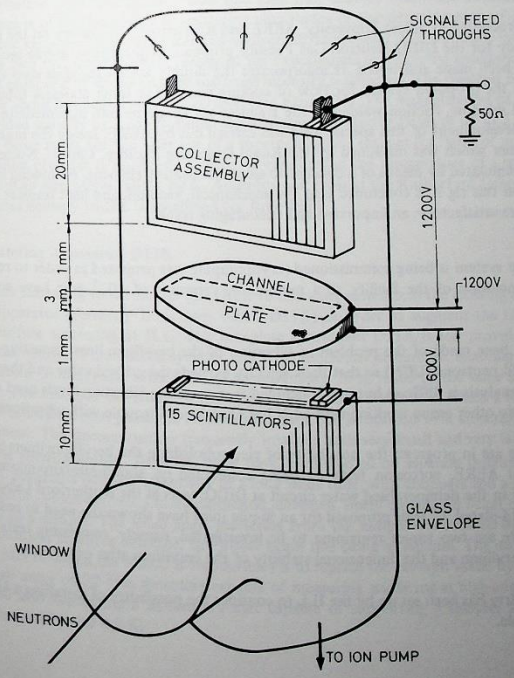

A prototype detector was constructed and is illustrated in Figure 93. The scintillator consists of 15 strips of NE905 (a cerium activated ^{6}Li loaded glass). The device was successfully tested at the AERE DIDO reactor. The positional resolution was demonstrated by scanning a 1 mm wide slit in a cadmium plate across the front of the detector with only one channel in use, the remainder being grounded. The response of the channel as a function of slit position is triangular in shape, as would be expected, and the base width is consistent with the 1 mm resolution of the detector, the slit width and the divergence of the neutron beam.

Guide Tubes

There has been continued development of a stacked film device for bending a 10 Å neutron beam through about 5°. Methods of stretching Melinex film have been developed and special spacers, formed by a photo etching process, have been obtained. The device has a bending radius of 180 cm, the films are 25 μ thick and are separated by air spaces of 250 μ.

An apparatus for measuring the variation of local surface slope of guide tube materials has been used on stretched film samples to show that the film surface will be close enough to the ideal for good results with 10 Å neutrons. For example the variation in slope of a flat specimen is within $\pm 4 \times 10^{-4}$, which is close to the surface quality specified for the cold neutron guides at the ILL.

A test rig for experimental trials of the bender was commissioned which can be mounted on the 4H5 hole at DIDO. To gain experience, measurements were made of the reflection of 10 Å neutrons from a nickel plated glass sheet curved to the same radius as the final bending device.

Ultra Cold Neutrons

Work has proceeded at Sussex University, AERE and Rutherford Laboratory on the project definition study for the DIDO Neutron Gas Facility proposal. A prototype in-pile section of the facility has been made and tested. It incorporates the double walled stainless steel vacuum envelope with the proposed system for flow of cooling water. The inner stainless tube has a zirconium end window, friction welded to the stainless via an aluminium intermediate tube. The successful development of this special weld was carried out by AERE. Inside the inner tube is a beryllium liner which was machined by the Royal Ordnance Factory, Cardiff. Nuclear heating of the rig is simulated by means of a concentric electrical heating element. Following many measurements on this rig it is concluded that the mechanical, vacuum, and heat transfer aspects of the design are satisfactory, an important and encouraging result.

A cryopump system is being commissioned (cryopumping was proposed in order to reduce possible contamination of the facility to a minimum). Pressures of 10^{-7} torr have so far been achieved.

A study has been made of the problem of vibration of the beryllium liner imparting energy to the ultra cold neutrons (UCN) so that their velocity exceeds the critical value and they are lost. Theoretical analysis is difficult but it is concluded that excessive vibration levels need not occur in practice. No other group working with UCN has experienced trouble with vibrations.

Other studies are in progress: the possibility of electropolishing the beryllium liners is being investigated; at AERE, corrosion tests are being conducted on aluminium/zirconium/stainless steel samples in the demineralised water circuit at DIDO; tests at the Rutherford Laboratory of the metal gold-plated 'C' seals proposed for an in-pile joint have shown the need to redesign this section. There are two topics remaining to be investigated, namely, outgassing tests on small samples of beryllium and the dimensional stability of the beryllium after outgassing.

A working party has been set up by the ILL to consider the possibility of installing a UCN facility at Grenoble.

Pressure Cells

Studies of the structure and dynamics of materials in different environments such as high or low temperatures are frequently made using neutron scattering techniques. Pressure, like temperature, is a useful thermodynamic parameter. For instance 2·5Kcal/mole can be stored in sodium chloride either by heating it from 0K to 300K or by applying a pressure of 50Kbar. In the former case there is a change in the interatomic distance of less than 1%, whereas in the latter case compression can change the atomic configuration in such a way that a new phase becomes stable, creating a change in interatomic distance of about 5%.

The potentialities of using pressures between 5 and 100Kbar in neutron scattering experiments have not been fully realised due to the difficulties of maintaining the pressure on the sample without interfering with the incident and scattered neutron beams. A survey of the construction techniques for high pressure sample cells has been started.

NEW INSTRUMENTS FOR THE INSTITUT LAUE-LANGEVIN

Polarized Neutron Diffractometer, D3

There are many experiments which can be done with beams of polarized neutrons without the use of polarization analysis especially now that high flux neutron beams are available at ILL; eg measurements of precise magnetic scattering amplitudes or the determination of extremely small magnetic cross-sections. The polarized neutron diffractometer, D3, will meet this requirement. It is a two axis diffractometer designed for experiments in which the specimen is placed in a beam of polarized neutrons and the scattered intensity is detected. The shielded detector of D3 can move about horizontal and vertical axes (see Figure 94). The magnetisation of the specimen is provided initially by a conventional electromagnet producing fields of up to 2 T, though provision is being made for the later use of a superconducting magnet for fields of up to 4·8 T. A liquid helium cryostat is provided, capable of maintaining the temperature of a specimen at 4·2 K, or with an alternative tail, at 80 K. Assembly and trials at the Rutherford Laboratory are in progress and delivery to ILL is scheduled for June 1974.

Diffuse Scattering Apparatus, D11B

A new diffuse scattering spectrometer (D11B) is to be incorporated into the existing small angle scattering apparatus (formerly D11, now called D11A) in order to augment the facilities for measuring diffuse scattering at ILL. The complete instrument D11A/B will provide a unique facility in the study of disordered systems and large molecular structures, enabling both high $|\underline{Q}|$ (momentum transfer) and ultra low $|\underline{Q}|$ measurements to be made on the same sample simultaneously. For example the study of decomposition of alloy systems, in which a heat-treated alloy passes through several phases to reach equilibrium, can be studied with advantage with the new instrument. The decomposition frequently involves both very small and very large precipitates existing simultaneously. Hitherto these have been studied on separate instruments. The present D11 apparatus consists essentially of a long guide tube, with choppers and a helical slot velocity selector, which delivers a monochromatic, chopped, finely collimated beam of neutrons (7 to 25 Å) to a sample. The small angle scattering from the sample is measured by a two dimensional position sensitive detector, the whole beam line being in vacuum. The modification, D11B, (for part of which the NBRU is responsible) is to replace the vacuum vessel by a new one containing an array of 32 ^{3}He detectors capable of measuring scattering at high angles (18° to 143°2θ) and also containing a helium cryostat capable of supporting 5 samples and cooling them to a temperature of 4·2 K.

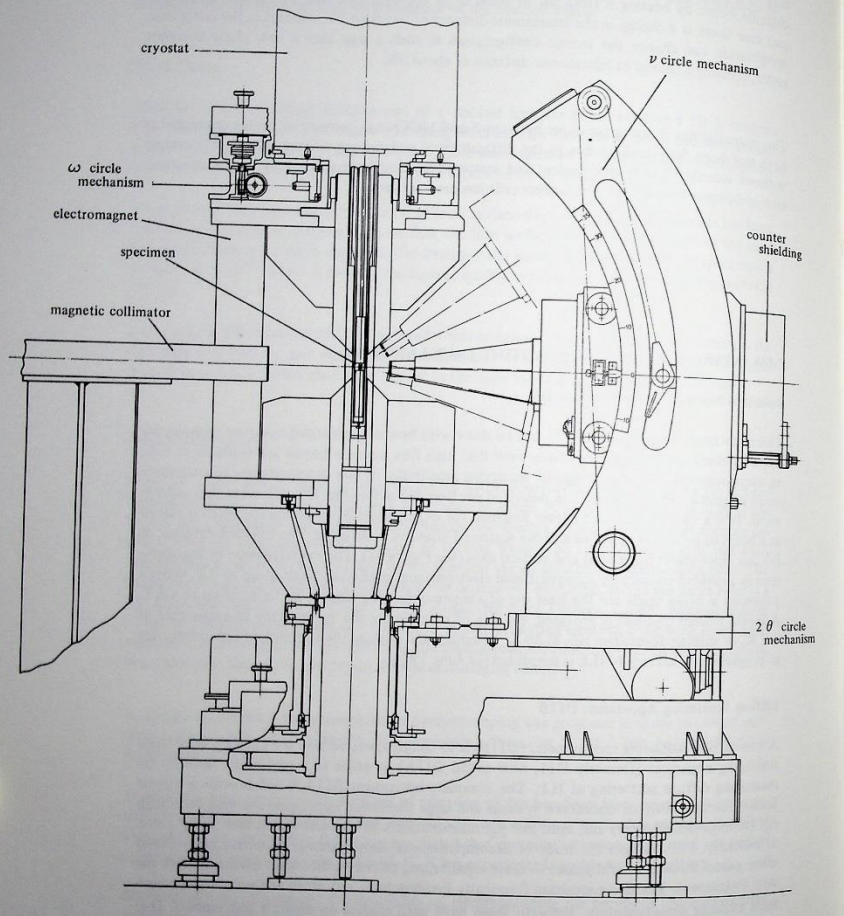

Figure 94. Machine drawing of the polarized neutron beam diffractometer, D3. The specimen is magnetized by a conventional electro-magnet (12571)

SUPPORT OF THE NEUTRON BEAM PROGRAMME

UK Programme

At the Herald reactor at AWRE, Aldermaston, modifications have been made to the Graphite Monochromating Chopper (GMC) blockhouse to reduce the background of unwanted particles. The NBRU provided a shielded door and shutter for the blockhouse and a vacuum flight path for the unscattered beam was installed. Further modifications are now in progress to provide a two-slot rotor and additional counter positions to uprate this instrument still further.

Improvements have been made to the SRC computing facilities at Herald. The objectives were to provide for an increase in the number of detectors and timing channels in the GMC apparatus, and for some expansion of the Rotating Crystal Spectrometer facility.

The DIDO-Rutherford Laboratory computer link has continued to function without failure during the whole year. Over 1340 jobs have now been submitted to the Rutherford IBM 370/195 using the remote ELECTRIC terminal and over 820 CASSANDRA neutron data tapes have been transferred to the IBM using the Remote Job Entry (RJE) Terminal. A Facit fast paper tape reader has been added to the RJE Terminal. The reader will allow neutron experimental data produced by the powder, polarized beam, and diffuse scattering diffractometers at AERE to be processed by the IBM 370/195 and archived to IBM 9 track magnetic tape.

ILL Programme

The NRBU is responsible for organising the collection and the processing of UK experimental proposals for transmission to the ILL. Each proposal is costed and particular attention is given to possible repercussions on the UK or ILL programme. So far a total of 116 proposals has been submitted to the ILL in three rounds of applications.

Support to the NBRC

Members of the Unit assist in the technical support for the NBRC and its Sub-Committees. This work includes preparation of papers and reports, the servicing of technical working parties, supervision of approved projects, processing of experimental proposals for the ILL and assistance with some aspects of proposals for domestic reactors.

PARTICIPATION IN NEUTRON BEAM SCIENCE

Neutron Incoherent Scattering and Absorption Cross-Sections

Unlike scattering lengths, the values of incoherent scattering and absorption cross-sections are not well documented. With the advent of higher fluxes, measurements can be performed more accurately resulting in a demand for higher accuracy in factors that correct data, such as absorption. The NBRU is assessing the extent to which further measurements are needed of absorption and incoherent scattering cross-sections for individual elements and isotopes. Special attention is being given to requirements arising from use of the AERE Linac.

Computer Simulation of Neutron Elastic Scattering (ref. 239)

A study has been made of the methods employed in data analysis, especially those pertaining to the measurement of absolute differential cross-sections at long wavelengths. A Monte-Carlo technique has been employed to study multiple scattering and absorption corrections. The Monte-Carlo technique has also been used to study the effects of window broadening on the angular resolution of small angle scattering data. This technique is of particular importance for experiments at the ILL where the high flux enables greater statistical accuracy to be obtained, which in turn requires more detailed data analysis.

Magnetic Studies

In collaboration with the University of Cambridge an analysis of the single crystal diffraction measurements using both polarized and unpolarized neutrons which had been made on $CoCO_3$ at 4·2 K has been completed. The measurements of the antiferromagnetic reflections have been used to establish a magnetic structure in which the cobalt moments lie wholly within the basal plane. This conclusion, which is contrary to that of previous workers, is a consequence of making a proper calculation of both spin and orbital scattering by the cobalt ion. This calculation is based on a ground state wave function for the cobalt ion in the structure of the carbonate deduced from spectroscopic and magnetization data. The model has also been used in calculating the scattering to be expected from the weak ferromagnetic component of moment which has been measured using the polarized neutron technique. The small differences between the observed scattering and that calculated for the model can in all cases be understood from the difference density distributions as being a consequence of covalency.

The programme is continuing with a study of magnetic scattering from ferrous salts. $FeCO_3$ and FeF_2 have been selected for examination. The former compound is chemically isostructural with $CoCO_3$. It has already been the subject of a single crystal, polarized neutron study to determine the magnetic scattering amplitudes of the [hhl] (rhombohedral) reflections with the sample at 79 K (Néel temperature $T_N = 35$ K) and in an external field of some 1·8 T. Below T_N, the sublattice magnetisation direction is [111] and the antiferromagnetic reflection intensities have been measured in an unpolarized neutron study at 4·2 K. The magnitude of the small extinction present is being confirmed by powder diffraction and the effects of spin-orbit coupling on the vector character of the moment density is the subject of a current experiment using the polarization analysis facilities available on the D5 diffractometer at the ILL.

A preliminary examination has been made of a small single crystal of CoS_2 in a collaborative study with the Centre National de la Recherche Scientifique, Grenoble. The experiment is an attempt to verify experimentally a theoretical suggestion that in ferromagnetic CoS_2 (Curie temperature, $T_C = 122$ K) the single equivalent set of cobalt atoms should split into two subsets having their single magnetic electron predominantly occupying a different set of orbitals with e_s symmetry. The initial measurements carried out at 4·2 K on the D2 diffractometer at ILL revealed no observable magnetic intensity at the half-order sublattice positions and they serve to put a lower limit on the sensitivity of this type of experiment to the proposed effect.

Alloy Precipitations

Titanium alloys are of great technological importance and there is considerable interest in the decomposition of their metastable phases. The use of neutron scattering for the study of these alloys is a powerful tool because the negative scattering length of Ti enables null-matrix alloys to be formed. For a random distribution of solute, the scattering is completely isotropic over the whole of Q space. However, any degree of order gives rise to a Q dependence that can be measured over a large range of |Q|, as there are no Bragg peaks. Measurements have been made on the binary alloy Ti–Zr and show a degree of short range order present. A series of measurements has been planned for the tertiary system Ti–Zr–Nb which is believed to exhibit a range of phase transformations.

Preparatory work, with Reading University, has been done on the Al–Zn system aimed at studying the modes of decomposition by diffraction measurements to see if the alloy exhibits satellite reflections on decomposition.

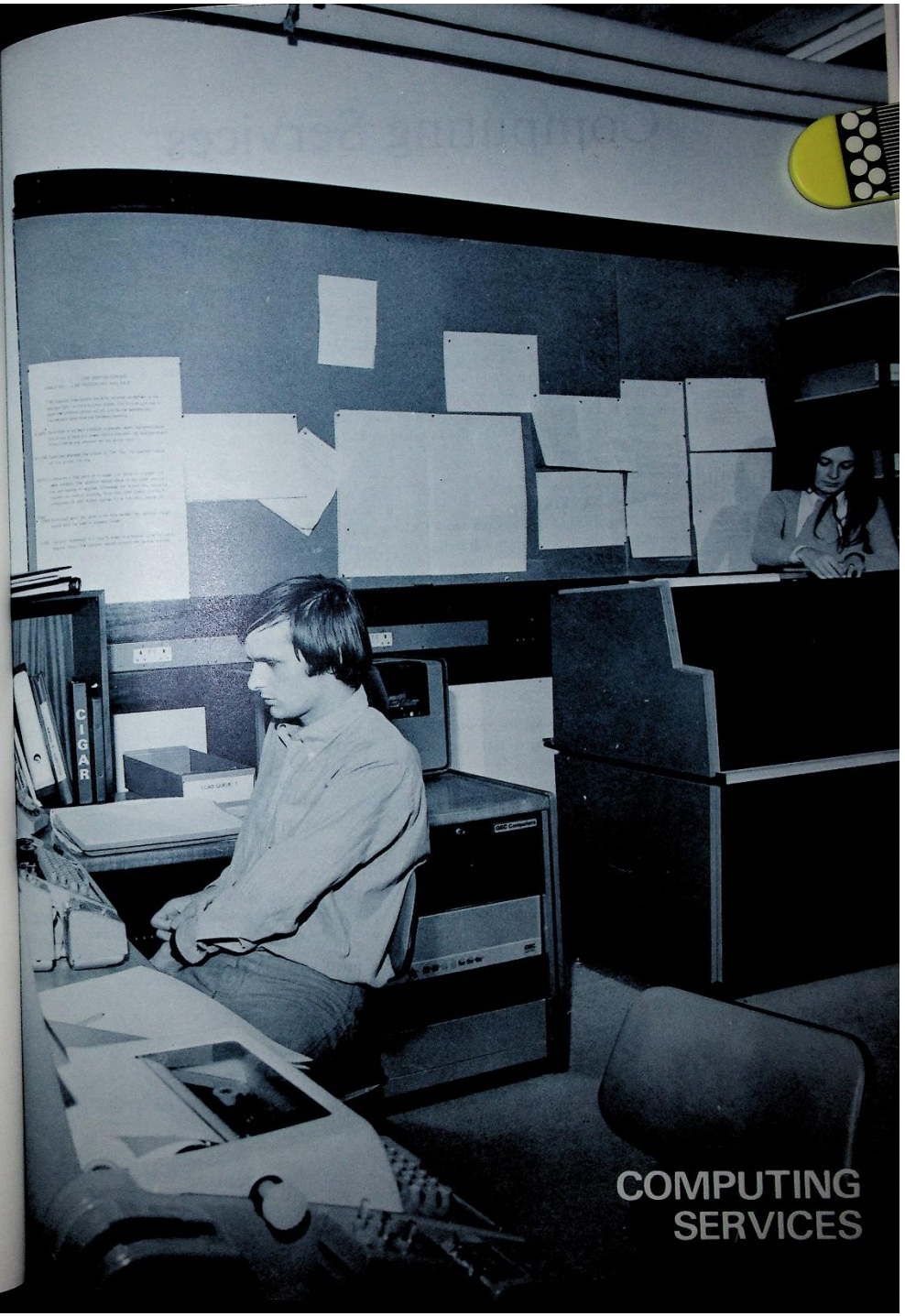

A work station at Oxford University connected to the central computer at the Rutherford Laboratory (14858)

COMPUTING SERVICES

Computing Services

At the beginning of the year the operating schedule of the Central Computer was extended to a full seven days (168 hours per week). The only new equipment added was a second set of IBM 3330 disks (eight drives), and no major changes were made to the operating system. In this stable atmosphere the performance and reliability of the machine have proved quite outstanding. Maintenance has been reduced to four hours every four weeks and system development to less than three hours per week, thus invariably leaving more than 160 hours available to Users in each normal working week.

The pressure of work has increased, so that for the greater part of the year all available CPU time has been used. With a full work load, CPU utilisation varies between 70% and 80%. This provides about 100 CPU hours per week to Users, and the total of jobs now exceeds 10,000 per week. The most notable growth during the year has come from Users sponsored by the Atlas Laboratory, who accounted for over 20% of the total work load by the end of the year.

Remote computing has undergone a quiet revolution during the year. This has arisen partly from the increased popularity of ELECTRIC: over 50% of jobs are now submitted from local or remote ELECTRIC terminals. The number of ELECTRIC users rose from 100 to 200 in the year. Fifteen remote work stations, based mainly on GEC 2050 computers supplied by the Laboratory, are now in service; in an average week about 4500 jobs are loaded on the central computer via work stations.

Early in December, after measuring 1·25 million bubble chamber events, HPD1 was taken out of service for rebuilding to HPD2 specification. HPD2 met all 70mm spark chamber film measuring requirements during the year, and had just measured a large sample of bubble chamber film satisfactorily.

CENTRAL COMPUTER

Operations (ref. 315–317)

This is the first year of full round-the-clock operation of the IBM 370/195, and the 450,000 total of jobs processed shows a rise of 70% on last year (which had itself shown a rise of 60% on 1971). A statistical summary of operations is made below and in Figures 96, 97, 98, 99, showing the numbers of jobs submitted from remote work stations, via ELECTRIC, and in total, and the CPU time in each case, the weekly averages of machine efficiency $\left(\frac{\text{scheduled - down time}}{\text{scheduled time}}\right)$ and CPU utilisation $\left(\frac{\text{CPU time used}}{\text{scheduled - down time}}\right)$, and other details.

Distribution of Jobs by CPU category

Category	Thousands of Jobs	Average CPU time used
Short (< 90 seconds CPU)	422	12 seconds
Medium (< 5 minutes CPU)	14	3 minutes
Long (> 5 minutes CPU)	13	14 minutes

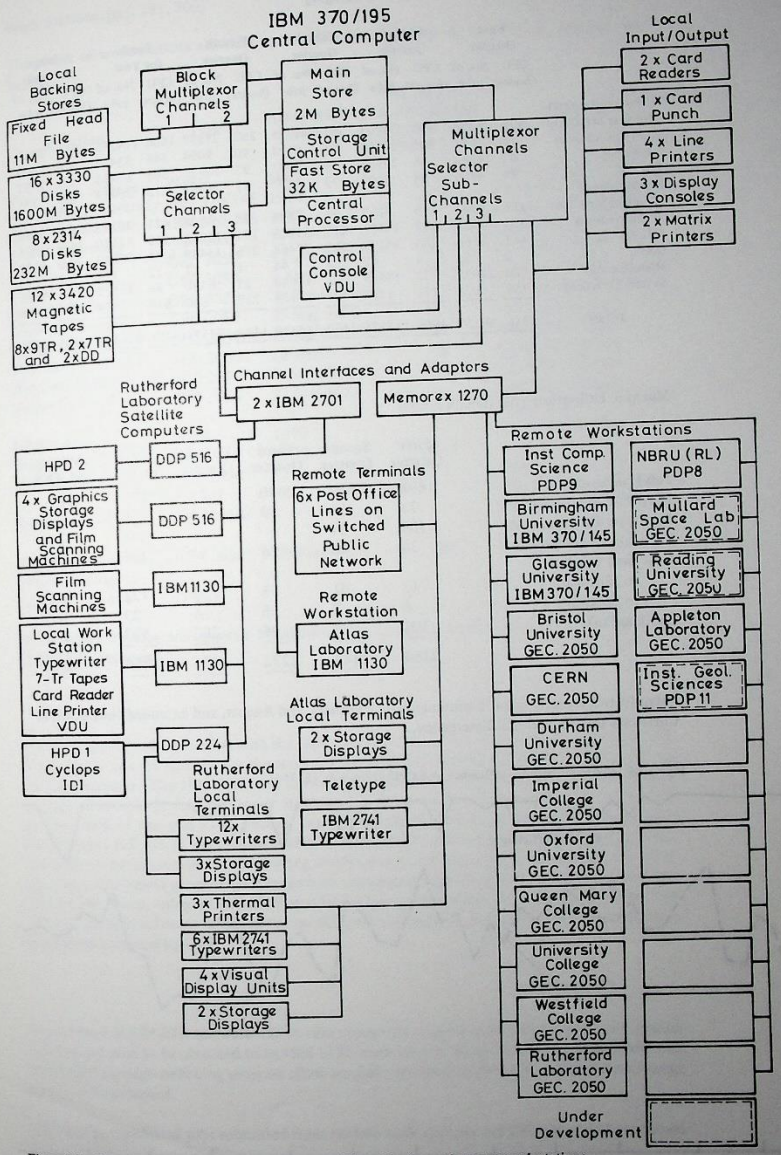

Figure 95. Organisation of the central computer, peripheral devices and remote work stations.

Distribution of CPU time and Jobs by User category

	First Quarter		Second Quarter		Third Quarter		Fourth Quarter		Total for Year		Average per week	
	CPU (hours)	No. of jobs	CPU (hours)	No. of jobs	CPU (hours)	No. of jobs	CPU (hours)	No. of jobs	CPU (hours)	No. of jobs	CPU (hours)	No. of jobs
HEP–Counters and Nuclear Structure	495	28250	420	31103	383	31735	302	27197	1600	118285	30·6	2265
RL–Film Analysis	74	7631	101	7959	81	8794	90	9094	346	33478	6·6	640
RL–Other	67	20542	88	20939	56	19077	97	22875	308	83433	5·9	1593
Theory	49	4154	98	5499	73	6297	55	4469	275	20419	5·3	391
Universities – Nuclear Structure	136	4367	119	6237	91	5293	75	4845	421	20742	8·1	396
Film Analysis	223	9528	247	13531	218	14213	195	16268	883	53540	16·9	1024
ATLAS	161	8566	285	14179	323	17468	278	19429	1047	59642	20·0	1140
DNPL	2	51	4	67	5	44	1	17	12	179	0·2	3
Miscellaneous	20	12035	22	13609	21	14688	23	16380	86	56712	1·6	1085
System Overheads	159	1033	222	1152	209	889	228	600	818	3674	15·7	70
Totals	1386	96157	1606	114275	1460	118498	1344	121174	5796	450104	110·9	8607

Machine Utilisation (All time in hours)

	First Quarter	Second Quarter	Third Quarter	Fourth Quarter	Total for Year	Average per week
Job Processing	1898	2059	2030	1885	7872	150·6
Hardware Maintenance	23	13	19	14	69	1·3
Hardware Development	109	24	–	5	138	2·6
Software Development	34	30	26	33	123	2·4
Lost time attributed to Hardware	13	31	53	35	132	2·5
to Software	6	7	6	4	23	0·4
Switched off *	101	20	98	208	427	8·2
	2184	2184	2232	2184	8784	168·0

*Mainly twice-yearly plant maintenance in February and August, and extended shut-down at Christmas due to National Emergency.

Figure 96. Central computer efficiency and CPU utilisation (15754)

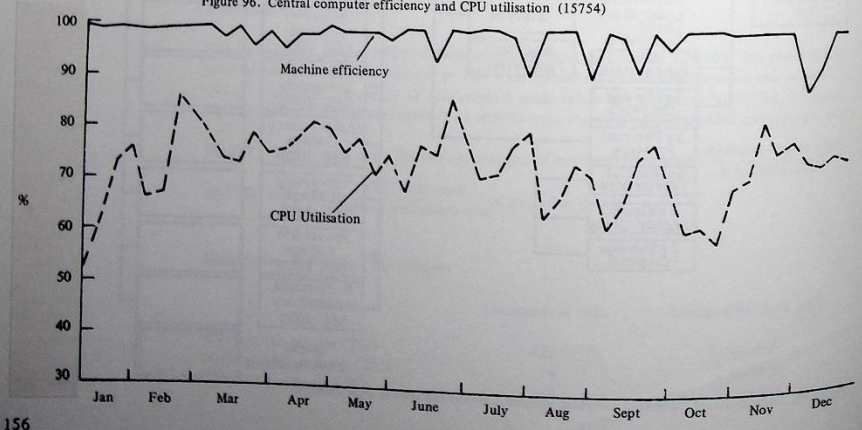

Work Stations (ref. 181, 303)

The status of work stations attached to the central computer at the end of 1973 is summarised below:

Location	Type	Acceptance date	No. of jobs in normal week (Average for November 1973)	Comments
Inst. Comp. Science	PDP 9	1968	321	Development Project
Birmingham University	IBM 370/145	1972	684	(Originally IBM 360/44)
Glasgow University	IBM 370/145	1972	137	(Originally IBM 360/44)
Bristol University	GEC 2050	10 April 1973	248	Purchased by RL
CERN	GEC 2050	5 June 1973	267	Purchased by RL
Durham University	GEC 2050	3 April 1973	197	Purchased by RL
Imperial College	GEC 2050	27 March 1973	324	Purchased by RL
Oxford University	GEC 2050	25 May 1973	407	Purchased by RL
Queen Mary College	GEC 2050	17 April 1973	58	Purchased by RL
University College	GEC 2050	29 March 1973	65	Purchased by RL
Westfield College	GEC 2050	7 June 1973	131	Purchased by RL
Rutherford Laboratory	GEC 2050	22 Feb 1973	–	Used for software development
NBRU(RL)	PDP8	1972	–	Used for data input
Atlas Laboratory	IBM 1130	1972	593	
Mullard Space Lab	GEC 2050	–	–	Purchased by ACL (PO link due Jan 1974)
Reading University	GEC 2050	–	–	Purchased by ACL (PO link due Jan 1974)
Appleton Laboratory	GEC 2050	29 June 1973	201	Purchased by ACL
Inst. of Geological Sciences, London	PDP11	–	–	

The Nuclear Physics workstation installations are complete except for attaching additional ELECTRIC terminals.

The software initially provided with the GEC 2050 computers was designed to emulate an IBM 2780, which can be handled by the work station support program HASP-RJE resident in the central computer. The IBM 2780 is a device which cannot be programmed, and this software package allowed only card reading or line printing. It was used successfully on all stations for the first half of the year. The package was subsequently replaced by 'multi-leaved' software which makes full use of the programmable facilities of the small computer, enabling ELECTRIC terminals to be connected and permitting simultaneous (and faster) card reading and line printing. This multi-leaved program package (which simulates an IBM 1130) was written at the Rutherford Laboratory, using a GEC 2050 simulation system (provided by GEC) for the IBM 370/195 to facilitate software development on the central computer. Responsibility for maintaining it has been accepted by GEC.

The normal HASP-RJE software allows one typewriter console plus a number of card-readers and line-printers to be attached to an IBM 1130 work station. Modifications made to HASP and the MAST message-switching program allow auxiliary terminals (typewriters, VDU's and storage tubes) to be attached.

The weekly number of jobs submitted from remote work stations and CPU time used are shown in Figure 97.

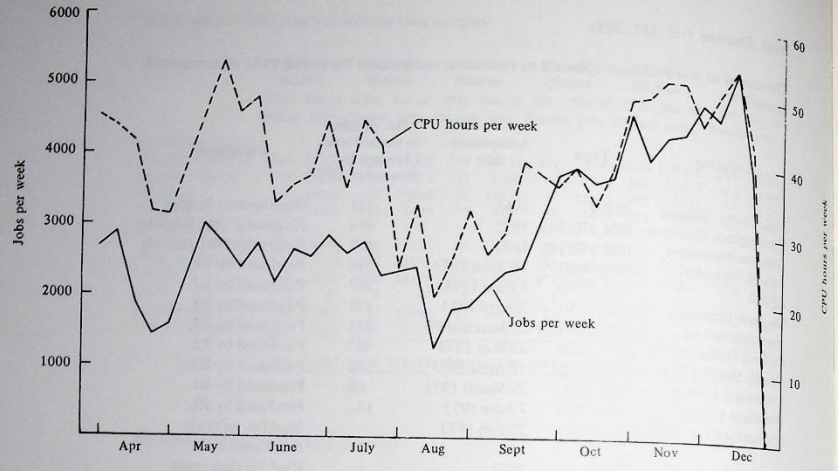

Figure 97. Remote work station statistics (15752)

Other Terminals

The Laboratory terminal facilities have hardly changed during the year, but several big users have acquired their own terminals. There is a Computek and a Tektronix T4010 graphics terminal dedicated to different Counter groups, and Applied Physics Division has a Computek and a thermal printer. The T4002 display installed for the Bubble Chamber Research Group was already in use last year and a VDU has been added this year. There are new VDU's in the Program Advisory Office and on the local GEC 2050 work station. Finally, there are four public terminals situated at the Atlas Laboratory (one teletype, one IBM 2741 typewriter and two T4010 graphics displays).

For external users in institutions without their own work stations there remain six lines on the public telephone network, to which teletypes or graphics terminals can be connected for low speeds (10 characters/second) transmission. Extensive use has been made of these facilities by more than a dozen user groups.

Tests have been made to enable users with terminals, who now dial directly to the central computer via the public network, to communicate instead by the public network to a nearby work station, at some saving in cost. Tests were also made on a fast (2400 bits/second) telephone link, which if successful would be a cheaper alternative to a leased private line for those work stations in contact with the central computer for only two or three hours per week.

OPERATING SYSTEM DEVELOPMENTS

The basic operating system software for the IBM 370/195 central computer remains OS/MVT/HASP as supplied by IBM but with some local additions to meet specific needs. The numerous on-line activities are supported by MAST/DAEDALUS/ELECTRIC, written locally. Late in the year IBM provided version 21.7 of OS/360. Version 3.1 of HASP 2 continues in use, but some further modifications to MVT have been made locally, as described below.

Local developments during the year have been primarily in the three areas of automating various operational tasks, introducing facilities specific to large multiprogramming machines, and monitoring system behaviour. Many of the developments are ultimately directed to maximum utilisation of main memory, which at two megabytes will eventually limit the growing use of the machine.

IBM software intended to conserve memory in management of the system queue ('Dynamic System Queue Area') was introduced and routine modifications to accommodate the second bank of 8 type 3330 disk drives were made; the opportunity was taken to re-distribute the system data-sets.

There are several long-lived programs (MAST, ELECTRIC, etc) for which the MVT system was modified to allocate reserved high-address partitions in main memory, leaving the remaining memory available to MVT in the standard way. During the year this principle has been extended to accommodate any one long-lasting application program in a core position where it will not cause prolonged fragmentation.

An 'autocleanup' program, which detects when a program library is nearly full, has been introduced to remove program modules which have been superseded or are no longer in use. This prevents jobs failing through lack of library space.

A program library will generally contain some defunct members, some which rarely change (because they are well developed and in production use), and some being developed which change frequently. By recording for each library member the date of creation or latest re-creation, the date of most recent use, and a use-count, new library management software ('automigration') now decides when to move unchanging members which are still in use to an associated library.

Another new library management facility, called autoarchiving, is just being put into effect. It will copy library members which have not been used at all for some pre-determined period, such as three months, to magnetic tape. Once on tape, the programs will not encumber disk management at all, but can be recalled at some future date if they are needed.

Fortran changes

Practically all Fortran programs need standard Fortran service routines (collectively known as Fortlib) when executing. This has hitherto been done by incorporating copies of these routines in each program, which meant there could easily be a dozen copies of some routines simultaneously taking space in main memory, and several hundred included in the user program libraries on disk. The situation is accentuated by the heavy dependence on Fortran for scientific programs at the Laboratory and heavy multiprogramming, and has led to pioneering arrangements to make Fortran 're-enterable' for the IBM 360/370 series.

In this re-enterable system a single copy of the most frequently used Fortlib members is held permanently in main memory, so that all concurrent jobs can use it without interference. Preparation and testing for this reform took most of one man-year, but it was introduced smoothly. The Fortlib version chosen was that accompanying the new H Extended Plus compiler (see below), but is compatible with programs compiled by the older G and H compilers.

IBM have provided a new Fortran compiler (Fortran H Extended Plus) specially designed for the model 195. The new compiler generates machine instructions in an order not usually achieved by the older compilers but which is particularly suited to the high degree of concurrency possible in the 195 central processor. This compiler, intended to be the standard for production jobs at the Laboratory, was introduced late in the year. It has already shown that 20–30% of CPU time can be saved for many programs, and bigger savings are likely for programs heavily dependent on the standard mathematical functions.

In addition, a collection of matrix algebra routines has been started, specially written for the model 195 and faster than any Fortran compilation. For example, the scalar product of two vectors of order N can be formed in 0·3N microseconds.

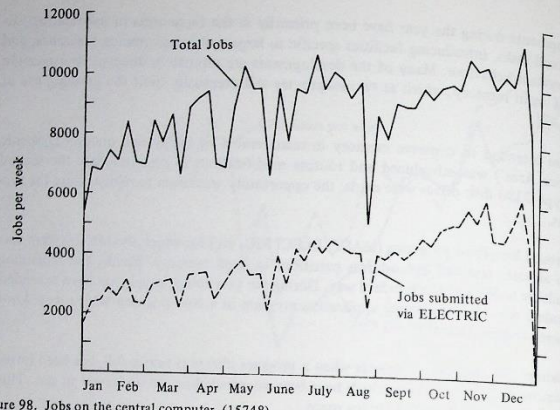

Figure 98. Jobs on the central computer (15748)

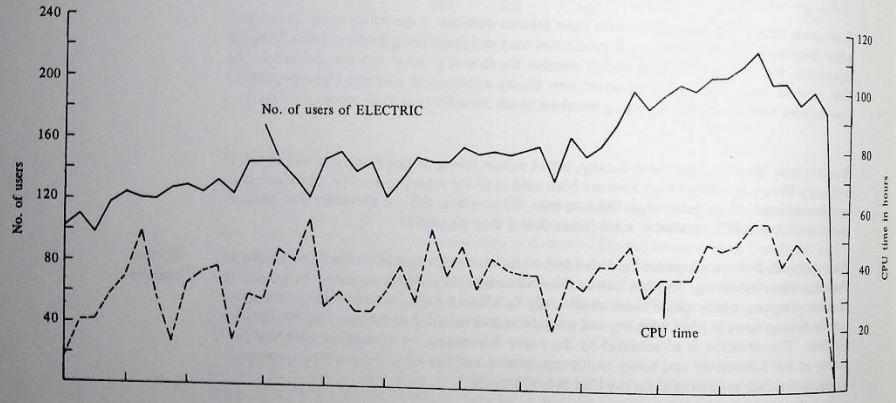

Figure 99. Use of ELECTRIC (15750)

DAEDALUS ELECTRIC and MAST (ref. 252)

This software is now reliable and robust. DAEDALUS-224 is not expected to need any further changes, though minor modifications were made to DAEDALUS-516 during the year as operational experience with HPD2 was gained.

Use of the ELECTRIC job entry/retrieval and file handling system continued to grow during the year. By the year end there were over 70 terminals, the number of active users had approximately doubled (100 to 200) and the number of jobs submitted weekly via ELECTRIC risen similarly (2500 to 5000), Figures 98, 99 show this growth. Provision was made for up to 30 simultaneous users (instead of 20), and the total space within ELECTRIC (currently a complete type 3330 disk) is now fully allocated. The graphics space is 70% occupied, and will shortly be doubled to accommodate future growth.

Developments of MAST continue as new on-line hardware devices, which it must control, are introduced, but the basic framework of 1966 remains.

COPPER and SETUP

COPPER checks that the user identifier and account number are a valid combination, and downgrades the requested priority if the user's allocation is exhausted, while SETUP tells the computer operators the tapes and disks required, and allocates them to drives. Both are sub-tasks of HASP which are on-line to MAST, and can thus participate in job control and employ standard methods of communication.

During the year, realistic values were inserted in the COPPER control tables. Most users require rapid turnround for short development jobs but can wait a while for long production jobs. Accordingly, most user groups have been allocated some time at high priority and much more at low priority. Development runs at high priority can be completed during the day in normal circumstances, while long production jobs at low priority are usually completed overnight or at weekends. Users can enquire from any terminal how much of their weekly time allocation remains.

The COPPER tables have been extended to handle more levels of priority, if this should prove necessary. It was also found convenient to use COPPER as a vehicle for messages to appear in a job's print-out heading, either from the computer operators or drawing the user's attention to any excessive (and thus wasteful) request for main memory.

Phase 2 of SETUP has been introduced. This not only displays messages for tapes and disks to be fetched in advance of need, but also takes over from OS the allocation of drives. At the end of a job it looks ahead to check if the same volume will soon be needed again. Overall, jobs now spend very little time waiting for appropriate mounting.

The job classes have been simplified by using SETUP, which can accommodate jobs with various peripheral requirements without separating them into different streams. It can also detect the memory and time demands for a job, so the only class a user need declare is X for express. All other classes are calculated internally.

The job status information given in response to a user's typed request has been improved, and will be extended to include reports on recent successfully finished jobs. Such refinements are increasingly desirable as more work is submitted from terminals.

Accounting and System Analysis

The SMF (System Management Function) records, which are produced for every job for accounting purposes, have been extended to include the data sets, magnetic tapes and disks which a job uses, and the time it spends in a waiting state. The collection of weekly statistics on utilisation of input/output channels has started, both in total and split by groups and division. In addition to the above recording, which proceeds continuously while the machine is running, special short-term monitor jobs are sometimes run at busy times of day to record fine detail of machine behaviour.

The waiting state time is important, for if it uses tapes or disks a job's duration bears little relation to its CPU time, which is the control quantity in COPPER. If the wait time (which is now reported to the user with each job printout) greatly exceeds the CPU time, the job is running inefficiently from the point of view of main memory utilisation. It may need redesigned input/output methods, or possibly to take more memory (for input/output buffers) so that its wait-time decreases and it releases memory more quickly.

It is of course important to foresee computing limitations before they become serious, and channel capacity could become a bottleneck as activities extend and diversify. There are now 16 (instead of 8) type 3330 disks on block multiplexor channel No 2, and while this allows a better spread of data sets and eases operations, with some disks mounted permanently and others free for anticipatory set-up, the load on the channel is considerably increased. ELECTRIC is one user of this channel, and it is important for a very wide spectrum of terminal users that overloading of the channel should not degrade the ELECTRIC response.

User Support

Work Stations (Ref. 303)

Bringing the new work stations into full operation was a major activity of User Support during the year. Visits to the sites were made to help users become familiar with the system and conventions, and to monitor performance of the stations. A Work Station Users Manual (RL-73-041) was issued during the year, and weekly accounts are now distributed to Work Station Representatives.

Disk Space

There is growing awareness of the advantages of permanently mounted disk space, and an increasing demand for it. When the second set of eight type 3330 disk drives became available and activity was conveniently low (over Easter) the user library space was increased from 180 to 250 Mbytes and that for users' private data sets from 80 to 275 Mbytes.

During the year a disk (called FREEDISK) was introduced on which users' data sets could reside for a limited period (about a month) without registration. This facility has become very popular and may prove worth extending at the cost of other, registered, data set space.

A computer based registration system was introduced during the year. It enables better records to be maintained and facilitates better control of disk space.

Accounting

The general accounting facilities have been improved. Daily, weekly, monthly and quarterly information can now be produced. Each User Group Representative receives monthly accounts of his group's usage and that of other groups in the same category.

The information has proved useful, for example in setting up data for COPPER (to speed jobs requiring quick turn-round) and in predicting possible new requirements, such as higher density tape drives or extra terminals.

Program Library

Considerable progress has been made in tidying-up routines in the Program Library. Some 80 routines have been scrutinised so far, and a short descriptive guide produced for each. New versions of the AERE library and of the CERN program SUMX were implemented. An easier method of accessing members of the Computational Physics Communications (CPC) library was devised, and some commonly used mathematical functions from the CERN library were converted for 370/195 usage. New versions of FORTRAN documentation programs were made available.

The extending use of ELECTRIC and consequent pressures on space have led to some tidying-up, particularly of the JOBFILE. This is an area set aside for general purpose programs and utilities, which it is hoped to make more readily accessible.

Advice and Information

The Program Advisory Office has continued to handle most day-to-day programming queries, which again totalled some 2500 in the year. Some special utility programs and procedures have arisen from queries, particularly in the field of tape and disk handling.

A new version of the main users' document CIGAR (Computer Introductory Guide and Reference) is being written and will be available in 1974. It will include description of routines in the Program Library.

FILM ANALYSIS

Automatic Measuring Machines

HPD1

On 24 January the machine measured its millionth bubble chamber event, and on 22 March its millionth from the CERN 2-metre chamber. Towards the end of the year measuring was transferred to HPD2, and on 3 December HPD1 was switched off. Conversion to HPD2 specifications began at once, with completion scheduled for mid-1974.

In terms of 3-view bubble chamber events and including remeasurements, the totals achieved were:

		Events
1968	82cm Saclay chamber	30,000
1969	2-metre CERN chamber	100,000
1970	"	210,000
1971	"	335,000
1972	"	315,000
1973	"	260,000
		1,250,000

Measurements were made for four experiments during the year and for five in all:

	Events	
	1973	Total
Low energy K^-p (1GeV/c) (including 30,000 in Saclay chamber)	158,000	625,000
$\bar{p}p$ (1 GeV/c)	–	120,000
High energy K^-p (14 GeV/c)	28,000	280,000
π^+d (4 GeV/c)	49,000	200,000
K^0p (1 GeV/c)	25,000	25,000
	260,000	1,250,000

Some of the π^+d film was pre-digitised at Durham University and some of the low energy K^-p at Imperial College, London. The total measured for Durham (including 4000 events measured in 1972) was 9000, and for Imperial College 28,000. Most of the measuring for all these experiments has been completed. There were periods during the year when no film was available for measuring; the total measuring time was 2720 hours or 31% of the year. The weekly average for each month is shown in Figure 100.

A sample of 1600 spark chamber events, on reverse-developed film from Experiment 5 (K13C) was measured in March but showed multiple digitising of wide spark images. This fault was attributed to the fine light spot in HPDs.

A modified version of the on-line control program, adapted for Reduced Guidance pre-digitising, was tested during the year (on both HPDs). With reduced guidance, digitisings were written to disk several times during measuring of a single chamber image for subsequent filtering. Tests are not complete but look encouraging.

Figure 100. Average weekly totals of events measured on HPD 1 during 1972 and 1973 (15753)

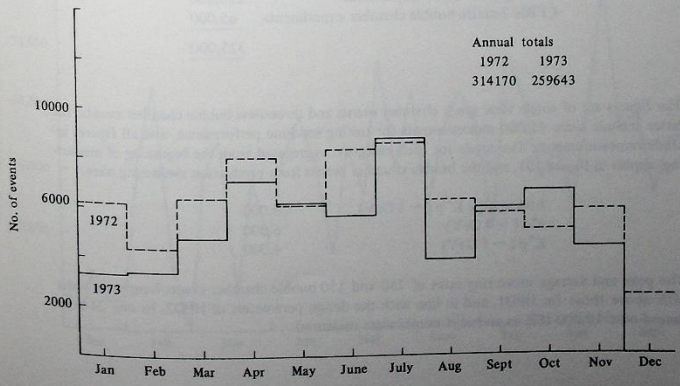

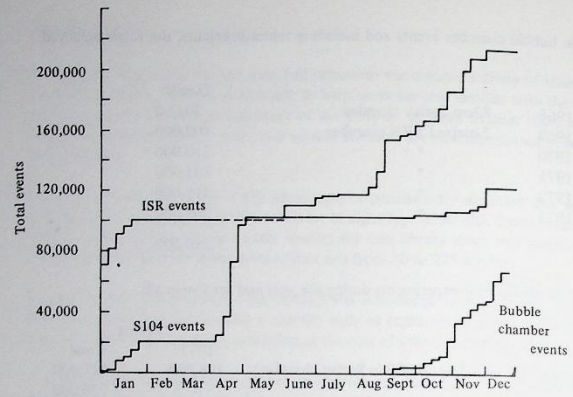

Figure 101. Measurement on HPD 2 (15749)

HPD2

During 1973 HPD2 measured film from two spark chamber experiments (number 17 at the CERN ISR and number 11 at CERN PS (S104)) and, towards the end of the year, from two bubble chambers (CERN 2-metre and, in test quantities, British National 1·5 metre chamber with track-sensitive target). Hardware and software changes improved the accuracy and reliability of measuring, and some further work was done in preparation for BEBC (Big European Bubble Chamber) film.

A 30 MHz clock system using integrated circuits was introduced in the spot digitising logic, with the main effect of improving measuring accuracy significantly. A new Automatic Gain Control circuit, particularly suited to bubble chamber measurement, was introduced to compensate for variations in spot intensity and film density. While satisfactory for bubble chamber work and ISR spark film, there were still difficulties with the flared sparks common in the S104 experiment, and with a sample from Experiment 5 (K13C) for a similar reason. The fine structure in their images often led to multiple digitising by the sensitive HPD detection system, but modifications to the track detection unit allowed S104 measuring to proceed.

During the year HPD2 measured over 300,000 events made up as follows:

ISR spark chamber experiment	140,000
S104 spark chamber experiment	120,000
CERN 2-metre bubble chamber experiments	65,000
	325,000

The figures are of single view spark chamber events and three-view bubble chamber events: the latter include some 25,000 measurements for testing machine performance, and all figures include remeasurements. The totals for each category, aggregated from the beginning of measuring, appear in Figure 101, and the bubble chamber events from production measuring were:

Low energy K^-p (~ 1 GeV)	28,000
π^+d (~ 4 GeV)	6,000
K^0p (~ 1 GeV)	4,000

The peak and average measuring rates of 250 and 150 bubble chamber events/hour were some 60% above those for HPD1, and in line with the design parameters of HPD2. In one 24-hour period over 10,000 ISR experiment events were measured.

As production measuring of bubble chamber film started on HPD2 detailed comparisons were made with HPD1 measurements of the same film. This checking, which involved studying results of Geometry, Ionisation and Kinematics program runs on several thousand events, showed but slight differences between the machines, with some advantage in accuracy on HPD2.

A few frames of film from BEBC, produced in various operating conditions, were digitised for test purposes during the year. Attempts were made to quantify the well-known problems of uneven chamber illumination, poor track contrast, small bubble size, etc, and establish the sources of electrical noise generated as the HPD spot scans across the film. It was confirmed experimentally and theoretically that the major noise source is the granular structure of the film itself, and this was studied in some detail.

Tandem HPD Complex

Plans were made last year to upgrade HPD1 to HPD2 specification and operate the two machines in tandem on the DDP-516 computer. During 1973 three electronic subsystems for the new HPD were built, and two of these (for film transport and stage control) were fully tested by substitution into HPD2. Extensive mechanical modifications to HPD1 are also necessary, and a start was made as soon as the machine was switched off in December.

CYCLOPS

The overhaul begun late in 1972, which included fitting and aligning a new cathode ray tube, was completed in January. Measurement of film from the Cambridge University/Rutherford Laboratory experiment (K13C) began in February. Problems, partly due to films of different densities, and partly to multiple and faulty digitisings of wide spark images (attributable to fine structure in the images) were overcome by installing a simple AGC circuit (to stabilise the photomultiplier response to the CRT spot), modifying the digitiser circuits, and making some softwear changes. With the benefit of these changes a long spell of good measuring was achieved, reaching a peak of over 45,000 events in one week. By the end of October all 880,000 events for this experiment (on 250 rolls of film) had been measured, easily a record year for CYCLOPS. Weekly totals of events measured are shown in Figure 102.

Figure 102. Weekly totals of events measured in CYCLOPS (15751)

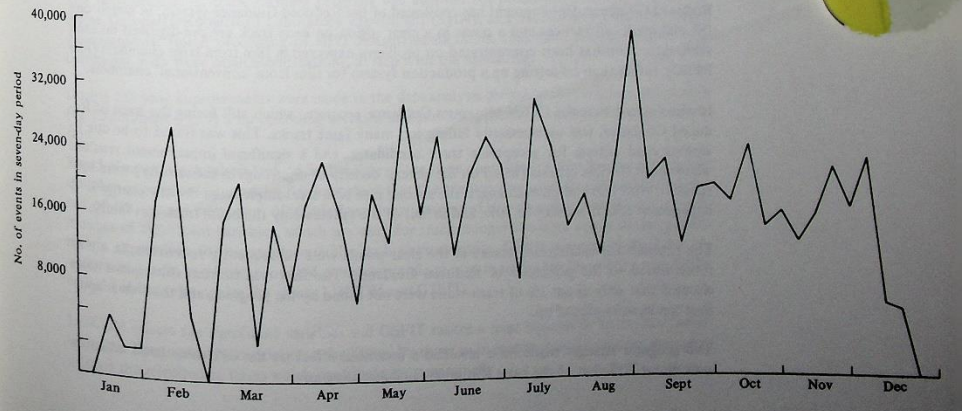

Light Pen Stations

The IDI display and light pen, which communicates with the central computer via the DDP224 satellite, was used for 'rescuing' bubble chamber tracks which had failed geometrical reconstruction criteria. Faulty tracks from 63,000 failed events measured with the HPD road guidance system were displayed during the year. Rescue action with the light pen, usually refiltering evident mistakes or cutting out the length of track beyond a kink, was attempted on 57,000 of these, in a total of 1,200 hours, with a 70% success rate. A new facility has been made available which allows the light pen operator to mark specific digitisings, selected to become new master points. This facility proved particularly useful with measurements of a sample of film from the 1·5 metre chamber with track-sensitive target, since track densities within and without the target often differ appreciably.

The IDI display is limited to a maximum of 1,500-2,000 points per picture before unacceptable flickering occurs, and in any case the picture quality is not up to modern standards. This limited number of points, which is due to the low speed deflection system employed, is just sufficient for bubble chamber patch-up with road guidance pre-digitising, but inadequate for the reduced guidance system or for chambers of the BEBC type. A new Hewlett Packard unit enables many thousands of points to be displayed without flicker. The unit uses a cathode ray tube but with electrostatic deflection (instead of much slower magnetic deflection). With a small Interdata Model 70 computer for refreshing the display, a sample bubble chamber picture of 4,000 points was written. The picture was quite free of flicker and individual points could easily be picked out by the light pen detector: the 4,000 limit was due to the computer memory size, and more economical data storage methods and an extended memory will be needed for a completely flexible patch-up station. Good quality pictures of 30,000 points have been displayed by using special pattern generators, and there is no doubt that the Hewlett Packard unit can display more points if necessary.

SOFTWARE FOR DATA ANALYSIS

Bubble Chambers

The HAZE–MATCH–EDGING program chain has remained the standard for processing HPD measurements of bubble chamber film. Only minor modifications have been made to the chain, primarily to meet problems arising from the K° experiment. This experiment is the first encountered with no visible beam track, and the first with all visible tracks nearly transverse in some cases (and hence no tracks on the HPD normal scan). Once the programs had been generalised to cope with the new situation, the pass rate through GEOMETRY reached a level sufficiently high (because of the small average number of tracks per event) that no light pen 'rescue' of failures was considered necessary.

Reduced Guidance. Development has continued of the Reduced Guidance system, in which one fiducial mark, all vertices and a point in a clear region on each track are pre-digitised on each view. Attention has been concentrated on problems expected in film from large chambers (like BEBC), rather than on setting up a production system for film from 'conventional' chambers.

It was noticed that the CERN Minimum Guidance program, which still forms the basis of Reduced Guidance, was unnecessarily failing too many faint tracks. This was found to be due to various rigid criteria for acceptable track candidates, and a significant improvement resulted when more flexible criteria (based on the general density of digitisings in the vicinity) were substituted. With this and other changes, the success rate on a test sample from the low energy $K^{-}p$ experiment rose from 40% to 70%, and in half of the failures only the beam track was faulty.

The routines for establishing tracks at the clear points were subsequently re-written, in a way more suited to the principles of Reduced Guidance. The first results from subsequent tests showed that only about 1% of track-views were not found by the program, and that fewer spurious tracks were picked up.

The program changes made have also had a beneficial effect on the CPU time used, which is now about 70% that of the basic Minimum Guidance program.

Large chambers, HYDRA system. A few frames of film from BEBC and the Argonne 12 ft chamber have been examined on HPD2, but no film was measured this year. However, the CERN HYDRA program system is being installed on the 370/195, and will be suitable for BEBC, etc.

The system consists at present of management and file handling programs, and packages ('processors') for geometrical reconstruction and kinematic fitting of events in conventional or large chambers. Tests are being made of satisfactory reconstruction by the geometry processors, using HPD measurements of 2-metre chamber film and an input processor written locally.

Track-sensitive target. HPD2 was used to measure a sample of film from the 1·5 metre chamber equipped with a track-sensitive target. The measurements were processed with the Road Guidance program chain, but using only the Rutherford filter program EDGING and omitting the CERN HAZE, which was considered unsuitable for tracks passing through the target material. Nevertheless there were problems with such tracks and others, particularly faint electron tracks in neon, and some modifications to the program chain are being made.

One extra facility has already been added to the light pen 'patch-up' program. It allows 'master points' to be added to tracks too faint to be filtered successfully, or to one section of a track (eg in hydrogen) when the other section (eg in neon/hydrogen) is already satisfactorily filtered. Work is in progress on adapting the geometry and kinematics programs to experiments with a track-sensitive target.

Kinematics. Major modifications to the treatment of convergence and hypothesis rejection are being made in the Kinematics program (see RL–73–084). It has long been known that the traditional method, which works very well in most cases and which is used in all existing programs, sometimes fails to converge for certain classes of events (eg those including slow sigmas). A different approach to the fitting problem has been developed and is currently being tested.

Spark Chambers

Spark Chambers. Three views of the K13C experiment multi-gap spark chambers were photographed, from the top (0°) and side (90°), plus a resolving view (11°). Close sparks are common in this experiment, so it was decided to reconstruct sparks in three dimensions first and then link sparks into tracks (instead of forming tracks in two dimensions and then reconstructing in three, as done for a previous experiment).

Nearly 90% of sparks were reconstructed successfully from all three views, and another 5% from two views only (because the spark image was not digitised for the third). The uncertainty in the lateral position of sparks was below ± 1mm. Tracks, spreading over five or more chamber gaps, are formed by linking established sparks and following towards the vertex origin. The tracks have already been used to check alignment of the chambers.

The two-dimensional track forming program was adapted for processing some data from the Rome University/Rutherford Laboratory experiment (S104), and successfully tested on HPD2 measurements. Initial processing of HPD measurements of the film from the ISR experiment continued, with some small modifications, in step with the measuring.

During the year improvements were made in the data analysis programs for various experiments (eg Experiment 4 (π9)) by re-coding sections and providing routines for fast matrix manipulation.

Rapid Momentum Analysis (ref. 255). Because of the large quantities of data produced in spark chamber experiments nowadays, it is important that the analysis programs should make efficient use of the central computer. Methods have been developed for describing tracks by a small number of significant variables, which are used for track recognition tests and in deriving parametric expressions for kinematic variables such as momentum. CERN programs have been re-written in a form convenient for IBM computers and are now in use at the Daresbury and Rutherford Laboratories, under the names LINCOM and GSFIT.

LINCOM selects the significant variables and GSFIT makes a least squares fit to the kinematic variables. Economical manipulation is facilitated by using an orthogonal set of vectors, thus permitting the rejection of terms which contribute only marginally.

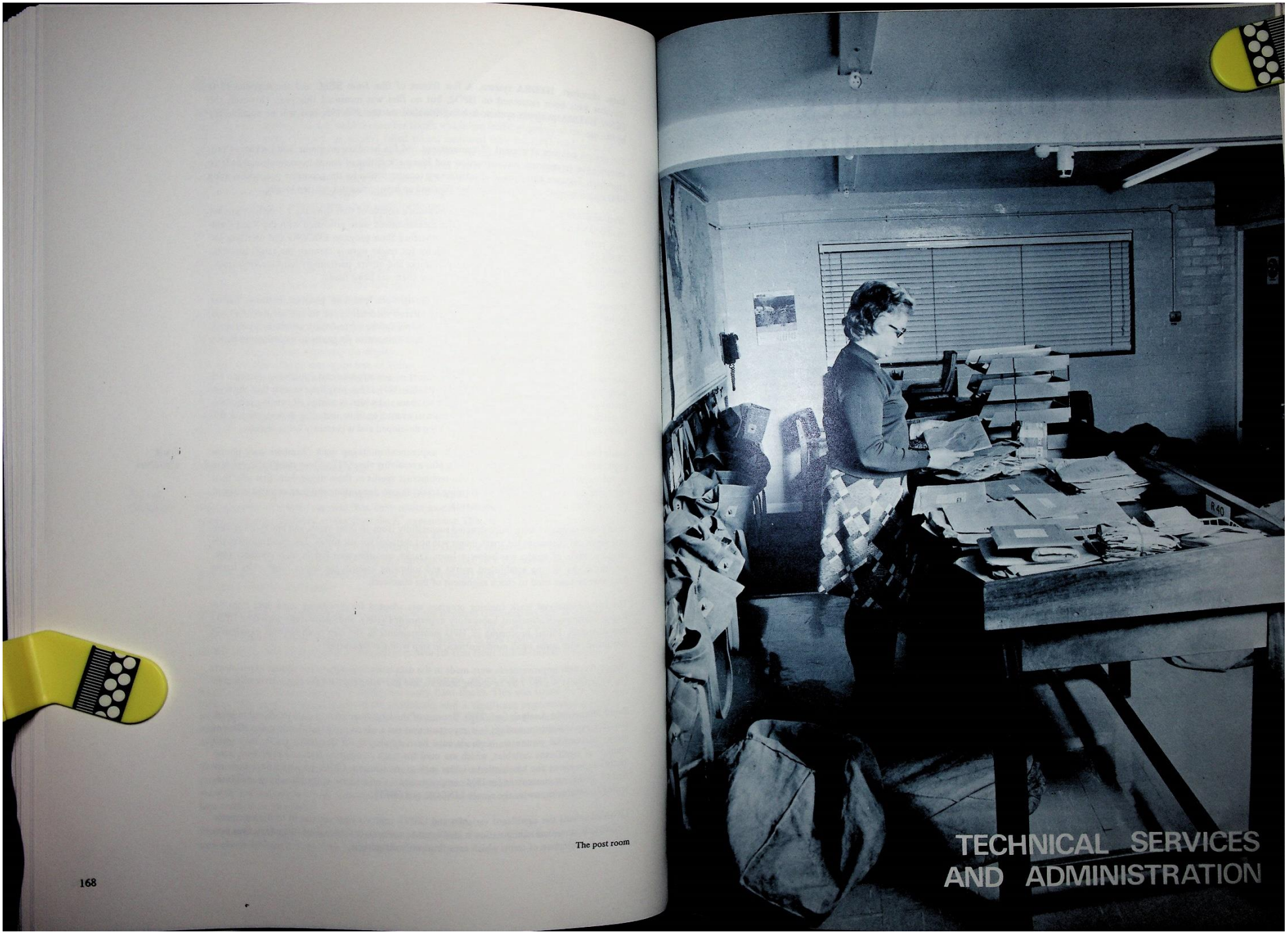

The post room

TECHNICAL SERVICES AND ADMINISTRATION

Technical Services and Administration

RADIATION PROTECTION

Personal Dosimetry

There have been no particularly noteworthy incidents or technical developments during the year. From personal dosimetry results no one working at the Laboratory exceeded the permitted levels for either external radiation or internal contamination.

Shielding Ref. 261, 263

Special radiation surveys and other measurements which provide data for the design of new or changed shielding arrangements have been carried out. Investigations performed during the year include recommendations for shielding at higher Nimrod intensities, preliminary estimates of the shielding for the EPIC project, advice on temporary shielding for the 70 MeV injector building operations and assistance in the diagnosis and cure of high radiation backgrounds in the hydrogen bubble chamber.

Induced Radioactivity (ref. 188, 189)

The highest personnel radiation doses tend to result from work on or near to radioactive accelerator components. This is primarily due to external gamma radiation, with no serious contamination problems. It is expected that control of these doses will be the most important radiation problem arising from increased Nimrod intensities. The increase in injection energy from 15 MeV to 70 MeV will greatly increase the activity produced by the injector. This has been carefully studied, particular attention being given to the safe disposal of cooling water containing ^{3}H and ^{7}Be. High resolution and low background gamma spectrometry systems have been of great value in these studies. The same equipment has been used in the development of accurately calibrated proton beam monitoring foil techniques, including a quick and simple system for routine use, in which allowance is made for the effect of short-lived isotopes. Autoradiographic techniques have also been developed for the accurate determination of proton distribution in the small focal spots of extracted beams.

GENERAL SAFETY

The maintenance of a high standard of safety is dependent upon the continued vigilance of all who work at the Laboratory. With the aim of re-emphasising and increasing the need for vigilance a large proportion of time was spent in communicating safety information to staff. The need to keep abreast of changing and improving standards, in particular with those arising from integration with the European Community and continued participation in CERN, is vital. Greater effort in this direction is planned. A particular instance was liaison on safety matters concerning the High Pressure Gas Cerenkov Counter for Experiment 13 at CERN. Liaison with external organisations having similar safety problems was maintained during the year and in several instances practical advice was given. Routine work to comply with statutory requirements and Laboratory rules for plant and buildings continued to show a steady increase. The Group continued to provide similar safety services to the adjacent Atlas Laboratory.

The formal authorisation of mechanical lifting operations was introduced during the first quarter of the year. The Highly Flammable Liquids and Liquefied Petroleum Gases Regulations came into effect in June and assistance to those responsible for carrying out the requirements was given by the Flammable Gases Section. A new Electrical Safety Code, which involved a major revision of existing arrangements, was introduced during the year. Discussions took place on the detailed implementation in several areas and a significant increase in registered high voltage apparatus occurred toward the end of the year as a result of the new requirements.

Basic safety training was provided for new entrants. It is hoped to resume practical safety training sessions, which are a necessary follow up, on a monthly basis in the near future. Two refresher sessions on mechanical handling were given and the Safety Officer participated in a training course for supervisors at the Atlas Laboratory.

Regular safety tours, looking for potential hazards, were again organised by the Group on behalf of the Safety Committee. Those taking part were full-time safety and fire prevention staff with the addition of a member of the Safety Committee on a rotation basis. The entire Laboratory was inspected twice during the year, the main observations being the need for constant vigilance in maintaining standards of good housekeeping. Administration Officers in the various areas of the Laboratory were co-opted and provided valuable assistance in following up the recommendations and advice given to the supervisors responsible. Publicity of hazards was continued by means of Safety News sheets and Showcase Displays. Several new Rutherford Laboratory Safety Notices, which are mandatory safety instructions, were prepared.

The total number of items recorded in the safety register continued at about the same level. The totals were as follows with the 1972 figures in brackets: Lifting Machines 405 (396), Lifting Tackle 2448 (2600), Pressure Vessels 889 (890), Safety Valves 289 (268), Breathing Apparatus and other Safety Equipment 147 (147), Fire Prevention 52 (52), and High Voltage Installations 420 (385). These registered items were given a total of 8377 (7524) inspections during the year either by Group staff or contract inspectors. Reports on these items were recorded and remedial action on defects and recommendations to improve safety were progressed as necessary.

The number of injuries involving Laboratory staff which were reported during 1973 were the lowest on record. The total was 78 (1972 - 94), and 6 (13) of these resulted in absence from work for one day or more; the average absence was 7·3 (10·2) days. The injuries were classified in the following categories:—

Handling goods	25
Stepping on or striking against objects	18
Falls of persons	11
Use of hand tools	7
Machinery	6
Falls of objects	3
Electricity	0
Miscellaneous	8

All were investigated and where appropriate, recommendations were made to prevent recurrence.

The national method of assessing accident performance is by means of an accident frequency rate. This is expressed as the number of injuries per 100,000 man hours worked, 100,000 hours is an approximate working lifetime. The Laboratory all-injury frequency rate was 3·1 (3·5) and the lost-time frequency rate was 0·23 (0·49).

The steady downward trend in reported injuries continues. The majority were, as in previous years, due to the failure of individuals to take personal care rather than resulting from the specialised nature of the work of the Laboratory. However, because of the wide range of potentially very hazardous materials and activities, there are no grounds for complacency.

ENGINEERING SERVICES

Mechanical and Electrical Manufacture

The number of separate jobs completed were 750 by the Mechanical Workshop and 110 by the Electrical Workshop. In addition, over 1,000 separate jobs amounting in value to £300,000 were placed with outside manufacturing contractors.

During the year the previously separate mechanical and electrical maintenance workshops were integrated into one combined workshop, improving facilities and the coordination of both disciplines. An extensive programme of plan improvement was carried out which has resulted in a considerable drop in the number of breakdowns and more effective use of plant. These range from the fitting of new sewage pumps to the rebalancing and modification of the IBM 370/195 computer air conditioning plant. A very extensive investigation into the operation efficiency and control of the Central Chilled Water facility brought about a reduction in breakdowns and a reduction in the number of compressors normally running from four to two. The fuel crisis at the end of November 1973 turned our attention to the more efficient use of steam and electricity and the necessity to control temperature to a maximum 63°F.

Track Analysis Machines

The track analysis machines section has had a busy year with operational duties to 30 digitising machines. Developments to improve production efficiency and throughput have included pneumatic film clamping and drive system modifications (SHIVA machines), fresnel lens system, film gate clamp and printed circuit motor drive (Hudson tables), and rationalisation of electronic counting and control systems (D'Mac machines). The new "BESSY" machines were provided with a modified, more flexible design to allow increased film drive speeds and the ability to accept 35 mm, 50 mm or 70 mm plain or sprocketted film on either large or standard reels. Work is continuing with greater involvement in HPD2, CYCLOPS, Vanguard machines with the CRYSTAL computer system, and adaption of visual display units to the digitisers. Operation on HPD1 ceased in December 1973 and work is now in progress to upgrade this machine to HPD2 standards.

Electronic Design and Manufacture

During the year 113 new designs of printed circuit boards were produced involving 350 drawings including the artwork (nearly 50% done off site). Electronics Manufacturing Section completed work to the value of £180,000 including component costs (60% done off site). The prototype workshop completed 220 jobs and the printed circuit board assembly line completed 100 jobs. The total in-house effort was approximately 30,000 man hours. The Electronic and Instrument repair section handled over 2,600 items for repair, calibration, first line servicing and "on-call" breakdown investigation with 20% being dealt with by specialist firms. The Electronic Instrument Loan Pool continued to function as a site service with 490 issues from over 500 instruments in the pool. The above three sections were transferred from Engineering Division to HEP Division from 1 September 1973.

Routine chemical analyses, advice on corrosion problems, trade waste and other effluents, and assistance in the safe usage and disposal of chemicals, and decontamination and monitoring of working areas following mercury spills have been provided during the year.

SCIENCE RESEARCH COUNCIL WORKS UNIT

During 1973 the Council Works Unit has been involved in giving advice, preparing schemes and tender documents and supervising works at the Atlas Laboratory, Appleton Laboratory, Chilbolton Observatory, Winkfield Observatory, RGO Herstmonceaux, London Office and the Rutherford Laboratory. A great deal of time and effort has been taken up on the three major jobs being carried out by Messrs. Turriff Construction Ltd., the Office and Colloquium extension at the Atlas Laboratory, the New Library and the New Injector Building at the Rutherford Laboratory. Work commenced on site during April and the work is progressing despite labour shortages, and severe shortages and long deliveries of building materials. It is anticipated that the new building work for the Atlas Laboratory will be completed by April 1974; the New Library by Mid 1974 and the Injector Building will be progressively handed over for plant installation from April 1974. An advisory service has been provided to other laboratories within SRC with regard to plant modifications and maintenance. The number of jobs over £1,000 handled at various stages of completion for each of the establishments during the year were: Atlas Laboratory 5, Appleton Laboratory 8, Chilbolton Observatory 2, RGO Herstmonceaux 5, Rutherford Laboratory 30, Winkfield Observatory 1.

Library Building. Construction of the New Library building continued during the year with completion and occupation expected mid 1974. By the end of 1973 the external shell was substantially complete and the general appearance of the building became apparent. The building was designed as an architectural feature of the Laboratory providing an attractive focal point to the easterly approach. A major feature is the 30 m span bridge section, which, with a new three storey block, links two existing buildings.

The bridge structure is concrete, with precast arch beams faced with exposed aggregate, hollow plank floor slab units and supported on circular concrete columns. A structural steel frame supports a low pitch metal deck roof, insulated with extruded polystyrene slabs and weather proofed with hypalon based single layer covering. The east facing wall of the bridge is a special feature, being formed of gold-tinted double-glazed solar-control glass units supported by an anodised aluminium glazing system. These solar-control units help to create stable conditions in the reading hall of the Library. The west wall is generally clad with corrugated profile steel panels. The thermal insulation of the building was given special consideration to reduce heat loss in the winter and solar heat gain in the summer.

A special floor construction was used to minimise noise transfer from the plant room to the building. Fresh air is used for cooling whenever possible, but the water from the main chilled water plant is used when the outside air temperature is high. A heater battery is used for heating the mainly recirculated air in the winter. Air is delivered to the library through a linear grille adjacent to the east side window and is extracted through the lighting fittings mounted in a sealed accoustic ceiling. By integrating the heating, lighting and ventilation system together with the accoustic and visual aspects of floor and ceiling treatment a very pleasing environment will be achieved.

The three-storey block, designed as a foil to the bridge, is of largely traditional construction with load-bearing brick walls faced with dark brown and multi-rustic bricks, concrete floors and metal deck roof. Windows are single glazed in aluminium, those at the east end being full height lancet type.

Accommodation provided in the three-storey block will include at ground level a main stack area, postroom, workshop and entrance. At first floor level the library reception area opens off the main reading hall with adjacent offices for library staff. A micro-fiche and card reader room is provided together with five individual study rooms. A public corridor runs the full length of the new building thus providing free circulation to the building complex at the first floor level.

Figure 103. Progress in construction of the new library

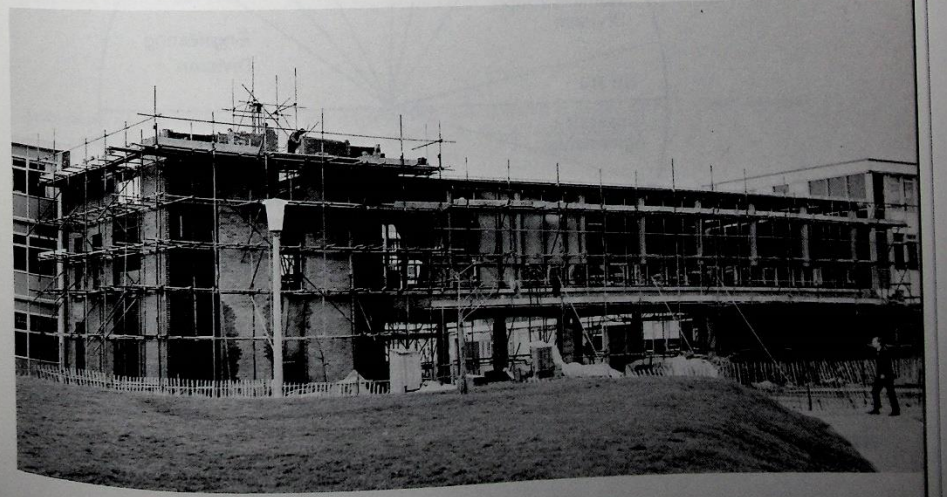

ADMINISTRATION

Finance

The Laboratory expenditure (financial year 1973/74) was £9·48 million of which £1·43 million was for capital (including major computer items amounting to £0·50 million) and £8·05 million was recurrent. Corresponding figures for 1972/73 were £8·35 million, £0·90 million and £7·45 million.

A brief analysis of the net expenditure is given below with corresponding figures for the previous year shown in brackets.

	£ million
Staff expenditure (salaries and wages, insurance, superannuation, etc)	3·70 (3·60)
Research and development (see below)	4·35 (3·85)
Plant and equipment	1·18 (0·82)
Building works	0·25 (0·08)
Total	9·48 (8·35)

A proportional representation of the breakdown of the Research and Development expenditure into divisional and the other main components is shown in the pie chart (Figure 104).

Figure 104. Break-down of the £4·35 million R and D expenditure

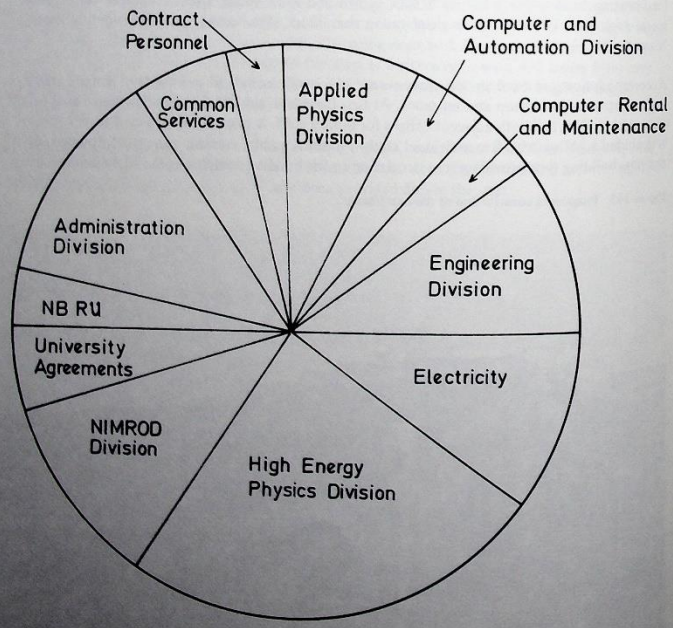

Staff Numbers 1973

The staff position at the beginning and end of the year.

	Opening Strength 1.1.73	Changes during 1973 Gains	Losses	Closing Strength 31.12.73
NON INDUSTRIAL				
Senior and Banded Staff	25	3	1	27
Science Group	247·5	11·5	16·5	242·5
Professional and Technology Group	337	6·5	13	330·5
Administration Group	76	11	13	74
Research Associates	54	29	28	55
Non-Techs and Stores	42	1	6	37
Librarian	1	0	0	1
Secretarial and Typing	27	8	5	30
Photographers	3	0	0	3
Photoprinters	5	0	0	5
Machine Operators	63·5	19·5	24·5	58·5
Hostel Manageress	2	2	2	2
Telephone Operators	2	0	0	2
Total Non Industrial	885	91·5	109	867·5
INDUSTRIAL				
Craft	172·5	27·5	33	167
Non-Craft	117	22·5	30·5	109
Apprentices	23	7	10	20
Total Industrial	312·5	57	73·5	296
GRAND TOTALS	1197·5	148·5	182·5	1163·5

The figures listed under "changes" include new entrants, resignations and promotions. Staff on sandwich courses, and those working part-time are counted as half.

Staff numbers continued to decline; the net decrease since 31 December 1970 has been 88·5 (7% of those in post at that date).

Staff Relations

Communications between management and industrial staff were provided by regular three monthly meetings of the Local Joint Consultative Committee. A special meeting of this body was held to discuss the use of contract labour at the Laboratory.

Shop stewards representing the various Trades Unions recognised at the Laboratory also continued their participation on Joint Productivity Sub-Committees and on the Restaurant, Safety and Staff Suggestions Committees, which further provided opportunities for useful exchanges of ideas between staff and management.

During the year, four shop stewards attended external training courses designed to further their knowledge of trades union affairs and methods of negotiation.

Four regular meetings of the Local Whitley Committee were held, including the Annual Meeting chaired by the Director, at which the scientific programmes of the Laboratory and of the Nuclear Physics Board for the years 1973/74 to 1978/79 were discussed.

Staff Side members continued to take a keen interest in the EPIC proposal, the setting up of the Council Works Unit and the Neutron Beam Research Unit, (both based at the Laboratory) and in the latter's participation in the now Anglo-French-German high flux research reactor collaboration at the Institut Laue-Langevin (ILL), Grenoble.

Several special meetings with management were held to discuss specific topics, including training, accommodation and home to Laboratory transport. Agreements were reached on a number of matters affecting staff working conditions.

Staff Side membership of the Restaurant, Safety and Staff Suggestions Committees continued, providing further opportunities for frank and friendly discussions on staff conditions.

In October, Staff Side members and Trades Union representatives informally met the new Chairman of the Council, Professor S F Edwards, FRS; discussion ranged freely over many topics related to the work of the Laboratory.

At the end of the year, Management/Trades Union/Staff Side discussions took place with a view to providing a joint approach to implementing the Government fuel economy measures and to mitigate the resultant difficult working conditions.

Training

The year has shown a further decline in the level of day-release and evening training in the Laboratory, but the success-rate has remained high and there has been a substantial increase in the level of management training, largely as a result of the programme of Staff Reporting Courses for members of the P & TO Group. There has also been an increase in interest in Open University courses, bringing the number of participants supported by the Laboratory up to seven.

The total number of part-time training concessions awarded during academic year 1972/73 was 76, about 6·5% of the total staff of the Laboratory compared with 8% last year. The 70 students who sat examinations or were subject to "continuous assessment" achieved an overall success-rate of 88%. Three members of staff received day-release concessions for specialist postgraduate courses and two are registered research students, one with the University of Surrey and one with the Council of National Academic Awards.

Three full-time students from the Laboratory completed their courses during the year. One was awarded First Class Honours in Electrical Engineering at Lanchester Polytechnic, one was referred in the CEI Part II examination following a course of study at Oxford Polytechnic and the third student failed the same examination. A fourth student satisfactorily completed the first year of a Mechanical Engineering degree course at Brunel University while on unpaid leave and has been awarded an SRC Bursary for the remainder of the course.

The main source of external training courses used by Laboratory staff has been the AERE Education and Training Department – to the extent of about 47% of the total (compared with 60% last year). SRC and CSD courses amounted to 14% of the total and the remainder was made up by courses run by a wide range of Universities, Polytechnics, Technical Colleges, Research Associations, professional bodies and commercial organisations. As in previous years the Laboratory has contributed to a number of the AERE technical courses on the teaching side.

The Laboratory has for several years assisted staff attending evening classes in French and occasionally in other languages. A new and more urgent need for oral French training has arisen as a result of the arrangements for British participation in the work of the Institut Laue-Langevin at Grenoble and all 13 members of the Neutron Beam Research Unit have been attending a special twice-weekly course at the North Berkshire College of Further Education. The Laboratory has acquired a language laboratory-type tape recorder and a set of the tapes being used by the College to enable the students to do private study.

The Laboratory has continued its collaboration with AERE in the training of Craft Apprentices. Commencing with the intake of 2 Student Engineers to the Laboratory in January 1973, AERE is providing only 5 months of basic workshop training and thereafter the training of Student Engineers will be directly controlled by the Laboratory. There were 25 Craft Apprentices, Student Engineers and Graduate Engineers in training at the beginning of the academic year and this number had fallen to 21 by August 1973. Five Craft Apprentices completed their "time" during the year and one Graduate Engineer transferred to the Atlas Laboratory as a P & TO II. Three Student Engineers graduated from University in 1973, one with First Class Honours in Electrical Engineering at Nottingham University, one with First Class Honours in Electrical and Electronic Engineering at Birmingham University and one with Upper Second Class Honours in Mechanical Engineering also at Birmingham.

This academic year's major internal training activity has been the programme of Staff Reporting Courses for members of the P & TO Group. Altogether 21 one-day courses for Reporting Officers were run, including one pilot course attended by observers from other SRC establishments, and a further half-day course was run for P & TO IVs. These courses were attended by 338 Laboratory staff, 7 staff from the Atlas Laboratory, 5 from the Appleton Laboratory and one from ROE.

The Laboratory's programme of metrication training was continued with a series of 6 brief courses open to all members of the Laboratory, but aimed particularly at Craftsmen and those P & TOs who did not attend one of the two-day courses for designers held last year. The Laboratory again acted as host establishment for two SRC Central Induction Courses, which were held in December 1972.

The Laboratory provided industrial training during the academic year for 48 college-based sandwich-course students in a variety of disciplines, bringing the overall total of such trainees in the Laboratory over the last 13 years to 415. Administration Division provided the usual fortnight's practical office training for 9 full-time Business Studies students from the North Berkshire College of Further Education and a new enterprise was the provision of a four-week extra-mural project for a student attending the Modern Studies degree course at Sheffield Polytechnic. HEP Electronics and Nimrod P.D. Groups jointly provided 6 months' practical training in electronics for a senior physics technician from the University of the West Indies, sponsored by the Inter-University Council for Higher Education Overseas.

General Administration

During the year the demand for general administrative services continued at an increasing rate. Typing and clerical services have had to be utilised with the utmost flexibility in order to satisfy Laboratory needs.

Full and effective use has been made of the Laboratory's furnished flats and houses and the majority of people entitled to this type of accommodation have been housed. The provision of unfurnished housing however has been very difficult. The problem has been exacerbated by the high cost of housing in the area and mortgage difficulties, preventing tenants purchasing their own property.

Considerable changes in office and laboratory accommodation have taken place during the year, to ensure more effective use is made of Laboratory facilities, and Groups with a need to interact with each other were strategically placed for this purpose.

Meetings and Schools

The Cosener's House has been well used during the year to provide conference facilities, particularly for the Council's Boards, Summer Schools and Training Courses.

The annual Theoretical Physics gathering took place from 3–5 January. Two summer schools on High Energy Physics were organised, one for experimental physicists (15–27 July) and the other for theoreticians (3–21 September). Meetings were held at The Cosener's House on Links between Weak and Electromagnetic Interactions (24–25 February), Physics with Polarized Targets at High Energies (17–18 March), Diffractive Scattering and Multiparticle Unitarity (17–18 November) and on Vertex Detectors (3–5 December). The Neutron Beam Research Group held a joint meeting with the Institute of Physics and the Chemical Society on 2 October to discuss New Developments in Neutron Beam Instrumentation.

Visits

The Engineering Board visited the Laboratory on 13 March and the Nuclear Physics Board held a meeting at The Cosener's House on 26 November. Parties of visitors during the year totalled 910, including 60 Italian school children on a UK visit.

Physics Exhibition

The Laboratory mounted a large working exhibit at the Physics Exhibition in London, 9–13 April 1973. It demonstrated the Remote Computing Facilities at the Laboratory, which serve workstations as far away as Geneva and Glasgow, and showed examples of interactive graphics programmes as an aid in magnet design. The exhibit consisted of an RJE workstation based on the GEC 2050 computer, connected via modems and a post office tarriff T line at 2400 bits/sec to the IBM 370/195 computer at the Laboratory.

A film describing the computing facilities and interactive magnet design work at the Laboratory was shown at the Exhibition.

Figure 105. A remote job entry work station at the Physics Exhibition

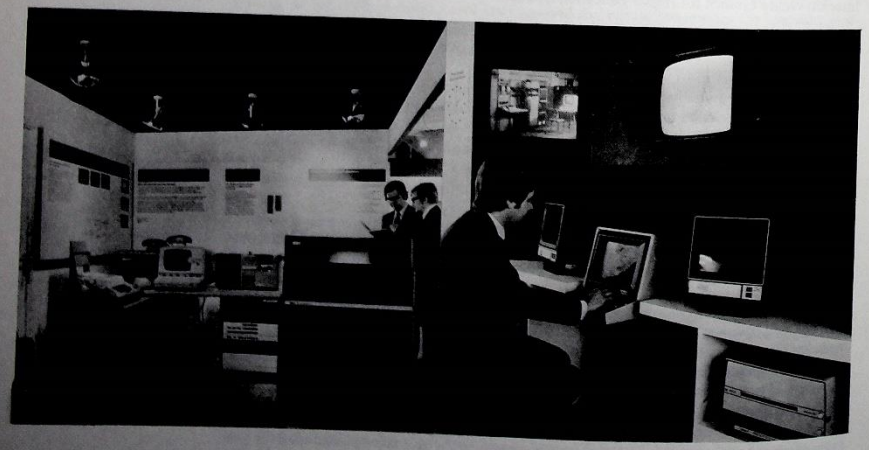

A view of the repro-graphics department

PUBLICATIONS AND LECTURES

Publications and Lectures

JOURNAL ARTICLES

1 B W Allardyce, C J Batty, D J Baugh, E Friedman, G Heymann, M E Cage, G J Pyle, G T A Squier, A S Clough, D F Jackson, S Murugesu, V Rajaratnam
Pion reaction cross-sections and nuclear sizes. Nucl. Phys. A209 (1973) 1 (RPP/NS10)

2 B W Allardyce, C J Batty, D J Baugh, E Friedman, G Heymann, M E Cage, G J Pyle, G T A Squier, A S Clough, D F Jackson, S Murugesu, V Rajaratnam
Total reaction cross-sections for pions on nuclei and neutron density distributions. J. Phys. (Paris), Colloq. 5 (1972) 157

3 B Alper, H Bøggild, G Jarlskog, G Lynch, J M Weiss, P Booth, L J Carroll, J N Jackson, M Prentice, G von Dardel, L Jönsson, G Damgaard, K H Hansen, E Lohse, F Bulos, L Leistam, A Klovning, E Lillethun, B Duff, F Heymann, D Quarrie
Production of High Transverse Momentum Particles in p–p– Collisions in the Central Region at the CERN ISR; Phys. Lett. 44B (1973) 521

4 B Alper, H Bøggild, G Jarlskog, J M Weiss, P Booth, L J Carroll, J N Jackson, M Prentice, G von Dardel, G Damgaard, F Bulos, W Lee, G Manning, P Sharp, L Leistam, A Klovning, E Lillethun, B Duff, K Potter, D Quarrie, S Sharrock
Particle Composition at High Transverse Momenta in p–p– Collisions in the Central Region at the CERN ISR; Phys. Lett. 44B (1973) 527

5 B Alper, H Bøggild, P Booth, F Bulos, L J Carroll, G von Dardel, G Damgaard, B Duff, F Heymann, J N Jackson, G Jarlskog, L Jönsson, A Klovning, L Leistam, E Lillethun, G Lynch, G Manning, M Prentice, D Quarrie, J M Weiss
Large Angle Production of Stable Particles Heavier than the Proton and a Search for Quarks at the CERN Intersecting Storage Rings; Phys. Lett. 46B (1973) 265

6 B Alper, H Bøggild, P Booth, F Bulos, L J Carroll, G von Dardel, G Damgaard, B Duff, F Heymann, J N Jackson, G Jarlskog, L Jönsson, A Klovning, L Leistam, E Lillethun, G Lynch, S Ølgaard-Nielsen, M Prentice, D Quarrie, J M Weiss
Large Angle Inclusive Production of Charged Pions at the CERN ISR with Transverse Momenta less than 1·0 GeV/c; Phys. Lett. 47B (1973) 75

7 R E Ansorge, J A Charlesworth, N Intizar, W W Neale, J G Rushbrooke
Analysis of $NN \to (\Sigma K)N$ and $NN \to (\Lambda K)N$ channels at 6 GeV/c without isospin-exchange interference; Nucl. Phys. B60 (1973) 157

8 G T J Arnison
Some Characteristics of a calacity read-out spark chamber; Nucl. Instrum. Meth. 108 (1973) 135

9 H W Atherton, B J Franek, B R French, B Ghidini, H G Hilpert, J B Kinson, L Mandelli, J Moebes, K Myklebost, B Nellen, E Quercigh, V Simak
Observation of narrow $(3\pi)^{\pm}$ peaks in the δ and A_1 regions in $\bar{p}p$ annihilations at 5·7 GeV/c; Phys. Lett. 43B (1973) 249

10 J F Ayres, T G Coleman, A R Damerell, C M Fisher, E W Fitzharris, J H Foster, P Gottfeldt, B Mack, A R Mortimer, P Seager, J R Stokoe, P R Williams, H Leutz, J Tischhauser, H Wenninger
The operation of a track sensitive hydrogen target in a 500 l. neon hydrogen bubble chamber; Nucl. Instrum. Meth. 107 (1973) 131

11 D A Bailin, A Love, D V Nanopoulos, G G Ross
Purely hadronic weak interactions in unified field theories of the weak and electromagnetic interactions; Nucl. Phys. B59 (1973) 177

12 R Bairstow, A Brandstetter, J H Hunt
A simple ionisation measuring device for bubble chamber pictures; Nucl. Instrum. Meth. 99 (1972) 345

13 M C Ball, G B Stapleton, J F Raffle
Fibrous structure in a hardened cement paste; Magazine of Concrete Research, Vol 25, No. 83 (1973)

14 P C Barber, T A Broome, W Busza, J K Davies, B G Duff, D A Garbutt, F F Heymann, D C Imrie, G J Lush, E N Mgbenu, K M Potter, D M Ritson, L A Robbins, R A Rosner, S J Sharrock, A D Smith, R C Hanna, P R Pitts, E J Sacharidis
Measurements of K^+p elastic scattering differential cross-sections in the incident momentum range 1368 to 2259 MeV/c; Nucl. Phys. B61 (1973) 125

15 V Barger, R J N Phillips, K Geer
Rising $d\sigma/dt$ probes pp diffraction mechanisms; Nucl. Phys. B54 (1973) 463

16 V Barger, F Halzen, R J N Phillips
Line reversal in baryon reactions and the energy dependence of dip locations; Nucl. Phys. B57 (1973) 401

17 V Barger, F Halzen, R J N Phillips
Scaling limit of pp-elastic scattering; Nucl. Phys. B61 (1973) 522

18 V Barger, R J N Phillips
Model independent analysis of the structure in pp scattering; Phys. Lett. 46B (1973) 412

19 R Barloutaud, A Borg, F Brun, D Denegri, C Louedec, F Pierre, M Spiro, K Paler, T P Shah, R J Miller, J J Phelan, B Chaurand, B Drevillon, G Labrosse, R Lestienne, D Linglin, R A Salmeron
Study of the diffractive $\bar{K}\pi\pi$ system produced in $K^- p \to \bar{K}\pi\pi N$ reactions at 14·3 GeV/c Nucl. Phys. B59 (1973) 374

20 C J Batty, A I Kilvington, A Marinov
Velocity measurements of recoil nuclei from α-decay and the determination of their mass; Nucl. Instrum. Meth. 99 (1972) 179

21 C J Batty, A I Kilvington, J L Weil, G W A Newton, M Skarestad, J D Hemingway
Search for superheavy elements and actinides produced by secondary reactions in a tungsten target; Nature 244 (1973) 429 (RL-73-048)

22 A G Bell
'Himmelbett'; The Computer Journal. Vol 16, p.269

23 A G Bell, P J Hallowell
Crawling round a cube edge; Computing, 15 February 1973

24 A G Bell, P J Hallowell, D H Long
A Universal Benchmark?; Software – Practice and Experience, Vol 3 (1973) 355

25 A de Bellefon, A Berthon, L K Rangan, J Vrana, T C Bacon, A Brandstetter, I Butterworth, S M Deen, C M Fisher, P J Litchfield, R J Miller, J R Smith, G Burgun, J Meyer, E Pauli, G Poulard, B Tallini, W Wojcik, J Zatz, R Strub
Channel cross sections of K^-p reactions from 1·26 to 1·84 GeV/c; Nouvo Cim. 7A (1972) 576

26 D M Binnie, L Camilleri, N C Debenham, A Duane, D A Garbutt, J R Holmes, W G Jones, J Keyne, M Lewis, I Siotis, P N Upadhyay, I F Burton, J G McEwan
Study of narrow mesons near their thresholds; Phys. Rev. D8 (1973) 2789(RL-73-016)

27 D M Binnie, J Carr, N C Debenham, A Duane, D A Garbutt, W G Jones, J Keyne, I Siotis, J G McEwan
Direct evidence for the S* meson near the K^+K^- threshold; Phys. Rev. Lett. 31 (1973) 1534

28 A Boksenberg, R G Evans, R G Fowler, I S K Gardner, L Houziaux, C M Humphries, C Jamar, J B Macau, E D Malaise, A Monfils, K Nandy, G I Thompson, H Wroe
The ultra-violet sky-survey telescope in the TD-1A satellite; Monthly notices of the Roy. Astron. Soc. Vol 163 (1973) 291

29 F Bradamante, S Conetti, C Daum, G Fidecaro, M Fidecaro, M Giorgi, G Kalmus, A Penzo, L Piemontese, P Schiavon, D Stairs, A Vascotto.
Polarization in backward elastic π^+p scattering at 2·0, 3·5 and 4·0 GeV/c; Nucl. Phys. B56 (1973) 356

30 F Bradamante, S Conetti, C Daum, G Fidecaro, M Fidecaro, M Giorgi, G Kalmus, A Penzo, L Piemontese, P Schiavon, D Stairs, A Vascotto
Polarization in $\pi^+p \to K^+\Sigma^+$ backward scattering at 3·5 GeV/c; Phys. Lett. 44B (1973) 202

31 A Brandstetter, I Butterworth, S M Dean, P J Litchfield, A Berthon, J Vrana, J Zatz, W Wojcik, J Meyer, B Tallini
The reaction $K^-p \to \omega\Lambda$ in the c.m. energy range 1915-2168 MeV; Nucl. Phys. B39 (1972) 13

32 P J Brown, P J Welford, J B Forsyth
Magnetisation density and the structure of cobalt carbonate; J. Phys. C: Solid State Physics Vol 6 (1973)

33 P J Brown, J B Forsyth
The crystal structure of solids; Edward Arnold (Publishers) Ltd. (1973)

34 D V Bugg
Coulomb corrections to π-n elastic scattering; Nucl. Phys. B58 (1973) 397

35 D V Bugg, A A Carter, J Carter
New values of π-n scattering lengths and f^2; Phys. Lett 44B (1973) 278

36 P J Bussey, J R Carter, D R Dance, D V Bugg, A A Carter, A M Smith
π-p elastic scattering from 88 to 292 MeV; Nucl. Phys. B58 (1973) 363

37 J R Carter, D V Bugg, A A Carter
π-p phase shifts from 88 to 310 MeV; Nucl. Phys. B58 (1973) 378

38 H M Chan, H I Miettinen, R G Roberts
Dual properties of inclusive spectra; Nucl. Phys. B54 (1973) 411

39 H M Chan, J E Paton
Multiparticle shadow effects on elastic scattering in the dual model; Phys. Lett. 46B (1973) 228

40 Y A Chao, A D Jackson
Optimized conformal mapping applied to the Lippmann-Schwinger equation; Phys. Lett. 43B (1973) 449

41 Y A Chao, R W Kraemer, D W Thomas, B R Martin
$\bar{K}N$ data and Λ (1405); Nucl. Phys. B56 (1973) 46

42 J A Charlesworth, R L Sekulin, M J Emms, J B Kinson, L Riddiford, B J Stacey, M F Votruba, P L Woodworth, I G Bell, M Dale, J V Major
A study of ρ° and f° production in 4 GeV/c π^+d interactions; Nucl. Phys. B65 (1973) 253 (RL-73-054)

43 R Y L Chu, G W London, Y P Yu, D Boyd, T Beggs, D J Candlin, A T Goshaw, H W K Hopkins, W Venus, P Alibran, S Kahn, J P Lowys, R Stump, J P Wuthrick, J Colas, C Farwell, A Ferrer, E Gombosi, T Hofmokl, J Six, D Camba, A Marzari, A Romero, A E Werbrouck
Channel cross sections for $K^-p \to \Lambda$ + neutrals between 0·525 and 0·820 GeV/c; Nucl. Phys. B64 (1973) 109

44 A S Clough, G K Turner, B W Allardyce, C J Batty, D J Baugh, W J McDonald, R A J Riddle, L H Watson, M E Cage, G J Pyle, G T A Squier
Coulomb effects in π^+ - C and π^- - C total cross-sections; Phys. Lett. 43B (1973) 476 (RPP/NS9)

45 T G Coleman, C M Fisher, E W Fitzharris, J H Foster, J G V Guy, P R Williams, H Leutz, H Wenninger
First physics run with a track sensitive target; Nucl. Instrum. 107 (1973) 399

46 J T Dakin, G J Feldman, W L Lakin, F Martin, M L Perl, E W Petraske, W T Toner
Measurement of ρ° and ϕ - meson electroproduction; Phys. Rev. D8 (1973) 687

47 J T Dakin, G J Feldman, F Martin, M L Perl, W T Toner
Electroproduction of hadrons from deuterium; Phys. Rev. Lett. 31 (1973) 786

48 L Dick, Z Janout, H Aoi, C Caverzasio, A Gonidec, K Kuroda, A Michalowicz, M Poulet, D Sillou, D G Aschman, N E Booth, K Green, C M Spencer
A measurement of the polarization parameter in backward π-p elastic scattering at 6 GeV/c; Nucl. Phys. B64 (1973) 45

49 T Eichten, H Faissner, F J Hasert, S Kave, W Krenz, J Von Krogh, J Morfin, K Schultze, G H Bertrand-Coremans, J Sacton, W Van Doninck, P Vilain, D C Cundy, D Haidt, M Jaffre, S Natali, P Musset, J B M Pattison, D H Perkins, A Pullia, A Rousset, W Venus, H Wachsmuth, V Brisson, B Degrange, M Haguenauer, L Kluberg, U Nguyen-Khac, P Petiau, E Bellotti, S Bonetti, D Cavalli, C Conta, E Fiorini, C Franzinetti, M Rollier, B Aubert, L M Chounet, P Heusse, L Jauneau, A M Lutz, C Pascaud, J P Vialle, F W Bullock, M Derrick, M J Esten, T W Jones, J McKenzie, A G Michette, G Myatt, W G Scott
Measurement of the neutrino-nucleon and antineutrino-nucleon total cross-sections; Phys. Lett. 46B (1973) 274

50 T Eichten, H Deden, F J Hasert, W Krenz, J Von Krogh, D Lanske, J Morfin, H Weerts, G Bertrand-Coremans, J Sacton, W Van Doninck, P Vilain, D C Cundy, D Haidt, M Jaffre, G Kalbfleisch, S Natali, P Musset, J B M Pattison, D H Perkins, A Pullia, A Rousset, W Venus, H Wachsmuth, V Brisson, B Degrange, M Haguenauer, L Kluberg, U Nguyen-Khac, P Petiau, E Bellotti, S Bonetti, D Cavalli, C Conta, E Fiorini, C Franzinetti, M Rollier, B Aubert, L M Chounet, P Heusse, A M Lutz, J P Vialle, F W Bullock, M J Esten, T W Jones, J McKenzie, G Myatt, J L Pinfold
High energy electronic neutrino and antineutrino interactions; Phys. Lett. 46B (1973) 281.

51 R T Elliot, P S Flower
High field pulsed magnets for a bubble chamber beam line; IEEE Trans. NS20 No. 3 (1973)

52 F Elvekjaer, T Inami, G A Ringland
Amplitude analysis of πN charge exchange to large momentum transfers; Phys. Lett. 44B (1973) 91

53 F Elvkjaer, T Inami, R J N Phillips
πN amplitudes at large momentum transfer; Nucl. Phys. B64 (1973) 301

54 Fayyazuddin, Riazuddin
Proton-neutron mass difference in gauge theories; Phys. Rev. D8 (1973) 1179

55 Fayyazuddin, Riazudden
Hadron-hadron scattering at large momentum transfer; Nuovo Cim. 17A (1973) 443

56 K Fialkowski
Correlation integrals for charged and neutral pions in inclusive production and the two-component picture; Acta Phys. Pol. B4 (1973) 561

57 K Fialkowski, H I Miettinen
A comment on the early onset of semi-inclusive scaling in proton-proton collisions; Phys. Lett. 43B (1973) 493

58 M Fukugita, T Inami
Impact parameter analysis of $\bar{K}$N and πN scattering in the intermediate energy region; Nucl. Phys. B57 (1973) 543

59 K. Gabathuler, C R Cox, J J Domingo, J Rohlin, N W Tanner, C Wilkin
Pion-deuteron scattering near the 3–3 resonance; Nucl. Phys. B55 (1973) 397

60 F J Hasert, H Faissner, W Krenz, J Von Krogh, D Lanske, J Morfin, K Schultze, H Weerts, G H Bertrand-Coremans, J Lemonne, J Sacton, W Van Doninck, P Vilain, C Baltay, D C Cundy, D Haidt, M Jaffre, P Musset, A Pullia, S Natali, J B M Pattison, D H Perkins, A Rousset, W Venus, H W Wachsmuth, V Brisson, B Degrange, M Haguenauer, L Kluberg, U Nguyen-Khac, P Petiau, E Bellotti, S Bonetti, D Cavalli, C Conta, E Fiorini, M Rollier, B Aubert, L M Chounet, P Heusse, A Lagarrigue, A M Lutz, J P Vialle, F W Bullock, M J Esten, T Jones, J McKenzie, A G Michette, G Myatt, J Pinfold, W G Scott
Search for elastic muon-neutrino electron scattering; Phys. Lett. 46B (1973) 121

61 F J Hasert, S Kabe, W Krenz, J Von Krogh, D Lanske, J Morfin, K Schultze, H Weerts, G H Bertrand-Coremans, J Sacton, W Van Doninck, P Vilain, U Camerini, D C Cundy, R Baldi, I Danilchenko, W F Fry, D Haidt, S Natali, P Musset, B Osculati, R Palmer, J B M Pattison, D H Perkins, A Pullia, A Rousset, W Venus, H Wachsmuth, V Brisson, B Degrange, M Haguenauer, L Kluberg, U Nguyen-Khac, P Petiau, E Bellotti, S Bonetti, D Cavalli, C Conta, E Fiorini, M Rollier, B Aubert, D Blum, L M Chounet, P Heusse, A Lagarrigue, A M Lutz, A Orkin-Lecourtois, J P Vialle, F W Bullock, M J Esten, T W Jones, J McKenzie, A G Michette, G Myatt, W G Scott
Observation of neutrino-like interactions without muon or electron in the Gargamelle neutrino experiment; Phys. Lett. 46B (1973) 138

62 P Hoyer, R G Roberts, D P Roy
New relations for two-body reactions from inclusive finite mass sum rules; Nucl. Phys. B56 (1973) 173

63 P Hoyer, J Kwiecinski
Analyticity and a finite-energy sum rule for the Reggeon-particle amplitude in $a + b \to c + d + e$; Nucl. Phys. B60 (1973) 26

64 P Hoyer, R G Roberts, D P Roy
Test of duality in baryon-antibaryon amplitudes from Reggeon-particle scattering; Phys. Lett. 44B (1973) 258

65 G E Kalmus
Recent advances in bubble chamber physics; Reports on Progress in Physics Vol 36 (1973) 961

66 A T Lea, B R Martin, R G Moorhouse, G C Oades
Multichannel analysis of $\bar{K}$N data 0·4 - 1·2 GeV/c; Nucl. Phys. B56 (1973) 77

67 D Linglin, B Chaurand, B Drevillon, G Labrosse, R Lestienne, R A Salmeron, R J Miller, K Paler, J J Phelan, T P Shah, R Barloutaud, A Borg, C Louedec, F Pierre, M Spiro
$K^-\pi^-$ elastic scattering cross-section measured in 14·3 GeV/c K^-p interactions; Nucl. Phys. B57 (1973) 64

68 A Love, D V Nanopoulos, G G Ross
Three triplet realizations of gauge models and deep inelastic scattering; Nucl. Phys. B55 (1973) 33

69 A Love, D V Nanopoulos, G G Ross
Three triplet realizations of gauge models and electromagnetic mass differences; Phys. Rev. D7 (1973) 3812

70 A Love, G G Ross
Neutral weak currents and the proton-neutron mass difference; Nucl. Phys. B56 (1973) 440

71 C J Marchese, N M Clarke, R J Griffiths
Collective model analysis of the inelastic scattering of 53 and 33 MeV helions by ^{56}Fe; Nucl. Phys. A202 (1972) 421

72 R J Miller, K Paler, J J Phelan, T P Shah, B Chaurand, B Drevillon, G Labrosse, R Lestienne D Linglin, R A Salmeron, R Barloutaud, A Borg, C Louedec, F Pierre, M Spiro
Two-body final states in K^-p interactions at 14·3 GeV/c; Lett. Nuovo Cim. 6 (1973) 491

73 I Montvay
High transverse momentum hadron jet production in a gluon exchange model; Nucl. Phys. B66 (1973) 115 (RL-73-045)

74 A C Newton, F Martin, S J St. Lorant, W T Toner
A method for producing long, cylindrical superconducting flux shields; Rev. Sci. Instrum. 44 (1973) 244

75 K Paler, T P Shah, R J Miller, J J Phelan, D Linglin, B Chaurand, B Drevillon, G Labrosse, R Lestienne, R A Salmeron, R Barloutaud, A Borg, C Louedec, F Pierre, M Spiro
A triple Regge analysis of the reactions $K^-p \to \Lambda + X$ and $K^-p \to \bar{K}^0 + X$ at 14·3 GeV/c; Phys. Lett. 43B (1973) 437

76 R Rader, R Barloutaud, J Griselin, J Prevost, B Tallini, H Filthuth, R Leibscher, H Schleich, J Meyer, J Petersen, J R Smith, J Vrana
The reaction $K^-p \to \Lambda\eta$ from 0·80 to 1·84 GeV/c; Nouvo Cim. 16A (1973) 178

77 R G Roberts, D P Roy
Prong cross sections from a realistic two-component model; Phys. Lett. 46B (1973) 201

78 R G Roberts, D P Roy
Dual property of diffractive resonances from semi-local factorization; Phys. Lett. 47B (1973) 247

79 R G Roberts, D P Roy
Duality and Regge analysis of inclusive reaction; Acta. Phys. Pol. B5 (1974) 1

80 R L Sekulin
Some remarks on the analysis of the decay density matrix of mixed scalar-vector-tensor boson systems; Nucl. Phys. B56 (1973) 227 (RPP/H/106)

81 B C Sinha
Second Order Nucleon Nucleus Optical Potential; Nucl. Phys. A203 (1973) 473

82 B C Sinha, D K Scrivastava, N K Ganguly
Energy Dependence of the Optical Potential; Phys. Lett. 43B (1973) 113

83 G T A Squier, M E Cage, G J Pyle, A S Clough, G K Turner, B W Allardyce, C J Batty, D J Baugh, W J McDonald, R A J Riddle, L H Watson
Pion-nucleus coupling constants for ^{7}Li and ^{9}Be; Phys. Rev. Lett. 31 (1973) 389 (RL-73-037)

84 G B Stapleton, R H Thomas
The effect of sorption on the migration of ^{7}Be from a high energy accelerator constructed on a chalk site; Water research, Vol 7 (1973)

85 G R Stevenson, D M Squier
An experimental study of attenuation of radiation in tunnels penetrating the shield of an extracted beam of the 7 GeV proton synchrotron Nimrod; Hlth. Phys. 24 (1973) 87

86 G C Stirling
Experimental techniques in chemical applications of thermal neutron scattering; (ed Willis) Oxford University Press (1973)

87 W H Tait, V R W Edwards
A study of 30 MeV Proton Inelastic Scattering from Isotopes of Molybdenum and Zinc; Nucl. Phys. A203 (1973) 193

88 G L Thomas, B C Sinha, F Duggan
Effective Interactions in the Proton Optical Model Potential; Nucl. Phys. A203 (1973) 305

89 C Wilkin, C R Cox, J J Domingo, K Gabathuler, E Pedroni, J Rohlin, P Schwaller, N W Tanner
A comparison of π^{+} and π^{-} total cross-sections of light nuclei near the 3–3 resonance; Nucl. Phys. B62 (1973) 61

90 M N Wilson
An improved technique for measuring hysteresis loss in superconducting magnets; Cryogenics p.361 (1973)

91 M N Wilson, G J Homer
Low loss heavy current leads for intermittent use; Cryogenics p.672 (1973)

92 B M Winston, R J Berry, D R Perry
Response of Vicia Faba to irradiation with a beam of negative pi-mesons under aerobic and hypoxic conditions; Brit. J. Radiology 46 (1973) 541

93 R P Worden
Duality and Regge absorption models; Nucl. Phys. B58 (1973) 205

PREPRINTS, REPORTS & MEMORANDA

94 C J Adams, G F Cox, J D Davies, J D Dowell, T Dimbylow, G H Grayer, P M Hattersley, R J Homer, R J Howells, C McLeod, T J McMahon, H B van der Raay, L Rob, C J S Damerell, M J Hotchkiss
$K^{+}p$ elastic scattering between 432 and 939 MeV/c and phase shift analysis. RL-73-071

95 B W Allardyce, C J Batty, D J Baugh, W J McDonald, R A J Riddle, L H Watson, M E Cage, G J Pyle, G T A Squier, A S Clough, G K Turner
$\pi^{\pm}$ Total cross-sections for ^{6}Li, ^{7}Li, ^{9}Be, C and 0 from 90 to 860 MeV. RL-73-038

96 A G A M Armstrong
Sector magnet shim sums; RL-73-047 (June).

97 A G A M Armstrong
Shimming a sector magnet: results from GFUN; RL-73-050 (June).

98 G T J Arnison
A magnet sensing device for beam transport systems; RHEL/M/H 26 (1973).

99 F Atchison, J Butterworth
A low emittance low halo extracted proton beam for Nimrod; RL-73-112 (October)

100 J F Ayres, E W Fitzharris
Argonne 12ft bubble chamber tract sensitive target tests; RL-73-141 (October)

101 T C Bacon
Study of the possibility of filling specific interaction channels and ep elastic scattering in particular; RL-73-194 (EPIC/WP5/P9)

102 R L Bailey, B Colyer, G J Homer
The indirect cooling of a superconducting magnet using supercritical helium; RHEL/R258 (December 1972)

103 R L Bailey
Heat transfer to liquid helium in pulse-heated channels; RL-73-089 (August).

104 M T Ball
A low temperature thermal conductivity apparatus and some typical data; RHEL/R 266 (January 1973).

105 A P Banford
The preparation of scientific and technical documents: notes for the guidance of authors, 2nd edition; RL-73-001 (March).

106 D P Barber
The generalisation of the van der Meer method to include the case of bunched collinear beams; RL-73-207 (EPIC/WP7/P5).

107 V Barger, R J N Phillips
Quark parton model relations in deep inelastic lepton scattering; University of Wisconsin preprint.

108 K Barnham
Kinematics of total EM and weak rates; RL-73-192 (EPIC/WP5/P7).

109 J E Bateman
Some preliminary measurements of X-ray transition radiation on the π-8 beam line at RHEL; RHEL/M/H 27 (1973).

110 J E Bateman
Some properties of the RHEL 20cm x 20cm x 2mm MWPC's; RL-73-055 (May)

111 J E Bateman
XTR spectra from plastic radiators; RL-73-121 (September).

112 J E Bateman
An approach to the amplification of MWPC signals; RL-73-136 (October).

113 C J Batty, G T A Squier, G K Turner
Forward pion nucleus scattering amplitudes; RL-73-118.

114 D J Baxter, I D Buckingham, I J Corbett, P A Dunn, J M C L Emmerson, J Garvey, F Hart, G Hughes, C M S Jones, R Maybury, N Middlemass, P R Norton, T W Quirk, J A Scheid, A M Segar
A study of neutral final states in K^-p interactions in the range from 690 to 934 MeV/c; Oxford preprint 63-73.

115 D E Baynham
A peaking strip magnetometer and its use at low temperature; RL-73-007 (April).

116 N E Booth
Feasibility of measuring the total photoabsorption cross-section with ep colliding beams; RL-73-171 (EPIC/WP2/P3).

117 B H Bracher
Notes on the rough digitising IBM 1130 macro library; RL-73-122 (September).

118 G R Brookes
Total γ-hadronic cross-sections; RL-73-170 (EPIC/WP3/P2).

119 C J Brown, D H Lyth
$e\bar{e} \rightarrow e\bar{e}$ + hadrons at EPIC energies; RL-73-161 (EPIC/WP1/P1, 5, 11, 12).

120 R Budny
EPIC ways of studying weak bosons; RL-73-162 (EPIC/WP1/P2).

121 R Budny
Effects of neutral weak currents in annihilation; RL-73-165 (EPIC/WP1/P8).

122 R Budny, A McDonald
W° effects in inclusive experiments at EPIC energies; RL-73-164 (EPIC/WP1/P7).

123 R Budny, A McDonald
W° effects in Bhabha scattering; RL-73-168 (EPIC/WP1/P18).

124 J W Burren, P M Girard, T G Pett, I Rose, D B Scott
ELECTRIC users' manual; RHEL 72-003.

125 J Butterworth, D H Reading
A proposed large aperture negative pion radiological beam line; RL-73-132.

126 J Butterworth, D H Reading
Properties of a proposed large aperture negative pion radiological beam line; RL-73-133.

127 A A Carter, J R Carter
A tabulation of pion-nucleon forward amplitudes up to 30 GeV/c; RL-73-024 (May).

128 A A Carter, D V Bugg, J R Carter
A new value for the σ commutator for πN scattering lengths; RL-73-036 (June).

129 H M Chan, J E Paton
Multiparticle shadow effects on elastic scattering in the dual model; RL-73-056 (June).

130 H M Chan
Multiparticle hadron dynamics – a personal view; RL-73-061 (July).

131 H M Chan
Duality and the Regge approach to inclusive reactions: lectures at the Spanish GIFT School, Barcelona; RL-73-062 (July).

132 Y A Chao, R K P Zia
Magnetic moment of the Δ^{++} in a bootstrap model: RL-73-012 (April).

133 Y A Chao, R K P Zia
On the extrapolation of πN amplitudes of the $\pi\pi$ cut; RL-73-013 (May).

134 Y A Chao, A D Jackson
The optimized polynomial approximation to solving integral equations: Lipmann-Schwinger equation; RL-73-033 (May).

135 W S Chapman
CONVERT – the program link between the Crystal film measurement system and the IBM 360/195; RL-73-125 (October).

136 A G Clark, R P Worden (eds.)
Physics with polarized targets at high energy: proceedings of a meeting held on 17 and 18 March 1973; RL-73-088 (September).

137 P T M Clee, C W Trowbridge (eds.)
Design study of a Tokamak fusion device with superconducting Bθ coils; RL-73-067 (October).

138 F Close, J Thompson
Rates for electroproduction inclusives (e + p → e + k); RL-73-172 (EPIC/WP3/P2).

139 T G Coleman, C M Fisher, E W Fitzharris, J H Foster, J G V Guy, P R Williams, H Leutz, M Thevenon, J Tishchhauser, H Wenninger
Physics run with an all plexiglas track sensitive target; RL-73-040.

140 C J Collie
KURLY – a program for computing the magnetic fields of 2-dimensional arrays of conductors; RL-73-032 (May).

141 P D B Collins
Some estimated cross-sections for EPIC; RL-73-188 (EPIC/WP5/P2).

142 B Colyer, M T Ball, M P Campbell
The work of fracture of epoxy resins; RL-73-104 (September).

143 B Colyer
Weibull's failure theory applied to an epoxy resin; RL-73-114 (November).

144 B Colyer
The geometry of constant perimeter dipole windings; RL-73-143 (November).

145 W N Cottingham
Aspects of photon-photon collisions in electron-positron colliding beams at EPIC energies; RL-73-163 (EPIC/WP1/P4, 17).

146 J H Coupland
The design, construction and testing of the superconducting magnet AC4; RL-73-105 (September).

147 G V Dass, H Fraas
Time-reversal-like relations for spin-effects in elastic and inelastic reactions, vector meson photoproduction vs. Compton scattering from nucleons; DESY preprint.

148 B J Day
Connecting a paper tape reader to the DDP 224 computer; RL-73-009 (May).

149 M H R Donald, J D Lawson
Reflections on Erice; RL-73-075 (July).

150 M H R Donald, G H Rees, M R Harold
A modified magnet lattice for the EPIC Booster; RL-73-160 (EPIC/MC/38) (December).

151 M H R Donald
Synchrotron-betatron stop bands; RHEL/M/NIM 18 (February).

152 G Domokos, S Kosevi-Domokos, B C Yunn
Electroproduction of pseudoscalar mesons at large transverse momenta; RL-73-076.

153 P J Dornan
Observations of weak interaction events in EPIC; RL-73-185 (EPIC/WP4/P3).

154 B Duff
Possible scheme for pp working party; RL-73-203 (EPIC/WP7/P1).

155 B G Duff, P I P Kalmus, G H Rees
Bunched or DC proton beam for EPIC; RL-73-208 (EPIC/WP7/P7).

156 A W Eastwood
A users guide to DC electrostatic separators at the Rutherford Laboratory; RL-73-128 (October).

157 J A Edgington, V J Howard, I M Blair, B E Bonner, F P Brady, M W McNaughton
A measurement of neutron-proton bremsstrahlung near 130 MeV; RL-73-072.

158 E Eisenhandler, W R Gibson, C Hojvat, P I P Kalmus, L C Y Lee Chi Kwong, T W Pritchard, E C Usher, D T Williams, M Harrison, W H Range, M A R Kemp, A D Rush, J N Woulds, G T J Arnison, A Astbury, D P Jones, A S L Parsons
Differential Cross-Sections for $\bar{p}p \to \pi^-\pi^+$, K^-K^+ between 0·8 and 2·4 GeV/c; RL-73-123.

159 E Eisenhandler, W R Gibson, C Hojvat, P I P Kalmus, L C Y Lee Chi Kwong, T W Pritchard, E C Usher, D T Williams, M Harrison, W H Range, M A R Kemp, A D Rush, J N Woulds, G T J Arnison, A Astbury, D P Jones, A S L Parsons
Interpretations of the Differential Cross-Sections for $\bar{p}p \to \pi^-\pi^+$ and $\bar{p}p \to K^-K^+$; RL-73-124.

160 R T Elliott, J E Ellis
Some recent developments of secondary emission chambers in Nimrod extracted proton beams; NIM-73-07.

161 R T Elliott, P S Flower
Possible hazards arising from the use of cobalt-iron in the 70 MeV injector; RL-73-058 (July)

162 R T Elliott
70 MeV injector: modifications to tank 2 input half drift tube quadrupole; RL-73-059 (July)

163 R T Elliott, P S Flower
70 MeV injector: effective lengths of drift tube DC quadrupoles; RL-73-060 (July).

164 F Elvekjaer, T Inami, R J N Phillips
πN amplitudes at large momentum transfer; RL-73-031 (May).

165 D Evans
An hypothesis concerning the training phenomenon observed in superconducting magnets; RL-73-092 (August).

166 F J M Farley
Electron polarization in EPIC; RL-73-209 (EPIC/WP8/P2).

167 Fayyazuddin, Riazuddin
Scale dimension of the chiral-symmetry-breaking Hamiltonian; RL-73-042 (June).

168 Fayyazzudin, Riazuddin
Analysis of electromagnetic mass shift in light cone algebra; RL-73-101 (September)

169 N Ferguson
Sonic survey — 1·2 MW DC power supplies unit in R25; NIM-73-03

170 O Fich, G C Oades
A study of A and R measurements in K^+p scattering; RL-73-119 (October).

171 C M Fisher
A toroidal magnetic field configuration for an EPIC detector; RL-73-200 (EPIC/WP5/P17)

172 C M Fisher
The kinematic analysis of 1C channels at high energy; CERN/ECFA/72-40.

173 C M Fisher, J G V Guy, J W G Wignall
Geometrical reconstruction of events from track sensitive targets; RL-73-142

174 E W Fitzharris
12ft chamber TST project. General description of target systems; NIM-73-08.

175 E W Hitzharris
12ft chamber TST project. Target installation and operation; NIM-73-12.

176 F Foster
Hole fragmentation and parton fragmentation – an experimental view; RL-73-181 (EPIC/WP3/P14).

177 F Foster
Exploitation of a double arm transverse field spectrometer at EPIC; RL-73-182 (EPIC/WP3/P15).

178 J H Foster
1·5m cryogenic bubble chamber operation (November/December 1972); NIM-73-06

179 G E Gallagher-Daggitt
Superconductor cables for pulsed dipole magnets; RHEL/M/A 25 (February 1973)

180 GESSS Collaboration (CEN Saclay, IEKP Karlsruhe, Rutherford Laboratory)
Towards a European superconducting synchrotron; GESSS-2 (May 1973).

181 P M Girard
HASP remote station handling and on-line console support; RL-73-074 (July).

182 P Gottfeldt, M Morrissey, W G Seddon
Computer based instrumentation of the 1·5m hydrogen bubble chamber; RL-73-097 (September).

183 D A Gray
Current accelerator design studies in the UK; RL-73-144 (November).

184 D E Gray (ed.)
Nimrod operation and development quarterly report October 1 to December 1 1972; RHEL/R 267 (January 1973).

185 D E Gray (ed.)
Nimrod operation and development – quarterly report January 1 to March 31, 1973; RL-73-002 (April).

186 D E Gray
Nimrod operation and development quarterly report April 1 to June 30, 1973; RL-73-129 (October)

187 E H de Groot, H I Miettinen
Shadow approach to diffraction scattering; RL-73-003 (April).

188 R C Hack
The prediction of induced activity levels in and around Nimrod; RHEL/R 268 (January)

189 R C Hack
Radiation Protection Group (Operations) progress report for 1972; RL-73-035 (April)

190 D E Hall
New approaches to convergence and hypothesis rejection in kinematics; RL-73-084 (August)

191 P J Hallowell, R A Lawes
Computer control of the HPD2 flying spot digitizer; RL-73-099 (September).

192 M R Harold
Magnet apertures and injection at 2·1 GeV/c; RL-73-217 (EPIC/MC/11)

193 M R Harold
Some EPIC parameters of interest to experimentalists; RL-73-218 (EPIC/MC/12)

194 M R Harold
Superconducting versions of the SPS – apertures, field errors and resonance widths; GESSS/MD/34.

195 M R Harold
Injection into the PR at 5 GeV/c; RL-73-015 (April)

196 J C Hart, J S Hutton, J H Field, P H Sharp, E W A Blackmore, H E Fisk, G Manning, A G Parham, D H Reading, D C Salter, R J Tapper
A test of the $\Delta S = \Delta Q$ rule in Ke3 decay; RL-73-085

197 B C Haywood, J B Hayter, J W White
The feasibility and applications of a 60Å time-of-flight spectrometer; RL-73-098 B.

198 E G Higgins
R57 plant room modifications, 1973-74, description of services for HPD measuring machines and scanning laboratories nos. 9, 10 and 11; RL-73-110 (October)

199 A R Hodges
A further report on the effect of radiation on selected silicon diodes from the Nimrod 900 KW power unit; NIM-73-17

200 V J Howard, J A Edgington, S S das Gupta, I M Blair, B E Bonner, F P Brady, M W McNaughton, N M Stewart
Differential cross-sections for np and nd elastic scattering near 130 MeV; RL-73-073

201 G Hughes
Preliminary design of an electron detector for EPIC; RL-73-176 (EPIC/WP3/P7).

202 M R Jane, B D Jones, N H Lipman, D P Owen, B K Penney, T G Walker, M Gettner, P Grannis, H Uto, J Anderson, E H Bellamy, M G Green, J Kirkby, P E Osman, J A Strong, D H Thomas, C M Solomonides
A measurement of the charge asymmetry in the decay $\eta \to \pi^+\pi^-\pi^0$; RL-73-139.

203 M R Jane, B D Jones, N H Lipman, D P Owen, B K Penney, T G Walker, M Gettner, P Grannis, H Uto, J Anderson, E H Bellamy, M G Green, J Kirkby, P E Osman, J A Strong, D H Thomas, C M Solomonides
A measurement of the charge asymmetry in the decay $\eta \to \pi^+\pi^-\gamma$; RL-73-140.

204 H Jarvis
70 MeV injector alignment proposals, Part 3: Alignment of floor datum and height reference points; RL-73-134 (November)

205 G Kalmus
Some considerations in the design of a solenoid for use with EPIC; RL-73-193 (EPIC/WP5/P8).

206 P I P Kalmus
Extracted beams from EPIC; RL-73-201 (EPIC/WP6/P2).

207 N M King (ed.)
Superconducting accelerator designs applicable at CERN; CERN/Lab II-DI-PA/Int. 73-1.

208 K M Knight
A high speed paper tape reader and paper tape punch interface for the Interdata Model 70 computer; RL-73-005 (April).

209 K M Knight
A Facit 4001 tape reader interface to a buffered digital I/O channel of a DEC PDP8E computer; RL-73-078 (July).

210 W S Lam, J Tran Thanh Van, I Uschersohn
Inclusive electroproduction in the photon fragmentation region; RL-73-135 (November).

211 P V Landshoff
Some physics questions about deep inelastic ep; RL-73-173 (EPIC/WP3/P3)

212 P V Landshoff, G Ringland
The physics interest of deep inelastic eN scattering at EPIC; RL-73-178 (EPIC/WP3/P9).

213 R Lascelles
70 MeV injector alignment proposals, Part 1: Tank and drift tube alignment; RL-73-107 (September).

214 R Lascelles
70 MeV injector alignment proposals, Part 2: LEDS and DC gun alignment; RL-73-127 (October).

215 R A Lawes, C M Fisher (eds.)
Proceedings of a seminar on track analysis for rapid cycling bubble chambers; RHEL/R 271 (February).

216 J D Lawson
High current and beam-beam effects in EPIC; RL-73-021 (April).

217 J D Lawson
Deuterons in EPIC; RL-73-057 (July).

218 J D Lawson
Q-shifts and Q-spreads associated with the head-on collision of bunches of unequal size; RL-73-079 (July).

219 J D Lawson
Multi-mode excitation of a lossy line by a pulsed beam; RL-73-117 (October).

220 J D Lawson
Particle scattering in EPIC – some preliminary comments; RL-73-156 (December).

221 M Le Bellac, H I Miettinen, R G Roberts
Structure of two-body correlations in high energy hadron production; RL-73-111.

222 H Leutz, P R Williams
The operation of track sensitive targets in a neon hydrogen bubble chamber; RL-73-026 (April).

223 J D Lewin
Path length adjustment for energy variation in EPIC; RL-73-046 (June).

224 B G Loach
Proposed reference numbering system for EPIC lattice components; RL-73-068 (July).

225 B Mack
A design loading analysis of a track sensitive target in a bubble chamber; RL-73-019 (May).

226 J R Maidment, C W Planner
Notes on beam instabilities; RL-73-213 (EPIC/MC/6).

227 J R Maidment
ESR 1: Sensitivity to closed orbit errors; RL-73-214 (EPIC/MC/7).

228 J R Maidment
ESR 1: Non-linear resonances and the working point; RL-73-215 (EPIC/MC/8).

229 J R Maidment
ESR 1: Momentum dependent Q-shifts; RL-73-216 (EPIC/MC/10).

230 J R Maidment
Closed orbit distortion due to energy loss by synchrotron radiation in ESR 1; RL-73-014 (April).

231 J R Maidment
Good field requirements in the electron ring of EPIC II/III; RL-73-052 (June).

232 J R Maidment
Beam separation in the EPIC II e^+ - e^- option; RL-73-070 (July).

233 J R Maidment
Good field requirements in the proton ring of EPIC II/III; RL-73-080 (July).

234 J R Maidment
Beam separation in the EPIC II e-p proton; RL-73-091 (August).

235 G Manning
Ideas on physics with EPIC; RL-73-154 (November).

236 W J McDonald, A I Kilvington, C J Batty, J L Weil
Identification of fission activity using thin film detectors; RL-73-086.

237 J G McEwan, G J Daniell
A note on determining resonance widths in the presence of Gaussian errors; RL-73-093 (September).

238 A D McInturff
Design study of iron configuration for beam line dipoles (superconducting); RL-73-109 (September).

239 B H Meardon
A Monte-Carlo computer programme for neutron elastic scattering simulation; Harwell Report AERE R-7302.

240 I Montvay
Statistical bootstrap of non-spherical fireballs; RL-73-029 (May).

241 D R Moore
70 MeV injector: close support services requirements; RL-73-131 (November)

242 D R Moore
70 MeV injector build and alignment requirements: a) Tank support structures, b) Tank nos. 1, 2, 3, 4, c) Drift tubes; RL-73-147 (November).

243 D R Moore
Survey datums for 70 MeV injector and Nimrod check calculations; RL-73-148 (December).

244 R H C Morgan
New injector control system; N/INJ/ 26 (March 1973).

245 A R Mortimer
Demineralised water supply to new injector; N/INJ/ 23 (March 1973).

246 A R Mortimer
70 MeV injector heat dissipation (new injector equipment in injector hall and magnet hall); N/INJ/ 24 (August 1973).

247 A R Mortimer, A T Gresham
Concrete insulated magnets; NIM-73-10.

248 A R Mortimer
70 MeV injector for Nimrod – building drawings; RL-73-069 (July).

249 G Myatt
Production of intermediate weak bosons by weak interactions in EPIC; RL-73-184 (EPIC/WP4/P2).

250 M J Newman, J Simkin, C W Trowbridge, L R Turner
GFUN user's guide – A users guide to an interactive graphics program for the computer aided design of magnets; RHEL/R244 (September 1972).

251 M J Newman
MNEMONIC: an interactive graphics program to generate a triangular mesh for TRIM; RL-73-126 (February 1972 (reprinted)).

252 S Norris
Daedalus version 2 in the DDP224: a description of the system software; RL-73-008 (April).

253 P Norton
Separation of σ_T and σ_L on EPIC; RL-73-174 (EPIC/WP3/P4).

254 P R Norton, H E Montgomery
EPIC rates; RL-73-180 (EPIC/WP3/P13).

255 M J O'Connell
Economical function fitting for momentum determination; RL-73-081 (August).

256 R J Ott
Two-body kinematics for EPIC; RL-73-189 (EPIC/WP5/P4).

257 K Paler, T P Shah, S N Tovey, R J Miller, J J Phelan, N M Cason, P H Stuntebeck, N N Biswas, V P Kenney, W D Shephard, B Chaurand, B Drevillon, G Labrosse, R Lestienne, R A Salmeron, M Bardadin-Otwinowska, A Borg, C Louedec, Y Pons, M Spiro
Factorisation in the inclusive reactions $\pi^{\pm}p \to \Lambda + X$ and $K^{-}p \to \Lambda + X$; RL-73-120.

258 F P Palou
A simple lower bound for the $\pi^{\circ}\,\pi^{\circ}$ total cross-section; RL-73-130 (November).

259 R D Peccei
Crossing symmetry and coherent states; RL-73-145 (November).

260 D H Perkins
Weak interaction rates in e-p collisions (EPIC) (Oxford Report 11/73); RL-73-183 (EPIC/WP4/P1).

261 D R Perry
Shielding for EPIC: first estimates; RL-73-087 (EPIC/MC/31)(August).

262 D R Perry
Radiation protection in particle accelerator areas; RL-73-106 (October).

263 D R Perry
Nimrod shielding: A brief guide; NIM-73-09.

264 R J N Phillips
Theoretical models of pp scattering; RL-73-004 (April).

265 R J N Phillips, D P Roy
Duality; RL-73-064 (July)

266 R J N Phillips, V Barger
Model independent analysis of the structure in pp scattering; RL-73-082 (August).

267 R J N Phillips
Comment on real parts of KN and $\bar{K}N$ elastic amplitudes; RL-73-149 (December).

268 E Pittet
A pedestrian approach to the dilatation group and some scaling laws; RPP/T/49.

269 W Range
Compton scattering; RL-73-169 (EPIC/WP2/P1).

270 B N Ratcliff
Determination of the transverse polarization of particles in EPIC; RL-73-212 (EPIC/WP8/P6).

271 G H Rees
A first magnet lattice design for EPIC II/III; RL-73-010 (April).

272 G H Rees
Energy variation for e-p collisions in EPIC II; RL-73-030 (May).

273 G H Rees
Initial studies of longitudinal space charge forces in e-p beam-beam interactions, for bunched and unbunched p beams; RL-73-044 (May).

274 G Ringland
The kinematics of the parton fragmentation region; RL-73-179 (EPIC/WP3/P11).

275 R G Roberts, D P Roy
Prong cross-sections from a realistic two-component model; RL-73-065 (July).

276 R G Roberts
Phenomenology of inclusive reactions: lectures at Scottish Universities Summer School 1973; RL-73-095 (September).

277 R G Roberts, D P Roy
Dual property of diffractive resonances from semilocal factorisation; RL-73-103 (September).

278 P S Rogers
Electronic circuit analysis with graphical output; RL-73-158 (December).

279 P S Rogers
Detection of Brenner Marks for the HPD; RHEL/M/C 54 (March 1973).

280 R Rosner, T G Walker (eds.)
Seminar on techniques for momentum reconstruction; RL-73-090 (October).

281 G G Ross
An SU(3) × SU(3) model for hadrons and leptons; RL-73-017 (April).

282 G G Ross
Errors in ν, Q^2 due to unobserved final states along the initial beam direction; RL-73-195 (EPIC/WP5/P10).

283 G G Ross
Effects of scaling breakdown; RL-73-196 (EPIC/WP5/P11).

284 G G Ross
Polarization at EPIC; RL-73-197 (EPIC/WP5/P12).

285 H I Rosten
The constant perimeter end; RL-73-096 (September).

286 H Rosten
Fortran routines for elliptic integrals – PSEUDO and 3rd kind (complete and incomplete); RL-73-097A (November).

287 H I Rosten
The magnetic field due to a current carrying helical block of rectangular cross section; RL-73-098A (October).

288 R G Russell
Modifications to Nimrod required for 70 MeV injection; N/INJ/ 25 (March 1973).

289 E J Sacharidis
Parity doublets and the Mandelstam-Sommerfeld-Watson transformation in backward K^+p elastic scattering; RL-73-025 (May).

290 D B Scott
Automatic spooling of SD-4020 output; RL-73-115 (October).

291 P Seager
Report on the NEF Group coating plant; NIM-73-23.

292 R L Sekulin, R J Ott
Kinematically allowed regions (in the Laboratory system) for reactions ep-ep ($n\pi$) etc.; RL-73-190 (EPIC/WP5/P5).

293 R L Sekulin
Calculations of total EM and weak rates; RL-73-191 (EPIC/WP5/P6).

294 J R Smith, F M Telling (eds.)
The work of the Rutherford Laboratory 1972; RHEL/R 270 (May 1973).

295 K Smith
A digital read-out for low temperatuve sensing resistors in the 2-7 K range; NIM-73-22.

296 K M Smith, P S L Booth, H R Renshall, P B Jones, G L Salmon, W S C Williams, P J Duke, W M Evans, R E Hill, W R Holley, D P Jones, J J Thresher
A search for CP-violating effects in the decays $K^{\pm} \to \pi^{\pm}\pi^{\circ}\pi^{\circ}$; RL-73-043.

297 P F Smith
A suggested experimental search for heavy long-lived integrally charged particles; RL-73-022.

298 A H Spurway, P F Smith
An assessment of possible enrichment processes for heavy metastable charged particles; RL-73-023.

299 R Stone
Re-installation of special Type II quadrupoles; NIM-73-11.

300 R J Stone
Procedure for installation, adjustment and removal of beam line components; NIM-73-18.

301 N W Tanner
Comparison of Pion Factories; CERN report PH III-73/14½ (December).

302 K W Taylor
An analysis of alternative data communication links between terminals and IBM 360/195 computer at the Rutherford Laboratory; RL-73-152 (December).

303 P C Thompson, C Balderson
Central cumputer system – Remote workstations operation manual; RL-73-041 (June).

304 W T Toner, R K P Zia (eds.)
Links between weak and electromagnetic interactions: proceedings of an informal meeting held at Rutherford Laboratory, 24-25 February 1973; RL-73-018 (May).

305 W T Toner
Beam-beam bremsstrahlung: the ultimate limit; RL-73-166 (EPIC/WP1/P9).

306 W T Toner
Separation of one-photon and two-photon events in electron positron collisions at EPIC energies; RL-73-167 (EPIC/WP1/P16).

307 W T Toner
Equivalent radiator for EPIC; RL-73-187 (EPIC/WP5/P1).

308 W T Toner
Detection of small-angle particles at EPIC, using a superconducting shield; RL-73-198 (EPIC/WP5/P14).

309 W T Toner
Controlled lepton polarization in EPIC; RL-73-199 (EPIC/WP5/P16).

310 L R Turner
Direct calculation of magnetic fields in the presence of iron as applied to the computer program GFUN; RL-73-102 (August).

311 I Uschersohn
Generalized rapidity for space-like particles; RL-73-094 (September).

312 L Vanryckeghon
Finite energy sum rule evaluations for hypercharge exchange reactions; Oxford University preprint.

313 W A Venus, H W Wachsmuth
Remarks on neutrino fluxes and their measurement in 200 and 400 GeV neutrino experiments using wide-band and narrow-band beams; RL-73-137 (October), (also CERN TC-L/Int 73-2).

314 T G Walker
Provision of test beams from the booster; RL-73-202 (EPIC/WP6/P3).

315 W Walkinshaw, A T Lea (eds.)
Computing and Automation Division quarterly report 30 December 1972 – 30 March 1973; RL-73-011 (April).

316 W Walkinshaw, A T Lea (eds.)
Computing and Automation Division quarterly report, 31 March 1973 – 29 June 1973; RL-73-051 (July).

317 W Walkinshaw, A T Lea (eds.)
Computing and Automation Division quarterly report, 30 June 1973 - 30 December 1973; RL-73-116 (October)

318 J G Watson
DDP224 to IBM 2701 PDA interface; RHEL/M/C46.

319 J G Watson, K M Knight
Serial (V24) to parallel (B S I) interface; RHEL/M/C 52 (1973).

320 N D West
Length dimensions of tanks 2 and 3 and proton acceleration rates; RL-73-157 (December).

321 F Wickens
The problem of accelerating polarized protons in EPIC; RL-73-210 (EPIC/WP8/P3).

322 J A Williams
The testing of rolling element bearings in cryogenic fluids with application to energy transfer system prototype; RL-73-063 (October).

323 P R Williams
12ft chamber TST project. Philosophy behind proposed Ne/H_2 handling scheme; NIM-73-04.

324 P R Williams
12ft chamber TST project. Containment of Ne/H_2 mixtures; NIM-73-05.

325 W G Williams
A design for thermal neutron polarization analysis diffractometer with a filter containing polarized samarium-149 nuclei as the spin analyser; RL-73-034.

326 W G Williams, J Penfold
Measurements of the efficiences of Mezei thermal neutron spin flippers; NBRU 73-1.

327 M N Wilson
Superconducting dipoles for beam transport; RL-73-108 (September).

328 R P Worden
$\gamma\pi$ scattering experiments at EPIC; RL-73-177 (EPIC/WP3/P8).

329 M Yates
A time-interval analyser for the measurement of RF structures in extracted beams; NIM-73-21.

330 V Zahra
Short DC separator; NIM-73-02.

CONFERENCE PAPERS (alphabetically by conference, then by author)

331 A S L Parsons
Baryon Exchange
American Physical Society (APS) Meeting, Berkeley, August 1973.

332 E Eisenhandler et al
$\bar{p}p$ elastic scattering 0·8 - 2·4 GeV/c
APS Meeting, Berkeley, December 1973

333 G P Gopal (Imperial College - Rutherford Laboratory Collaboration)
K^-p elastic scattering between 0·96 and 1·36 GeV/c
APS Meeting, Washington, April 1973.

334 D Baxter, I Buckingham, I Corbett, P Dunn, J Emmerson, A Engler, J Garvey, F Hart, G Hughes, C Jones, R Maybury, N Middlemass, P Norton, J Scheid, A Segar, T Quirk
Neutral particle final states from K^-p interactions in the range 690 to 934 MeV/c
Baryon Resonances, Conferance on, Purdue, 1973.

335 J D Dowell
Review of K^+p scattering experiments and phase shift analyses since 1970; **Ibid.**

336 A Kernan, S Y Fung, U Mehtani, Y Williamson, W Michael, G E Kalmus, R W Birge
Partial wave analysis of $\pi^+p \to \pi^o\pi^+p$ and $K^+ \Sigma^+$ at 1·28 - 1·84 GeV/c; **Ibid.**

337 R T Ross, J L Lloyd, D Radojicic
Production of strangeness – 2 baryons in the mass region 1600 to 2100 MeV/c² in K^-p interactions at 3·1, 3·3 and 3·6 GeV/c; **Ibid.**

338 R T Ross, J L Lloyd, S Radojicic
Ξ(1530) resonance in K^-p reactions at 3·1 - 3·6 GeV/c; **Ibid.**

339 C Hojvat, E Eisenhandler, W R Gibson, P I P Kalmus, L C Y Lee Chi Kwong, T W Pritchard E C Usher, D T Williams, M A R Kemp, A D Rush, J N Woulds, M Harrison, W Range, G Arnison, A Astbury, D P Jones, A S L Parsons
Differential cross-sections for $\bar{p}p \to \bar{p}p$, $\pi^+\pi^-$, K^+K^- in the range 0·8 – 2·4 GeV/c
Canadian Association of Physicists Meeting, Montreal, June 1973.

340 D B Thomas
Prospects of superconducting synchrotrons
Charged Particle Accelerators, III All Union Conference for Scientific Problems of, Moscow, October 1972.

341 C M Fisher
Rapid cycling bubble chambers
ECFA Study Meeting, Tirrenia, September 1972 (CERN/ECFA/72-4).

342 C M Fisher
A two arm spectrometer design to accommodate dispersion in a vertical magnetic field associated with a vertex detector; **Ibid.**

343 B Alper, H Bøggild, P Booth, L J Carroll, G von Dardel, G Damgaard, B Duff, J N Jackson, G Jarlskog, A Klovning, L Leistam, E Lillethun, M Prentice, D Quarrie, P Sharp, S Sharrock, J M Weiss
Preliminary results on charged particle production at high transverse momenta in p-p collisions at 90° at the CERN ISR
Elementary Particles, International Conference on, Aix, September 1973.

344 S L Baker, S Banerjee, J R Campbell, G Hall, A K M A Islam, G May, D B Miller, J E Allen, P V March, S H Morris, K O'Brien, C E Peach
A study of $K^+\pi^-$ elastic scattering in the reaction $K^+n \to K^+\pi^-p$ between 2·0 and 3·0 GeV/c; **Ibid.**

345 D M Binnie, L Camilleri, J Carr, N C Debenham, A Duane, D A Garbutt, W G Jones, J Keyne, I Siotis, J G McEwan
A study of the reaction $\pi^-p \to \omega n$ near threshold; **Ibid.**

346 D M Binnie, L Camilleri, J Carr, N C Debenham, A Duane, D A Garbutt, W G Jones, J Keyne, I Siotis, J G McEwan
Search for neutral mesons near 1 GeV/c²; **Ibid.**

347 D M Binnie, L Camilleri, J Carr, N C Debenham, A Duane, D A Garbutt, W G Jones, J Keyne, I Siotis, J G McEwan
A high resolution missing-mass measurement near the X° threshold; **Ibid.**

348 D M Binnie, L Camilleri, J Carr, N C Debenham, A Duane, D A Garbutt, W G Jones, J Keyne, I Siotis, J G McEwan
Measurements of the background differential cross-sections for $\pi^\pm p$ scattering, $\pi^\circ n$ charge exchange scattering and ηn production between 0·6 → 1·05 GeV/c; **Ibid.**

349 Birmingham – Durham – Rutherford Collaboration
Forward ω° production in 4 GeV/c π^+d interactions; **Ibid.**

350 Birmingham – Durham – Rutherford Collaboration
Backward production of meson resonances in 4 GeV/c π^+d interactions; **Ibid.**

351 Birmingham – Durham – Rutherford Collaboration
Branching ratios of the f° meson; **Ibid.**

352 H Bøggild, P Booth, L J Carroll, G von Dardel, G Damgaard, B Duff, K H Hansen, J N Jackson, G Jarlskog, L Jönsson, A Klovning, L Leistam, E Lillethun, G Lynch, S Ølgaard-Nielsen, M Prentice, S Sharrock, D Quarrie, J M Weiss
Preliminary results concerning two-particle correlations and associated multiplicity at the CERN ISR; **Ibid.**

353 H M Chan
Mueller-Regge phenomenology; **Ibid.**

354 R Y L Chu, G W London, Y P Yu, D Boyd, T Beggs, D J Candlin, A T Goshaw, H W K Hopkins, W Venus, P Alibran, S Kahn, J P Lowys, R Stump, J P Wuthrick, J Colas, C Farwell, A Ferrar, E Gombosi, T Hofmokl, J Six, D Gamba, A Marzari, A Romero, A E Werbrouck
Analysis of the interaction $K^-p \to \Sigma^\circ\pi^\circ$ in the 1575 - 1750 MeV/c² mass region; **Ibid.**

355 R Y L Chu, G W London, Y P Yu, D Boyd, T Beggs, D J Candlin, A T Goshaw, H W K Hopkins, W Venus, P Alibran, S Kahn, J P Lowys, R Stump, J P Wuthrick, J Colas, C Farwell, A Ferrar, E Gombosi, T Hofmokl, J Six, D Gamba, A Marzari, A Romero, A E Werbrouck
$K^-p \to \Lambda\pi^\circ\pi^\circ$ and $K^-p \to \Sigma^\circ\pi^\circ\pi^\circ$ formation in the 1570 - 1750 MeV/c² mass region; **Ibid.**

356 E Eisenhandler, W R Gibson, C Hojvat, P I P Kalmus, L C Y Lee Chi Kwong, T W Pritchard, E C Usher, D T Williams, M A R Kemp, A D Rush, J N Woulds, M Harrison, W Range, G T J Arnison, A Astbury, D P Jones, A S L Parsons
The differential cross-sections for $\bar{p}p \to \pi^+\pi^-$ and $\bar{p}p \to K^+K^-$ in the momentum range 0·8 - 2·4 GeV/c; **Ibid.**

357 H I Miettinen
S-channel phenomenology of diffraction scattering; **Ibid.**

358 G A Ringland
Models for non-diffractive two-body reactions; **Ibid.**

359 Rutherford – Saclay – Ecole Polytechnique – Notre Dame Collaboration
Test of the factorisation hypothesis for the polarization of the Λ in the inclusive reactions $K^-p \to \Lambda + X$ and $\pi^\pm p \to \Lambda + X$
Elementary Particles, International Conference on, Aix, 1973 and
High Energy Collisions, V International Conference on, Stony Brook, 1973

360 Rutherford – Ecole Polytechnique – Saclay Collaboration
Study of ΛK° associated production in K^-p interactions at 14·25 GeV/c; **Ibid.**

361 Rutherford – Ecole Polytechnique – Saclay Collaboration
Study of the inclusive reactions $K^-p \to \gamma$ + anything at 14·3 GeV/c; **Ibid.**

362 Rutherford – Ecole Polytechnique – Saclay Collaboration
Search for double diffractive dissociation in K^-p interactions at 14·3 GeV/c; **Ibid.**

363 Rutherford – Ecole Polytechnique – Saclay Collaboration
Determination of the $K^-\pi^-$ total elastic and inelastic cross sections up to 2·8 GeV c.m. energy; **Ibid.**

364 Rutherford – Ecole Polytechnique – Saclay Collaboration
A triple Regge analysis of the reaction $K^-p \to pX$ at 14·3 GeV/c; **Ibid.**

365 Rutherford – Ecole Polytechnique – Saclay Collaboration
P_t correlations in hadron interactions with and without baryon exchange; **Ibid.**

366 British-Scandinavian Collaboration
Inclusive charged particle production at large angles at CERN ISR
High Energy Particle Collisions, International Conference on New Results from Experiments on, Vanderbilt University, Nashville, March 1973.

367 R Barloutaud, A Borg, F Brun, D Danegri, C Louedec, F Pierre, M Spiro, R J Miller, K Paler, J J Phelan, T P Shah, B Chaurand, B Drevillon, G Labrosse, R Lestienne, D Linglin, R A Salmeron
Distribution of charged multiplicities in K^-p interactions at 14·3 GeV/c
High Energy Physics, XVI International Conference on, Chicago and NAL, 1972.

368 R D Baker
Isotensor π - π phase shifts below the ρ mass; **Ibid.**

369 A S Clough, G K Turner, B W Allardyce, C J Batty, D J Baugh, W J McDonald, R A J Riddle, L H Watson, M E Cage, G J Pyle, G T A Squier
π^+ and π^- total cross-sections for ^{6}Li, ^{7}Li, ^{9}Be, C and O from 90 to 860 MeV
High Energy Physics and Nuclear Structure, Fifth International Conference on, Uppsala, 1973.

370 V R W Edwards
Anisotropic Momentum Distribution in Deformed Nuclei; **Ibid.**

371 V R W Edwards, B C Sinha, P W Tedder
Exchange Contribution to Inelastic Scattering from Collective Nucleus; **Ibid.**

372 T Ekelof, A J Herz, E Hagberg, S Kullander, P C Bruton, C S Curran, J K Davies, S M Fisher, F F Heymann, D C Imrie, G J Lush
The coherent interaction of high energy protons with ^{4}He; **Ibid.**

373 B C Sinha, F Duggan
A Three Parameter Optical Model on the Energy Shell; **Ibid.**

374 A D Bryden
Progress in reduced guidance at Rutherford Laboratory;
HPD Annual Conference, CNAF Bologna, September 1973.

374a R A Lawes, W T Welford
Analysis of film noise in flying spot scanners; **Ibid.**

375 C M Fisher
Track sensitive targets and rapid cycling bubble chambers; (RL-73-053)
Instrumentation for High Energy Physics, International Conference on, Frascati, 1973.

376 J Garvey
Television cameras in high energy physics experiments; **Ibid.**

377 J Garvey, G Amato, O Gildmeister, P Briandet, E Huffer, L Appleby, R Barnard, N. Lipman, D Morris, D Owen, D White, P Wilde, J Lister
A television camera system for data acquisition on the Omega spectrometer; **Ibid.**

378 J G V Guy, C M Fisher, W J Chapman, W Wignall
Geometrical reconstruction of events in a track sensitive target; **Ibid.**

379 R W Newport, D David, B R Diplock, B W H Edwards, W Turner, J D Wheatley
A rapid cycling bubble chamber with good access for use with counters; **Ibid.**

380 P R Williams, H Leutz
The operation of track sensitive targets in neon-hydrogen bubble chambers; **Ibid.**

381 C J Collie, N J Diserens, M J Newman, C W Trowbridge
Progress in the development of an interacting computer program for magnetic field design and analysis in two and three dimensions; (RL-73-077).
Magnetic Fields, IV Conference on Analysis of, Nevada, 1973.

382 E H de Groot, H I Miettinen
Shadow approach to diffraction scattering
Moriond, VIII Rencontre de, Meribel, March 1973.

383 D P Roy
Duality in Reggeon-particle scattering; **Ibid.**

384 D P Roy
Inelastic diffraction and total cross-section rise
Multiparticle Hadrodynamics, IV International Symposium on, Pavia, August, 1973.

385 B Chaurand, B Drevillon, G Labrosse, R Lestienne, D Linglin, R A Salmeron, R Barloutaud, A Borg, F Brun, D Denegri, C Louedec, F Pierre, M Spiro, R J Miller, K. Paler, J J Phelan, T P Shah
Some properties of transverse momenta and their correlations in semi-inclusive K^-p reactions at 14·3 GeV/c
Multiparticle Reactions, 3rd International Colloquium on, Zakopane, 1972.

386 R Lestienne, K Bockmann, M Rost, J Major, C L Pols, R T Van de Walle, G Rinaudo, A E Werbrouck, R J Miller, K Paler, J J Phelan, T P Shah, B Chaurand, B Drevillon, G Labrosse, R Lestienne, D Denegri, C Louedec, F Pierre, M Spiro, D Linglin, R A Salmeron, R Barloutaud, A Borg, F Brun
Some features of transverse momentum distributions in inclusive reactions; **Ibid.**

387 M Harrison et al.
$\bar{p}p \to K^+K^-$ over the momentum range 0·8 - 2·4 GeV/c;
Nuclear Structure and High Energy Physics, Institute of Physics Conference on, Liverpool, March, 1973.

388 B C Sinha
An analytic local expansion of a non-local exchange potential; **Ibid.**

389 B C Sinha, F Duggan
A three parameter nucleon-nucleus optical model on the energy shell; **Ibid.**

390 E C Usher et al.
$\bar{p}p \to \pi^+\pi^-$ over the momentum range 0·8 - 2·4 GeV/c; **Ibid.**

391 S Weisrose, R J Griffiths, N M Clarke
The Interaction of 83 MeV helions with ^{56}Fe; **Ibid.**

392 B C Sinha, F Duggan
The microscopic optical potential for Helions
Nuclear Structure International Conference on, Munich, August, 1973.

393 E G Sandels, R A Church, I S K Gardner, H C Whitby
A 2nd R F system for Nimrod;
Particle Accelerator Conference, San Francisco, March, 1973.
(IEEE Transactions on Nuclear Science, Vol. NS-20, No. 3 p.418).

394 British–Scandinavian Collaboration
New results on charged particle production in the central region of proton-proton collisions at the CERN ISR
Physique Hadronique aux Energies des ISR, Colloque de, Marseilles, November, 1973.

395 J A Charlesworth, R L Sekulin, D C Colley, M J Emms, J B Kinson, L Riddiford, B J Stacey, M F Votruba, P L Woodworth, I G Bell, M Dale, J V Major
Production of ρ° and f° in 4 GeV/c π^+d interactions
$\pi\pi$ Scattering and Associated Topics, International Conference on, Florida State University, 1973.

396 R J N Phillips
Theoretical models of pp scattering
Proton-proton Scattering at very High Energies, Royal Society Discussion Meeting on, London, March, 1973.

397 D Evans, M A Crook
Stress relaxation of polyethylene during irradiation
Polymer Physics, Institute of Physics Conference on, Shrivenham, September, 1972.

398 G W Dolphin, D C Lloyd, R J Purrott
Applications of chromosome aberration analysis to problems in radiobiology, (NRPB-R13)
Radiology, XIII International Congress of, Madrid, October, 1973.

399 A G Bell
Training to write real time systems
Real Time Computing, Info Conference on, October, 1973.

400 A E Stormer
Automatic management of partitioned data sets
SEAS Anniversary Meeting, Leuven, 1973.

401 P J Hallowell, R A Lawes
The automatic measurement of photographic negatives from high energy physics experiments
Software for Control, IEE Conference on, University of Warwick, July, 1973.

THESES FOR HIGHER DEGREES

402 T Azemoon (University College, London)
The lifetime of the neutral cascade hyperon and other properties of the hyperons

403 N C Debenham (Imperial College, London)
A high resolution study of backward π^-p reactions between 0·6 and 1·0 GeV/c

404 A Duane (Imperial College, London)
A measurement of the width of the X° (958) meson

405 F Duggan M.Phil. (Kings College, London)
The proton optical model and effective interactions

406 J Keyne (Imperial College, London)
A study of the ω-meson near its production threshold

407 J A Kirkby (Westfield College)
A search for the C-violating decay mode $\eta \to \pi^\circ e^+e^-$

408 G May (Imperial College, London) HEP/T/44
A study of KN, Kπ and Kd interactions at intermediate energies

409 T A Montgomery (University of Sussex) HEP/T/41
A measurement of the decay $\Sigma^+ \to p\pi^\circ$ as a test of the $\Delta I = \frac{1}{2}$ rule

410 R S Orr (Imperial College, London) HEP/T/42
K^+n charge exchange scattering

411 T G Pett (University of London)
The elastic scattering of low energy neutrons by deuterons

412 H R Renshall (University of Liverpool) HEP/T/40
A search for CP violation in the decays $K^+ \to \pi^+\pi^\circ\pi^\circ$ and $K^- \to \pi^-\pi^\circ\pi^\circ$

413 A M Shahabuddin (University of London)
Studies of nuclear inelastic scattering and of two step processes in single nucleon transfer reactions

414 E C Usher (Queen Mary College, London)
Measurements of differential cross-sections for the interaction $\bar{p}p \to \pi^+\pi^-$ in the momentum range 0·8 - 2·4 GeV/c

RUTHERFORD LABORATORY LECTURES

(on subjects of general scientific interest)

C Ford (Sir William Dun School of Pathology, Oxford, 18 January): New ways of looking at chromosomes and genes.

D T N Williamson (Molins Ltd. 8 February): The future of the mechanical engineering industry.

B T Price (Vickers Ltd. 15 March) Transport in the eighties.

W T Welford (Imperial College, 26 April): Holography for beginners.

R Wilson (UCL, 24 May): The solar corona.

H R A Dedow (Hydraulics Research Station, 28 June): The Hydraulics Research Station.

T Mulvey (Aston, 4 October): Electron microscope — a meeting point of science and technology.

E Laithwaite (Imperial College, 29 November): Three dimensional engineering.

NIMROD LECTURES ON PARTICLE PHYSICS

G Oades (Aarhus, 8 January): πK Phenomenology below 1 GeV.

G Kalbfleisch (Brookhaven, 22 January): 1. Eta primes. 2. Tachyons.

J Tran Than Van (Orsay, 29 January): Proton-proton scattering at all angles.

F Bradamante (CERN, 5 February): π^+p elastic and $\pi^+p \to \Sigma^+K^+$ scattering in the backward direction using a polarized target.

A J Van Horn (R L, 12 February): Barrelet zeros and resonance ambiguities in $K^-p \to \Lambda\pi^\circ$.

G Bellettini (Pisa and CERN, 16 February): Proton-proton total cross-sections at ISR.

M Derrick (ANL and UCL, 19 February): Neutrino interactions in hydrogen and deuterium.

N Byers (Oxford and UCLA, 26 February): Relativistic quark model results.

K Schultze (Aachen, 5 March): Experimental study of deep inelastic neutrino reactions.

D H Miller (Purdue and CERN, 12 March): Recent results in the 'R' region from bubble chambers and Omega.

A Yokasawa (ANL, 19 March): New data on πN charge exchange polarization.

R A Carrogan (NAL, 20 March): Proton-proton interactions at NAL.

J Rosner (Minnesota, 26 March): Resonances and Symmetries.

J D Hansen (CERN, 2 April): Partial wave analysis of the 3π and $K\pi\pi$ systems.

S Berman (SLAC, 9 April): PEP physics – high energy ep and $e\bar{e}$ colliding beam system.

R P Worden (RL, 14 April): Polarization in strong interactions.

C Wohl (Oxford, 30 April): The reactions $K^-p \to \bar{K}^\circ n$, $K^-p \to \Lambda\pi^\circ$, $K^-p \to \Lambda\eta$, $K^-p \to \Sigma^+\pi^-$, $K^-p \to \Sigma^-\pi^+$ between 3 and 4 GeV/c.

A Roberts (NAL, 2 May): Photon spectra at large transverse momenta from 300 GeV proton interactions at NAL.

M Ferro Luzzi (CERN, 7 May): Measurement of the real part in $\pi^\pm p$, $K^\pm p$, $\bar{p}p$ scattering between 1 and 2·6 GeV/c by means of the coulomb-nuclear interference.

R Stroynowski (CERN, 14 May): Comparison of medium energy data with ISR results.

A Parsons (RL, 21 May): $\bar{p}p \to 2\pi$, 2K between 0·7 and 2·4 GeV/c.

J Dowell (Birmingham): K^+p elastic scattering below 1 GeV/c and phase shift analysis.

D Faiman (CERN, 11 June): Symmetry schemes vs the Rosenfeld tables: some open experimental questions.

L Montanet (CERN, 18 June): What have we learned from a K^+p experiment done between 1·2 and 1·7 GeV/c incident momentum.

I Siotis (Imperial College, 25 June): Results on $pp \to pX$ from NAL.

R Rand (Stanford, 5 July): EM interactions at SPEAR.

C Franzinetti (Torino, 9 July): High energy neutrino physics – recent results.

G Fox (CERN, 12 July): Multiplicity distributions and inclusive spectra from 20 GeV/c to ISR in a multiperipheral cluster model.

B Duff (UCL, 14 July): Production of high transverse momentum particles at the ISR.

H I Miettinen (RL, 23 July): The role of the pomeron in multihadron physics – a global view.

G Chadwick (SLAC, 30 July): Helicity conservation: a comparison in ρ – photoproduction and πp scattering

M Le Bellac (Nice, 13 August): Correlations in multi-particle production.

E D Bloom (Caltech, 17 August): Inelastic μ^-p scattering in the SLAC rapid cycling hybrid bubble chamber.

J D Jackson (Berkeley and NAL, 20 August): Physics research programme at NAL.

S Coleman (Harvard, 28 August): The price of asymptotic freedom.

S Weinberg (Harvard, 29 August): Gauge models of weak interactions.

T A Filippas (Demokritos and CERN, 17 September): The inclusive charged pion spectra in $\bar{p}N$ interactions at rest.

G Trilling (Berkeley, 15 October): Recent results from a 205 GeV/c π–p bubble chamber experiment at NAL.

C J Batty (RL, 22 October): Searches for superheavy elements: an "Elementary Review".

J C Polkinghorne (Cambridge, 29 October): Hadronic processes at large p_T.

G Alexander (Tel Aviv and CERN, 5 November): $K^\circ_L p$ interactions between 0·8 – 3·0 GeV/c.

W Willis (Yale, 12 November): Results with BNL hyperon beam.

D Olive (CERN, 19 November): Recent progress in dual models.

L Holloway (RL and Illinois, 26 November): $\pi^- C^{12} \to 3\pi C^{12*}$ at 6 GeV/c.

R G Moorhouse (Glasgow, 3 December): Dynamics and non-symmetries of recent results in $N^* \to N\gamma$, Np, $\Delta\pi$ decays.

M R Jane (RL, 10 December): A measurement of the charge asymmetry in the decays $\eta \to \pi^+\pi^-\pi^\circ$ and $\eta \to \pi^+\pi^-\gamma$.

APPLIED PHYSICS LECTURES

P F Smith (26 February): An unorthodox review of the superconducting applications programme

D A Gray (7 May): What is EPIC?

J D Lawson (25 June): Basic concepts in accelerators and storage rings
(5 lectures: 25 June to 23 July)

C M Fisher and P R Williams (29 October): Track sensitive targets and bubble chamber physics.

MEETINGS AND SUMMER SCHOOLS

January 3-5	Informal Theoretical Physics Meeting
February 24-25	Weekend Meeting on "Links between Weak and Electromagnetic Interactions" (at Coseners House)
March 17-18	Weekend Meeting on "Physics with Polarized Targets at High Energies" (at Coseners House)
July 15-27	Summer School for Experimentalists in High Energy Nuclear Physics
September 3-21	Theoretical Elementary Particle Physics Summer School
November 17-18	Weekend Meeting on "Diffractive Scattering and Multiparticle Unitarity" (at Coseners House)
December 3-5	Meeting on "Vertex Detectors" (at Coseners House)

SEMINARS IN COMPUTING

V R Saunders (Atlas Computing Laboratory, 12 January): Computational aspects of quantum chemistry

M J O'Connell (26 January): Momenta in milliseconds

(14 February): Track analysis with rapid cycling chambers (whole day meeting). Arranged by R A Lawes and C M Fisher (RHEL/R 271)

A J Oxley, R A Lawes (23 February): Measuring machines – progress report

J Barlow, B Franek (9 March): Some more programs of the RL Film Analysis Group

J W Burren, D B Scott, T G Pett (14 March): Getting the best out of the ELECTRIC system (half-day meeting)

M M Curtis, A R Mayhook (23 March): Why COPPER?

F R A Hopgood (Atlas Computing Laboratory, 6 April): Computer Animation

A Bell (4 May): Observations on machine intelligence

P Girard, P J Hemmings (18 May): Telecommunications on the 195

H Wind (CERN, 8 June): Developments in Momentum Parameterisation

H Renshall (15 June): The π9 experiment and its data processing requirements

(13 July): Remote computing and teleprocessing (whole day meeting). Arranged by J F MacEwan

J Hart, R Maybury (27 July): The analysis of a spark chamber experiment (K13C)

(12 October): General Meeting

A Stormer (26 October): Automatic Program Library Management

M Jane (9 November): The analysis of the eta charge asymmetry experiment (π8)

J Lewis (Atlas Computing Laboratory, 23 November): POLYGRAPHICS – yet another graphics system?

M J O'Connell (7 December): Models for rapid momentum fitting

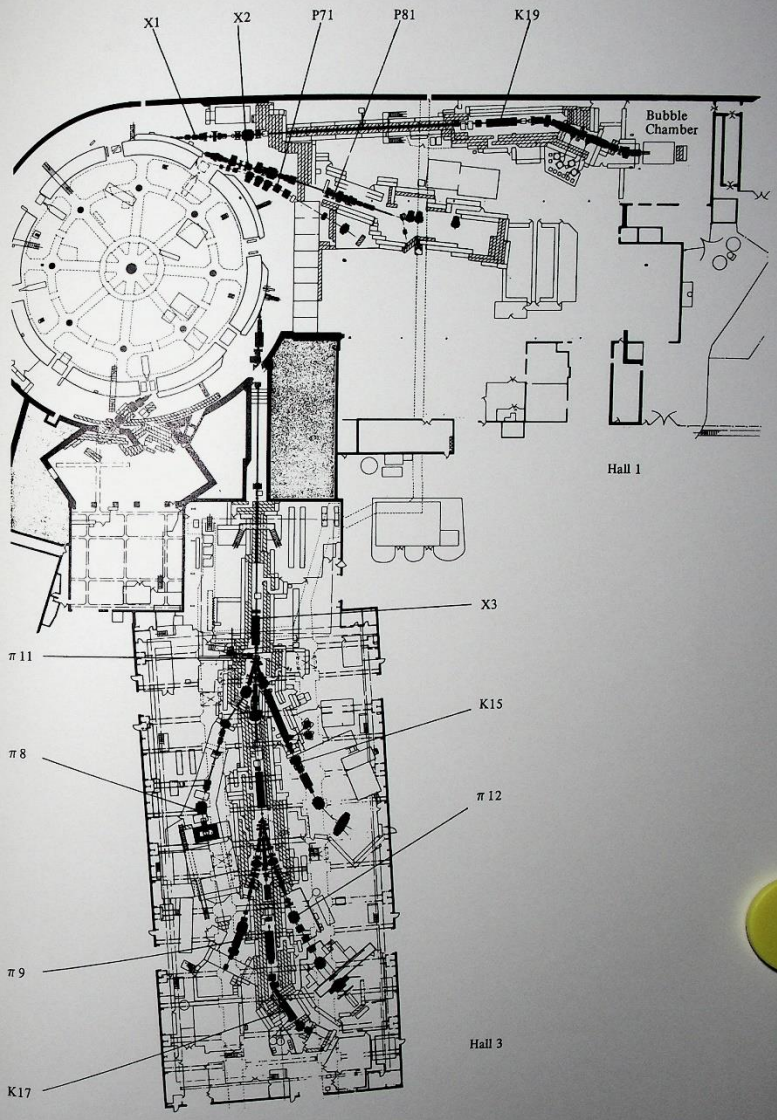

Figure 106. Beam lines in the experimental halls during 1973